RICE UNIVERSITY

Biomimetic PEG Hydrogels for *ex vivo* Hematopoietic Stem Cell Expansion

by

Maude Lucille Rowland

A THESIS SUBMITTED
IN PARTIAL FULLFILLMENT OF THE
REQUIREMENTS FOR THE DEGREE

Doctor of Philosophy

APPROVED, THESIS COMMITTEE:

Jennifer L. West
Isabel C. Cameron Professor, Chair
Bioengineering

K. Jane Grande-Allen, Associate
Professor, Bioengineering

M. Cindy Farach-Carson, Professor,
Biochemistry and Cell Biology

HOUSTON, TX

DECEMBER 2011

Abstract

Biomimetic PEG Hydrogels for *ex vivo* Hematopoietic Stem Cell Expansion

by

Maude Lucille Rowland

Hematopoietic stem cells (HSCs) are commonly used in the treatment of blood cancers, like leukemia, and other cancers where radiation or chemotherapy damages the native HSC population. The development of a novel system to study and maintain HSCs *ex vivo* would give researchers and clinicians the ability to investigate the basic biological processes of HSCs, improve current treatment regimens, and explore their use in new therapies. The work in this thesis focuses on the development of a synthetic PEG hydrogel scaffold that accurately mimics aspects of the HSC microenvironment and can expand clinically relevant HSC populations.

PEG hydrogel well surfaces were covalently functionalized with bioactive factors known to be critical in controlling HSC fate *in vivo*. In initial studies, 32D cells, a myeloid progenitor, were cultured in the wells for 6 days. On surfaces with the adhesive RGDS peptide sequence, 32D cell adhesion increased concurrently with RGDS surface concentrations. With the immobilization of two niche cytokines, SCF and SDF1α, onto hydrogel surfaces, 32D cells demonstrated significant increases in adhesion and spreading. These results confirmed that hematopoietic cell behavior could be controlled through the design of the bioactive PEG scaffold.

In studies with a primary hematopoietic cell population (c-kit$^+$, lin$^-$), the effects of bioactive molecules on cell expansion and differentiation were investigated after 2 weeks

in culture. The adhesive peptides sequences, RGDS and CS1, and four niche proteins, SCF, SDF1α, JAG1, and IFNγ, were covalently tethered to hydrogel well surfaces. Primary cells proliferated significantly on gels containing SCF and IFNγ though only SCF was capable of preventing HSC differentiation. Cells cultured on surfaces functionalized with JAG1 and SDF1α did not proliferate extensively, but they were able to maintain primitive HSC populations. Primary c-kit$^+$ cells were also encapsulated within biodegradable PEG hydrogels and cultured for 2-5 weeks. Cells remained viable for 5 weeks in culture, and preliminary results indicated minimal cell differentiation. In this work, biomimetic PEG hydrogels were successfully employed to expand HSC populations in both two and three dimensions. The ability to generate large populations of primitive HSCs *ex vivo* has broad clinical and research implications.

Acknowledgements

I would first like to thank my committee members, Dr. Jennifer West, Dr. Jane Grande-Allen, and Dr. Cindy Farach-Carson for their support and guidance. Jennifer, you have been a great mentor, and I genuinely appreciate your help in my career development. Jane, thank you for always being there and taking such an interest in me and all of your students. Cindy, thanks for joining my committee in the late stages and having so much good advice.

A big thank you to my peers in the West lab, past and present. Your support through these past five years has been much needed. You guys were always there when I needed someone to give me a hand, some advice, or just to listen.

A big dose of gratitude goes to my friends especially those in NC, Jac and Bre, who have always been there and still love me even if I don't call for months at a time. You guys are awesome.

Thank you to my family, without whom I wouldn't be here. Five fams, you know how special you are. My future family in CO, thank you for keeping me on track and giving me love and support. To Ruth, thank you for keeping me grounded and helping me remember what's important in life. Mom and Dad, you guys have given me everything I need to be successful and always pushed me to be my best. I love you.

And the biggest thank you to Michael. You have always supported me and pushed me and believed in me when I didn't. You are the reason that I made it through, and I couldn't have done it without you. I love you.

This thesis was financially supported by an NSF Graduate Research Fellowship and grants from the NIH.

Table of Contents

Abstract ii

Acknowledgements iv

List of Figures xi

List of Tables xvii

List of Abbreviations xviii

Chapter 1: Introduction 1

1.1 The Need for *ex vivo* Hematopoietic Stem Cell Expansion 1

1.2 HSC Transplants 2

1.3 Transplantation Process 5

1.4 Challenges Facing HSC Therapy 7

1.5 Hematopoietic Stem Cell Biology 8

1.6 The Hematopoietic Stem Cell Microenvironment 14

1.7 HSC Expansion Strategies 22

1.7.1 Advantages of and Obstacles to *ex vivo* HSC Expansion 22

1.7.2 Evaluation of Expanded HSCs 24

1.7.3 Cytokine Cocktails 25

1.7.4 Coculture 27

1.7.5 Biomimetic Surfaces and Scaffolds 27

Chapter 2: Hematopoietic Cell Behavior on Hydrogel Surfaces Containing Immobilized Fibronectin-derived Peptide Sequences 33

2.1 A Hydrogel System for HSC Expansion 33

2.1.1 Hydrogels 33

2.1.2 Poly(ethylene glycol) Hydrogels 35

2.1.3 Hydrogel Wells for Stem Cell Culture 38

2.1.4 Fibronectin-derived Adhesive Peptide Sequences: RGD and CS1 41

2.1.5 Selection of Hematopoietic Cells 42

2.2 Materials and Methods **43**
2.2.1 Polymer Synthesis and Characterization 43
2.2.2 PEG Hydrogel Wells 45
2.2.3 Cell Maintenance 48
2.2.4 Evaluation of Hematopoietic Cells in Culture 51
2.2.5 Statistical Analysis 55
2.3 Results and Discussion **55**
2.3.1 Polymer Synthesis and Characterization 55
2.3.2 Primary Cell Isolation 57
2.3.3 32D Cell Adhesion 58
2.3.4 32D Cell Spreading 61
2.3.5 Hematopoietic Cell Proliferation 64
2.3.6 Primary Cell Differentiation 68
2.4 Conclusions **77**
Chapter 3: The Effect of Covalently Immobilized SCF on Hematopoietic Cell Fate in Hydrogel Wells **78**
3.1 Introduction **78**
3.1.1 Stem Cell Factor 78
3.1.2 The Use of Stem Cell Factor in HSC Expansion 80
3.2 Materials and Methods **82**
3.2.1 Polymer Synthesis and Characterization 82
3.2.2 Cell Maintenance 85
3.2.3 Evaluation of Hematopoietic Cells in Culture 86
3.2.4 Statistical Analysis 87
3.3 Results and Discussion **87**
3.3.1 Polymer Synthesis and Characterization 87
3.3.2 32D Cell Adhesion 89
3.3.3 32D Cell Proliferation 92

3.3.4 32D Cell Spreading 94

3.3.5 Primary Cell Expansion 98

3.3.6 Primary Cell Differentiation 102

3.4 Conclusions 111

Chapter 4: The Effects of Immobilized SDF1α on Hematopoietic Cell Behavior in Hydrogel Wells 113

4.1 Background 113

4.1.1 Stromal Derived Factor 1α 113

4.1.2 Use of SDF1α in Biomimetic Scaffolds 114

4.2 Materials and Methods 116

4.2.1 Polymer Synthesis and Characterization 117

4.2.2 Cell Maintenance 118

4.2.3 Evaluation of Hematopoietic Cells in Culture 119

4.2.4 Statistical Analysis 120

4.3 Results and Discussion 120

4.3.1 Polymer Synthesis and Characterization 120

4.3.2 32D Cell Adhesion 122

4.3.3 32D Cell Proliferation 124

4.3.4 32D Cell Spreading 126

4.3.5 Primary Cell Expansion 129

4.3.6 Primary Cell Differentiation 132

4.4 Conclusions 140

Chapter 5: Effects of Surface Immobilized Jagged1 on the Expansion of Hematopoietic Stem Cells in Hydrogel Wells 142

5.1 Background 142

5.1.1 Jagged1 142

5.1.2 JAG1 for HSC Expansion 144

5.2 Materials and Methods 145

5.2.1 Polymer Synthesis and Characterization 145

5.2.2 Cell Maintenance 146

5.2.3 Evaluation of Expanded Hematopoietic Cells 147

5.2.4 Statistical Analysis 147

5.3 Results and Discussion 147

5.3.1 Polymer Synthesis and Characterization 147

5.3.2 Primary Cell Expansion 148

5.3.3 Primary Cell Differentiation 151

5.4 Conclusions 159

Chapter 6: Hematopoietic Stem Cell Behavior in Hydrogel Wells Functionalized with IFNγ 160

6.1 Background 160

6.1.1 Interferon γ 160

6.1.2 IFNγ for HSC Expansion 162

6.2 Materials and Methods 163

6.2.1 Polymer Synthesis and Characterization 163

6.2.2 Cell Maintenance 164

6.2.3 Evaluation of Expanded Hematopoietic Cells 164

6.2.4 Statistical Analysis 165

6.3 Results and Discussion 165

6.3.1 Polymer Synthesis and Characterization 165

6.3.2 Primary Cell Expansion 167

6.3.3 Primary Cell Differentiation 171

6.4 Conclusions 180

Chapter 7: Encapsulation of Hematopoietic Stem Cells in Bioactive Degradable Hydrogels 181

7.1 Background 181

7.1.1 Cell Encapsulation within Degradable PEG Hydrogels 181

7.1.2 Advantages of Encapsulation for HSC Expansion 183
7.2 Materials and Methods 184
7.2.1 Polymer Synthesis and Characterization 184
7.2.2 Cell Encapsulation and Maintenance 186
7.2.3 Cell Retrieval 188
7.2.4 Cell Proliferation 188
7.2.5 Evaluation of Differentiation Potential 189
7.2.6 Statistical Analysis 189
7.3 Results and Discussion 190
7.3.1 Polymer Synthesis and Characterization 190
7.3.2 Cell Viability within PEG Hydrogels 192
7.3.3 Cell Proliferation within Gels 196
7.3.4 Differentiation Potential 198
7.4 Conclusions 203
Chapter 8: The Biomimetic PEG Hydrogel System for HSC Expansion 204
8.1 Introduction 204
8.2 32D Cell Culture in PEG Hydrogel Wells 204
8.3 Primary Cell Culture in Bioactive Hydrogel Wells 206
8.4 Primary HSC Culture in Three-dimensional Bioactive PEG Hydrogels 211
8.5 Conclusions and Future Work 213
Bibliography 216
Appendix 242

List of Figures

Figure 1.1: Bone marrow transplantation process 6

Figure 1.2: Stem cell fates in the niche 9

Figure 1.3: Differentiation pathway of HSCs 11

Figure 1.4: Models for HSC mobilization and homing 13

Figure 1.5: The HSC microenvironment or niche 15

Figure 1.6: Proposed relationships between HSC sub-niches 17

Figure 1.7: A model of the interface between an HSC and a specialized niche osteoblast 18

Figure 1.8: HSCs from umbilical cord blood cultured on surface aminated nanofibers .. 31

Figure 2.1: Chemical structures of synthetic polymers that can form hydrogels.. 35

Figure 2.2: Methods to crosslink PEG chains and form hydrogel networks 36

Figure 2.3: General schematic for encapsulation of cells within a bioactive, proteolytically degradable PEG hydrogel 38

Figure 2.4: PEG hydrogel well fabrication techniques 39

Figure 2.5 PEG-Diacrylate synthesis 44

Figure 2.6: PEG-RGDS synthesis 44

Figure 2.7: PEG-CS1 synthesis 45

Figure 2.8: Microfabrication of PEG-DA hydrogel wells 46

Figure 2.9: Surface conjugation of hydrogel wells 47

Figure 2.10: GPC plots of PEG-RGDS and PEG-CS1 55

Figure 2.11: Flow cytometry analyses of c-kit$^+$, lin$^-$ cells immediately following magnetic sort 58

Figure 2.12: 32D cell adhesion on bioactive PEG hydrogels after 48 hrs 59

Figure 2.13: 32D cell spreading on RGDS surfaces 62

Figure 2.14: 32D cell area on hydrogel surfaces 63

Figure 2.15: 32D cell area distribution on differing surface RGDS concentrations..... 64

Figure 2.16: Change in 32D cell number in 48 hrs..... 65

Figure 2.17: c-kit$^+$, lin$^-$ primary cells on hydrogel surfaces with RGDS and CS1..... 66

Figure 2.18: Total cell expansion on surface immobilized RGDS and CS1 68

Figure 2.19: Colonies formed after 14 days in methylcellulose media following expansion 69

Figure 2.20: Distribution of colonies formed from cells expanded on gels with surface immobilized CS1 and RGDS..... 70

Figure 2.21: Individual colony formation organized by colony type from cells expanded on RGDS and CS1 functionalized hydrogels)..... 71

Figure 2.22: Flow cytometry analysis of c-kit$^+$, lin$^-$ cells after 14 days in culture on PEG-RGDS..... 73

Figure 2.23 Flow cytometry analysis of c-kit$^+$, lin$^-$ cells after 14 days in culture on PEG-CS1..... 75

Figure 2.24: Percent change in the c-kit$^+$, lin$^-$ population after 14 days in culture 76

Figure 2.25: Percent change in the KSL population after 14 days in culture..... 76

Figure 3.1: SCF structure and signaling pathways 79

Figure 3.2: Reaction scheme for the PEGylation of SCF (or any biomolecule)..... 84

Figure 3.3: Surface conjugation technique for multiple PEG-biomolecules..... 85

Figure 3.4: Western blot confirming PEGylation of SCF..... 88

Figure 3.5: The bioactivity of SCF is maintained after PEGylation..... 89

Figure 3.6: 32D cells adhere significantly to gels with surface immobilized SCF 90

Figure 3.7: At high concentrations of RGDS the effects of SCF are masked 91

Figure 3.8: SCF does not affect the proliferation of 32D cells..... 93

Figure 3.9: 32D cells spread extensively on hydrogels containing SCF 95

Figure 3.10: 32D cell area on bioactive hydrogels 96

Figure 3.11: Distribution of 32D cell size on hydrogel surfaces..... 97

Figure 3.12: Primary cells cultured on immobilized SCF over 2 weeks 99

Figure 3.13: The addition of SCF to hydrogel surfaces results in primary cell expansion 101

Figure 3.14: Colonies formed from expanded primary cells 103

Figure 3.15: Distribution of colonies formed from cells expanded on gels with surface immobilized SCF 104

Figure 3.16: Individual colony formation organized by colony type from cells expanded on SCF functionalized hydrogels 105

Figure 3.17: Flow cytometry analysis of c-kit$^+$, lin$^-$ cells after 14 days in culture on PEG-RGDS with PEG-SCF 107

Figure 3.18: Flow cytometry analysis of c-kit$^+$, lin$^-$ cells after 14 days in culture on PEG-CS1 with PEG-SCF 108

Figure 3.19: SCF immobilized on gel surfaces results in an increase in the c-kit$^+$, lin$^-$ population 109

Figure 3.20: The addition of SCF to hydrogel wells causes a significant increase in the KSL population 110

Figure 4.1: Structure of SDF1α 114

Figure 4.2: Process of transendothelial migration of HSCs triggered by the release of soluble SDF1α 116

Figure 4.3: Western blot of SDF1α and PEG-SDF1α 120

Figure 4.4: Bioactivity of PEGylated SDF1α 121

Figure 4.5: 32D cell adhesion on surfaces with immobilized SDF1α 123

Figure 4.6: Cell adhesion on gels with high RGDS concentrations (250 μg/cm^2) 124

Figure 4.7: 32D cell growth over 48 hrs. on hydrogels with immobilized RGDS and SDF1α 125

Figure 4.8: 32D morphology on bioactive PEG hydrogels with covalently immobilized SDF1α 126

Figure 4.9: Average 32D cell area on hydrogels with immobilized RGDS and SDF1α 127

Figure 4.10: Distribution of 32D cell sizes on surface immobilized RGDS and SDF1α 128

Figure 4.11: c-kit$^+$, lin$^-$ primary hematopoietic cells on hydrogels with surface immobilized SDF1α with PEG-CS1 or PEG-RGDS 130

Figure 4.12: The total expansion of primary cells on surface immobilized SDF1α after 14 days in culture 131

Figure 4.13: Colony distribution of colonies formed from cells expanded on gels with surface immobilized SDF1α 133

Figure 4.14: Distribution of colonies formed from cells expanded on gels with surface immobilized SDF1α 134

Figure 4.15: Individual colony formation organized by colony type from cells expanded on SDF1α functionalized hydrogels 135

Figure 4.16: Flow cytometry analysis of c-kit$^+$, lin$^-$ cells after 14 days in culture on PEG-RGDS with PEG-SDFα 136

Figure 4.17: Flow cytometry analysis of c-kit$^+$, lin$^-$ cells after 14 days in culture on PEG-CS1 with PEG-SDF1α. 137

Figure 4.18: Increase in c-kit$^+$, lin$^-$ cells over 14 days in culture 139

Figure 4.19: Expansion of the primitive KSL population on gels with covalently immobilized SDF1α 140

Figure 5.1: Jagged-Notch signaling pathway 144

Figure 5.2: Western blot of PEG-JAG1 148

Figure 5.3: c-kit$^+$, lin$^-$ cells on hydrogel surfaces modified with JAG1 and CS1 or RGDS 149

Figure 5.4: Total cell expansion on bioactive hydrogel surfaces functionalized with JAG1 after 2 weeks in culture 150

Figure 5.5: Colony formation from cells expanded on gels with surface immobilized JAG1 152

Figure 5.6: Distribution of colonies formed from cells expanded on gels with surface immobilized JAG1 153

Figure 5.7: Individual colony formation organized by colony type from cell expanded on JAG1 functionalized hydrogels 154

Figure 5.8: Flow cytometry analysis of c-kit$^+$, lin$^-$ cells after 14 days in culture on hydrogels functionalized with PEG-RGDS and PEG-JAG1 155

Figure 5.9: Flow cytometry analysis of c-kit$^+$, lin$^-$ cells after 14 days in culture on hydrogels functionalized with PEG-CS1 and PEG-JAG1 156

Figure 5.10: Increase in c-kit$^+$, lin$^-$ population during 14 days in culture on gels functionalized with JAG1 157

Figure 5.11: Expansion of the primitive KSL population on gels with covalently immobilized JAG1 158

Figure 6.1: Structure of IFNγ and its receptor. 161

Figure 6.2: Western blot image of IFNγ 166

Figure 6.3: Bioactivity of PEGylated IFNγ 167

Figure 6.4: c-kit$^+$, lin$^-$ cells on hydrogels functionalized with IFNγ and RGDS or CS1 169

Figure 6.5: Total cell expansion on hydrogel surfaces with immobilized IFNγ after 2 weeks in culture 170

Figure 6.6: Colony formation from cells expanded on gels with surface immobilized IFNγ 172

Figure 6.7: Distribution of colonies formed from cells expanded on gels with surface immobilized IFNγ 173

Figure 6.8: Individual colony formation organized by colony type from cells expanded on IFNγ functionalized hydrogels 174

Figure 6.9: Flow cytometry analysis of c-kit$^+$, lin$^-$ cells after 14 days in culture on hydrogels functionalized with PEG-RGDS and PEG-IFNγ 175

Figure 6.10: Flow cytometry analysis of c-kit$^+$, lin$^-$ cells after 14 days in culture on hydrogels functionalized with PEG-CS1 and PEG-IFNγ. 176

Figure 6.11: Increase in c-kit$^+$, lin$^-$ population during 14 days in culture on gels functionalized with IFNγ 177

Figure 6.12: Expansion of the primitive KSL population on gels with covalently immobilized IFNγ 178

Figure 7.1: PEG-PQ-PEG synthesis 185

Figure 7.2: Encapsulation of HSCs in degradable PEG-PQ-PEG hydrogels 187

Figure 7.3. Mass spectrometry plot of PQ peptide 191

Figure 7.4: Gel permeation chromatography (GPC) analysis of PEG-PQ-PEG 192

Figure 7.5: Viability of encapsulated c-kit$^+$ cells within PEG-PQ-PEG hydrogels with immobilized RGDS 193

Figure 7.6: Primary cell viability in PEG-PQ-PEG hydrogels 194

Figure 7.7: Representative phase contrast images of c-kit$^+$ cells encapsulated within degradable biomimetic PEG-PQ-PEG hydrogels at days 1 and 14 197

Figure 7.8: Colonies formed from c-kit$^+$ cells after 14 days of encapsulation 198

Figure 7.9: Colony distribution as a proportion of total colony number 199

Figure 7.10: Flow cytometric analysis of c-kit$^+$ cells after culture in degradable PEG hydrogels with 2 mM RGDS 201

Figure 8.1: Percent change in total cell population after 14 days in culture within hydrogel wells functionalized with biomolecules 207

Figure 8.2: Colony formation of c-kit$^+$, lin$^-$ cells cultured for 14 days on hydrogel surfaces functionalized with biomolecules 208

Figure 8.3: Percent change in c-kit$^+$, lin$^-$ population after 14 days in culture within hydrogel wells functionalized with biomolecules 210

Figure 8.4: Percent change in KSL population after 14 days in culture within hydrogel wells functionalized with biomolecules 211

Figure A1: Colonies formed during the colony forming unit assay. 242

List of Tables

Table 1.1: Distribution of diseases treated with HSC transplants from 1970-2007. 4

Table 1.2: Molecules implicated in HSC adhesion within the niche 21

Table 8.1: Overview of the effects of surface immobilized bioactive factors on hematopoietic cell behavior 212

List of Abbreviations

32D.....32D Clone 3

ANG1.....Angiopoietin 1

APC.....Allophycocyanin

BMEC.....Bone Marrow Endothelial Cell

C.....CS1

CCD.....Charge-coupled Device

CFU.....Colony Forming Unit

CS1.....Connecting Segment 1

CXCR4.....C-X-C Chemokine Receptor Type 4

DCM.....Dichloromethane

DIPEA.....Diisopropylethylamine

DMSO.....Dimethylsulfoxide

ECM.....Extracellular Matrix

EDTA.....Ethylenediaminetetraacetic Acid

ELISA.....Enzyme-linked Immunosorbent Assay

EPO.....Erythropoietin

FBS.....Fetal Bovine Serum

FEP.....Fluorinated Ethylene Propylene

FGF.....Fibroblast Growth Factor

FITC.....Flurescein Isothiocyanate

FN.....Fibronectin

G.....Granulocyte

G-CSF.....Granulocyte Colony Stimulating Factor

GEMM.....Granulocyte, Erythrocyte, Macrophage, Megakaryocyte

GM.....Granulocyte, Macrophage

GPC.....Gel Permeation Chromatography

GVHD.....Graft Versus Host Disease

GVT .....Graft Versus Tumor

HA.....Hyaluronic Acid

HBS.....HEPES Buffered Saline

HPC.....Hematopoietic Progenitor Cell

HSC.....Hematopoietic Stem Cell

IFNγ .....Interferon γ

IL.....Interleukin

JAG1 .....Jagged1

KSL .....c-kit^{+}, Sca1^{+}, lineage marker^{-}

Lin.....Lineage Marker

LT-HSC.....Long-term Hematopoietic Stem Cell

M.....Macrophage

MCM.....Methylcellulose Media

MMP .....Matrix Metalloprotease

MPP .....Multipotent Progenitor

MSC .....Mesenchymal Stem Cell

MW .....Molecular Weight

NMR .....Nuclear Magnetic Resonance

NVP .....*N*-Vinyl Pyrrolidone

OPN .....Osteopontin

PBS .....Phosphate Buffered Saline

PDMS.....Poly(dimethylsiloxane)

PE.....Phycoerythrin

PEG.....Poly(ethylene glycol)

PEG-DA.....Poly(ethylene glycol) Diacrylate

PEG-PQ .....PEG-GGGPQGIWGQGK-PEG

PES.....Poly(ether sulfone)

PET .....Poly(ethylene terephthalate)

PFA .....Perfluoroalkoxy

PHEMA .....Poly(hydroxyethyl methacrylate)

PMP .....Poly(methyl pentene)

pNIPAAm .....Poly(*N*-isopropylacrylamide)

PQ .....GGGPQGIWGQGK

PTFE .....Poly(tetrafluoroethylene)

PVA .....Poly(vinyl alcohol)

R.....RGDS

Sca1 .....Stem Cell Antigen 1

SCF .....Stem Cell Factor

SCM .....Succinimidyl Carboxymethyl

SDF1α .....Stromal Derived Factor 1α

SLAM .....Signaling Lymphocyte Action Molecule

SNO .....Spindle-shaped N-cadherin Expressing Osteoblast

SS .....Stainless Steel

ST-HSC.....Short-term Hematopoietic Stem Cell

SVA .....Succinimidyl Valerate

TEA.....Triethylamine

TFA.....Trifluoroacetic Acid

VLA .....Very Late Antigen

Chapter 1: Introduction

1.1 The Need for *ex vivo* Hematopoietic Stem Cell Expansion

45,000 patients worldwide receive potentially life-saving bone marrow transplants each year, though many more who could benefit from this procedure are unable to receive a transplant due to a limited number of suitable donors (1). Hematopoietic stem cells (HSC) in bone marrow transplants replace diseased or damaged blood and immune cells. Transplanted HSCs home to the bone marrow, engraft, and begin hematopoiesis, the process of becoming mature blood and immune cells. These procedures are most prominently carried out to treat multiple myeloma, non-Hodgkin's lymphoma, and acute leukemia, all cancers of the immune system or blood cells (2). They have also been effective in treating blood diseases like sickle cell anemia and β-thalassaemia, various autoimmune diseases (*e.g.* Crohn's disease, multiple sclerosis), as well as cancers where radiation treatment or chemotherapy damages the immune system (1, 3-9). Additionally, research is underway to expand the use of HSC therapy to treat genetic disorders, neurological disorders, diabetes, liver diseases, muscular dystrophies, acute myocardial infarction, and myocardial chronic ischemia (10-17).

HSCs have the potential to treat a wide variety of debilitating diseases, but they are not used extensively in clinical applications outside of cancer. This is due to a lack of available HSCs resulting from a limited number of donors, the low level of HSCs in bone marrow and peripheral blood, and the inability to culture HSCs successfully. The development of a system to study and maintain these cells *in vitro* would give researchers and clinicians the ability to investigate basic biological processes of HSCs, explore their

use in new therapies, and improve current treatment regimens. The work in this thesis focuses on the development of a synthetic scaffold for these purposes.

1.2 HSC Transplants

Currently, HSCs for transplantation can come either from the patient himself (autologous) or from a donor (allogeneic). Autologous transplants are the most common, but they are only possible in cases where the immune cells and blood cells themselves remain healthy despite the disease, but after aggressive treatment (like radiation), the immune system is lethally harmed or compromised (14). Approximately 30,000 autologous transplants occur annually as opposed to 15,000 allogeneic transplants (2). Table 1.1 displays the number of autologous and allogeneic transplants that have been performed for various diseases in the past forty years and registered with the Center for International Blood and Marrow Transplant (18). Before an allogeneic transplant can be performed, a donor who is a "match" to the patient must be found. This means that cells from both the donor and patient must express similar types of proteins on their surfaces. Typically "matches" are found in family members such as a sibling, but the existence of a bone marrow registry has made transplants from nonrelated donors possible. It is especially important to match when doing HSC transplants because the implanted immune cells are capable of attacking the patients' native cells, an outcome termed graft versus host disease (GVHD) (19). This undesired reaction is possible because all mammalian cells express major histocompatibility complex (MHC) proteins, which serve to identify them as non-foreign to immune system cells (20). There are three important MHC proteins in matching HSC donors and recipients: human leukocyte antigen (HLA) - A, HLA-B, and HLA-DR (19, 20). Every person has two alleles of these proteins, one

from each parent. Thus, a perfect match is termed a 6:6 match, and siblings have a one in four chance of being a 6:6 match (19). There are at least 20 varieties of each HLA, meaning that there are approximately 3 billion different possible combinations of the six significant HLAs. As a result, not every patient can receive HSCs from a 6:6 match, and 5:6, 4:6, and 3:6 matches must also be used. As less perfect matches are used, the likelihood of rejection or GVHD increases concurrently (2, 19). Though GVHD is not a desirable outcome, one possible patient benefit is the graft versus tumor (GVT) effect (3, 21). In the GVT effect, donor immune cells actually attack and kill any malignant cells they encounter within the body.

Table 1.1: Distribution of diseases treated with HSC transplants from 1970-2007. As reported to the Center for International Blood and Marrow Transplant through 2007. Adapted from (18).

Disease	Allogeneic Transplants	Autologous Transplants
Acute lymphoblastic leukemia	23,766	1,517
Acute myelogeneous leukemia	36,562	7,149
Chronic myelogeneous leukemia	25,137	729
Chronic lymphocytic leukemia	2,417	597
Hodgkin disease	1,095	14,107
Non-Hodgkin lymphoma	9,204	33,770
Plasma cell disorders	2,935	28,641
Breast cancer	193	23,206
Neuroblastoma	174	2,993
Ovarian cancer	22	1,688
Melanoma	48	59
Lung cancer	10	226
Sarcoma (soft tissue, bone, and other)	38	698
Ewing sarcoma	71	803
Wilm tumor	7	273
Myelodysplastic syndromes	10,701	244
Other leukemia	1,691	388
Medulloblastoma	5	688
Germ cell tumor	10	623
Brain tumors	5	1,104
Testicular cancer	8	1,288
Other malignancies	1,059	1,300
Autoimmune diseases	59	348
Severe aplastic anemia	8,682	15
Inherited erythrocyte abnormalities	4,836	5
SCID and other immunodeficiencies	3,378	4
Inherited disorders of metabolism	1,666	4
Histiocytic disorders	637	7
Other non-malignancies	330	321
Total	134,746	122,795

1.3 Transplantation Process

To prepare for an HSC transplant, the patient first receives myeloablation: high dose radiation or chemotherapy to ablate bone marrow cells, suppress the immune response, and kill malignant cells (19). Some patients cannot withstand the severity of myeloablation, and as a result, a new technique has been established that uses lower doses of radiation or chemotherapy, nonmyeloablative regimens, to suppress the immune system and decrease the chance of rejection. Since 2006, approximately 40% of allogeneic transplants utilize nonmyeloablative regimens (3). This procedure relies on implanted HSCs to kill cancer cells, and results in complete or partial remission in more than half of patients (3, 19, 22-25).

HSCs are typically collected from the donor's peripheral blood or bone marrow in the pelvis (19). However, HSCs can also be harvested from newborn umbilical cord blood. Cord blood HSCs are less likely to cause an immune response in imperfect matches as compared to equal mismatches in bone marrow HSCs. However, there are not as many stem cells in cord blood so adults must pool cord blood from more than one donor (21, 26). This increases the risk of GVHD because two types of non-self cells in the patient are capable of attacking the host tissue. Cord blood HSCs also take longer to home to and repopulate the bone marrow cavity (19, 21).

Harvested HSCs are filtered to remove debris such as bone fragments and may be processed to remove T-cells that could initiate GVHD (21). The purified cells are then infused into the patient intravenously. If the transplant is successful, the HSCs will migrate to the bone marrow cavity and begin hematopoiesis, repopulating the immune system (19). A schematic of the transplantation process is shown in Figure 1.1.

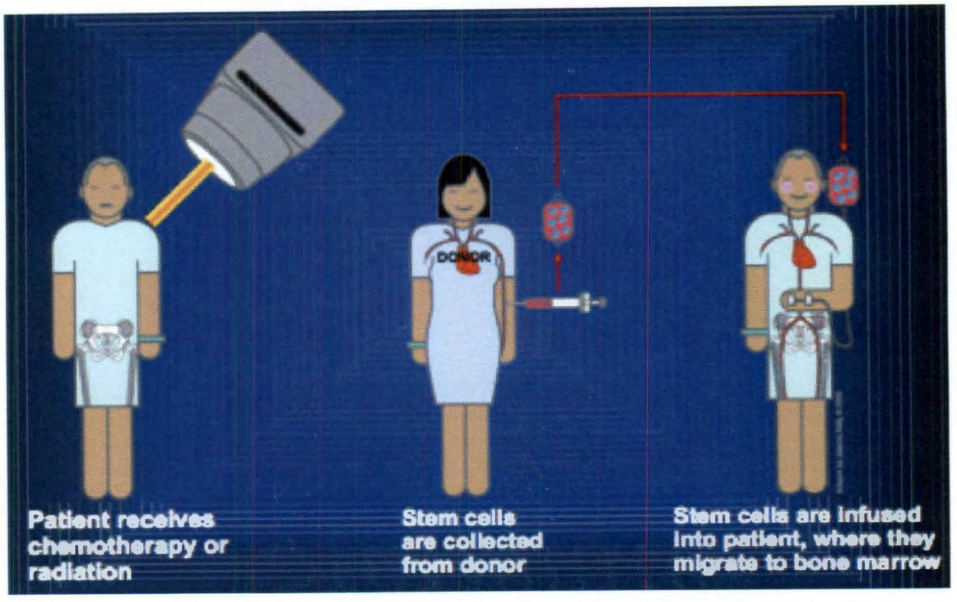

Figure 1.1: Bone marrow transplantation process. Image adapted from (19).

Survival rates after transplantation vary widely depending on the type of transplant, donor age, recipient age, and stage of the disease but rates of remission and survival are still higher than alternative treatments. The main concerns are infection after transplant—since the patient will have no functional immune system for about two weeks post-transplant, rejection, GVHD, and relapse (21). Autologous transplants are usually more successful (approximately 90 % survival rate) due to the fact that the patients' own cells are used, eliminating the risk of rejection and GVHD. Overall, transplants for non-malignant diseases have a survival rate of 70-90% if the HSCs come from an HLA identical sibling and 36-65% if the HSCs are received from an unrelated 6:6 match. The survival rates for acute leukemias are 55-68% if the donor is a HLA identical sibling and 26-50% if the donor is an unrelated HLA identical match (21). Because a variety of factors can contribute to the success of a transplant, the US Department of Heath and Human Services maintains a database of patient outcomes that can be sorted by disease,

donor type, patient age, patient race, patient gender, and cell source to serve as a resource to patients and healthcare providers (27).

1.4 Challenges Facing HSC Therapy

As aforementioned, one of the main obstacles facing HSC treatment is the limited number of HSCs available. Donors are in short supply, and finding a perfect match is difficult. Collecting HSCs from the pelvis is risky for the donor, but peripheral blood collection does not yield as many cells. HSCs from a single newborn's cord blood are insufficient and must be combined with other donations to successfully repopulate the patient. Even if large numbers of cells are implanted, only about 10% of the implanted cells are capable of self-renewal and repopulation, processes that are necessary for the transplant to be successful (28).

In addition, it is difficult to expand HSCs *ex vivo* because they do not readily self-renew, and they quickly begin to differentiate in culture. As a result, cultured cells cannot currently be used for therapy. Many research groups have begun to develop new methods for expanding self-renewing HSCs *ex vivo*. This could make HSCs from one donor or from a single cord blood isolation available to multiple patients and allow patients to receive higher HSC doses and/or multiple treatments more easily. Previous work has shown that higher numbers of implanted HSCs are more successful in therapies (29). The ability to culture HSCs *ex vivo* would also allow scientists to study the basic biological processes of the cells more easily. Having an available cell source would make large-scale experiments possible and reduce the frequency of primary cell harvests. For these reasons, this thesis will concentrate on the development of a bioactive polymer

scaffold for the maintenance of HSCs *ex vivo*. The system immobilizes important signaling molecules into the polymer matrix to mimic the HSC microenvironment.

1.5 Hematopoietic Stem Cell Biology

In order to engineer a successful *ex vivo* culture system, it is important to consider the biology of HSCs. HSCs are a type of adult stem cell typically found in the bone marrow cavity of long bones. They were first identified when they formed colonies in the spleens of irradiated mice after a bone marrow transplant (30, 31). These multipotent cells represent 1/20,000 of the total bone marrow cell population and can differentiate into all blood and immune cells in a process called hematopoiesis (1). Hematopoiesis is a continual process but is upregulated at times of stress such as at high altitudes and after injury (19, 32).

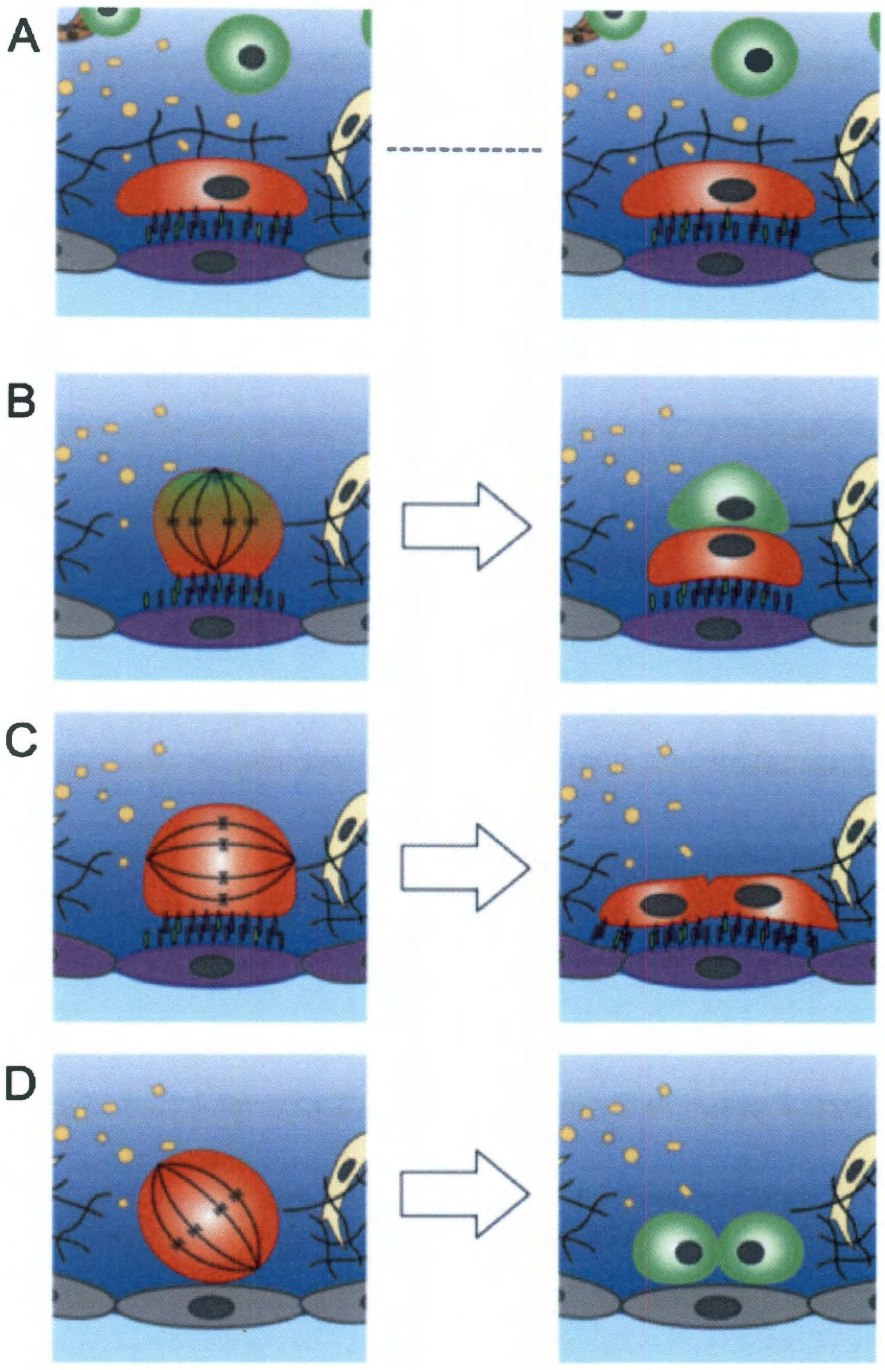

Figure 1.2: Stem cell fates in the niche. [red cells are hematopoietic stem cells (HSC), green cells are hematopoietic progenitor cells (HPC)]: A. HSC remains quiescent, B. HSC divides asymmetrically, one daughter cell remains an HSC and the other daughter cell begins to differentiate, C. HSC divides symmetrically and both daughter cells remain undifferentiated, D. HSC divides symmetrically and both daughter cells begin to differentiate. Figure adapted from (33).

HSCs possess a special characteristic called self-renewal, meaning that HSCs are capable of repopulating themselves and remaining in a multipotent state. Self-renewing HSCs can repopulate all blood cell lineages in irradiated hosts (34). However, HSCs are typically in a quiescent state and divide infrequently, approximately once every sixty days (35). The specific signals that regulate HSC self-renewal and differentiation remain the subject of scientific investigation and debate (19). It is hypothesized that it is not one signal but a combination of environmental cues and interactions that regulate HSC fate. The complexity of this system makes it difficult to control HSC behavior using standard tissue culture techniques.

There are two hypotheses that address the question of how HSCs self-renew. In divisional asymmetry, the HSC divides in such a way that one daughter cell receives all of the information to begin differentiation, and the other daughter cell remains in an undifferentiated state. In environmental asymmetry, the two daughter cells are identical and receive the signals that determine their fate from the external environment. Typically, one daughter cell remains an HSC and the other begins to differentiate (34). In symmetrical division, HSCs divide, and both daughter cells remain stem cells. It is theorized that HSCs can switch between symmetrical and asymmetrical divisions depending on physiological conditions (36, 37). Figure 1.2 pictorially depicts the fate of HSCs within the bone marrow: quiescence, self-renewal, and differentiation (32)

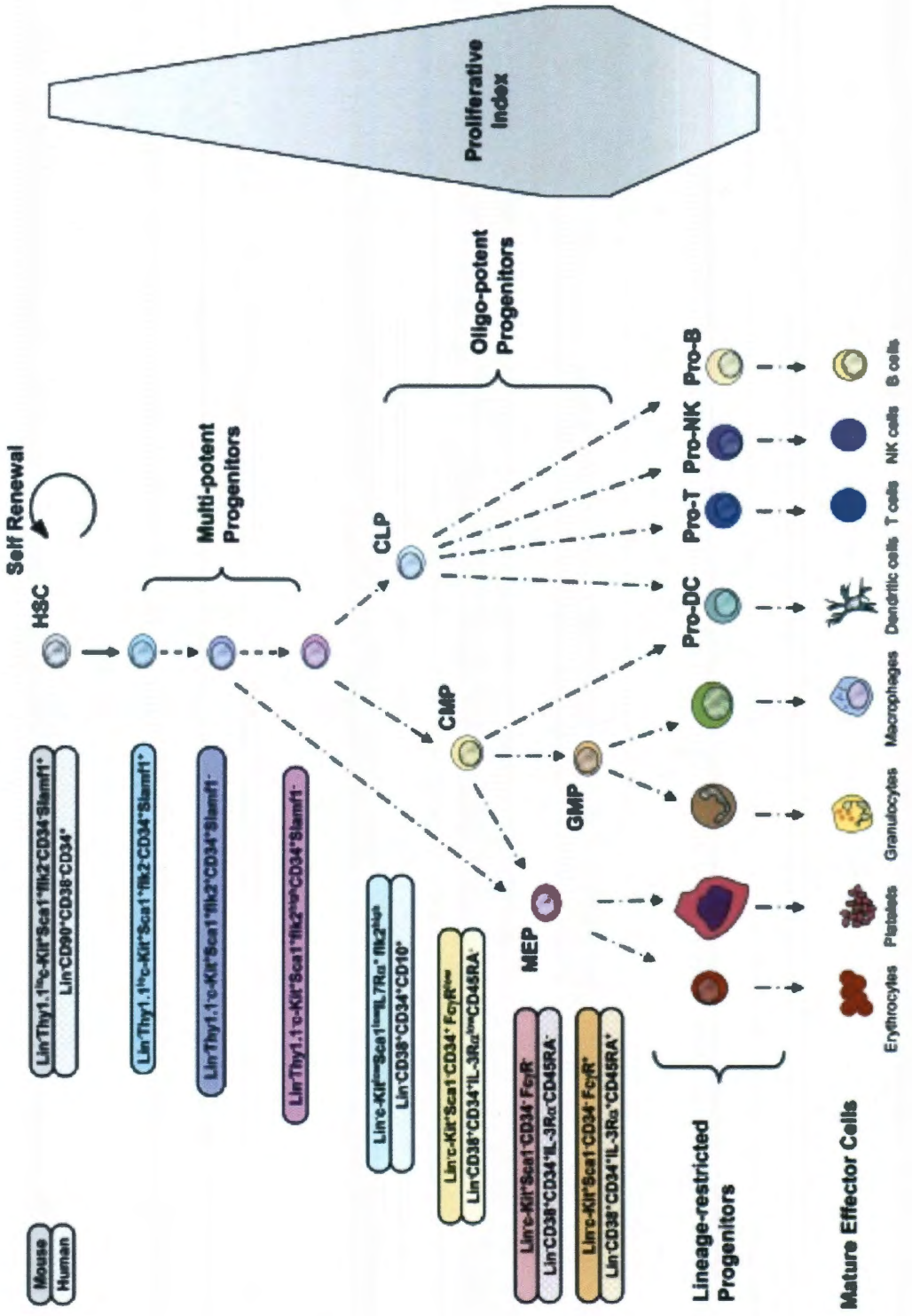

Figure 1.3: Differentiation pathway of HSCs. To the left of the colored cells, are matching colored ellipses indicating the surface markers that the cells express. Image adapted from (38).

Studying HSC function is complicated by the fact that the isolation of pure HSC populations from bone marrow is difficult. Many groups define HSC populations by a combination of surface markers that the cells express, all of which contain HSCs as well as a variety of progenitor cells. A specific combination of signaling lymphocytic action molecule (SLAM) family receptors has been used to describe HSCs: $CD150^+$, $CD48^-$, and $CD41^-$ (39, 40). Another group, the KSL population, is defined as c-kit^+, stem cell antigen 1 $(Sca\text{-}1)^+$ and lin^- (39, 40). lin^- cells are negative for a combination of lineage markers that are representative of differentiated HSCs. These include: Ter-119 (erythroid cells), Gr-1 (granulocytes), Mac-1 (monocytes), B220 (B cells), IL-7 Receptor (B and T cells), CD4 (T-cells), and CD8 (T cells) (40-43). $Endoglin^+$, $Sca\text{-}1^+$, and $Rhodamine^{low}$ also define a population of long term repopulating stem cells (20, 41, 44). Another population, side population HSCs, is defined by its ability to efflux Hoechst dye (45). Figure 1.3 shows how the surface markers of murine and human HSCs change as they differentiate down myeloid and lymphoid pathways.

However, none of these populations contain a pure population of self-renewing HSCs; they contain long-term and short-term reconstituting stem cells (LT-HSC and ST-HSC respectively) as well as multipotent progenitors (MPP) (34, 41, 46-48). LT-HSCs can renew extensively as opposed to ST-HSCs, which have a limited ability to self-renew, and MPPs, which do not self-renew (49-51). By combining different populations of HSCs, the percentage of long-term repopulating (self-renewing) cells can increase (41, 46, 47). Self-renewal is an important and critical process because it is the self-renewing HSCs that engraft in the bone marrow and repopulate the immune system, making transplantation successful. In fact, one self-renewing HSC can repopulate the entire

hematopoietic system of a mouse (43, 47, 52-55). There are also other HSC functions that must be maintained for therapies to work: mobilization and homing (Figure 1.4) (56).

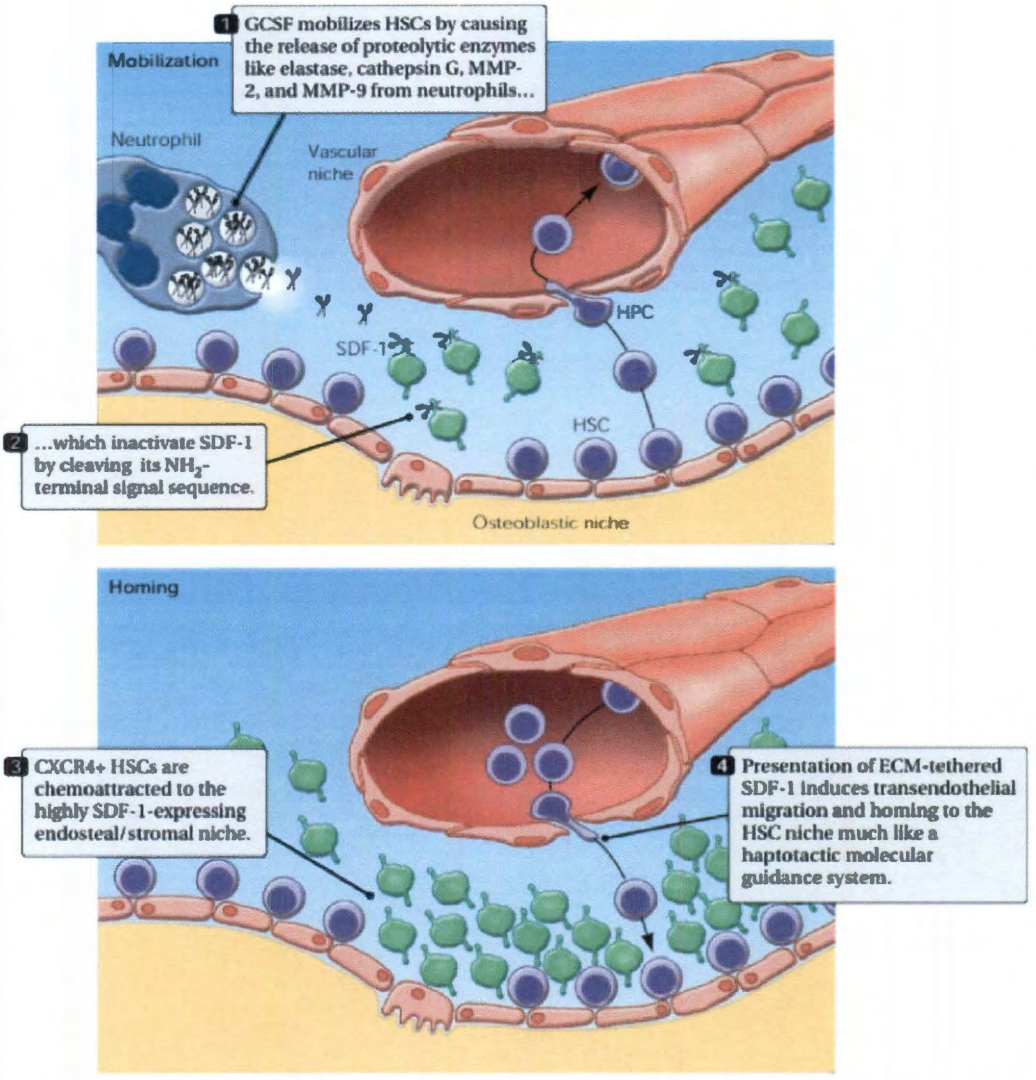

Figure 1.4: Models for HSC mobilization and homing. The protein stromal derived factor 1α (SDF1α) plays a critical role in both of these processes. Image adapted from (56).

Mobilization is the HSCs' response to injury or foreign invasion (34). During this process, proteolytic enzymes cleave adhesion molecules that keep the HSCs attached to stromal cells in the bone marrow cavity. This allows the HSCs to differentiate and move into the circulation where they can migrate to sites in the body where they are needed. The expression of c-kit and very late antigen 4 (VLA-4), both important adhesion

integrins, is decreased, and the production of matrix metalloproteases (MMPs) 2 and 9, which cleave adhesion molecules is increased on mobilized HSCs (57, 58). Granulocyte colony stimulating factor (G-CSF) triggers osteoclasts to resorb bone and release calcium, which also induces mobilization (59). Cyclophosphamide can also mobilize HSCs (34). HSCs that are unable to mobilize would be incapable of responding to injury or invasion by foreign bodies.

Homing is the ability of implanted or circulating HSCs to find their way to the bone marrow cavity (34). Transplanted HSCs must be able to be home to succeed in therapies because it is at this site that they receive signals for both self-renewal and differentiation. Several integrins (VLA-4 and VLA-5) and selectins (E and P) are critical in homing (34). Homed HSCs are found close to osteoblasts expressing osteopontin, N-cadherin, and bone morphogenic protein receptor 1 (BMPR-1) (34). In addition, there is an increase in the expression of C-X-C chemokine receptors type 4 (the receptors for stromal derived factor 1α) on the surface of HSCs during homing (28). Both mobilization and homing require signals that are coordinated by the HSCs' natural microenvironment or niche.

1.6 The Hematopoietic Stem Cell Microenvironment

In the design of a system for *ex vivo* HSC culture, it may be important to accurately recapitulate the native microenvironment. The HSC niche is defined as a "spatial structure in which [hematopoietic] stem cells are housed and maintained by allowing self-renewal in the absence of differentiation" (28). To preserve the delicate balance between quiescence, self-renewal, and differentiation, HSCs receive signals from their *in vivo* microenvironment. The majority of signals originate from membrane bound

proteins—via cell-cell interactions, local extracellular matrix components, and soluble molecules such as growth factors and cytokines (32). It has been proposed that stem cell potency relies heavily on extrinsic cues in the niche as opposed to intrinsic signals within the cell (32). To support this theory, researchers have shown that progenitor cells may be able to revert back to a stem-cell state when placed back into the niche (60, 61). Thus, the ability to control or mimic these cues *ex vivo* may retain HSCs in a multipotent state, which is critical if the cells will be used therapeutically.

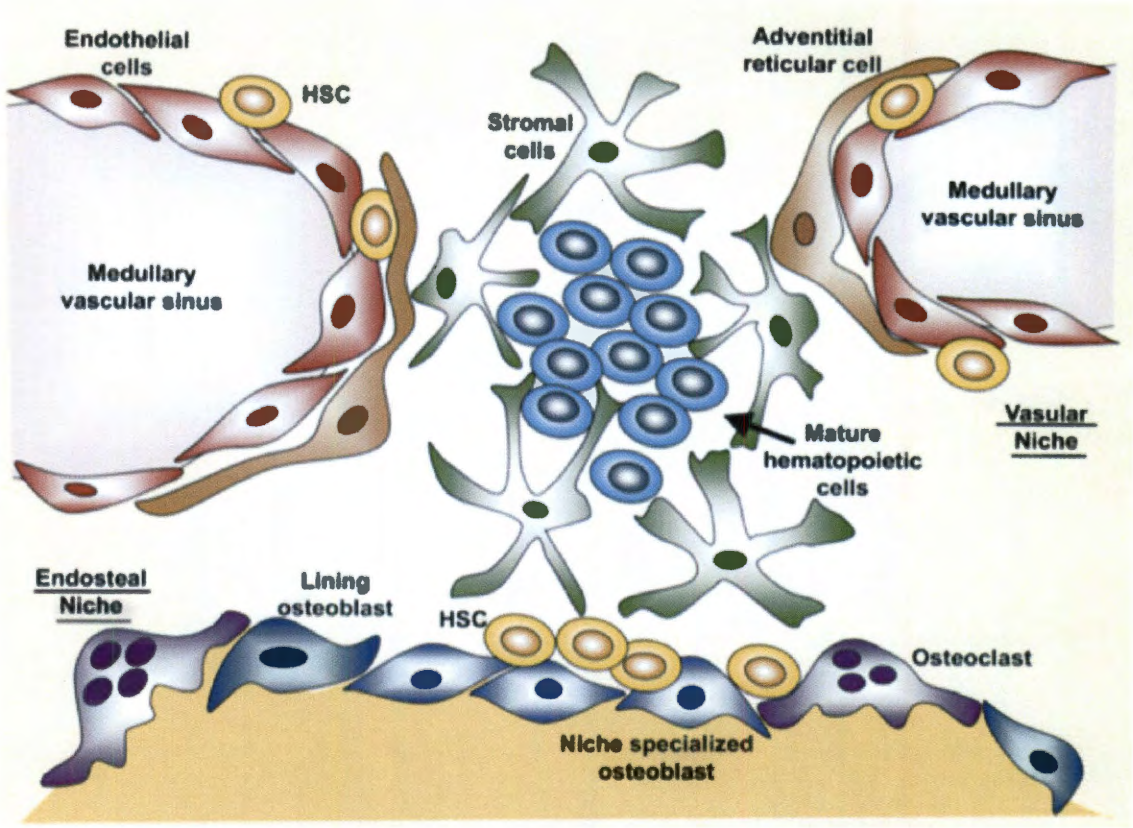

Figure 1.5: The HSC microenvironment or niche. The HSC niche is divided into two sub-niches: the endosteal niche—where HSCs interact with osteoblasts—and the vascular niche—where HSCs interact with endothelial cells. The functions of each niche are still under investigation, but it is known that several molecules and stromal cells regulate HSC fate. Image adapted from (62).

The niche was first discovered in a Steel Dickie mouse that had a mutation in the gene encoding for membrane bound stem cell factor (SCF). This mutation resulted in

changes to the niche and the inability of the mouse to maintain HSCs in vivo (34, 63). The niche is located in the bone marrow cavity, though HSCs can also be found in peripheral blood (~1 circulating HSC for every 100 located in the niche) and the liver and spleen after bone marrow injury (34). The presence of HSCs in circulation is thought to be important in repopulating areas of damaged bone marrow and thymus (1, 19, 28, 39, 64, 65). The HSC niche is divided into two sub-niches: the endosteal (or osteoblast) niche and the vascular niche as seen in Figure 1.5. These niches cooperate to ensure HSC self-renewal and hematopoiesis, though it is unclear precisely where these two processes take place within the niches (34, 66).

In general, it is thought that HSCs remain quiescent in the endosteal niche and when mobilized, due to stress or injury, they will migrate to the vascular niche where they begin to differentiate and leave the niche to circulate. In contrast, self-renewal could occur in the vascular niche because these cells would be in closer proximity to vasculature meaning they could act more quickly upon injury. The endosteal niche would then replenish the vascular niche by supplying it with HSCs (34). It has also been proposed that the sites for HSC self-renewal and differentiation are not predetermined. These events can occur in either the vascular or endosteal niche and depend more on the cells' proximity to specific stromal cells (67).

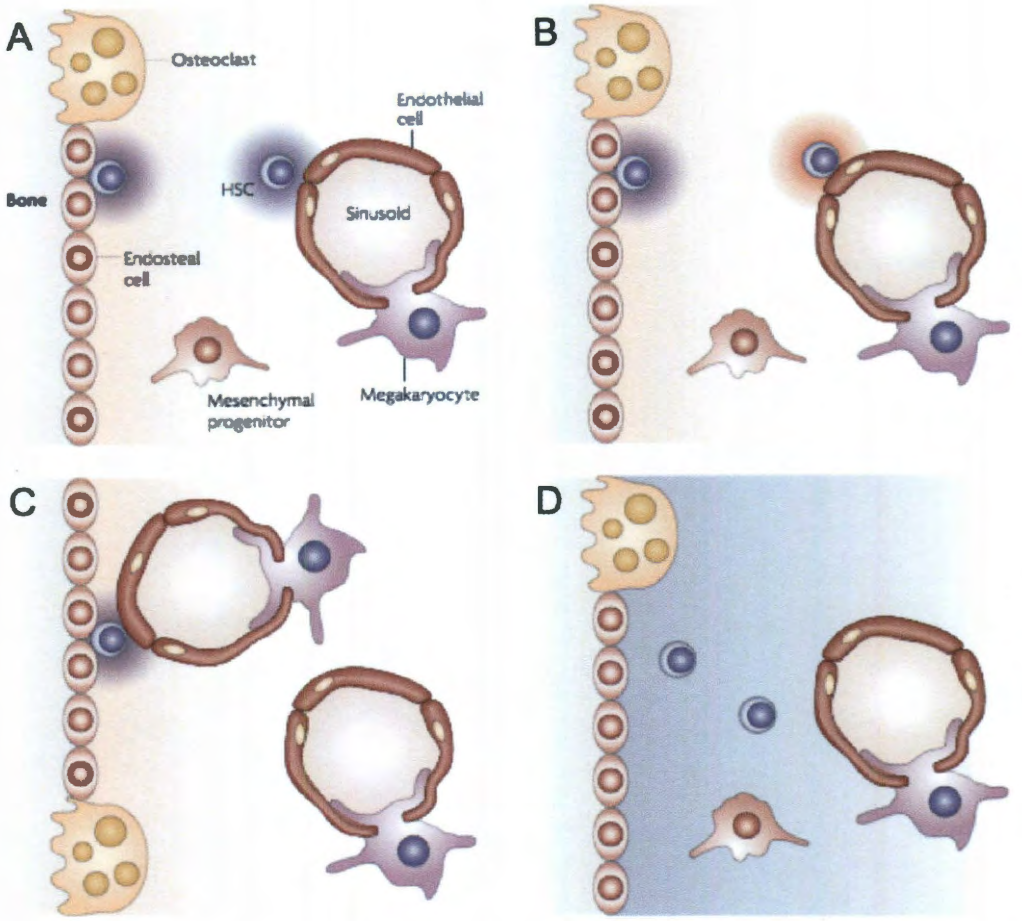

Figure 1.6: Proposed relationships between HSC sub-niches. A. Niches are spatially distinct but function similarly, B. Niches are spatially distinct but serve different roles in HSC maintenance, C. No sub-niches, HSCs are influenced by osteoblasts and endothelial cells in one larger niche, D. Unidentified cells maintain HSCs outside of endosteal or vascular zone. Image adapted from (66).

Figure 1.6 summarizes theoretical relationships between the sub-niches as well as a scenario challenging the idea of specific sub-niches and describing one comprehensive niche. The uncertainty surrounding the properties and functions of the sub-niches demonstrates another potential application of a synthetic niche environment. A system that is capable of recapitulating the cellular and molecular organization of both niches could help elucidate the distinct differences and similarities between the two.

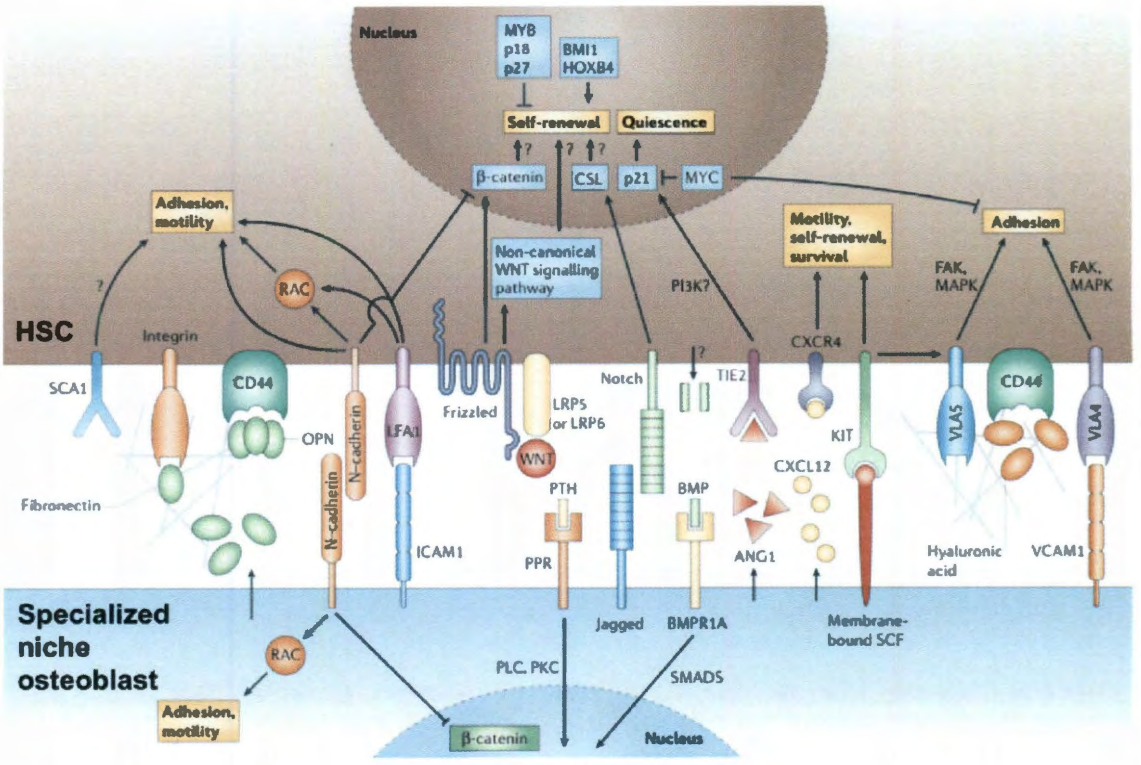

Figure 1.7: A model of the interface between an HSC and a specialized niche osteoblast. The interaction between osteoblasts is complex and has been well characterized. However, there are still many unknowns. Image adapted from (34).

Several different cell types compose the niche and many are specialized to control HSC behavior. These include fibroblasts, bone marrow endothelial cells (BMEC), mesenchymal stem cells (MSCs), spindle-shaped N-cadherin-expressing osteoblasts (SNOs), and CXCL12-abundant reticular (CAR) cells (34, 39, 56, 68). CXCL12 will be referred to by its other common name, stromal cell derived factor 1α (SDF-1α), in any subsequent discussion of the protein. These cells help to coordinate HSC behavior through secreted factors as well as cell-cell signaling.

The interactions between HSCs and SNOs are very complex and have been the most studied (Figure 1.7) (34, 39, 56, 68). The precise signaling pathways that control quiescence, self-renewal, and mobilization are still the subject of research and are most likely a combination of various signaling molecules. These molecules include soluble

factors (such as cytokines), membrane bound receptors, extracellular matrix proteins, and transcription factors (34). Though there is a multitude of signaling factors, we will only elaborate on a few of the most important.

SNOs (and other niche cells) express Jagged1 (JAG1), the ligand for Notch family receptors (1, 69). Notch receptors are expressed by HSCs and have been shown to prevent the differentiation of other cell types (1, 70, 71). Notch1 prevents HSC differentiation by maintaining the expression of GATA2, a transcription factor (72). However, Notch signaling is not necessary for HSC survival, indicating the redundancy of some of the signaling pathways (73-76).

Angiopoietin-1 (ANG1) on SNOs and TIE2 on the HSCs interact causing HSC quiescence and preventing apoptosis (1). Although this interaction prevents differentiation, it also prevents self-renewal (77). ANG1 can also encourage the adhesion of HSCs to SNOs through the TIE2 ligand (78).

Wnt signaling is also thought to promote self-renewal though the source of Wnt signaling molecules, osteoblast or vascular niche, is unknown (79-81). Hematopoietic progenitors can be expanded *in vitro* through the activation of Wnt signaling, and inhibiting Wnt signaling results in a lack of HSC growth *in vitro* and reduced repopulation abilities *in vivo* (34, 81). It is believed that Wnt signaling acts through HoxB4 (discussed later) and Notch1 pathways though the exact intracellular mechanisms are unclear (48, 81).

SDF1α has been shown to be important for both HSC retention and migration. It is expressed by both SNOs and BMECs and interacts with CXCR4 on HSCs (34). Membrane bound SDF1α can retain HSCs in the niche by binding to CXCR4 while

soluble SDF1α can induce mobilization by activating IL-8, MMP-2, and MMP-9 leading to the migration of HSCs out of the bone marrow and into the vasculature (28, 56).

Similarly, stem cell factor (SCF) has distinct effects on HSCs in its differing forms. Membrane bound SCF expressed on SNOs can cause HSC adhesion through the c-kit integrin on HSCs (28, 56). Though SCF does not seem to be necessary for the initial expansion of HSCs, it is critical for long-term maintenance and self-renewal (34). SCF can also stimulate adhesion by activating VLA-4 and VLA-5 integrins on HSCs, changing their shape (34). Osteoblasts without membrane bound SCF are unable to maintain HSCs *in vivo* (82, 83).

N-cadherin is expressed by both SNOs and HSCs (84, 85). N-cadherins in HSCs localize to their side of attachment to the SNOs (85). N-cadherin interactions between SNOs and HSCs are thus thought to aid in anchoring HSCs in the endosteal niche and, along with β-catenin, HSC asymmetrical division (34, 86). However, the subset of the HSC population that is capable of repopulation does not express N-cadherin suggesting it is not necessary for HSC maintenance (87).

Osteopontin (OPN), secreted from osteoblasts, also regulates HSC fate. Soluble OPN induces apoptosis in HSCs, and OPN deficient mice have a higher HSC population due the fact that there is a decreased level of apoptosis (34, 86). Osteopontin may also help maintain HSC quiescence (88).

Table 1.2: Molecules implicated in HSC adhesion within the niche. Table adapted from (89).

Major Stromal Adhesion Molecules			
	Type	**Adhesive Pathway Stroma: Hematopoietic Cell**	**Hematopoietic Target**
Collagen I	**ECM GP**		**HSC, E**
Collagen VI	ECM GP	Collagen VI : HSPG	HSC (lines)
Collagen XIV	**ECM GP**	**Collagen XIV : HSPG**	**HSC (lines)**
Laminin-10	ECM GP	Laminin-10 : β-1 Integrin	HSC (lines)
Fibronectin	**ECM GP**	**FN (RGD) : VLA-5 Integrin**	**HSC, E**
		FN (LDV) : VLA-4 Integrin	HSC, L
		FN (IDAPS) : CD44, VLA-4, CSPG	**HSC**
Thrombospondin-1	ECM GP	Thrombospondin-1 : CD36	Meg
Tenascin	**ECM GP**	**Tenascin : HSPG**	**HSC**
Fibulin	ECM GP	Fibulin: β-3 integrin	Meg
Perlecan	**HSPG**	**Antiadhesion**	**HSC (lines)**
Heparan Sulfate	HSPG	HSPG : pil protein	HSC
VCAM-1	**IgCAM**	**VCAM-1 : VLA-4 integrin**	**E, L**
HCA/ALCAM	IgCAM	HCA: HCA	HSC
		HCA: CD6	**HSC, L**
CD44	CAM	CD44 : hyaluronate	HSC, E, L
CD34	**Sialomucin**		**HSC**
CD164	Sialomucin		HSC
M-CSF Beta	**Cytokine**	**M-CSF β: c-fms**	**M**
transmembrane SCF	Cytokine	tm SCF : c-kit	HSC, E
transmembrane FL	**Cytokine**	**tm FL ; flt-3**	**HSC**

IgCAM: immunoglobulin cell adhesion molecule, GP: glycoprotein, HSPG: heparan sulfate proteoglycan, CSPG: chondroitin sulfate proteoglycan, pil: phosphatidyl inositil linked, L: lymphoid precursor, E: erythroid precursor, M: macrophage precursor, Meg: megakaryocytic precursor

Other ECM components such as fibronectin (FN) and hyaluronic acid (HA) help to keep the HSCs anchored in the endosteal niche through various integrins. An unidentified integrin on the HSCs adheres to FN, and VLA-5 on the HSCs adheres to HA (See Figure 1.7). Table 1.2 shows many of the major adhesion molecules that help HSCs adhere to either the ECM or stromal cells (89).

The concentration of different ions in the niche can also play a role in HSC behavior. Calcium gradients may be involved in HSC homing and retention of HSCs in the niche (90). The concentration of oxygen increases moving from the endosteal to the vascular niche, and lower oxygen levels are associated with HSC quiescence (39, 77, 91).

There are several other factors affecting HSCs that have been studied. Interferon-γ (IFN-γ), an inflammatory cytokine, is believed to negatively regulate hematopoiesis and promote HSC differentiation (92). It has been shown to promote the proliferation of LT-HSCs *in vitro* but leads to reduced engraftment capabilities (93). In addition, p21 (a gene) maintains quiescence, cmyc (also a gene) maintains the balance of HSC self-renewal and differentiation, and HoxB4 (a transcription factor) encourages self-renewal (39, 77, 91). The enumeration and detailed description of every molecule within the HSC niche are outside the scope of this work. However, it is important to keep in mind the complexity of the niche and variety of signaling pathways present when designing an *ex vivo* expansion system. In fact, many niche components have been incorporated into current HSC expansion strategies

1.7 HSC Expansion Strategies

1.7.1 Advantages of and Obstacles to *ex vivo* HSC Expansion

The expansion of HSCs has the ability to improve HSC therapy in several ways. First, *in vitro* culture would effectively increase the number of available donors because peripheral blood HSCs could be collected for both autologous and allogeneic transplants and expanded in place of harvesting HSCs from bone marrow in a more risky procedure. Cord blood would also be a more worthwhile source of HSCs because therapeutic numbers could be generated *ex vivo* eliminating the need for pooling. Also, HSCs would be readily available in cases where multiple HSC transplants are necessary such as when a patient receives successive rounds of damaging chemotherapy. Furthermore, the *in vitro* culture of stem cells would allow for concurrent gene therapy strategies and prevent rejection, graft v. host disease, and the need for immunosuppressant drug regimens (94).

Ex vivo expansion would also provide a way to conduct large-scale experiments with HSCs. Many of the molecular mechanisms governing HSC behavior are still not well understood. By creating a culture system, scientists could more easily study these cells (1, 95). An increased knowledge of HSCs could potentially help improve and broaden therapeutic applications (1).

Unfortunately, there are many hurdles to the culture of HSCs *in vitro*. As aforementioned, it is difficult to isolate HSCs. Harvested tissue contains numerous cell types, and current processing strategies are unable to produce pure HSC populations. This means that culture systems also support the maintenance of more differentiated cell types, which can mask the effects of the system on more primitive cells. Furthermore, though HSCs are capable of adhering to other cells and ECM components within the niche, they are typically non-adherent or weakly adherent in *in vitro* settings (96). Thus, culture on 2D surfaces is problematic, as the cells are highly mobile and readily leave the surface.

In addition, homeostatic conditions that are precisely controlled in the niche allow HSCs to proliferate while maintaining a pool of HSCs that remains undifferentiated. The signals that drive these processes are highly complex and have not been fully characterized. This makes it very difficult to mimic the niche accurately and maintain HSCs in a primitive state. In turn, once the cells have been expanded, there are several *in vitro* and *in vivo* assays that must be conducted to evaluate the success of the system. The expression of specific surface markers does not necessarily signify that the cells are capable of repopulation. Several research groups have addressed these challenges in attempts to culture HSCs in the laboratory.

1.7.2 Evaluation of Expanded HSCs

Expansion approaches have included cytokine cocktails (43, 97-107), coculture with niche stromal cells (34, 68, 96, 108-119), and engineered surfaces (94, 96, 120-125), as well as the use of synthetic polymer scaffolds (125-132). All of these systems used the same techniques to evaluate the potential of expanded HSCs. One of the simplest evaluation methods is to use flow cytometry analysis. In this assay, expanded cells can be stained with fluorescently tagged antibodies to surface markers defining HSC populations described in Section 1.5. The cells then flow through the pathway of a laser in a single cell stream to excite the fluorophores. The emission data for each cell is stored and can be analyzed to determine the expression profile of each marker within the cell population. However, this information should also be coupled with an assay that has a functional output.

The colony forming unit (CFU) assay can be used to determine pluripotency but cannot assess homing ability (133). In the CFU assay, progenitors are seeded within methylcellulose medium. Methylcellulose supports the growth of 3D cultures due to its viscosity. Cells are allowed to proliferate/differentiate and their ability to form various colonies signifies their differentiation potential. Colonies are observed and identified using an inverted microscope. Cells that are more primitive form colonies composed of multiple cell types. However, this technique can be subjective because different laboratories have developed their own scoring protocols, making it difficult to compare data from various laboratories. Also, some colonies form more quickly than others so various timepoints are typically evaluated (134).

The long-term culture initiating cell (LTC-IC) assay is used to quantify the number of cells that are capable of long-term repopulation. These cells are termed LTC-

ICs and are very primitive. To perform this assay, cells are seeded onto an irradiated feeder layer and kept in culture for a few weeks. They are then seeded in methylcellulose for the CFU assay. Colonies are counted, and if colonies are formed, the cells are marked as positive. LTC-IC frequency is calculated based on the number of seeded cells and applying Poisson statistics (134).

The best method to evaluate HSC potential is to perform a repopulation assay. In this assay, expanded cells are injected into an irradiated mouse and their ability to repopulate the host mouse indicates their potential. A variation of this assay is the competitive repopulating units assay. Donor bone marrow is mixed with cells from a genetically distinguishable control. The ability of the donor to repopulate the recipient is evaluated in both assays by looking at the percent of the donor's cells in the bone marrow compared to the number of control cells in the marrow (134). This is done using flow cytometry. In long term repopulating assays, bone marrow is retransplanted from the primary recipient into secondary recipients and from secondary to tertiary recipients. Stem cells that retain their potency should be able to repopulate the secondary and tertiary recipients (34).

1.7.3 Cytokine Cocktails

Many different cytokines have been added to the media to encourage HSC/HPC expansion. Thrombopoietin (TPO) induces the self-renewal of HSCs both *in vitro* and *in vivo* (97, 98). This is thought to be because TPO stimulates HoxB4 expression, which in turn encourages self-renewal (135). TPO may also play a role in suppressing HSC apoptosis (100). A combination of SCF and TPO was also shown to be effective in promoting HSC self-renewal compared to combinations of SCF and IL-3 or SCF and IL-

6 (101). Fibroblast growth factor (FGF) also promotes the expansion and the long-term growth of HSC/HPCs in culture (105). Both Jagged 1 and Wnt proteins can also lead to expansion of HSCs when added to the media (102, 103).

Flt3 has also been added to the media particularly in combination with TPO and SCF. Flt3 is thought to be early acting, involved in homing, and a survival factor. It induces the proliferation of human HSCs and when added with SCF it can improve engraftment (43, 104, 107). However, it has been shown that the Flt3 receptor (Flk2) is not expressed by LT-HSCs; populations expressing the receptor do not self-renew and are only capable of lymphoid reconstitution (50, 136). This suggests that Flt3 acts on a more differentiated population of hematopoietic cells.

The addition of cytokines to the media is a simple method to expand HSCs, but its simplicity is also its limitation. Many of the cytokines that are added to the media to encourage expansion and aid in survival, such as SCF, are also implicated in the differentiation pathways of HSCs. Though the addition of these signaling molecules can help the cells to proliferate, it concurrently triggers their differentiation. The half-life of these molecules is also very short because they are cleaved by proteases, and they must be replenished every few days, which can be very expensive (137). Furthermore, all of the factors that are added to the media are in a soluble form, which can have very different effects than if they are presented in a membrane bound form. One way to overcome these limitations is to use a feeder layer of cells to reproduce the multitude of signaling molecules that are present in the niche and the cell-cell interactions that are lacking in a system containing only soluble factors.

1.7.4 Coculture

Coculturing HSCs with other cell types found in the niche can also promote expansion. Several different types of endothelial cells have been used including BMEC (96), human umbilical vein endothelial cells (113, 119), and yolk sac endothelial cells (108, 109). HSCs have been shown to adhere to these endothelial cells and expand in culture significantly. Other stromal cells have seen similar results including NIH 3T3 fibroblasts (114, 115), osteoblasts (111, 117), and mesenchymal stem cells (68, 116, 118).

It is not entirely clear whether HSCs need to be in contact with stromal cells to survive and expand or if soluble factors released from these cells are capable of sustaining HSCs and encouraging their expansion. It has been shown that cell-cell contact is critical for the expansion of HPCs on osteoblasts (111). However, other studies show that contact is unnecessary and that soluble factors are enough to expand HSCs (110, 112).

The main problem with utilizing a coculture system is the lack of control that researchers have over the system. Although, the feeder cells can be manipulated genetically to secrete or express certain proteins, the interactions between the cells are so complex that it is difficult to parse out which signaling pathways are driving particular HSC processes. In addition, stromal cells could also signal undesired responses in HSCs, and it is hard to predict and/or prevent this.

1.7.5 Biomimetic Surfaces and Scaffolds

To better control the presentation of signaling molecules to HSCs without the use of other cells, several different types of surfaces have been fabricated for HSC expansion.

In one study, several surfaces, all approved for blood contact, were tested for human HSC biocompatibility and expansion. These included glass, stainless steel (SS) 316, SS 304, Teflon perfluoroalkoxy (PFA), Teflon fluorinated ethylene propylene (FEP), polytetrafluoroethylene (PTFE), polymethylpentene (PMP), polycarbonate, Barex (polyacetonitrile-methylacrylate), polyethylene (PE), high density PE (HDPE), polypropylene, acetyl polyformaldehyde, cellulose acetate, polyethylene terephthalate (PET), polysulfone, titanium, and aluminum (94). Teflon PFA, Teflon FEP, PMP, and titanium all did well in the expansion of human HSCs. SS 304, PTFE, HDPE, PET, and polysulfone all performed poorly. Overall, the investigators found that the expansion of primitive progenitor cells (those able to form CFU-GM—a combination of granulocyte and macrophage—colonies) was very sensitive to the material (94).

ECM proteins have also been coated onto polystyrene plates to test their effects on HSC adhesion. In one study, several different cell lines and ECM proteins were tested. Overall, they found that ECM proteins can encourage adhesion, and that the glycoproteins (fibronectin, vitronectin, and laminin) supported the largest percentages of cell adhesion (96). However, they also discovered that the cell lines responded very differently to the same ECM protein. For example, 80% of NALM-6 cells (B-cell lymphoma line) adhered to fibronectin as opposed to only 30% of KG1a cells (acute myelogenous leukemia). These results indicate the need for caution when presuming that the findings of studies with hematopoietic cell lines will apply to primary HSC populations.

FN has been widely studied in the expansion of HSCs/HPCs and has been shown to encourage the largest area of adhesion (120). When cultured in FN coated flasks,

human CD 34^+ cells were able to expand and maintained their ability to engraft (121). In another study, human $CD34^+$ cells also lost their clonogenic ability in the absence of FN (122). HPC adhesion to immobilized fibronectin has also been shown to stimulate proliferation whereas nonadherent cells stop in G1/S phase (123, 124). Two different peptide sequences derived from FN, CS-1 (LDV) and RGD, have also been used to successfully expand human umbilical cord HSCs (125).

The manipulation of surfaces is a fairly simple and versatile process. Many different molecules from the HSC niche can be tethered to surfaces. It is also possible to pattern them in specific arrangements to mimic their *in vivo* presentation, which is not an option with the addition of soluble cytokines or coculture techniques. However, surfaces are limited in their ability to translate into three dimensions. While surfaces are useful for studying basic cell-protein interactions and signaling pathways, it is difficult to recapitulate native bone marrow tissue accurately in only two dimensions. The HSC niche is a three-dimensional structure with multiple components, and the spatial arrangement of the various cell types and extracellular matrix components (ECM) affects the fate of HSCs *in vivo*. The creation of a synthetic HSC niche comprised of various cell types, signaling moieties, and appropriate ECM proteins has the potential to maintain these cells *in vitro* (34, 62). Outside of the niche, HSCs rapidly differentiate due to the absence of signals balancing the processes of self-renewal and differentiation. A three-dimensional system that recapitulates the *in vivo* HSC microenvironment may be able to control both of these events.

The use of polymer scaffolds in the design of such a system has great potential, yet it has not been studied extensively. Scaffolds not only provide mechanical support to

cells, but ideally they can be "selectively functionalized with regulatory cues" and the presentation of these molecules can be spatially controlled (32). RGD, LDV, and FN covalently conjugated to PET films showed successful *ex vivo* expansion of $CD34^+$ cells (125, 129). After ten days of culture, Jiang *et al.* observed a 600 fold increase in total nucleated cells on surfaces with CS1 and 500 fold increase on surfaces with RGD though only obtained successful engraftment of cells cultured on CS1 (125). Feng *et al.* cultured cells in both 3D and 2D PET scaffolds with surface immobilized FN. In ten days, cells expanded 200 fold in three-dimensions as compared to 100 fold in two-dimensions and maintained their ability to repopulate irradiated hosts (129).

Several different electrospun nanofibrous scaffolds (Figure 1.8) have also been developed to promote HSC adhesion and proliferation (126, 130, 131). Ma *et al.* electrospun a copolymer of poly(DL-lactide-*co*-glycolide) and collagen and coated it with E-selectin to capture HSCs; they were able to significantly increase the number of captured cells by 40% compared to controls (126). Chua *et al.* electrospun surface-aminated PES nanofibers to encourage HSC adhesion and expansion and obtained almost 200 fold expansion after 10 days compared to only 50 fold on TCPS (131). In another study, Chua *et al.* investigated the effects of various spacer types and lengths for the surface conjugation of amine groups to PES on HSC proliferation and differentiation potential. They found that the type of spacer used heavily influenced the expansion of HSCs (130).

Bagley *et al.* used tantalum-coated porous biomaterials to culture HSCs in three dimensions and observed a 7 fold increase in HSCs after 6 weeks in culture. Expanded cells retained their multipotency as demonstrated by the ability to form myeloid,

erythroid, and lymphoid progeny, though the *in vivo* repopulation ability of the cells was not evaluated (132). Despite their successes, none of these scaffolds has been effective in maintaining HSCs in culture for longer than a few weeks because they were unable to sufficiently mimic the complexity of the niche environment.

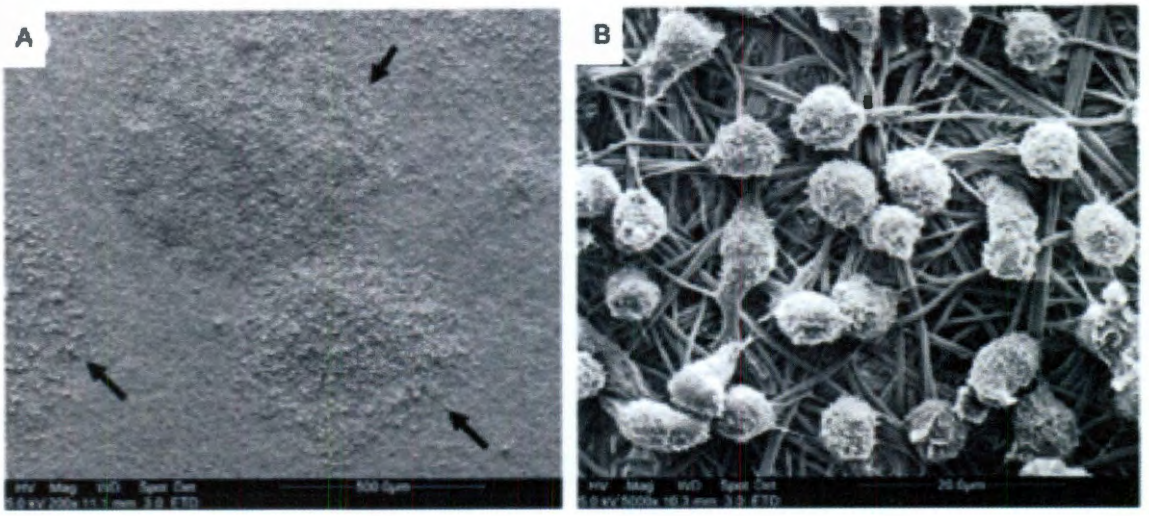

Figure 1.8: HSCs from umbilical cord blood cultured on surface aminated nanofibers. A. HSCs formed colonies on the nanofiber surface after 8 days (designated by black arrows) B. HSCs within the colonies on the nanofiber surface. Figure adapted from (130).

There is still a great need to develop novel scaffolds for HSC/HPC culture and expansion. The work in this thesis draws from research characterizing the HSC microenvironment and applies it to the design of a novel poly(ethylene glycol) based hydrogel scaffold. Recent work by Kobel *et al.* and Lutolf *et al.* demonstrated the utility of poly(ethylene glycol) diacrylate (PEG-DA) microwell arrays for studying the effects of specific proteins on the proliferation kinetics of single HSCs in a high-throughput manner (127, 128). In their system, they immobilized specific proteins, such as FGF, onto the surfaces of hydrogel wells and observed proliferation rates of single cells as well as their ability to engraft after multiple cell divisions. I have adapted this idea for the expansion of large populations of HSCs *ex vivo*. The following studies investigate the

potential of engineered niche components to manipulate HSC behavior in both two and three dimensions. The ability to control HSC fate *ex vivo* will improve current treatments that employ these multipotent cells and allow for development into new areas of research. These precisely designed materials will also provide researchers with a platform on which to study basic HSC biology.

Chapter 2: Hematopoietic Cell Behavior on Hydrogel Surfaces Containing Immobilized Fibronectin-derived Peptide Sequences

2.1 A Hydrogel System for HSC Expansion

The development of an *ex vivo* culture system for primary HSCs would greatly expand the clinical applicability of these cells. Currently, HSC therapy is limited by the inability to obtain large populations of these cells and maintain them in culture. The work in this thesis focuses on the development of a PEG hydrogel culture system that mimics aspects of the native bone marrow microenvironment. It is hypothesized that through the recapitulation of *in vivo* signaling processes, the ability to control HSC fate will be possible. We have designed a novel hydrogel well system for the culture of hematopoietic stem and progenitor cells. The surfaces of these wells can be functionalized with multiple biomolecules. This chapter investigates the effects of the short adhesive peptide sequences RGD and LDV on hematopoietic cell adhesion, spreading, proliferation, and differentiation.

2.1.1 Hydrogels

Hydrogels have been used for several years in the fields of tissue engineering (138-144) and drug delivery (139, 145-149) and have been investigated for other uses in diagnostics and biosensing (150). They have garnered attention due to their similarity to native tissues, which has been attributed to their high water content, and excellent biocompatibility (150). Hydrogels owe their structure to a network of polymer chains that are chemically crosslinked or physically entangled (151, 152). The hydrophilicity of polymer chains causes the gels to absorb high amounts of aqueous solutions, and in turn,

the gels swell extensively (138). Hydrogels can be formed from both natural and synthetic polymers.

Natural hydrogels can be generated from collagen, hyaluronic acid, fibrin, alginate, agarose, and chitosan (148). These hydrogels have intrinsic cytocompatibility and bioactivity, and many are naturally degraded by cells. However, hydrogels formed from natural polymers are typically weaker than synthetic matrices, though they can be chemically modified to increase their structural stability (150). In addition, researchers have less control over the biological properties of natural polymers as opposed to synthetic polymers.

Researchers can easily tune the mechanical, biological, and chemical properties of synthetic hydrogels. Synthetic hydrogels can be formed from poly(hydroxyethyl methacrylate) (PHEMA), poly(vinyl alcohol) (PVA), poly(ethylene glycol) (PEG), poly(acrylic acid), poly(methacrylic acid), and poly(acrylamide) (150). Figure 2.1 shows the chemical structures of these polymers. The mechanical properties of synthetic hydrogels can easily be controlled by altering the molecular weight of the polymer, the weight percent of the polymer, and/or the number of crosslinking sites on the polymer backbone (153). Synthetic polymers can be engineered to be biodegradable or nondegradable by the selection of the crosslinking process or the inclusion of degradable elements. For example, PVA readily degrades by hydrolysis if it is physically crosslinked but can be rendered nondegradable by chemical crosslinking (150). In addition, "smart" hydrogels can be formed that are responsive to changes in pH or temperature. One example of this is poly(*N*-isopropylacrylamide) (pNIPAAm), which can cycle between a swollen and collapsed state in response to temperature. (150).

pNIPAAm has been investigated for uses in *in vivo* drug delivery where it exists in a swollen form at room temperature and collapses at body temperature to release a drug (154, 155). Copolymers composed of one or more synthetic (or natural) polymer can also be synthesized to take advantage of various properties of each polymer.

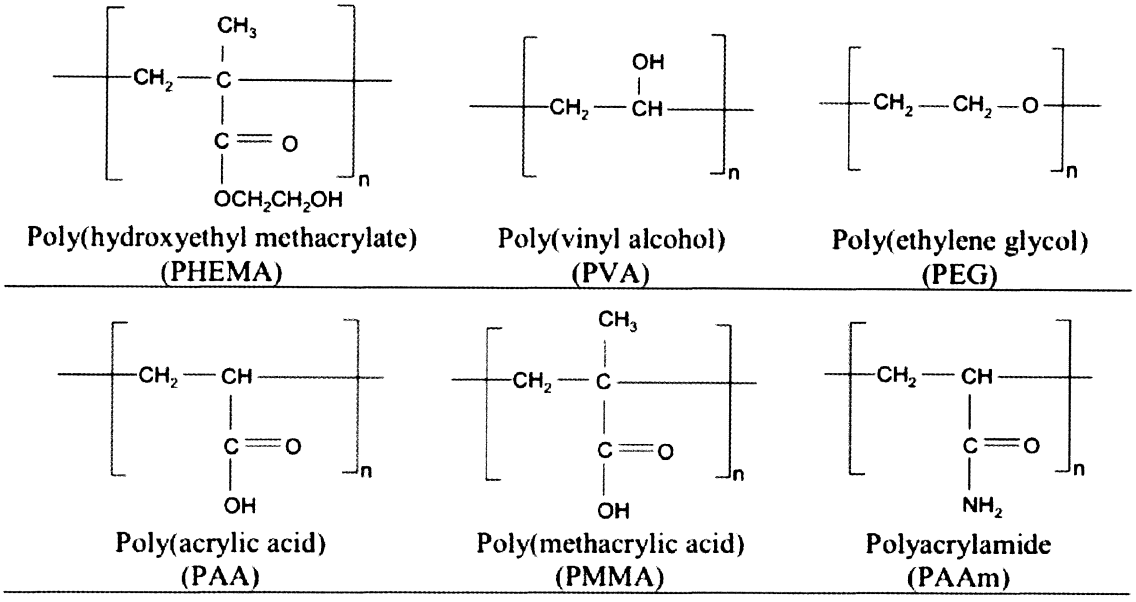

Figure 2.1: Chemical structures of synthetic polymers that can form hydrogels. Image adapted from (150).

2.1.2 Poly(ethylene glycol) Hydrogels

One type of synthetic hydrogel that has been used extensively in medical applications is PEG. PEG is non-toxic, non-immunogenic, and approved by the United States Food and Drug Administration for a number of applications. PEG resists protein adsorption and subsequent nonspecific cell adhesion (156, 157). Due to this property it has often been used as a "stealth" material to coat implanted devices and other materials to render them protein resistant and prevent immune rejection (150).

One PEG derivative, PEG diacrylate (PEG-DA) can be crosslinked rapidly via its acrylate groups. In an aqueous PEG-DA prepolymer solution, the PEG chains attract

water molecules causing the hydrophobic acrylate groups to cluster together and form micelles; this process prepares the polymer for subsequent crosslinking. There are two common strategies for the covalent crosslinking of PEG-DA: photopolymerization and Michael-type addition (Figure 2.2).

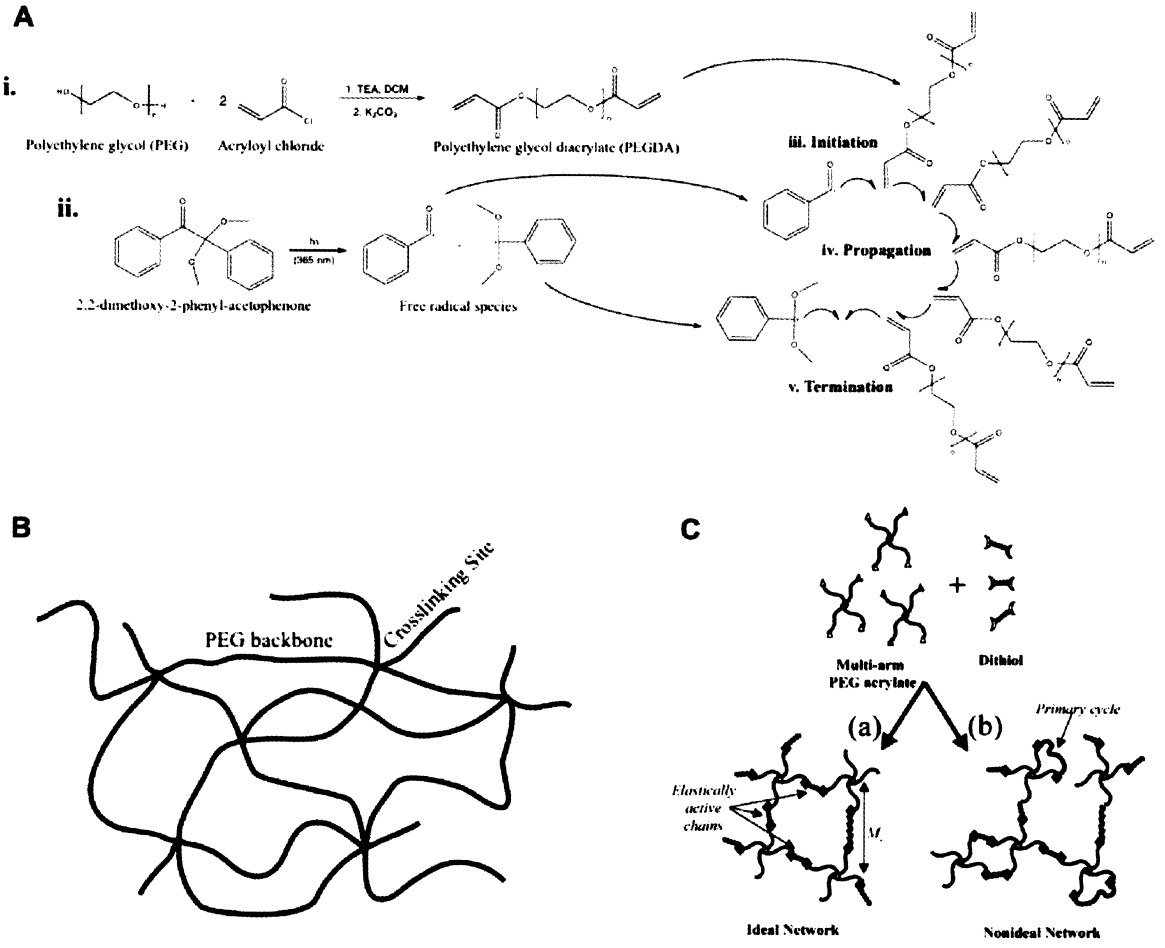

Figure 2.2: Methods to crosslink PEG chains and form hydrogel networks. A. Photopolymerization. i. PEG diacrylate (PEG-DA) synthesis. ii. UV light generates free radicals from the photoinitiator. iii. PEG-DA organizes into micelles in solution. iv. The addition of free radicals initializes the crosslinking of acrylate groups flanking each PEG chain. v. The reaction terminates upon the annihilation of two free radicals. B. The PEG hydrogel structure that forms as a result of the process shown in A. C. Michael-type addition. The reaction of dithiols and esters results in crosslinking of the PEG chains. This reaction can be catalyzed through an increase in pH and/or temperature. Images in A and B were adapted from (158) and in C from (159).

Photopolymerization uses the combination of a photoinitiator and light (UV or white) to initialize and accelerate free radical polymerization (160-162), a process that has been

shown to be cytocompatible (34, 163). Michael-type addition can also be used to form PEG-DA hydrogels through the reaction of free thiols and esters in an additive reaction (164, 165). This process proceeds slower than free radical polymerization, but utilizing a base catalyst and increasing the temperature can speed the reaction (165).

PEG-DA hydrogels are one of the most commonly used synthetic polymers in tissue engineering. These hydrogels can be designed to mimic the native ECM environment and provide a structural support for cells in the formation of new tissues (150). Though unmodified PEG hydrogels are biologically inert, there have been many approaches to modify the gel with bioactive elements (166-168). The ability to select the biomolecules that are covalently tethered to the matrix allows for complete control over the cell environment. Adhesive peptide sequences, such as RGDS, have been successfully immobilized onto PEG hydrogel surfaces to promote cell adhesion and spreading (161, 168-171). In addition, larger molecules such as growth factors and other proteins can be covalently incorporated into PEG hydrogels to drive cell behavior (172-175). The spatial arrangement of these molecules within a photopolymerized hydrogel can be controlled in both two and three dimensions using photolithography and laser scanning lithography techniques (176-180).

PEG-DA hydrogels can also be rendered biodegradable by incorporating proteolytically degradable peptide sequences into the PEG chain backbone (167, 181, 182) (Figure 2.3). Chapter 7 provides more information regarding the selection of peptide sequences. Cells release matrix metalloproteases (MMPs), which can degrade the sequences specifically and in turn break down the hydrogel (167, 183). Cells migrate through the matrix and remodel the scaffold as they organize into a three-dimensional

tissue-like structure. The advantage of this degradation scheme over hydrolytically degradable hydrogels is the ability to tune the degradation of the synthetic scaffold with the reorganization of the native tissue.

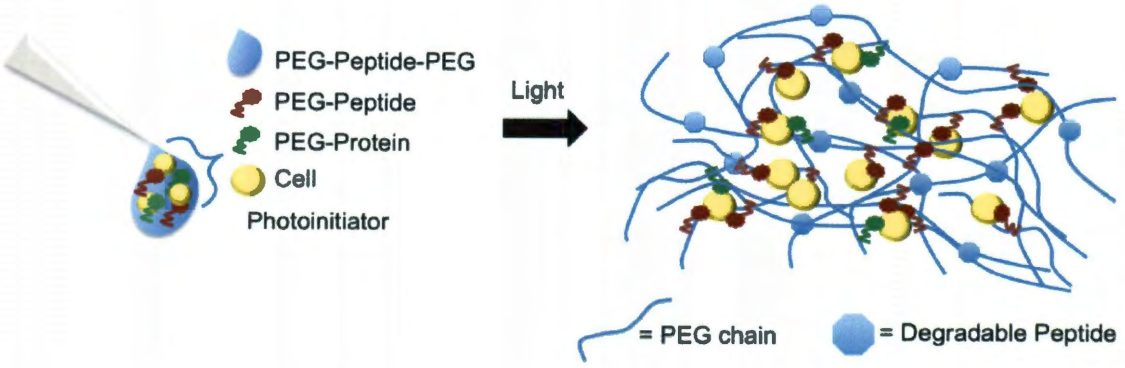

Figure 2.3: General schematic for encapsulation of cells within a bioactive, proteolytically degradable PEG hydrogel

2.1.3 Hydrogel Wells for Stem Cell Culture

Culturing cells within hydrogel wells is advantageous for HSC culture because it allows the cells to be contained. HSCs are highly mobile and during *in vitro* culture will migrate significantly (127, 128). In previous work, PEG hydrogel wells were developed for the culture of various types of stem cells (Figure 2.4). Moeller *et al.* and Karp *et al.* fabricated hydrogel microwells for the culture of embryoid bodies from embryonic stem cells and were able to obtain more homogenous differentiation (184, 185). Jongpaiboonkit *et al.* cultured encapsulated mesenchymal stem cells within wells of a PEG hydrogel microarray to simplify the analysis of material properties on MSC viability (186). In these studies, researchers used the hydrogels as a way to contain cells or gels containing encapsulated cells, and microarrays of hydrogel wells were utilized for high-throughput processing and/or analysis. The gel wells in these studies did not contain bioactive elements and thus, on their own, would not be applicable for HSC culture.

However, they do utilize a base PEG-DA hydrogel system, which can easily be functionalized with bioactive molecules as aforementioned, particularly peptides and proteins critical in HSC function.

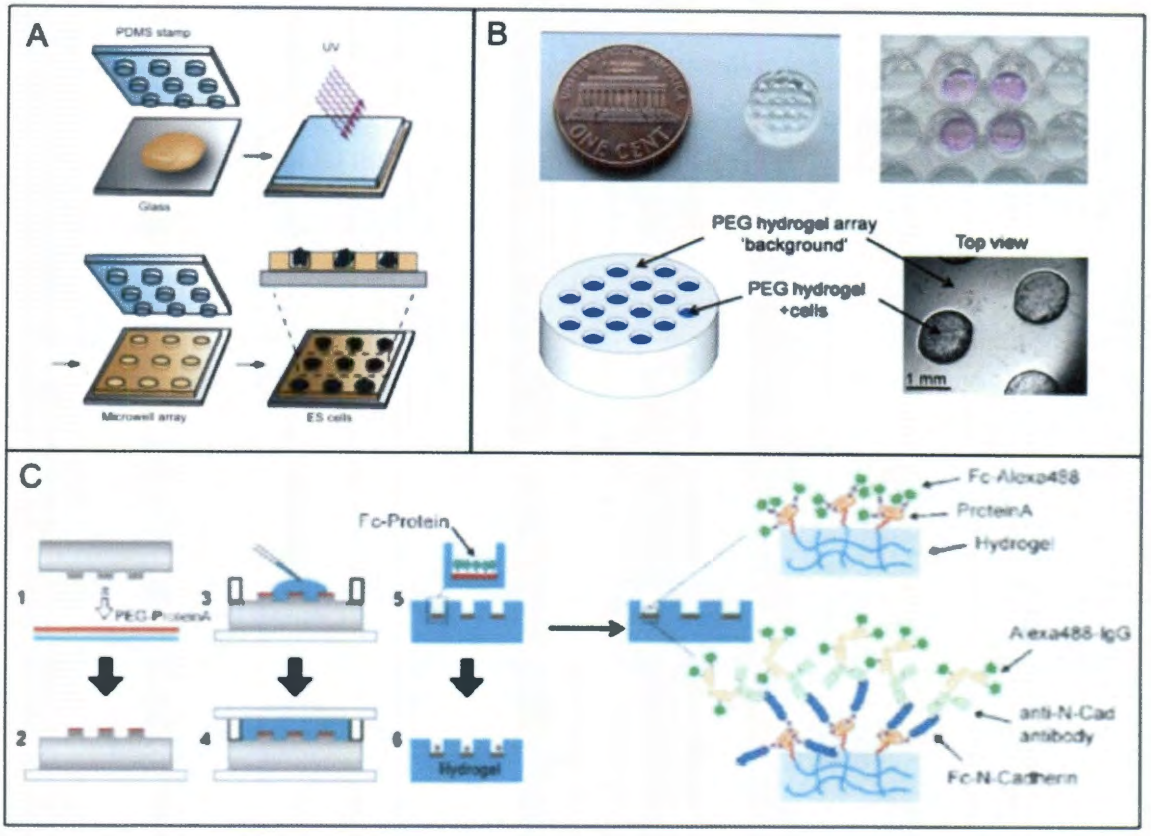

Figure 2.4: PEG hydrogel well fabrication techniques. A. Karp *et al.* molded a poly(dimethylsiloxane) (PDMS) stamp against the prepolymer solution (yellow) and crosslinked with UV light to create microarrays for embryonic stem cell culture. Image adapted from (184). B. Jongpaiboonkit *et al.* used a Teflon mold to create PEG wells to evaluate the effects of different material properties on the viability of encapsulated mesenchymal stem cells. Image adapted from (186). C. Lutolf *et al.* inked a PDMS stamp with PEG-ProteinA and then used this as a mold to create hydrogel wells whose surfaces were functionalized with ProteinA. ProteinA was then reacted with different proteins (to which it has a high binding affinity) such as the chimeric protein Fc-N-Cadherin. The surface proteins were visualized by tagging first with primary antibodies and secondly with fluorescent secondary antibodies. Image adapted from (127).

Lutolf *et al.* demonstrated the ability to functionalize hydrogel well surfaces for the study the effects of specific molecules on single HSC proliferation kinetics. Figure 2.4C shows a schematic of this work. The ability to control the spatial presentation of biomolecules is critical in containing HSCs in the well. When hydrogel wells were

functionalized with bioactive molecules throughout their bulk, HSCs were able to migrate up the gel walls (32, 127). By only functionalizing the surfaces of the gel wells, cells are unable to attach to the PEG-DA gel walls and leave the gel surface. This helps to maintain the interactions between HSC surface receptors and molecules presented on the gel surface.

One disadvantage of the system described by Kobel *et al.* and Lutolf *et al.* is the chemistry that is utilized (127, 128). Their systems use Michael-type addition to crosslink the polymer. In this application, Michael-type addition works well, but the translation to 3D necessitates a polymerization process that is more rapid to ensure that encapsulated cells are homogenously distributed throughout the matrix (187). Photopolymerization not only offers a way to quickly form covalently bonded hydrogels, but the use of light in the crosslinking process also allows patterning in two- and three-dimensions (176-180). This could prove critical in controlling the spatial presentation of specific adhesive ligands or niche proteins to HSCs.

In addition, this system investigated the proliferation of single cells; the wells were used as a tool to gain a better understanding of the kinetics of HSC proliferation and the effects of cell division on engraftment potential. Knowledge gained from the system will benefit the design of future culture systems and could potentially be used in the scale-up of this particular system. However, in its current form, the cells wells are too small to be plausible for generating the large populations of HSCs that are required for therapeutic applications.

The system described in this thesis modifies the hydrogel well work performed by Lutolf *et al.* and Kobel *et al.* In place of Michael-type addition, hydrogels were

crosslinked using photopolymerization due to the advantages described previously. The inert PEG-DA hydrogel was modified with several biomolecules that are present in the niche and known to affect HSC behavior: RGDS and CS1 (Chapter 2), SCF (Chapter 3), SDF1α (Chapter 4), JAG1 (Chapter 5), and IFNγ (Chapter 6). Proteolytically degradable PEG hydrogels were also used for three-dimensional culture of HSCs, which will be discussed in greater detail in Chapter 7. The use of PEG hydrogels that are easily tunable allows precise control of the mechanical, chemical, and biological properties of the gel.

2.1.4 Fibronectin-derived Adhesive Peptide Sequences: RGD and CS1

Work in the current chapter focuses on the covalent incorporation of short adhesive peptide sequences onto hydrogel well surfaces. One of the key regulators of HSCs in the niche is adhesion to ECM proteins, specifically fibronectin (FN). These interactions are not only important in cell adhesion and spreading but are also implicated in many signaling pathways within the cells, such as hematopoiesis and proliferation (122, 125, 188, 189). As HSCs differentiate they lose their ability to bind to FN (122). *In vitro*, HSC adhesion to FN has proven critical in maintaining the regenerative capabilities of HSCs during expansion (121, 190, 191). Additionally, Feng *et al.* demonstrated that FN that was covalently immobilized onto a poly(ethylene terephthalate) (PET) scaffold, as opposed to adsorbed onto the scaffold, resulted in increased HSC expansion (129).

HSCs adhere to FN through several cell surface integrins. The VLA-5 (very late antigen-5, α5β1) integrin binds to the minimal essential amino acid sequence, RGD, of FN, and the VLA-4 (very late antigen-4, α4β1) integrin binds to the CS-1 (LDV) segment of FN (192-194). These short peptide sequences can be utilized *in vitro* to mimic whole

FN. HSCs adhere differentially to various portions of FN. It is thought that more primitive hematopoietic cells bind to the CS1 portion of FN and less significantly to the RGD segment (125). Studies have been contradictory on which section is important for the growth of hematopoietic cells in culture, and both CS1 and RGDS have been used to trigger HSC proliferation (122, 191).

Cyclic forms of the RGD and CS1 peptides have been used in solid lipid monolayers to successfully promote the adhesion of hematopoietic progenitor cell lines (194, 195). RGD and CS1 have also been tethered to PEGylated glass surfaces, via avidin-biotin binding, and have succeeded in promoting hematopoietic cell adhesion (188). When conjugated to PET substrates, RGD and CS1 promoted the expansion of hematopoietic cells (125).

2.1.5 Selection of Hematopoietic Cells

To evaluate the effects of the peptide sequences on adhesion, proliferation, and differentiation, two different cell types were utilized. Various parameters of the hydrogel system were optimized through the culture of 32D Clone 3 (32D) cells on the gel surfaces. 32D cells are a semi-adherent, IL-3 dependent, myeloid progenitor cell line conventionally used to study the effects of knocking down specific genes on hematopoietic cell function. With these cells, we assessed cell adhesion, spreading, and proliferation.

Primary murine HSC populations were also cultured within hydrogel wells. A c-kit$^+$, lineage marker negative (lin$^-$) population of whole bone marrow was magnetically isolated. This population was selected as a derivation of the KSL (c-kit$^+$, Sca1$^+$, lin$^-$) population. As aforementioned, the KSL population is a heterogeneous population of

hematopoietic stem and progenitor cells containing a significant number of LT-HSCs that are capable of reconstitution (39, 40). In fact, 100 KSL cells are capable of repopulating a lethally irradiated host (196). The reason for selecting only two of the markers was primarily to allow for manual sorting within a sterile laminar flow hood. The c-kit$^+$, lin$^-$ selection also resulted in the collection of several million cells enabling us to evaluate a broad array of hydrogel and culture parameters easily. Though this population contains a heterogeneous mixture of cells and limited numbers of LT-HSCs, critical information regarding HSC self-renewal and differentiation can still be revealed from the culture of these cells. In addition, through the inclusion of biomolecules specific to the niche onto the hydrogel surface more primitive HSC populations can potentially be selected for, and it is possible that placing progenitors into the synthetic hydrogel niche could promote them to return to a less differentiated state (60, 61). The presence of more differentiated cell types in the culture system should not hinder the repopulation capabilities of LT-HSCs as whole bone marrow is typically used in bone marrow transplants. However, there is a concern that more differentiated cell types may overtake the culture, and thus, critical analysis of the expanded cells is necessary.

2.2 Materials and Methods

All materials were obtained from Sigma unless otherwise noted.

2.2.1 Polymer Synthesis and Characterization

2.2.1.1 PEG-DA

Poly(ethylene glycol) diacrylate was synthesized by reacting 6 kDa poly(ethylene glycol) (PEG) (Fluka) with acryloyl chloride at a molar ratio of 4:1 (PEG:acryloyl chloride) and triethylamine (TEA) at a molar ratio of 2:1 (PEG:TEA) in anhydrous dichloromethane (DCM) to acrylate both ends of the PEG chains (Figure 2.5). The

resulting product was then rinsed with K_2CO_3 and phase separated overnight to remove hydrochloric acid. The organic layer containing the PEG-DA was collected and dried with $MgSO_4$. The PEG-DA solution (in DCM) was rotary evaporated, and then PEG-DA was precipitated in diethyl ether. The precipitate was filtered and lyophilized. A sample of the resultant polymer was dissolved in chloroform, and acrylation was confirmed with proton nuclear magnetic resonance analysis.

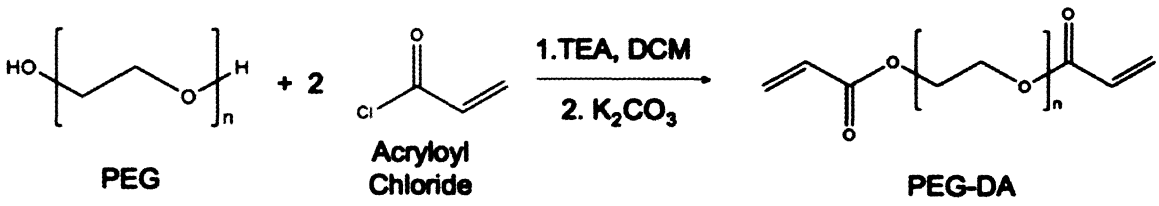

Figure 2.5: PEG-Diacrylate synthesis Poly(ethylene glycol) is reacted with acryloyl chloride and TEA in DCM. The reaction solution is subsequently phase separated in K_2CO_3, dried, and precipitated in diethyl ether. The final product is lyophilized and stored at -20 °C

2.2.1.2 PEG-RGDS for 32D Cell Studies

For studies with 32D cells, 3400 MW acrylate PEG-succinimidyl carboxymethyl (PEG-SCM, Laysan, Arab, AL) was reacted with RGDS peptide (American Peptide, Sunnyvale, CA) at a molar ratio of 1:1.1 (PEG-SCM:RGDS) with diisopropylethylamine (DIPEA) at a 1:2 molar ratio (PEG-SCM:DIPEA) in dimethylsulfoxide (DMSO) overnight at 4°C (Figure 2.6). The resulting product was purified by dialysis and lyophilized. The conjugation was verified using gel permeation chromatography (GPC).

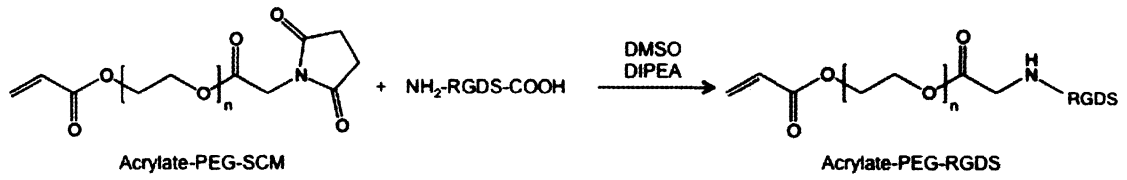

Figure 2.6: PEG-RGDS synthesis. RGDS was reacted with Acrylate-PEG-SCM overnight in DMSO to form a heterobifunctional PEG chain with an acrylate group on one end and a bioactive peptide sequence, RGDS, at the other end.

2.2.1.3 PEG-RGDS and PEG-CS1 (PEG-LDV) for Primary Cell Studies

An alternative PEG derivative was used to PEGylate RGDS and CS1 in experiments conducted with primary cells. 3400 MW Acrylate PEG-Succinimidyl valerate (PEG-SVA, Laysan) was reacted with the RGDS or CS1 (EI**LDV**PST) peptides (American Peptide) at molar ratios of 1.1:1 (PEG-SVA:Peptide) (Figure 2.7). The reactions were performed in phosphate buffered saline (PBS) overnight at 4°C while maintaining the pH at 8.0. The next day the pH was restored to 7.4, and the solution was dialyzed against milliQ water to remove unconjugated peptide. The solution was then lyophilized and stored at -80°C. The conjugation efficiency was quantified with GPC.

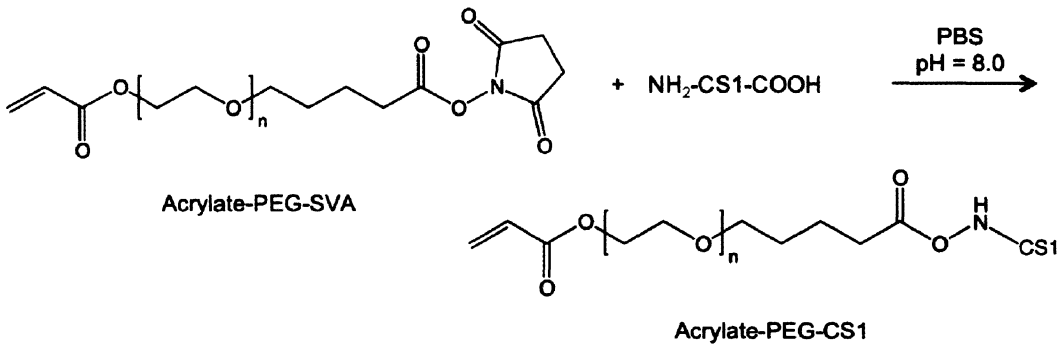

Figure 2.7: PEG-CS1 synthesis. The peptide sequence EILDVPST (the CS1 portion of fibronectin) was reacted with Acrylate PEG-SVA in PBS at pH 8.0 to form PEG-CS1. The carbon molecule spacers between the PEG chain and the reactive SVA group slow reaction with water in the aqueous buffer. The same reaction can be performed with the RGDS peptide sequence.

2.2.2 PEG Hydrogel Wells

2.2.2.1 Fabrication of PEG-DA Hydrogel Wells

To form PEG-DA hydrogel wells, microfabrication techniques were used to create photoresist pillars as previously described (197). Briefly, SU-8 2100 photoresist (Microchem, Newton, MA) was spincoated onto Piranha (7:3 v/v solution of H_2SO_4: 30% H_2O_2) etched glass slides. The photoresist was then exposed through a high-resolution (20,000 dpi) transparency mask (CAD/Art Services, Bandon OR) using a Mask Aligner

(SUSS, Garching, Germany). The resulting photoresist masters had 500 μm high pillars with pillar diameters of 5.34 mm.

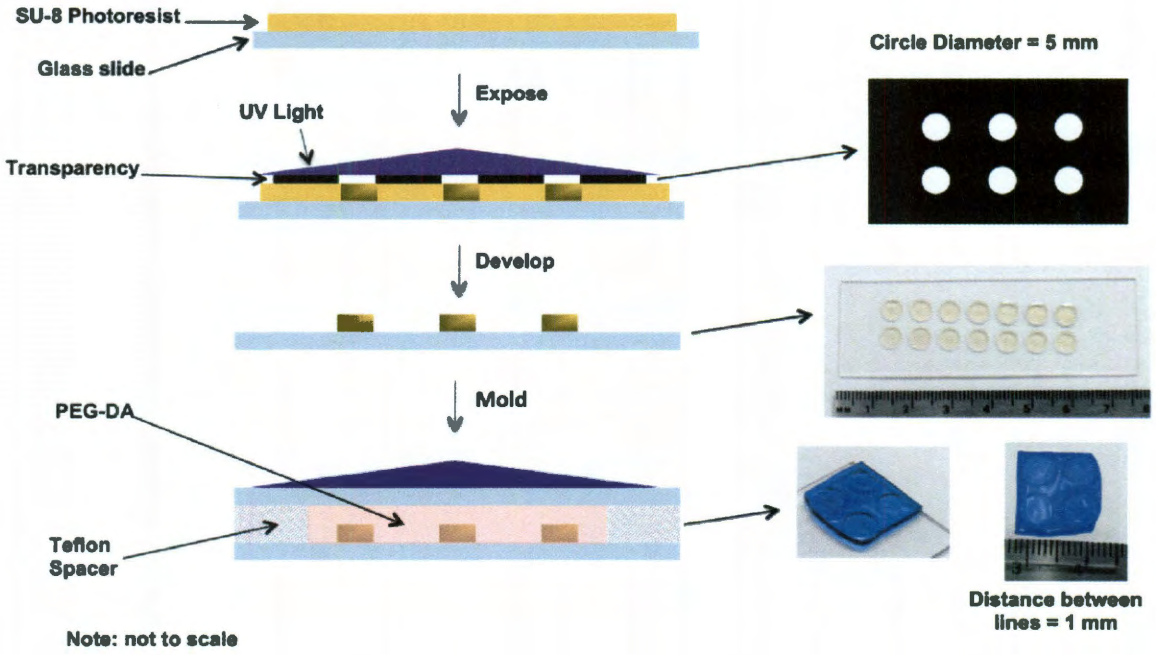

Figure 2.8: Microfabrication of PEG-DA hydrogel wells. To generate PEG-DA wells, SU-8 2100 photoresist was spincoated onto glass slides. The photoresist slab was then exposed with UV light through a high-resolution photomask. After removing the unexposed photoresist, PEG-DA was molded between two glass slides, one containing SU-8 pillars, separated by a Teflon spacer to generate PEG-DA wells.

To form hydrogel wells, PEG-DA was dissolved in HEPES buffered saline (HBS) (10% w/v) at pH 7.4, and the photoinitiator 2,2-dimethoxy-2-phenyl acetophenone (300 mg/ml in *n*-vinylpyrrolidone, NVP) was added to the polymer solution at 10 μl/ml. The PEG solution was then filtered in a laminar flow hood using a poly(ether sulfone) (PES) 0.22 μm syringe filter. The polymer solution was placed into a mold consisting of two glass slides coated with SigmaCote, one with SU-8 pillars, separated with a 1 mm PTFE spacer and clamped together. The polymer was crosslinked using long wavelength UV light (365 nm, 10 mW/cm^2) for 45 s/3.75 cm^2 creating a PEG-DA base hydrogel with wells. A schematic of the process can be seen in Figure 2.8 (not to scale).

2.2.2.2 Surface Conjugation of Hydrogel Wells with PEG-Peptides

PEG-DA hydrogel wells were soaked in sterile PBS with 0.1% NaN_3 overnight to allow for swelling and maintain sterility. A PEG-RGDS solution containing 10 µl/ml acetophenone was added to each hydrogel well to achieve a concentration of 250 µg/cm^2. A gel containing 4 wells was exposed to UV light for three min. (Figure 2.9). After UV exposure, gels were placed in well plates with sterile PBS containing 0.1% NaN_3. This process was repeated for each concentration of PEG-RGDS (2.5 and 25 µg/cm^2) and PEG-CS1 (25 µg/cm^2). To remove any NaN_3 before cell seeding, gels were soaked twice in fresh PBS for one hr. at 37°C. Gels were subsequently soaked in media for 1 hr. at 37°C to prepare them for cell seeding.

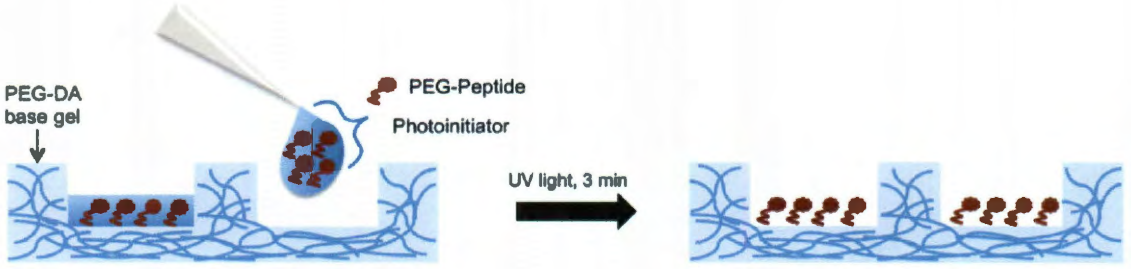

Figure 2.9: Surface conjugation of hydrogel wells. A solution of PEG-peptide and photoinitiator was made and added to wells (10 µl). Groups of four gel wells were than exposed to UV light for 3 min. The resulting gel was soaked in PBS with NaN_3 overnight to prevent contamination and allow diffusion of free peptide from the gel surface.

2.2.2.3 Quantification of Peptide Concentration on Gel Surfaces

To determine the efficiency of the surface conjugation reaction (i.e. the percentage of peptide that is successfully immobilized on the gel surface), a ninhydrin assay was conducted as previously described (179). Briefly, PEG-RGDS (synthesized with PEG-SVA) was conjugated to hydrogel well surfaces. A standard curve was created using known concentrations of PEG-RGDS in solution and PEG-DA gel wells. Individual gel wells were then degraded in 6 M HCl for 3 hrs. at 150°C. Samples were

rotary evaporated and subsequently lyophilized to remove the acid. Dry samples were dissolved in 0.1 M sodium citrate buffer (pH 5.0), and the ninhydrin reagent was added. Samples were boiled for 15 min., and absorbance was read at 570 nm.

2.2.3 Cell Maintenance

2.2.3.1 32D Cell Culture

Murine 32D clone 3 cells (32D cells, ATCC, Manassas, VA) were cultured in RPMI-1640 media (Invitrogen, Carlsbad, CA) supplemented with 2 mM L-glutamine, 10% IL-3 culture supplement (Becton Dickinson, Franklin Lakes, NJ), 10% heat-inactivated fetal bovine serum (FBS), 100 U/L penicillin, and 100 mg/L streptomycin. Cells were maintained at 37 °C at 5% CO_2. Media was refreshed every 2 to 3 days, and cells were subcultured when they reached a concentration of 1 million cells/ml.

2.2.3.2 Isolation and Culture of Murine c-kit$^+$, lin$^-$ Cells

C57/B6 mouse strains were bred and maintained at Baylor College of Medicine. The Institutional Animal Care and Use Committee (IACUC) of BCM approved all experiments using animals. To obtain murine bone marrow, 8-12 week old C57/B6 mice were sacrificed by isofluorene exposure followed by cervical dislocation. The femurs and tibias were removed and maintained in cold HBSS+ medium (HBSS, 10 mM HEPES, 2% FBS). The ends of bones were cut to expose the bone marrow cavity, which was flushed with DMEM+ medium (DMEM, 10 mM HEPES, 2% FBS) into 50 ml conical tubes using a 26 G needle equipped syringe. To eliminate tissue debris, the solution was filtered through a 40 μm nylon cell strainer (BD) and centrifuged at 200 x g for 8 min. at 4°C. To lyse red blood cells, the pellet was resuspended in 5 ml PharMlyse (BD) diluted

1:10 in DIH_2O and incubated 5 min. at room temperature. Cells were counted using a hemacytometer.

The whole bone marrow cells were then centrifuged for 5 min. at 200 x g and resuspended in recommended media (PBS containing 2% FBS, 1 mM ethylenediaminetetraacetic acid (EDTA), and 1% Gentomycin-Amphotericin (GA, Invitrogen)) at a concentration of $1x10^8$ cells/ml. Cells were then negatively sorted magnetically with the mouse hematopoietic progenitor cell enrichment kit as per the manufacturer's protocol (StemCell Technologies, Vancouver, BC, Canada). The collected cells (lineage negative) were then counted, centrifuged at 200 x g for 5 min., and resuspended in recommended media at a concentration of $1x10^8$ cells/ml. Cells were then positively sorted magnetically with the CD117/c-kit positive selection kit as per the manufacturer's protocol (StemCell Technologies). After the final magnetic sort, c-kit^+, lin^- cells were resuspended in StemSpan media (Stem Cell Technologies) supplemented with 50 ng/ml stem cell factor (R&D, Minneapolis, MN) and 1% GA. A portion of these cells as well as a portion of the c-kit^-, lin^- population were set aside and stained for flow cytometry analysis.

The reserved cells were centrifuged and resuspended in fluorescence activated cell sorting (FACS) buffer (PBS containing 1% bovine serum albumin, and 0.1% NaN_3) at a concentration of $1x10^6$ cells/ml. They were subsequently stained with fluorescently tagged primary antibodies for one hr. at 4°C: rat anti-mouse Sca1 (tagged with fluorescein isothiocyanate, FITC) (Abcam) at a concentration of 2 µl/10^6 cells and rat-anti mouse lineage marker cocktail (allophycocyanin, APC) (BD) at a concentration of 20 µl/10^6 million cells. Since the antibody staining occurred immediately following the

magnetic sort, c-kit positive cells should still possess their magnetic nanoparticle tag, which also contains a fluorescent phycoerythrin (PE) label. Cells were washed twice with FACS buffer by centrifugation for 10 min. at 200 x g at 4°C. Cells were then fixed in 4% paraformaldehyde in PBS for 15 min. at room temperature. Cells were centrifuged for 5 min. at 200 x g at room temperature and resuspended in cold PBS at a concentration of 10^6 cells/ml. The stained cells were stored at 4°C protected from light until analysis. A control group of cells from each population underwent the same process except for the antibody staining.

2.2.3.3 Cell Seeding into Hydrogel Wells

32D cells were seeded into the hydrogel wells at 5000 cells/cm^2. The experimental groups consisted of wells with 2.5, 25, and 250 μg/cm^2 RGDS. PEG-DA wells (0 μg/cm^2 RGDS) served as controls. Each group consisted of 4 gel wells. Cells within hydrogel wells were maintained in culture for 6 days at 37°C with 5% CO_2.

c-kit$^+$, lin$^-$ cells were seeded in gel wells ([RGDS]=25 μg/cm^2 or [CS1]=25 μg/cm^2) at 13,000 cells/cm^2. PEG-DA gel wells with (0 μg/cm^2 RGDS) and a 96-well FN plate served as controls. Each group consisted of 4 gel wells. Media was added around gels to keep them hydrated. Cells within hydrogel wells were maintained in culture for 14 days at 37°C with 5% CO_2 with changes of media every 2-3 days. Media was removed by vacuum aspiration around the gel but not within the gel well while the plate was kept flat. 250 μl of media was added to the plate by gently pipetting 1 drop of media into the gel well and adding the rest around the gel well. In the FN plates, 50 μl of media was removed and 75 μl of media was added to each well. After culture, the cells

from each group were combined so that enough cells were available for flow cytometry. The experiment was conducted a total of three times.

2.2.4 Evaluation of Hematopoietic Cells in Culture

2.2.4.1 Evaluation of 32D Cell Adhesion

Cell adhesion is a critical process in the HSC microenvironment. HSCs use cell surface integrins to lodge in the niche and retain their differentiation potential. To evaluate 32D cell adhesion, gels were rinsed by the addition of fresh media after 48 hrs. in culture to eliminate non-adherent cells. Nine phase contrast images of each well were captured using a Zeiss Axiovert 135 inverted microscope (Zeiss, Oberkochen, Germany) and Jenoptik ProgRes C5 charge-coupled device (CCD) camera (Jenoptik, Jena, Germany). Eight hydrogel wells made up each group: three surface concentrations of RGDS (2.5, 25, and 250 $\mu g/cm^2$) and a PEG-DA control. Cells were counted using ImageJ software (NIH, Bethesda, MD). Images were first changed to 8-bit, and the "find edges" function was used to outline the cell perimeters. The images were then thresholded individually to highlight the cells, and the "analyze particle" feature was run to count cells larger than 100 pixels. Images were thresholded individually due to the varying degree of background resulting from the PEG gels.

2.2.4.2 Evaluation of 32D Cell Spreading

To determine the effects of RGDS on 32D cell spreading, cells were fixed with 4% paraformaldehyde, permeabilized with 0.1% Triton-X, and blocked in PBS containing 1% bovine serum albumin after 6 days in culture. Cells were then stained with Alexa-Fluor 488 phalloidin (Invitrogen), which stains actin filaments, and counterstained with DAPI, which stains cell nuclei. The stained cells were imaged using

epifluorescent microscopy on a Zeiss Axiovert 135 inverted microscope equipped with an EXFO X-Cite 120 Fluorescent Illumination System (EXFO, Quebec, Canada) and a Jenoptik ProgRes C5 CCD camera. Cell size was determined using the phalloidin images and ImageJ software. The image processing followed the same steps as when counting the cells except the "close edges" and "fill holes" functions were employed prior to the "analyze particles" function to ensure that all of the pixels were counted when determining cell size. Cell nuclei were used to locate cells, and the "skeletonize" tool was used to distinguish individual cells when cells were in contact or overlapped. Five images from each hydrogel well were analyzed and each group contained eight gel wells. The number of cells per image varied due to differences in 32D cell adhesion.

2.2.4.3 Evaluation of Hematopoietic Cell Expansion

32D cells in the phase images were counted using ImageJ software to determine the total cell number in hydrogel wells after 2, 4, and 6 days in culture. The percent change in cell number over 48 hrs. was calculated for each well by comparing the cell number at days 4 and 6 to days 2 and 4 respectively. 9 images were counted per well, and each group contained 8 gel wells.

To monitor c-kit$^+$, lin$^-$ cell growth and morphology, images were taken every 48 hrs. Expansion was determined after 14 days by removing cells from the surfaces of the hydrogel or FN plates by rinsing each well 20 times with media. Cells were then counted with a hemacytometer. Four wells composed each group during each experiment. These four wells were combined for analysis purposes, due to time restraints and the requirement of large populations for flow cytometry. The experiment was conducted a total of three times.

2.2.4.4 Colony Forming Unit Assay

To evaluate the functional potential of expanded c-kit$^+$, lin$^-$ cells to differentiate down multiple lineages, a colony forming unit (CFU) assay was performed. 10,000 cells from each surface were resuspended in 1 ml of methylcellulose media (MCM) supplemented with erythropoietin, IL-3, IL-6, and stem cell factor (Stem Cell Technologies) as well as 1% GA to prevent contamination. The MCM containing cells was pipetted into 48-well non-tissue culture treated plates. Empty wells were filled with milliQ water to prevent dehydration of the MCM. The plates were kept in an incubator at 37°C and 5% CO_2, and colonies were counted, characterized, and imaged after 10-14 days in culture. Figure A1 in the Appendix contains images and brief descriptions of each type of colony that was counted. Throughout the incubation period, MCM was added to wells that were beginning to dry out or wells that were consuming media rapidly. Due to extensive dehydration during one experiment, the results of the CFU assay are from two studies.

2.2.4.5 Flow Cytometry Analysis

To determine the expression of primitive cell surface markers on expanded cell populations, the remaining cells from the gel surfaces and plates were stained for flow cytometry as described previously in Section 2.2.2.2. They were also stained with a rat anti-mouse c-kit antibody (tagged with PE) in addition to the Sca1 and lineage marker antibodies. According to the manufacturer, StemCell Technologies, the magnetic nanoparticle should be purged from the cell surface due to antigen renewal within 1-2 days of sorting. Cells were washed twice with 1 ml of FACS buffer by centrifugation for 10 min. at 200 x g at 4°C. Cells were then fixed in 4% paraformaldehyde in PBS for 15

min. at room temperature. Cells were centrifuged for 5 min. at 200 x g at room temperature and resuspended in cold PBS at a concentration of 1 million cells/ml. The stained cells were stored at 4°C until analysis. A group of cells obtained from a flask underwent the same process except for the antibody staining to serve as a control. The purpose of this control was to determine the level of fluorescent intensity that distinguished between positive and negative antibody staining. This knowledge aided in the set-up of gates on the flow cytometry plots.

Flow cytometry was performed on a BD FACScanto (BD). Positive CompBeads containing an anti-rat IgG antibody and negative CompBeads (BD) were incubated with primary antibodies individually or a control (no antibody) for 20 min., centrifuged for 5 min. at 200 x g, and resuspended in FACS buffer at a concentration of ~1 million beads/ml. These beads served as positive controls and negative controls to determine compensation levels on the machine. Compensation controls ensure that signal from the various fluorophores does not get collected incorrectly. After these controls were evaluated, an unstained cell sample was run to determine where the gates would be set for the various fluorophores. A primary gate was set-up to exclude cell debris and aggregates as well as other contaminants such as dust. A secondary gate was set at low fluorescent intensities for APC to count lineage negative cells. Thirdly, a dot-plot of Sca1 vs. c-kit for the lineage negative population was set up to determine the number of c-kit$^+$, Sca1$^+$, lin$^-$ cells. For each group, 20,000-30,000 cells were counted.

2.2.5 Statistical Analysis

One-way ANOVAs and Tukey's post-hoc analyses were performed to evaluate statistical differences between groups in all studies using a 95% probability level ($p<0.05$).

2.3 Results and Discussion

2.3.1 Polymer Synthesis and Characterization

PEG-DA, PEG-RGDS, and PEG-CS1 were synthesized in the laboratory and characterized using NMR and GPC analysis. According to the NMR data, the degree of acrylation on the PEG-DA chains was >80%. The GPC plots of PEG-RGDS (SCM) and PEG-CS1 (SVA) (Figure 2.10) showed conjugation efficiencies of greater than 90%. This was also observed when using PEG-SVA to synthesize PEG-RGDS. These findings are consistent with previous work in the laboratory.

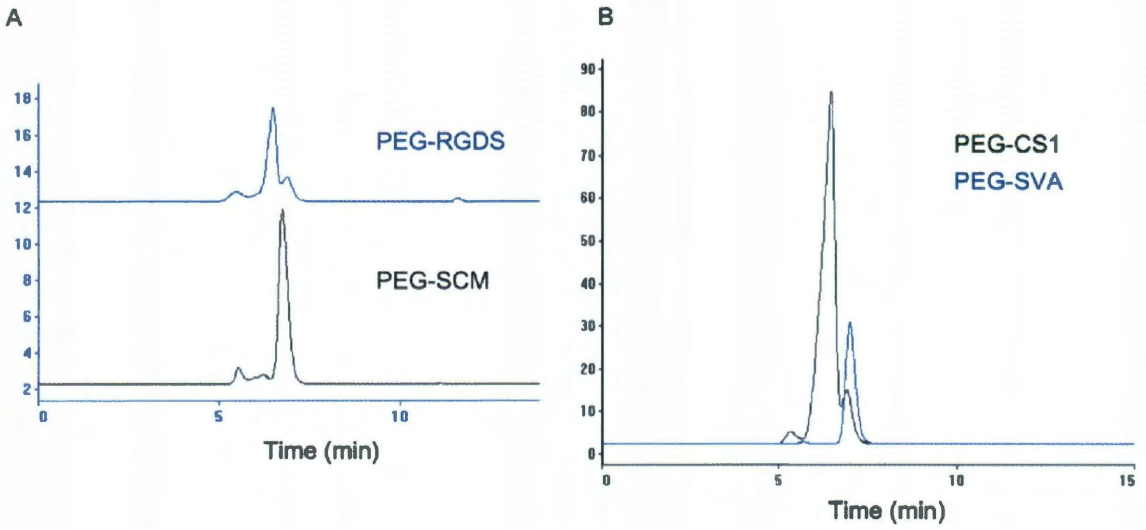

Figure 2.10: GPC plots of PEG-RGDS and PEG-CS1. After conjugation to RGDS (A) or CS1 (B), the peak of the PEG chain shifts left indicating an increase in molecular weight. Larger molecular weight molecules travel more quickly through the column because they are not trapped within the beads packing the column length. The units of the y-axis are relative signal intensity.

The ninhydrin assay determined that 37.7% ± 5.9% of the 500 μg/cm^2 PEG-RGDS, 50.6% ± 21.4% of the 250 μg/cm^2, and 76.1% ± 22.6% of the 125 μg/cm^2 are conjugated to the surfaces of the hydrogel well. As the amount of peptide increased, there was a corresponding decrease in percent conjugation. The same phenomenon has previously been reported (179). This can be attributed to a saturation of the free acrylates on the surface with acrylated peptide. There is a finite area on the gel well and due to steric hindrance, not all molecules that are added to the surface can crosslink into the hydrogel matrix. These results emphasize that the addition of more peptide to the surface does not necessarily lead to an increase in crosslinking to the surface. It was assumed that surface conjugation efficiencies for PEG-CS1 would be of a similar magnitude due to relative similarity in size and amino acid makeup. In the following sections, the groups are distinguished by the initial RGDS concentrations (2.5, 25, and 250 μg/cm^2) to avoid confusion, though the true surface concentrations are approximately 50% of this.

The degree of conjugation is higher than what has previously been reported. Hahn *et al.* observed that only about 10% of the initial peptide concentration was actively immobilized onto gel surfaces (179). This may be due to the fact that previous surface conjugation techniques did not utilize the well system. Instead, hydrogel rectangular slabs were used as the base and a solution of PEG-peptide was added to the entire gel surface. The well system restrains the PEG-peptide solution to a smaller area and allows focusing of the highest intensity UV light across the entire area to be modified. In addition, in previous work a different PEG derivative was utilized to PEGylate the peptides. The differences in the purity or chemistry of the molecules may affect their

abilities to crosslink to the hydrogel surface. These factors may both contribute to the ability to reach higher conjugation efficiencies using this system.

2.3.2 Primary Cell Isolation

To determine the purity of the c-kit$^+$, lin$^-$ immediately following magnetic sorting, a portion of the sorted cells were stained for flow cytometry. Figure 2.11 shows the flow cytometry plots that were generated from these cells. The magnetic sorting resulted in a population in which approximately 70% of the cells were lin$^-$ and 76% were c-kit$^+$. Of the cells that were lin$^-$, an estimated 82% were c-kit$^+$. This number was deemed sufficient for the following studies, but in the future, more washes could be performed to obtain a purer population.

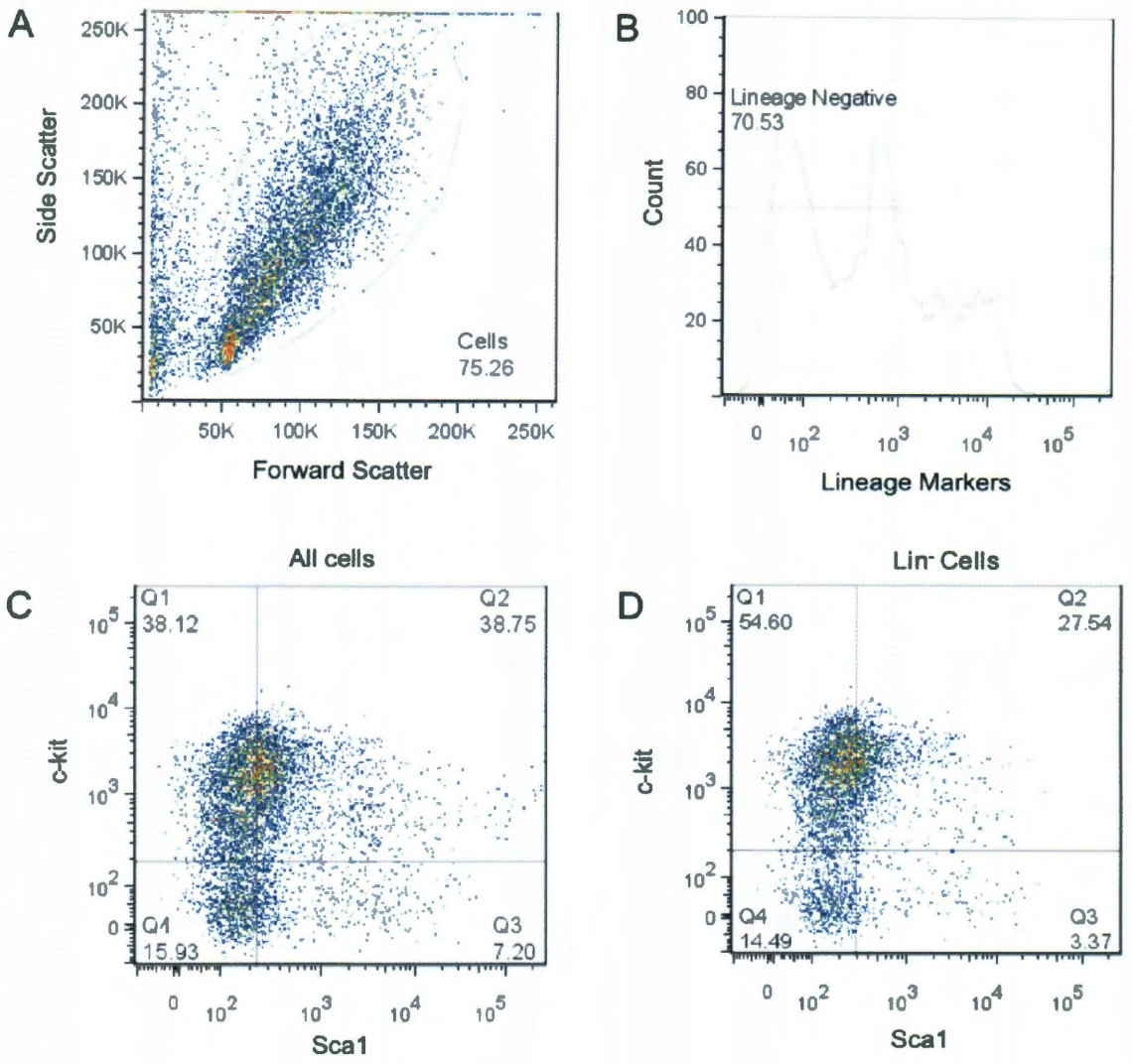

Figure 2.11: Flow cytometry analyses of c-kit$^+$, lin$^-$ cells immediately following magnetic sort. A. Particles were gated to eliminate debris and aggregates. B. Cells were gated to include those that were lin$^-$. C. A plot of all cells showing the fluorescence intensities of the Sca1 and c-kit markers. Cells were gated to delineate between positive and negative cells. D. A plot of lineage negative cells gated similarly to those in C. Numbers on the graphs indicate the percentage of cells falling within that gate. Units on unlabeled axes are relative fluorescent intensity.

2.3.3 32D Cell Adhesion

The adhesion of 32D cells to RGDS functionalized hydrogels was evaluated because adhesive interactions within the HSC niche have been shown to affect HSC fate. Figure 2.12 shows the number of adherent cells on the PEG-RGDS hydrogels after 48

hrs. As the RGDS concentration is increased, there is a corresponding increase in adherent 32D cells. At the low concentration (2.5 μg/cm^2), there was minimal cell adhesion comparable to that seen on PEG-DA hydrogels, indicating that this amount of RGDS is insufficient to enable surface adhesion.

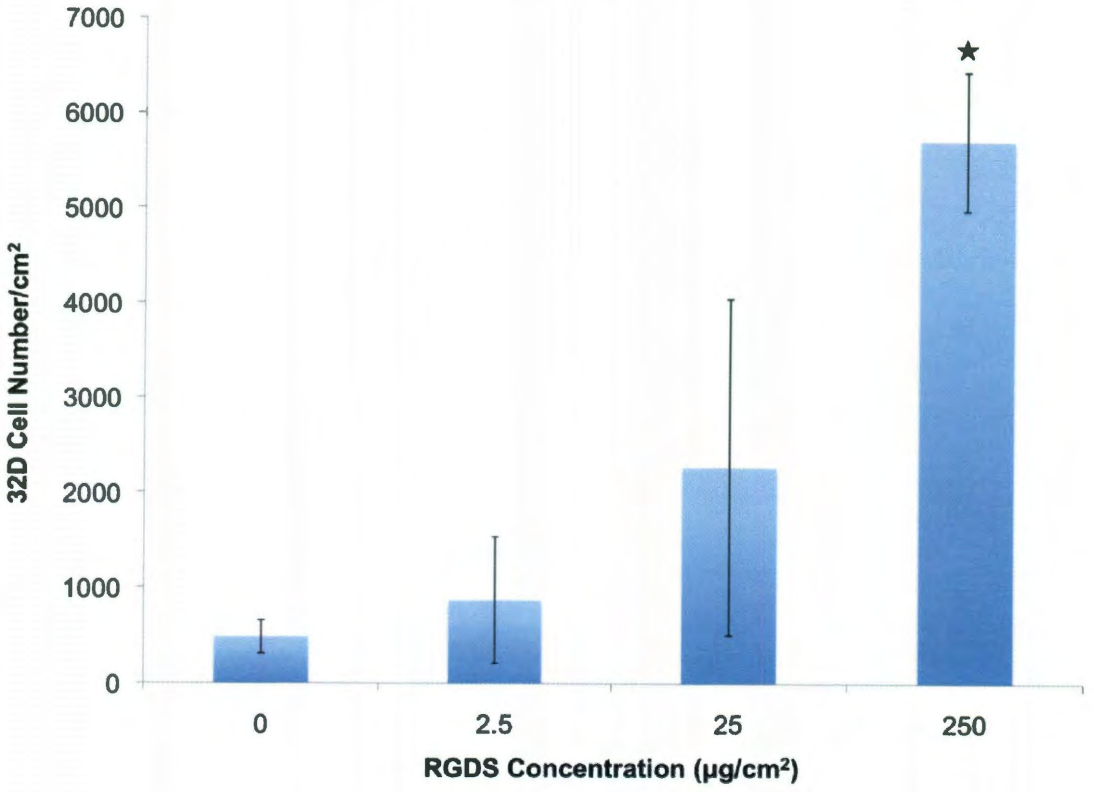

Figure 2.12: 32D cell adhesion on bioactive PEG hydrogels after 48 hrs. 32D cells were cultured on gels with increasing amounts of RGDS on the well surfaces. As the surface concentration of RGDS increased, there was a corresponding, significant increase in adherent 32D cells. Bars represent mean ± standard deviation. (★ denotes significance compared to all other groups, n=4, $p < 0.05$)

At the high concentration of RGDS (250 μg/cm^2), there is a significant increase in cell adhesion compared to all other groups. This suggests that 32D cells require binding to multiple RGDS molecules to adhere to the gel surfaces with enough strength to withstand the rinsing process. When the starting RGDS concentration was raised above 250 μg/cm^2, an increase in 32D cell number was not observed (data not shown). This is

probably due to saturation of the surface with RGDS as described in Section 2.3.1. There are not enough free acrylates to incorporate all of the RGDS molecules, and thus the difference in surface concentrations between a starting solution with 500 $\mu g/cm^2$ of RGDS and that of 1000 $\mu g/cm^2$ is minimal. As a result, cells adhere similarly on these surfaces.

RGDS was selected for incorporation onto the hydrogel surfaces to investigate the ability to mimic the *in vivo* interactions between HSCs and the ECM using the hydrogel system. In the niche, hematopoietic cells express the VLA-5 integrin, which binds specifically to the RGD sequence found in FN. With more available RGD on the surface, more 32Ds were able to bind and individual cells were able to bind to the surface with multiple integrins resulting in an increase in adherent cells on gel surfaces. The same trend has been observed in previous work (171, 198). Chollet *et al.* immobilized cyclic RGDS molecules onto PET surfaces and found that raising the surface RGDS concentration led to augmented endothelial cell and osteoblast adhesion and the production of more focal contacts (198). Gonzalez *et al.* utilized PEG hydrogels with bulk modified RGDS to culture neutrophils and could increase the percentage of neutrophils that adhered to the gel by increasing the RGDS concentration (171). The work in this chapter demonstrates a similar ability to affect hematopoietic cell adhesion by altering the surface RGDS concentration. Adhesive interactions retain cells in the HSC niche and help maintain them in a multipotent state. As cells differentiate they lose the ability to adhere to FN and travel out of the niche to sites of injury (191, 199-202). Thus, the ability to promote cell adhesion to our synthetic niche is critical to the successful expansion of clinically relevant HSCs.

2.3.4 32D Cell Spreading

The morphology of adherent 32D cells was observed and quantified using the fluorescent DAPI/phalloidin images of 32D cells on PEG-RGDS surfaces (Figure 2.13). Qualitatively, the cells do not spread on the gels to a high degree and appear very round in shape, similar to those seen on the unmodified PEG-DA gels. A quantification of this data shows that the average cell area is slightly significantly higher on the medium RGDS concentration (25 $\mu g/cm^2$) compared to all other groups (Figure 2.14), though the total number of cells on the surface after staining was low. The increase in cell size could result from the fact that during the staining process, which has multiple rinse steps, numerous cells were washed from the surfaces. On the medium RGDS concentration, it is likely that only cells that were more spread and attached to the surface with multiple integrins were able to remain on the surface. The standard deviations are large due to the heterogeneity of the 32D cell population. The data can also be plotted as histograms to obtain a better sense of the cell sizes (Figure 2.15). A similar cell size distribution can be seen between the low and high RGDS (250 $\mu g/cm^2$) concentrations with cell sizes clustered between 100-300 μm^2. The medium RGDS concentration (25 $\mu g/cm^2$) is shifted slightly right with cell sizes from 200-400 μm^2, which correlates with the data shown in Figure 2.14.

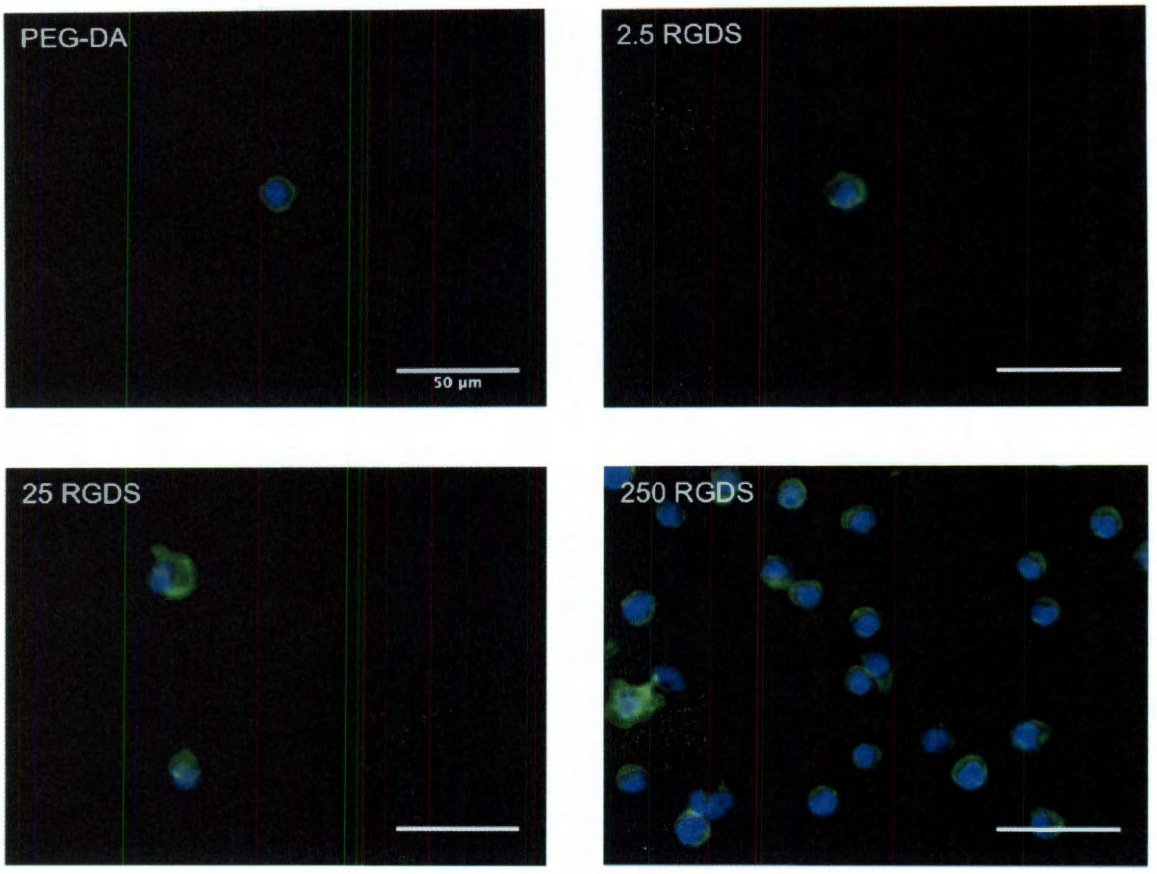

Figure 2.13: 32D cell spreading on RGDS surfaces. The nuclei of cells were stained with DAPI (blue) and the actin filaments with phalloidin (green). Cells did not spread extensively on the surfaces, but on the surfaces with RGDS there is more actin surrounding the cell nuclei. On the high RGDS surfaces some of the cells started to extend filopodia. (Scale bars = 50 µm)

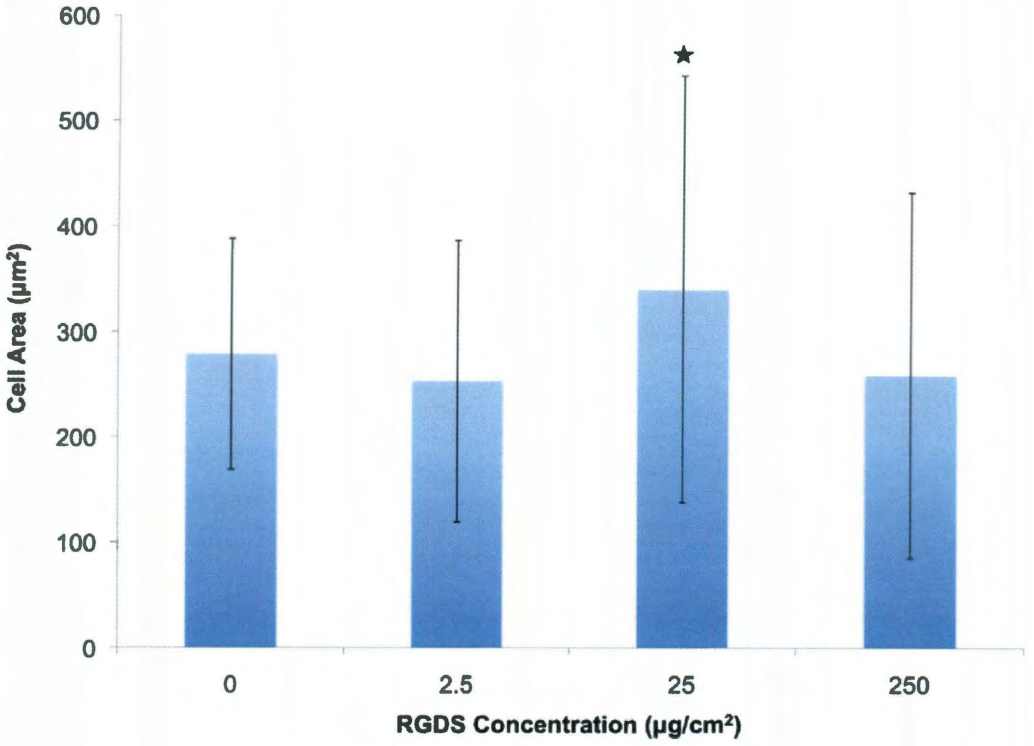

Figure 2.14: 32D cell area on hydrogel surfaces. The average cell size on the hydrogels was significantly higher on gels with 25 μg/cm^2 RGDS, though the total cell number was low. The large standard deviations result from the heterogeneity of the cell population, which is comprised of cells of varying sizes. Bars = mean ± standard deviation. (★ denotes significance compared to all other groups, n= 20 (0 μg/cm^2), 58 (2.5 μg/cm^2), 130 (25 μg/cm^2), 863 (250 μg/cm^2), $p < 0.05$)

In addition, at the medium RGDS concentration, cells were stimulated to proliferate (discussed later) and thus detached from the surface to divide making them particularly vulnerable to being washed away during staining. This is consistent with what was seen on the gel surfaces in terms of the percent change in cell number.

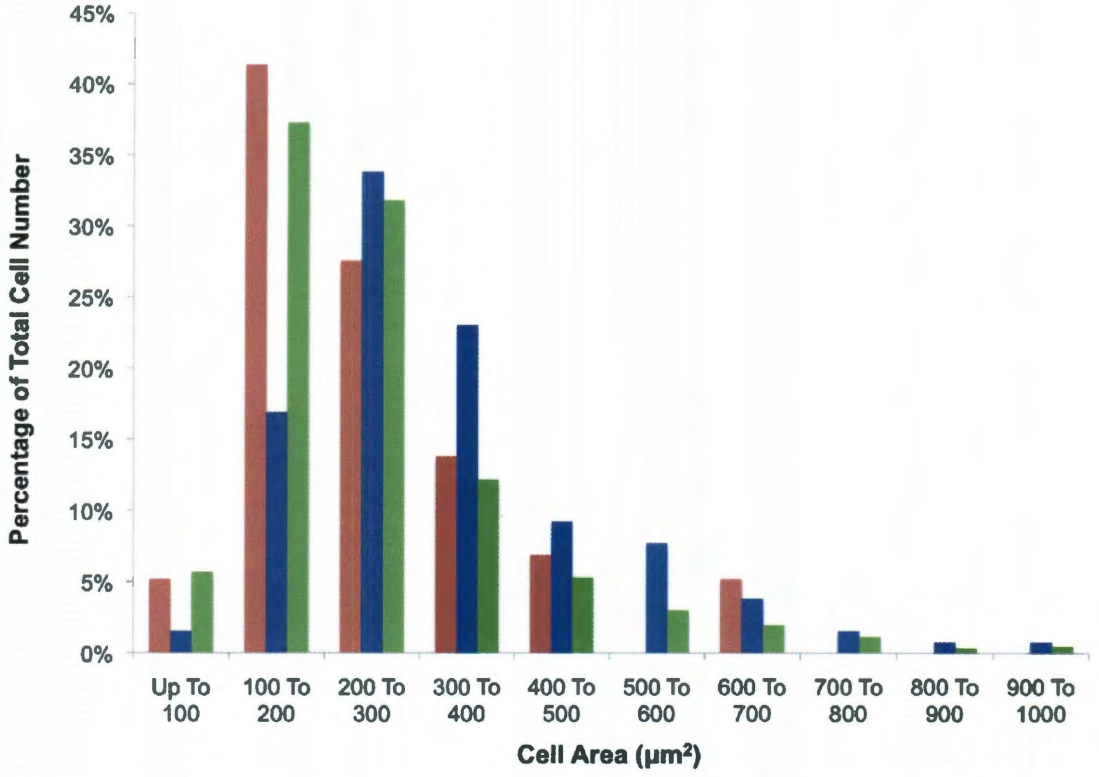

Figure 2.15: 32D cell area distribution on differing surface RGDS concentrations. The cell area profile was fairly consistent on all three RGDS concentrations with most cells in the 100 – 300 μm^2 range. On the medium RGDS concentration, there was a significant shift in cell size of about 100 μm^2 resulting in cells centered around 200 – 400 μm^2. (RGDS concentrations: **2.5 $\mu g/cm^2$**, **25 $\mu g/cm^2$**, **250 $\mu g/cm^2$**)

2.3.5 Hematopoietic Cell Proliferation

The effects of RGDS on 32D cell proliferation were investigated to determine the role the peptide plays in this process. The gels with the high concentration of RGDS (250 $\mu g/cm^2$) had the greatest number of cells after 6 days. However, the percent change in cell number over 48 hrs. is slightly lower, 33 ± 14.5%, than that observed on the medium concentration (25 $\mu g/cm^2$), 48.1 ± 10.2% (Figure 2.16). The percent changes in cell number on PEG-DA and the lowest concentration of RGDS (2.5 $\mu g/cm^2$) are much lower, 16.3 ± 0.6% and 22.8 ± 1.3% respectively. 32D cell adhesion to fibronectin has previously been shown to trigger cell proliferation, and we have shown the ability to

induce this response with the short RGDS peptide at concentrations of 25 μg/cm^2 (124). At the high concentration of RGDS the percent change in cell number drops, but the drop is not significant. Overall, the higher concentrations of RGDS (25 μg/cm^2 and 250 μg/cm^2) promote more cell proliferation than PEG-DA and 2.5 μg/cm^2.

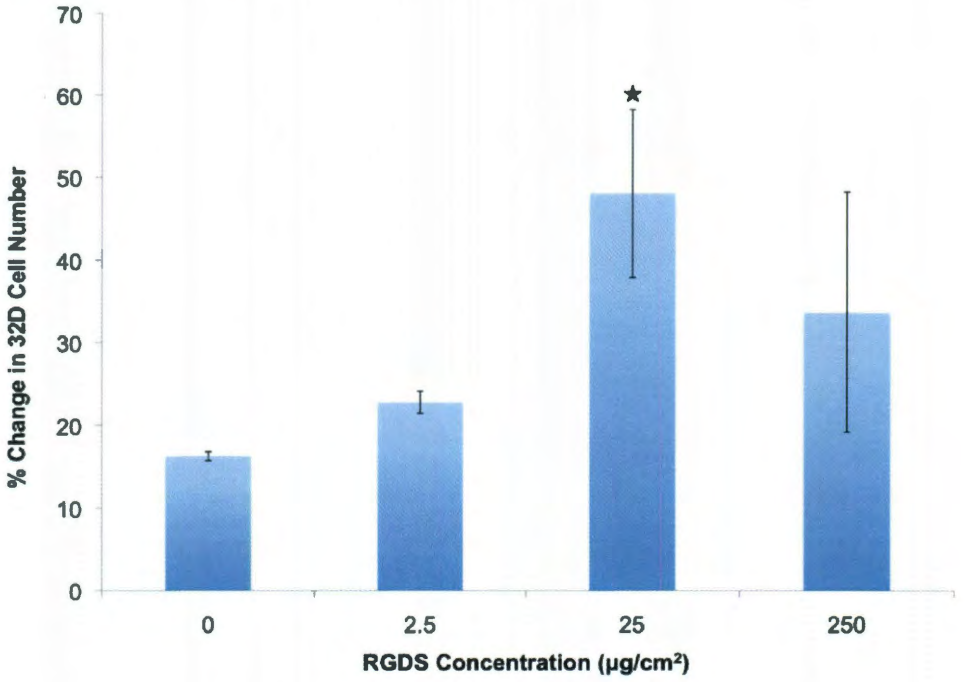

Figure 2.16: Change in 32D cell number over 48 hrs. Cells proliferated at a faster rate on surfaces containing RGDS. The medium concentration of RGDS produced a significantly higher percent increase in cells compared to PEG-DA and the low concentration of RGDS. At high RGDS concentrations (250 μg/cm^2) the change in cell number was greater than on PEG-DA or low concentrations of RGDS but significantly lower than on medium concentrations of RGDS. Bars are mean ± standard deviation. (★ denotes significance compared to PEG-DA and 2.5 μg/cm^2 RGDS, n=4, $p < 0.05$)

As a result, in studies with primary cells, the medium concentration of RGDS (25 μg/cm^2) was used; this concentration was also used for the CS1 peptide. On gels with RGDS and CS1, c-kit$^+$, lin$^-$ cells attached and proliferated. Figure 2.17 shows representative images of wells at varying timepoints. Over time, some of the cells have a definitive change in morphology and size, which may be indicative of differentiation.

Figure 2.18 shows the percent change in cell number on RGDS and CS1 gels compared to PEG-DA and FN controls.

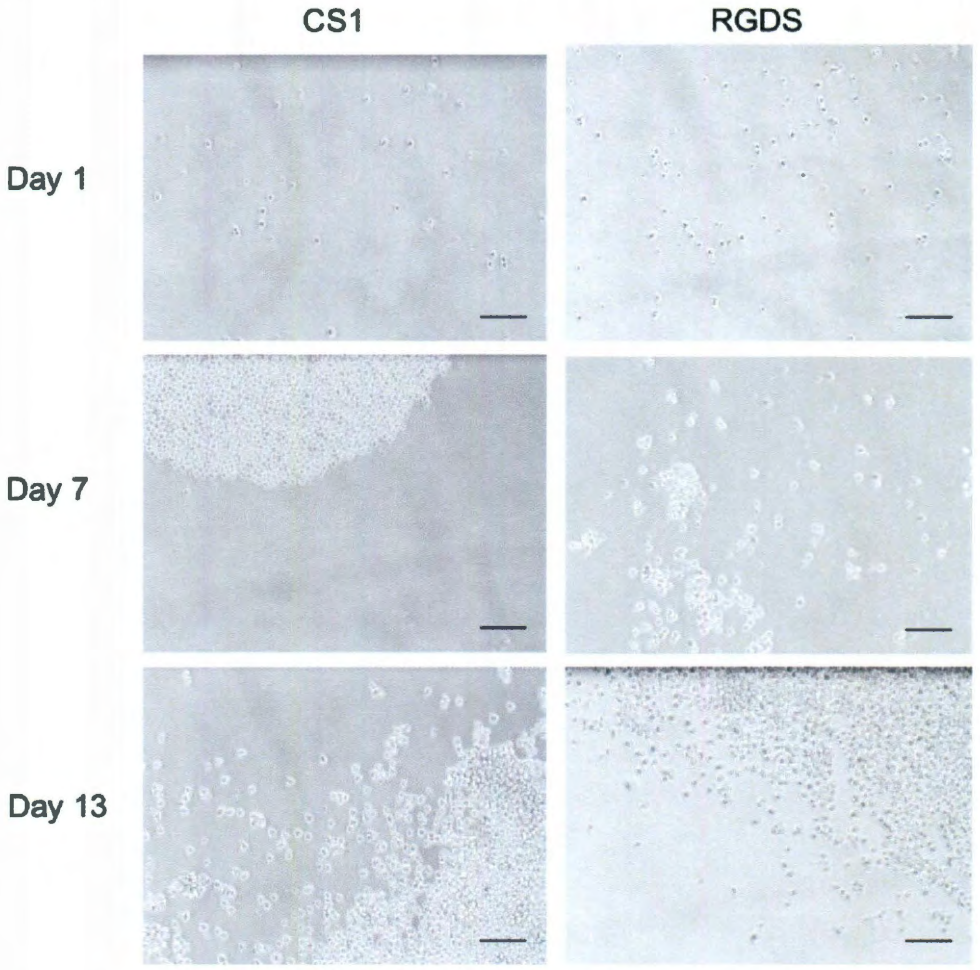

Figure 2.17: c-kit$^+$, lin$^-$ primary cells on hydrogel surfaces with RGDS and CS1. Cells proliferated over time and most of the population remained round with a cell diameter of approximately 10 μm. Some of the cells did increase in size and start to spread more on the gel surface, which could be an indicator of differentiation. (Scale bars = 100 μm)

On RGDS functionalized gels, the cells proliferated significantly compared to the PEG-DA control but none of the other differences were significant. Interestingly, the cells did not expand to a great extent on the FN plate. This could be due to a strong adherence to the plate similar to that seen with 32Ds on high RGDS concentrations. It may also be

due to physical differences between the FN plate and the hydrogel such as stiffness or ability to adsorb proteins from the media.

The proliferation rate likely varied amongst cells within the heterogeneous cell populations on the gel and plate surfaces as more differentiated cell types typically proliferate much faster than self-renewing, undifferentiated HSCs (127). During analysis of single cell proliferation kinetics, Lutolf *et al.* found that cells that proliferated more slowly within hydrogel wells in response to surface immobilized biomolecules were more likely to retain the ability to reconstitute the immune system of an irradiated mouse (127). Thus, lower proliferation rates could signify that a larger portion of the cell population on FN is in a less differentiated state. Alternatively, higher proliferation rates could also indicate that the fibronectin-derived peptides encouraged self-renewal to a greater extent than FN itself. There is a greater percent change in cell number in all groups compared to on PEG-DA controls. Fibronectin and peptide sequences derived from it have both been shown to be capable of supporting HSC self-renewal, and in these studies, both surfaces are promoting proliferation to some extent (121, 124, 125, 129, 191, 203). However, it is unclear whether the FN alone has reduced proliferative activity compared to RGDS and CS1 due to the ability of FN to maintain the cells in a less differentiated, slower proliferating state or because the RGDS and CS1 are more potent in their ability to trigger HSC self-renewal. To further investigate these theories, the expanded cells were evaluated for differentiation potential.

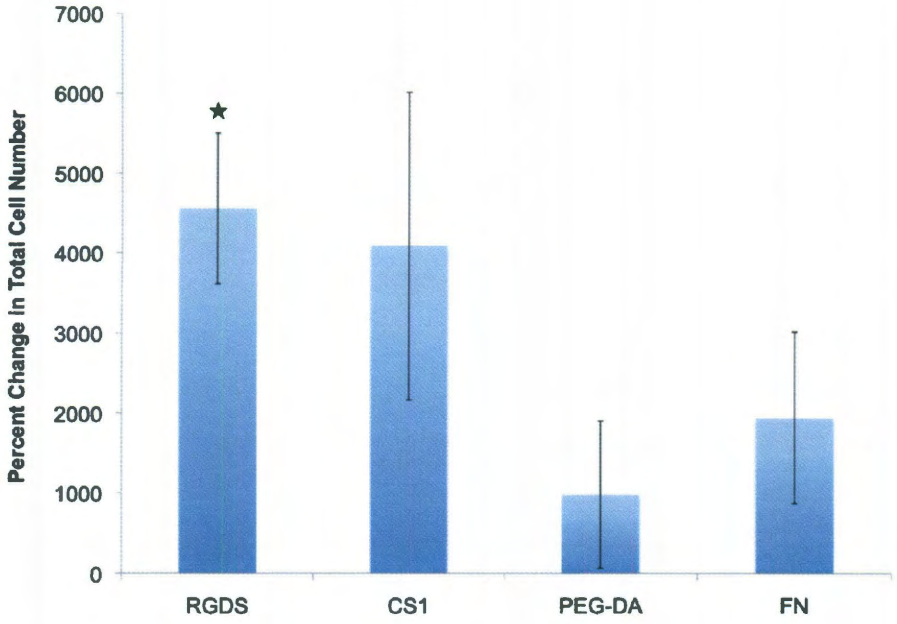

Figure 2.18: Total cell expansion on surface immobilized RGDS and CS1. Total cell number increased significantly on surfaces with PEG-peptides compared to PEG-DA and FN after 14 days in culture. (RGDS, CS1 concentrations = 25 μg/cm^2) Bars are mean ± standard deviation. (★ denotes significance compared to PEG-DA, n=3, $p < 0.05$)

2.3.6 Primary Cell Differentiation

2.3.6.1 Colony Forming Unit Assay

To first evaluate the differentiation potential of expanded cells, a functional analysis was performed. Colony forming unit (CFU) -GEMM, -GM, -G and -M colonies (where G=granulocyte, M=macrophage, E=erythrocyte, GM= granulocyte and macrophage, and GEMM=granulocyte, erythrocyte, macrophage, and megakaryocyte) formed from the cells in the PEG-RGDS, PEG-CS1 and FN groups (Figure 2.19).

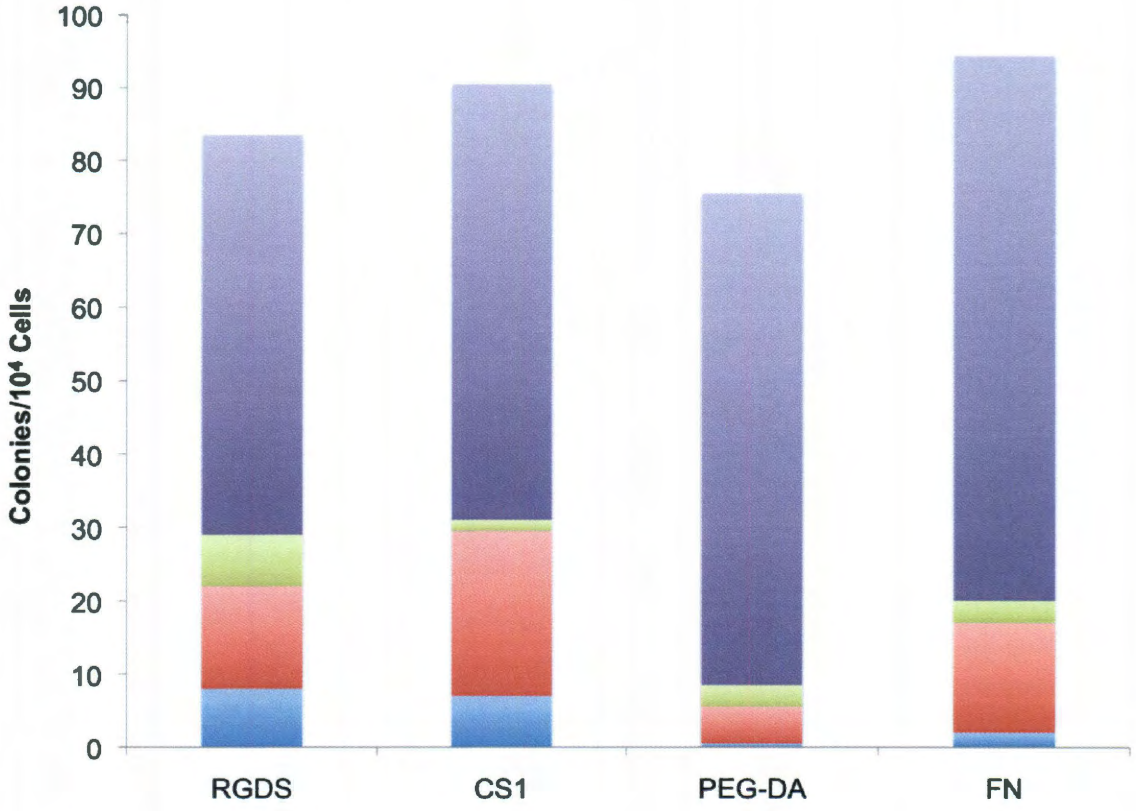

Figure 2.19: Colonies formed after 14 days in methylcellulose media following expansion. Cells from the RGDS and CS1 samples formed more primitive GEMM colonies than PEG-DA and FN controls. Cells from PEG-DA surfaces formed fewer colonies and displayed a reduced ability to form both GM and GEMM colonies. Bars are mean, n=2. (**CFU-M=Macrophage, CFU-G=Granulocyte, CFU-GM=Granulocyte/Macrophage, CFU-GEMM=Granulocyte, Erythrocyte, Megakaryocyte, Macrophage**)

All colonies were able to form in all sample groups albeit to different degrees. In terms of total colonies, all the samples had statistically similar numbers of colonies. The distribution of the colonies can be better seen in Figures 2.20 and 2.21.

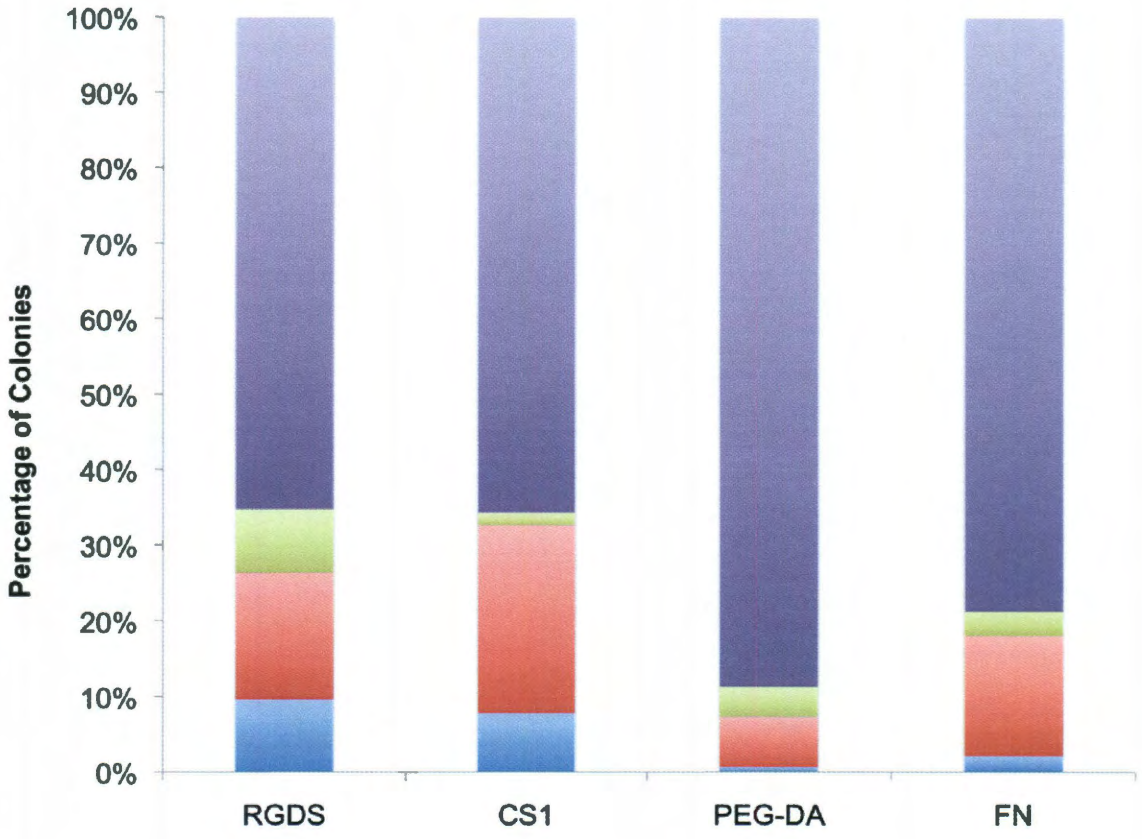

Figure 2.20: Distribution of colonies formed from cells expanded on gels with surface immobilized CS1 and RGDS. More primitive GM and GEMM colonies form in the RGDS and CS1 groups. The percentage of GEMM colonies is minimal on PEG-DA and FN. However, the percentage of primitive colonies (both GM and GEMM) is not significantly different between any of the groups. Bars are mean, n=2. (**CFU-M=Macrophage, CFU-G=Granulocyte, CFU-GM=Granulocyte/Macrophage, CFU-GEMM=Granulocyte, Erythrocyte, Megakaryocyte, Macrophage**)

The number of GEMM colonies (stemming from the least differentiated cells) was higher in the RGDS and CS1 groups than on FN, however, not significantly. The number of GM colonies was similar on CS1, RGDS, and FN. PEG-DA had very low levels of GM and GEMM colonies. Most of its colonies were M. GEMM colonies and GM colonies are comprised of more than one cell type, meaning they are derived from cells that are less differentiated and more progenitor-like. The presence of these colonies at higher proportions in the RGDS and CS1 groups may indicate that these samples were able to

maintain the primary cells in a more undifferentiated state. However, the experiments must be repeated to gain significance.

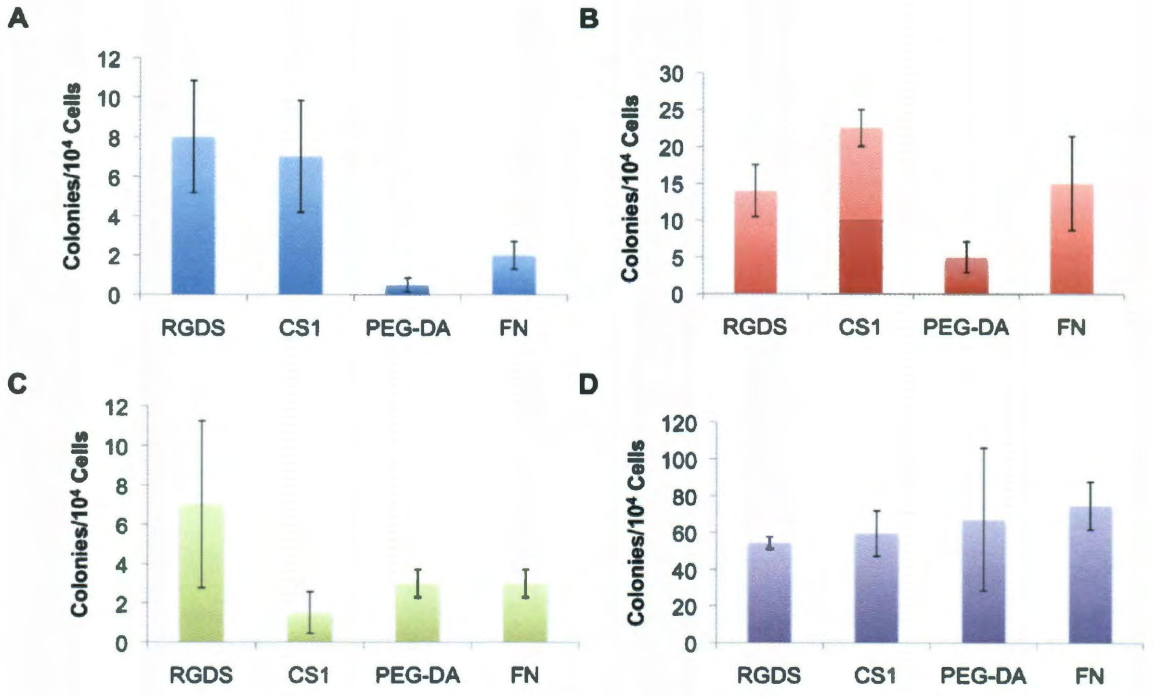

Figure 2.21: Individual colony formation organized by colony type from cells expanded on RGDS and CS1 functionalized hydrogels. GEMM and GM formation was highest on CS1 and RGDS. Bars are mean ± standard deviation, n=2. There was no statistically significant difference between any of the groups. (**A. CFU-GEMM=Granulocyte, Erythrocyte, Megakaryocyte, Macrophage, B. CFU-GM=Granulocyte/Macrophage, C. CFU-G=Granulocyte, D. CFU-M=Macrophage**)

2.3.6.2 Flow Cytometry Analysis

Flow cytometry analysis was performed to observe the expression of specific surface markers that define HSC populations. The flow cytometry plots show that a portion of the cells on all surfaces were no longer c-kit$^+$, lin$^-$ after expansion and the percentage of cells that were c-kit$^+$, lin$^-$ out of the total cells counted decreased (Figures 2.22 and 2.23). The fact that there is a decrease in the percentage of total cells that are primitive (c-kit+, lin- and KSL populations) was expected. The initial population of cells was not a pure collection of primitive cells; it contained cells that were c-kit$^-$ and lin$^+$. In

addition, the c-kit$^+$, lin$^-$ population is not a definitive set of markers for HSCs. Thus, the initial population contains LT-HSCs, ST-HSCs, as well as multipotent progenitors, and as aforementioned, progenitors are known to proliferate more quickly than undifferentiated cells (127). As a result, the percentage of primitive cells out of the total number of cells may decrease. Therefore, the absolute percent increase in specific cell populations was calculated. Any increase in these populations is significant because it means that the bioactive hydrogels are capable of maintaining primitive HSC populations.

The quantity of c-kit$^+$, lin$^-$ and KSL cells increased in all groups indicating that these populations were able to self-renew on the gels even in the presence of many more differentiated cell types (Figures 2.24 and 2.25). Though the percent increase in the KSL population was lower on RGDS and CS1 compared to controls, the differences were not significant. This data is somewhat contradictory to what was observed in the functional colony assay. The colony assay results suggest that RGDS and CS1 are more supportive of HSC maintenance as indicated by the ability of cells from these groups to form a higher percentage of primitive colonies compared to FN and PEG-DA. It is unclear the reason for this disparity. One explanation is that the wide standard deviations in all samples are masking the true effects of the surfaces on HSC behavior. The standard deviations are likely due to the fact that the primary cell populations were harvested from different sets of mice. In addition, the surface markers that define these populations are not definitive for HSCs. The ability of cells to form various colonies or engraft into host bone marrow is not necessarily dependent on the expression of these markers.

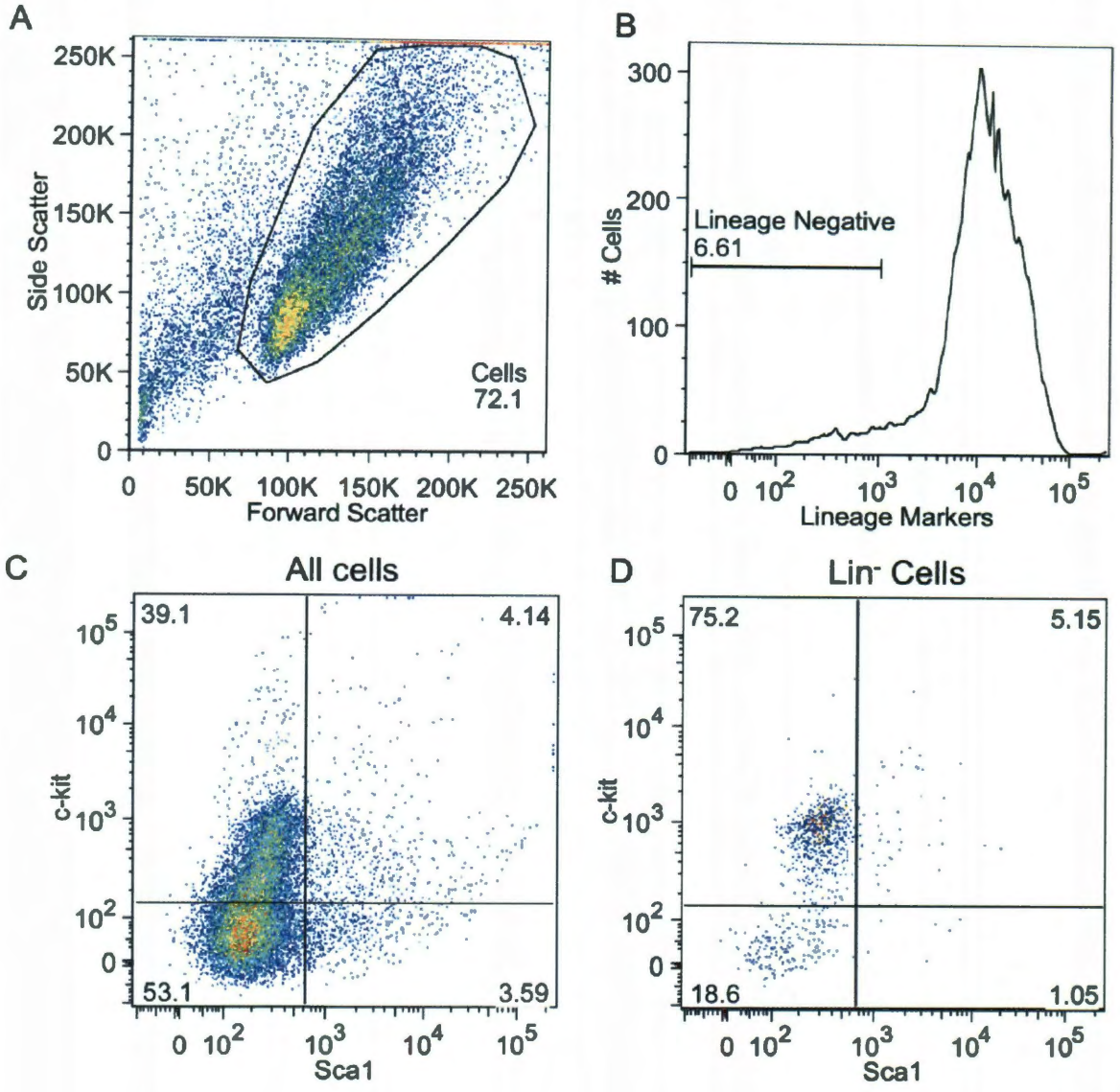

Figure 2.22: Flow cytometry analysis of c-kit$^+$, lin$^-$ cells after 14 days in culture on PEG-RGDS. A. Particles were gated to eliminate debris and aggregates. B. Cells were gated to include those that were lin$^-$. C. A plot of all cells showing the fluorescence intensities of the Sca1 and c-kit markers. Cells were gated to delineate between positive and negative cells. D. A plot of lineage negative cells gated similarly to those in C. Numbers on the graphs indicate the percentage of cells falling within that gate. The data shows that many of the cells have gained lineage markers after culture. However, there is still a high percentage of c-kit$^+$ cells, and there is a KSL population remaining after culture.

Previous studies have shown that adhesion to FN leads to HSC expansion with increased success in engraftment (121, 125, 129, 203). During *in vitro* culture, cells capable of long-term repopulation are typically found in the adherent layers of the culture

(122). Both RGD and CS1 have also shown the ability to encourage expansion of HSCs while maintaining their reconstitution ability, though typically adhesion to CS1 through the VLA-4 integrin leads to better engraftment (125). Taking both the colony assay and the flow cytometry results into account, it appears that hydrogels with the fibronectin derived peptides RGDS and CS1 immobilized on their surfaces are capable of preventing differentiation of primitive hematopoietic cells while supporting their self-renewal. Furthermore, the differences observed in cell proliferation on RGDS and CS1 compared to FN may be due to the ability of FN to prevent differentiation by slowing cell proliferation. On FN plates, expanded cells could form all colonies and a portion of the population retained the surface marker expression profile of primitive HSCs. However, in the design of a culture system, the ability to expand HSC populations extensively is required. Because the peptide sequences promoted greater cell expansion compared to the FN plate (significantly on RGDS) while still maintaining the cells in an undifferentiated state, they were selected for use in the culture system. These peptides are also much easier to work with than large proteins. Their relatively small size (3.8 kDa) compared to FN (>250 kDa) and other proteins means that they can be conjugated to hydrogel surfaces in combination with larger molecules without disrupting the ability of PEGylated versions of the proteins to crosslink to the PEG matrix. In addition, the short peptide sequences are more stable than entire proteins with more complex structures.

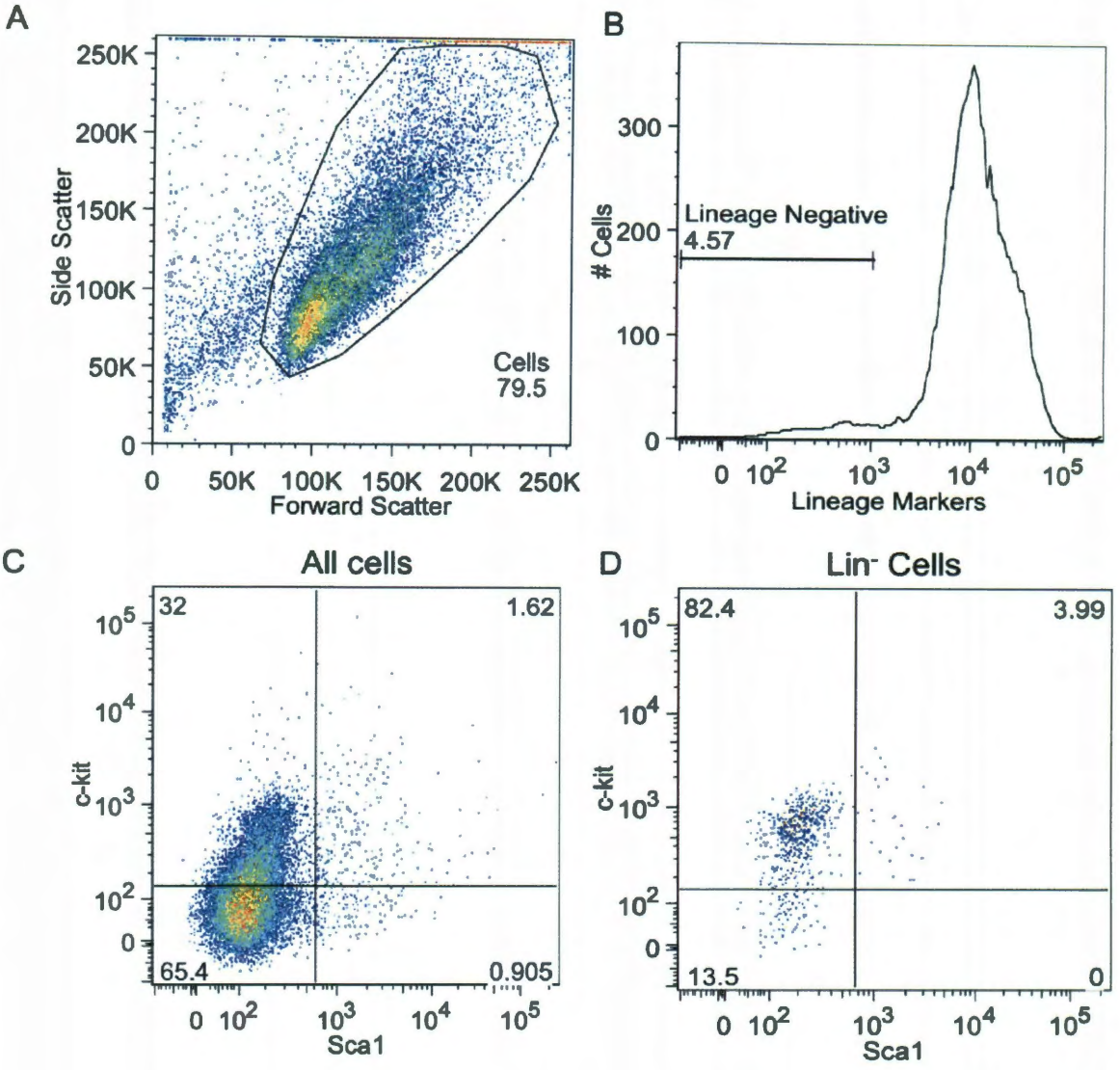

Figure 2.23 Flow cytometry analysis of c-kit$^+$, lin$^-$ cells after 14 days in culture on PEG-CS1. A. Particles were gated to eliminate debris and aggregates. B. Cells were gated to include those that were lin$^-$. C. A plot of all cells showing the fluorescence intensities of the Sca1 and c-kit markers. Cells were gated to delineate between positive and negative cells. D. A plot of lineage negative cells gated similarly to those in C. Numbers on the graphs indicate the percentage of cells falling within that gate. Similarly to cells from RGDS surfaces, many of the cells are lineage positive after expansion. However, there is still a high percentage of c-kit$^+$ cells, and there is a KSL population remaining after culture. The percentages of cells in each population are very similar to those seen in the RGDS sample.

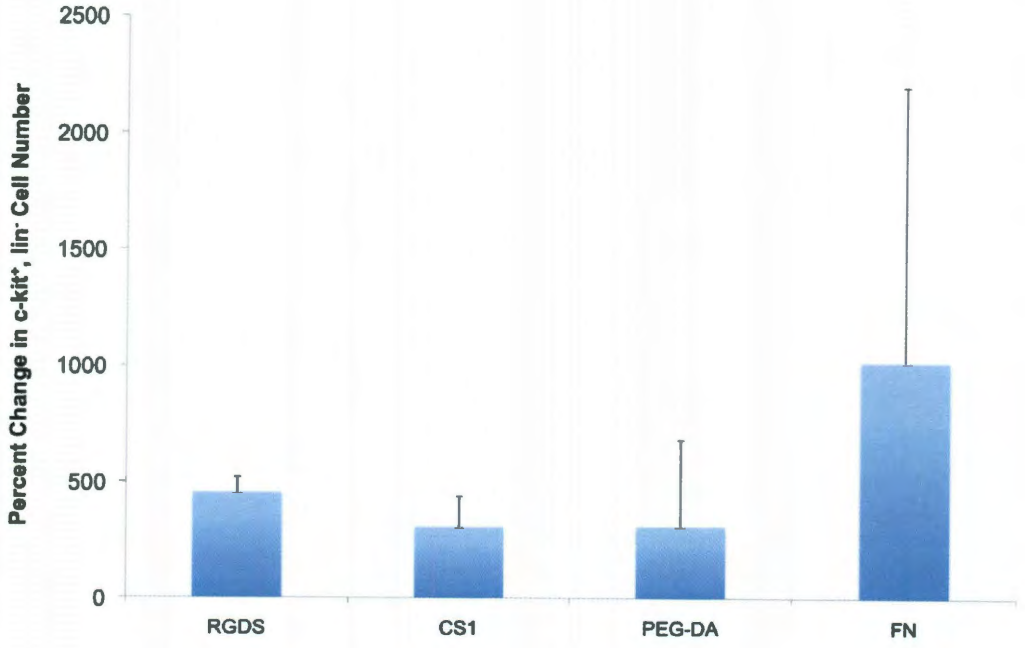

Figure 2.24: Percent change in the c-kit$^+$, lin$^-$ population after 14 days in culture. The c-kit$^+$, lin$^-$ population increased in all groups, and there was no significant difference between groups. (Bars are mean + standard deviation, n=3)

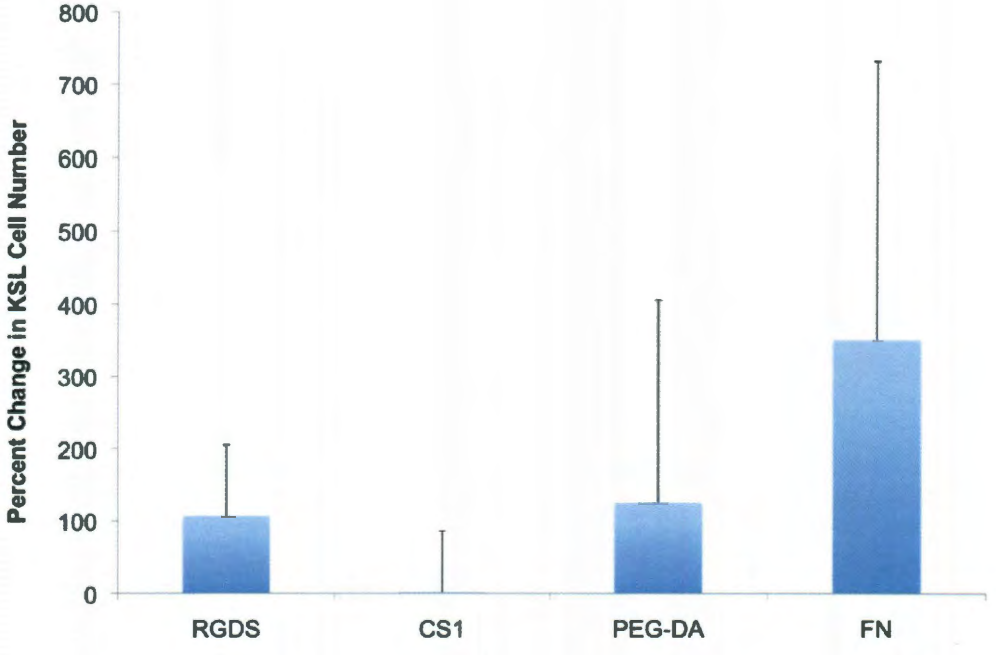

Figure 2.25: Percent change in the KSL population after 14 days in culture. The percent increase in the KSL cell population was fairly low on RGDS and CS1 compared to the controls though the differences were not significant. (Bars are mean + standard deviation, n=3)

2.4 Conclusions

RGDS and CS1 can be successfully conjugated to the surfaces of hydrogel wells and possess the ability to alter hematopoietic cell behavior in both a myeloid cell line (32Ds) and a primary hematopoietic progenitor population. 32Ds were able to adhere and proliferate in hydrogel wells, and altering the surface RGDS concentrations could control both of these processes. c-kit$^+$, lin$^-$ hematopoietic progenitor cells proliferated extensively within RGDS and CS1 functionalized hydrogel wells, and these cells were able to form more primitive colonies than those cultured in control groups. There was an increase in the total number of c-kit$^+$, lin$^-$ and KSL cells after 14 days in culture signifying a population of cells with potential reconstitution ability.

These studies demonstrate that the hydrogel well system is a viable option for hematopoietic cell expansion. The advantage of this system is the ability to functionalize the surfaces with specific niche proteins, which is not possible in a well plate. Due to the success of the fibronectin-derived peptides, hydrogels were next functionalized with RGDS and CS1 in combination with several proteins that are known to affect HSC fate. The following chapters investigate the ability of these proteins to promote hematopoietic cell expansion while maintaining multipotency.

Chapter 3: The Effect of Covalently Immobilized SCF on Hematopoietic Cell Fate in Hydrogel Wells

3.1 Introduction

The HSC niche is comprised of stromal cells, which regulate HSC behavior by the secretion of cytokines and expression of transmembrane proteins. However, the coculture of HSCs with stromal cells involves multiple signaling interactions. To isolate the effects of specific molecules on HSC fate, cell-cell interactions can be mimicked through the immobilization of individual molecules on hydrogel surfaces. This chapter focuses on the incorporation of stem cell factor (SCF) into the hydrogel matrix. SCF was selected due to its ability to spur HSC proliferation, promote hematopoiesis, and aid in HSC survival (104, 188, 204-209). SCF was surface immobilized onto hydrogel wells, and 32D cells and HSCs were cultured for 6 or 14 days respectively. We evaluated the effects of SCF on hematopoietic cell behavior by quantifying cell adhesion, spreading, proliferation, and differentiation potential.

3.1.1 Stem Cell Factor

Stem Cell Factor (SCF), also known as Steel factor or c-kit ligand, is a 28-30 kDa transmembrane glycoprotein (210). Figure 3.1 displays the structure of the protein as well as details the signaling pathways it initiates in mast cells. SCF exists in two forms: a 248 amino acid sequence that is cleaved to generate the soluble 165 amino acid form of SCF and a 220 amino acid sequence that forms the membrane-bound form of the protein (209, 211, 212). The soluble form of the protein exists as a dimer; however, the monomers are not linked via disulfide bonds (210, 212-217). Osteoblasts and other stromal cells in the niche secrete SCF as well as present it on their surfaces.

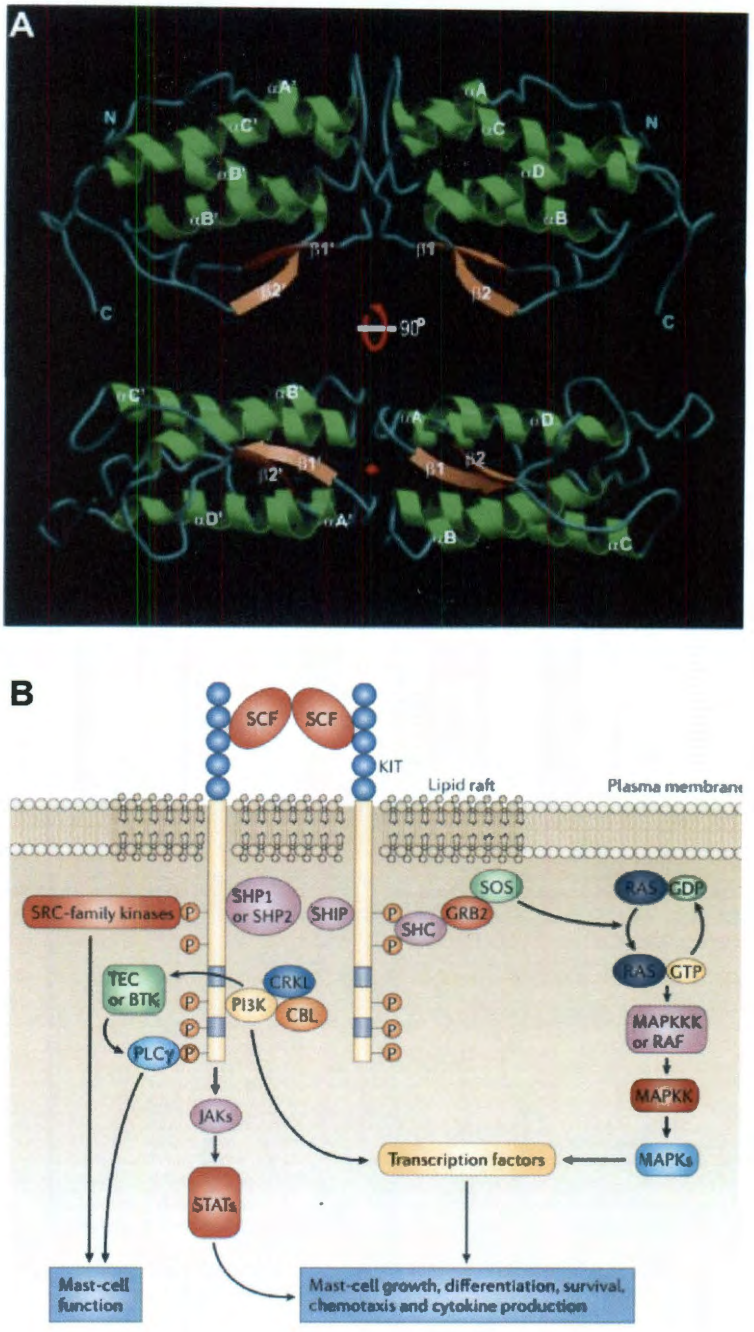

Figure 3.1: SCF structure and signaling pathways. A. Structural representation of human SCF. The lower structure is a 90° rotation of the upper structure. The N and C termini and secondary structures are labeled; the β-strands are orange, the helices are green, and the loop regions are grey. Schematic adapted from (218). B. The signaling pathways activated in mast cells when SCF binds to the c-kit receptor. Many of these same pathways are implicated in more primitive hematopoietic progenitors as well as HSCs and aid in proliferation, survival, and hematopoiesis. Image adapted from (219).

Both forms of the protein bind to and activate c-kit, the tyrosine kinase receptor expressed on the surfaces of HSCs and other hematopoietic progenitors, which can trigger the proliferation and differentiation of HSCs (220-223).

Soluble SCF has been used clinically to promote mobilization of stem cells (224-226). Kovach *et al.* treated hematopoietic cell lines with soluble SCF and demonstrated that soluble SCF did not alter the expression of VLA-4 and VLA-5 integrins but did affect their avidity in a biphasic manner. SCF promoted adhesion at early timepoints followed by increased mobilization at later timepoints (220). Other studies have shown that SCF can enhance adhesion of hematopoietic cells to fibronectin (227-229). Soluble SCF is also commonly used in colony forming assays to promote the differentiation of murine HSCs into both myeloid and lymphoid progenitors (205, 207, 212, 230, 231).

As opposed to soluble SCF, which is endocytosed and degraded, membrane or surface bound SCF has been shown to maintain c-kit activation and promote cell adhesion via the VLA-4 and VLA-5 integrins (208, 220, 232-234). Gunawan *et al.* used streptavidin-biotin binding to immobilize SCF onto glass surfaces coated with biotinylated PEG chains and observed that hematopoietic progenitors adhered to the surfaces in a dose-dependent manner (188). In addition, HSCs from mice lacking membrane bound SCF (Steel Dickie mice) are unable to self-renew (235).

3.1.2 The Use of Stem Cell Factor in HSC Expansion

In vitro, soluble and surface immobilized SCF have both been used to enhance HSC expansion and have been shown to prevent apoptosis and prolong hematopoiesis (188, 206, 208, 209). Soluble SCF has been added to media in combination with other cytokines and growth factors, such as thrombopoietin, Flt-3 ligand, Granulocyte

Macrophage Colony Stimulating Factor (CSF), Granulocyte-CSF, IL-3, IL-6, and IL-11, to maintain HSCs in long-term culture (204, 205, 207). A combination of soluble SCF and Flt-3 ligand promoted the expansion of hematopoietic progenitors for 2 to 3 days followed by successful engraftment in irradiated hosts (104). Due to its success, SCF is one of the most common components added to media in the *in vitro* culture of HSCs, though alone it is insufficient to maintain the HSCs in an undifferentiated state for long periods of time.

The membrane bound form of SCF has been shown to promote hematopoiesis in culture longer than the secreted form as a result of sustained activation of the c-kit ligand (209, 236-238). Toksoz *et al.* genetically altered stromal cells to express either the membrane bound or soluble form of SCF and observed expansion in both groups, though membrane bound SCF promoted expansion for 1-2 weeks longer than the soluble form (209). Doran *et al.* successfully physioadsorbed SCF to the wells of tissue culture plates and observed increased expansion of hematopoietic cell lines compared to similar SCF concentrations in a soluble form; in addition, c-kit expression on cells was at levels similar to low concentrations of soluble SCF, indicating low receptor saturation and/or internalization (206).

Kishimoto *et al.* immobilized SCF on fragmin/protamine microparticle-coated plates to help preserve the bioactivity of SCF and mimic the role the ECM plays in binding cytokines. This study found that a hematopoietic cell line could bind to the particles and proliferated in response to the immobilized SCF. However, the binding of the SCF to the microparticles was transient, and the SCF was released after five days (137). These studies indicate the importance of the interactions between SCF and the c-

kit receptor in HSC survival and maintenance. Toksoz *et al.* was able to present immobilized SCF to HSCs by expressing it in a feeder layer of stromal cells, but the use of another cell type during *in vitro* culture makes it difficult to have fine control over the system and the signaling events that take place. In addition, although both Doran and Kishimoto's groups demonstrated the ability to immobilize SCF and maintain its bioactivity in a synthetic system and prolong activation of the c-kit receptor, SCF is ultimately cleaved from the surfaces.

The PEGylation of SCF allows the protein to be displayed to cells in a manner that mimics the membrane-bound form of the protein. This is crucial because the soluble and membrane-bound forms of the protein play distinct roles in HSC function. In its soluble form, SCF is more likely to drive differentiation as the protein is endocytosed. In contrast, the membrane bound form allows for sustained activation of the c-kit receptor and maintains HSCs in a less-differentiated state for longer time periods. The presentation of immobilized SCF on hydrogel surfaces can replicate this interaction specifically and gives total control over the concentration of protein displayed to the HSCs. The following work investigates the effects of SCF on the adhesion, proliferation, and spreading of 32D cells as well as its efficiency in the expansion of primitive HSC populations.

3.2 Materials and Methods

All materials were obtained from Sigma unless otherwise noted.

3.2.1 Polymer Synthesis and Characterization

3.2.1.1 PEG-DA

6kDa PEG-DA was synthesized as described in Section 2.2.1.1.

3.2.1.2 PEG-RGDS and PEG-CS1

PEG-RGDS for studies with 32Ds was synthesized as describe in Section 2.2.1.2. PEG-RGDS and PEG-CS1 for studies utilizing primary cells were synthesized as previously detailed in Section 2.2.1.3.

3.2.1.3 PEG-SCF

PEG-SCF was made using the same methods as PEG-CS1 and PEG-RGDS for primary cell studies (described in detail in Section 2.2.1.3). Briefly, PEG-SVA was reacted with carrier-free murine SCF (R&D, Minneapolis, MN) at a molar ratio of 42:1 (PEG-SVA:SCF) (Figure 3.2). The reactions were performed in PBS overnight at 4° C while maintaining the pH at 8.0. To determine if SCF was PEGylated, a Western blot was performed on the PEGylated and unPEGylated forms of the proteins using a 15% Tris-HCl precast polyacrylamide gel (BioRad, Hercules, CA). A rabbit polyclonal to SCF was used as the primary antibody (Abcam, Cambridge, MA). The secondary antibody, a goat polyclonal to rabbit IgG, was conjugated with horseradish peroxidase (Abcam). To detect the proteins, the ECL chemiluminescent Western blotting analysis system (GE Healthcare, Chalfont St. Giles, UK) was applied, and chemiluminescent images of the blot were captured on an LAS 4000 (Fuji, Tokyo, Japan).

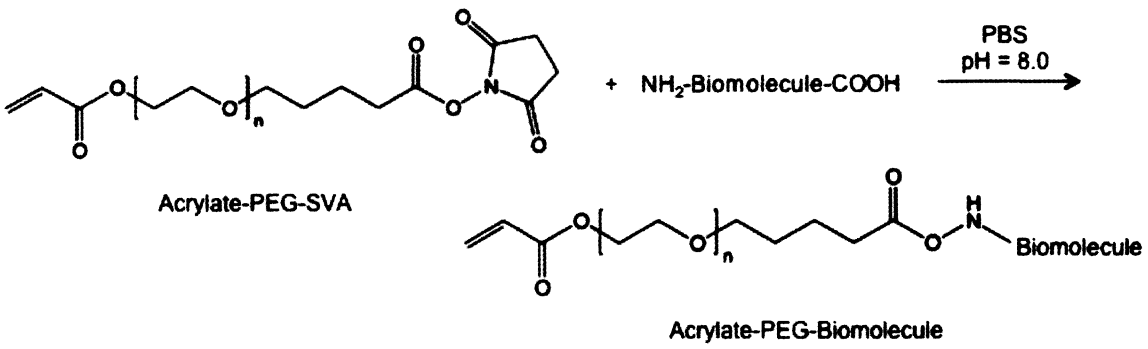

Figure 3.2: Reaction scheme for the PEGylation of SCF (or any biomolecule). Acrylate-PEG-SVA reacts with free amines on biomolecules to form a heterobifunctional polymer that can covalently crosslink to the PEG hydrogel matrix.

3.2.1.4 Bioactivity of PEG-SCF

To evaluate the bioactivity of PEG-SCF, 32D cells were seeded into TCPS plates at a density of 5000 cells/cm^2 in three formulations of media: control media (RPMI-1640 with 10% IL-3 supplement), control media with SCF (200 ng/ml) and control media with PEG-SCF (200 ng SCF/ml). After 24 hrs., the wells were imaged, and cell number was calculated using ImageJ software as described in Section 2.2.4.1. The imaging and analysis were repeated after 5 days, and the percent change in cell number during this time was determined.

3.2.1.5 Surface Immobilization of SCF within PEG Hydrogel Wells

6 kDa PEG-DA hydrogel wells were fabricated as detailed in Section 2.2.2. To functionalize the surfaces with biomolecules, solutions of PEG-RGDS and PEG-SCF or PEG-CS1 and PEG-SCF were made to obtain surface concentrations in the PEG wells of 400 ng/cm^2 (for PEG-SCF) and 250 or 25 μg/cm^2 (for PEG-CS1 and PEG-RGDS). The photoinitiator 2,2 dimethoxy, 2-phenyl acetophenone (300 μg/ml, dissolved in NVP) was added at 10 μl per ml of polymer solution. 10 μl of the polymer solution was added to each well and groups of four wells were crosslinked with long wavelength UV light (365

nm, 10 mW/cm^2) for 3 min. Figure 3.3 shows a schematic of this process. After crosslinking, gels were soaked and rinsed to prepare them for cell preparation as previously described in Section 2.2.2.2.

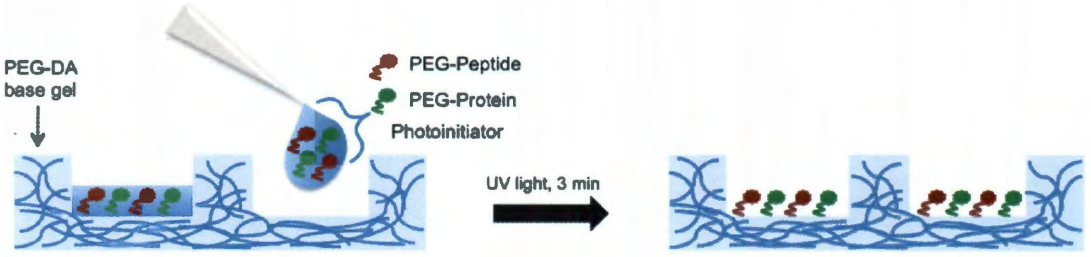

Figure 3.3: Surface conjugation technique for multiple PEG-biomolecules. PEG-DA hydrogel wells are coated with a 10 µl droplet containing PEG-peptide, PEG-protein, and a photoinitiator. Gels containing 4 wells are placed under UV light for 3 min. to covalently immobilize the biomolecules on the gel surfaces.

3.2.1.6 Quantification of SCF on Gel Surfaces

To confirm the surface protein concentrations, two concentrations of SCF (200 and 400 ng/cm^2) in combination with PEG-RGDS (25 µg/cm^2) were conjugated to the surfaces of hydrogel wells. After UV exposure, the 10 µl solution was removed from each hydrogel well, and the gels were soaked in PBS. An enzyme-linked immunosorbent assay (ELISA, Quantikine ELISA kit for SCF, R&D) was performed on the aspirated liquid as well as the soak solutions as previously described and using PEGylated versions of the proteins for the standard curve (174).

3.2.2 Cell Maintenance

3.2.2.1 32D Cell Culture

32D cells were maintained as explained in Section 2.2.3.2. Briefly, 32D cells were cultured in RPMI-1640 with 1% penicillin-streptomycin, 10% heat-inactivated FBS, and 10% IL-3 culture supplement. Media was replenished every 2-3 days. Cells were subcultured upon reaching a concentration of 1 million cells/ml.

3.2.2.2 Primary c-kit$^+$, lin$^-$ Cell Isolation and Culture

Whole bone marrow from 8-12 week old C57/B6 mice was isolated and processed in the manner described in Section 2.2.3.2. c-kit$^+$ lin$^-$ cells were isolated magnetically and cultured in StemSpan Media supplemented with 1% GA and 50 ng/ml SCF.

3.2.2.3 Cell Seeding into Hydrogel Wells

32D cells were seeded into the hydrogel wells at 5000 cells/cm^2. The experimental groups consisted of wells with 400 ng/cm^2 SCF and 25 μg/cm^2 RGDS. PEG-DA and PEG-RGDS gels (2.5, 25, and 250 μg/cm^2) served as controls. Each group consisted of 4 gel wells. Cells within hydrogel wells were maintained in culture for 6 days at 37°C with 5% CO_2 with media renewal every 2 days.

c-kit$^+$ lin$^-$ cells were seeded in gel wells ([SCF]=400 ng/cm^2, [RGDS]=25 μg/cm^2 or ([SCF]=400 ng/cm^2, [CS1]=25 μg/cm^2) at 13,000 cells/cm^2. Gel wells with only RGDS or CS1 (25 μg peptide/cm^2) served as controls. Each group consisted of 4 gel wells. Media was added around gels to keep them hydrated. Cells within hydrogel wells were maintained in culture for 14 days at 37°C with 5% CO_2 as described in Section 2.2.3.3. After culture, the cells from each group were combined so that enough cells were available for flow cytometry. The experiment was conducted a total of three times.

3.2.3 Evaluation of Hematopoietic Cells in Culture

The adhesion, proliferation, and spreading of 32D cells were evaluated as previously described in Sections 2.2.4.1 and 2.2.4.2 to determine the effects of SCF on these properties.

c-kit$^+$ lin$^-$ cell expansion and differentiation potential were quantified in the same manner as delineated in Sections 2.2.4.3-2.2.4.5.

3.2.4 Statistical Analysis

One-way ANOVAs and Tukey's post-hoc analyses were performed to evaluate statistical differences between groups in all studies using a 95% probability level ($p<0.05$).

3.3 Results and Discussion

3.3.1 Polymer Synthesis and Characterization

3.3.1.1 PEG-SCF

The conjugation of SCF to PEG was confirmed with a Western blot. Figure 3.4 shows an image of the blot. In the SCF lane, there is an expected band near 18 kDa, the molecular weight of the soluble version of the cytokine. In the PEG-SCF lane, a smear is visible beginning at 28 kDa. The increase in molecular weight indicates that the SCF has been successfully conjugated to PEG chains with a polydisperse molecular weight, and many of the SCF molecules are attached to multiple PEG chains generating a range of molecular sizes. The presence of a band at 18 kDa in the PEG-SCF lane indicates that a portion of the SCF is unconjugated, though the low intensity of the band signifies that it is a small amount of protein.

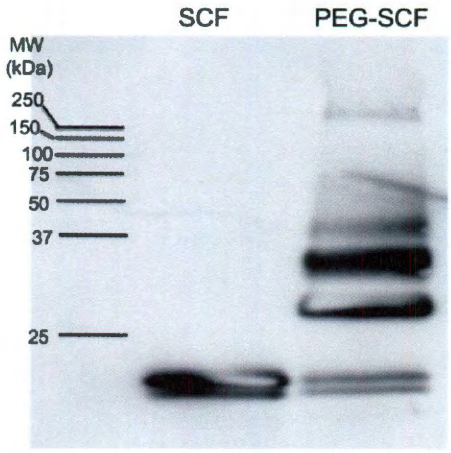

Figure 3.4: Western blot confirming PEGylation of SCF. In the SCF lane, a band at 18 kDa corresponds to the molecular weight (MW) of the extracellular domain of SCF. In the PEG-SCF lane, there is a smear beginning at a MW of ~28 kDa. The increase in MW confirms the addition of PEG chains to the SCF molecule, and the resulting smear indicates that some SCF molecules have multiple PEG chains.

3.3.1.2 Bioactivity of PEG-SCF

In order to ensure that SCF remained bioactive after PEGylation, a soluble form of the PEG-SCF was added to 32D cells in culture. The effects of SCF on 32D cell proliferation were then evaluated. The addition of both unmodified SCF and PEG- SCF to culture media resulted in significant increases in cell numbers compared to control wells without any form of the protein (Figure 3.5). There was no significant difference between the PEGylated and unmodified forms of the protein suggesting that the PEG chains do not affect the bioactivity of the protein.

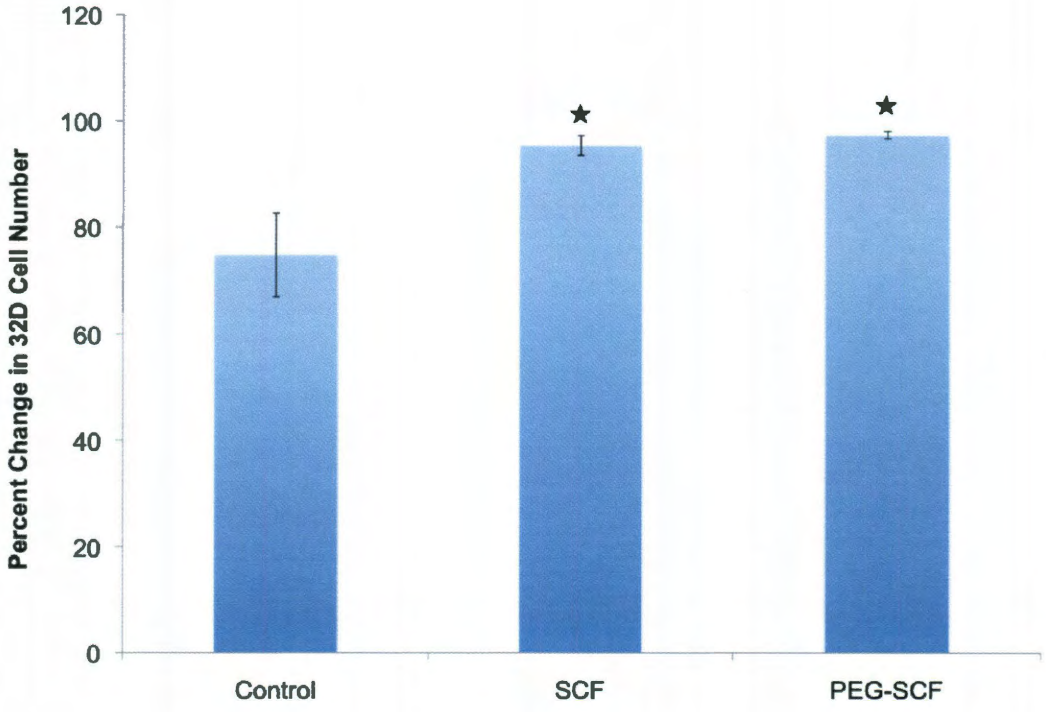

Figure 3.5: The bioactivity of SCF is maintained after PEGylation. 32D cells were cultured in media containing: no SCF, the natural occurring form of SCF, or the PEGylated SCF. The effects on 32D cell proliferation were evaluated. There was a significantly higher percent change in 32D cell number after 5 days when SCF or PEG-SCF was added to the media. We saw no significant difference between the PEGylated and unPEGylated versions of the protein. Bars are mean ± standard deviation (★ indicates significance compared to control, n=8, $p < 0.05$)

3.3.1.3 Quantification of SCF on Gel Surfaces

To determine the concentration of SCF on our surfaces, we performed an ELISA on the surface solution after crosslinking. The amount of SCF on the well surface after crosslinking an initial solution of 400 ng/cm^2 (89.52 ng/well) was 73.5 ± 6.7 ng, which is approximately 80% of the initial protein in the crosslinking solution. This finding confirms that SCF can be immobilized onto hydrogel surfaces.

3.3.2 32D Cell Adhesion

Cell adhesion is a critical process in the niche because it retains HSCs within the bone marrow and allows interaction with numerous other cell types. The ability of SCF

to alter 32D cell adhesion to hydrogel surfaces was evaluated by imaging cells after 48 hrs. in culture (Figure 3.6). Compared to the samples containing the medium concentration of RGDS (25 μg/cm^2), gels with surface immobilized SCF (also containing 25 μg/cm^2 RGDS) have significantly more adherent 32Ds after 48 hrs.: 2278.9 ± 1775.6 cells/cm^2 on the RGDS compared to 6797.9 ± 1327.2 cells/cm^2 on the SCF and RGDS combination.

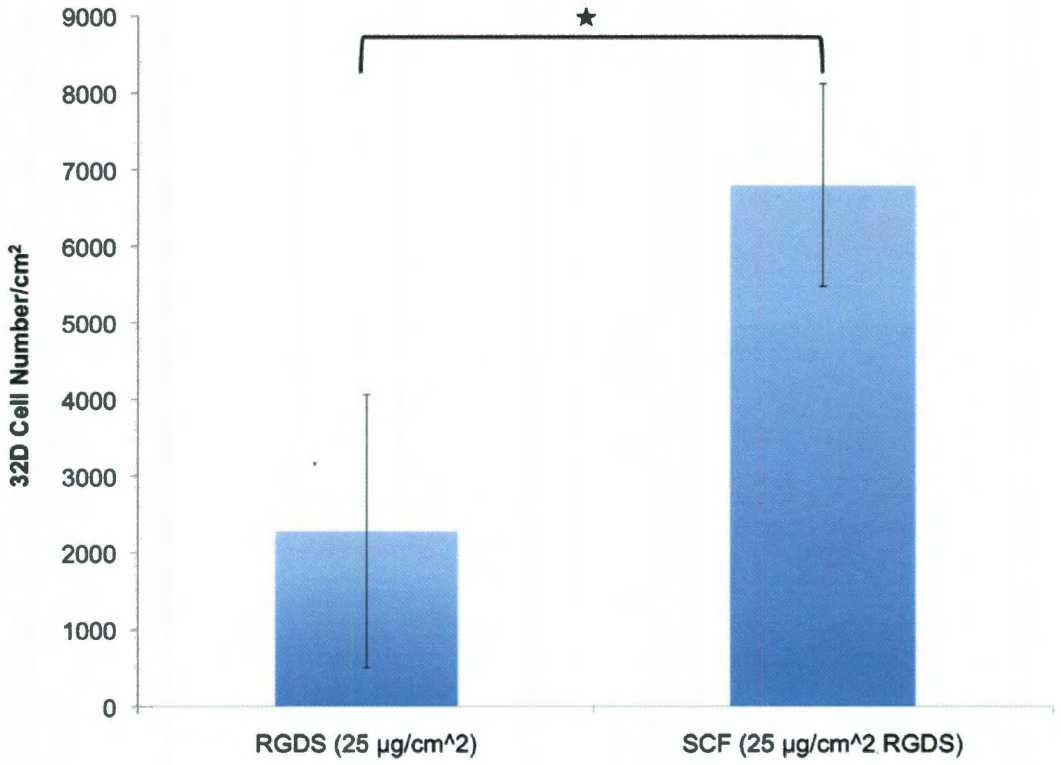

Figure 3.6: 32D cells adhere significantly to gels with surface immobilized SCF. After 48 hrs., there were significantly more 32Ds on surfaces with SCF and RGDS compared to surfaces containing only RGDS. Bars are mean ± standard deviation (★ denotes significance, n=4, $p < 0.05$)

These results are consistent with previous suggestions that fibronectin works with cytokines in the niche to promote cell adhesion (122). The incorporation of SCF onto the gel surfaces in conjunction with RGDS caused an additive response by the cells in terms of 32D cell adhesion. Binding to SCF through the c-kit receptor activates α5β1 integrins

on the cell surface to promote adhesion to RGDS (220, 239, 240). Because SCF is immobilized onto the hydrogel, there is sustained activation of the c-kit receptor, which maintains 32D cell adhesion. Additionally the SCF protein itself can act as a binding site for the HSCs further reinforcing their retention on the hydrogel surfaces.

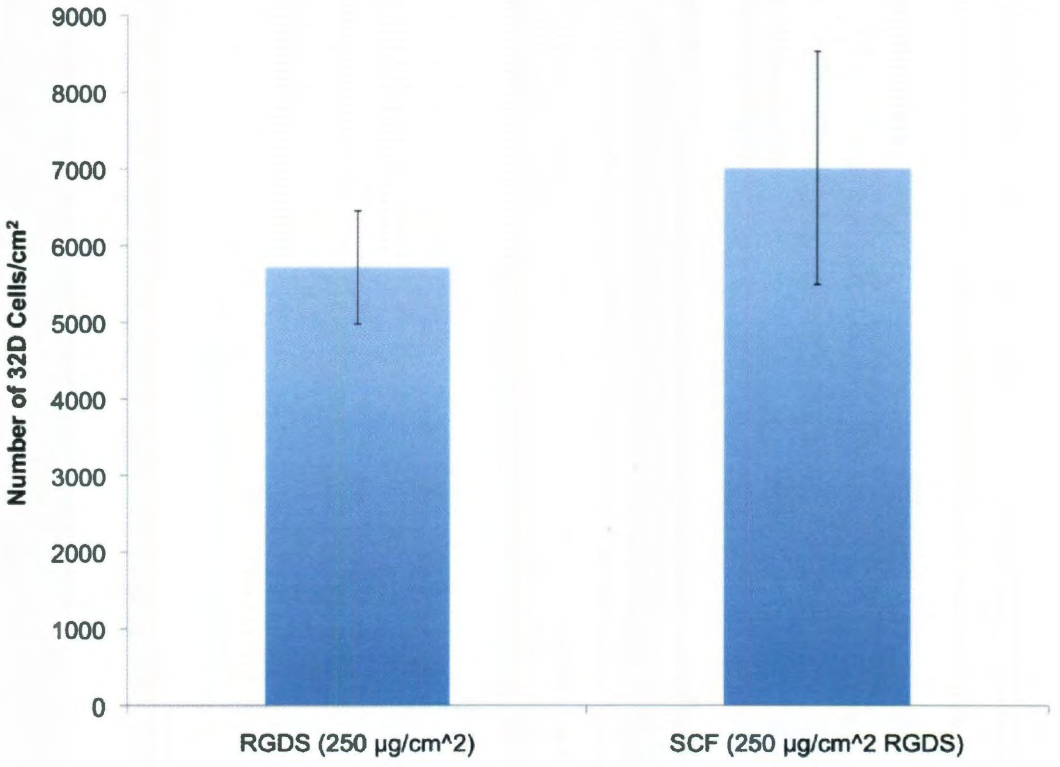

Figure 3.7: At high concentrations of RGDS the effects of SCF are masked. On surfaces with high RGDS concentrations, SCF does not significantly alter the adhesion of 32D cells. Bars represent mean ± standard deviation (n=4)

At higher concentrations of RGDS (250 µg/cm^2), the effects of SCF are masked, and cell number is maintained at the same level with and without these proteins (Figure 3.7). This may be due to the activation of similar signaling pathways by both RGDS and SCF. As aforementioned, binding to SCF through the c-kit receptor activates α5β1 integrins, which in turn bind to RGDS. The presence of additional RGDS molecules on the surface at the high RGDS concentration (250 µg/cm^2) can also lead to an increase in 32D adhesion (171, 198). The RGDS and SCF work through similar pathways to

encourage cell adhesion. At the high RGDS concentration, the addition of SCF likely does not enable greater adhesion because the integrins have already been activated by RGDS. However, the cell spreading differs greatly on these two surfaces indicating that the activation of c-kit is likely involved in cell spreading to some degree. These effects are discussed later in Section 3.3.4.

3.3.3 32D Cell Proliferation

In comparison to the medium RGDS concentration (25 $\mu g/cm^2$), the addition of SCF seems to slow the proliferation of 32D cells, though not significantly (Figure 3.8). The percent change in 32D cells over 48 hrs. was 48.1 ± 10.2% on the RGDS compared to 13.6 ± 42.0% on the SCF and RGDS combination. Note that the standard deviations of these changes were rather large due to the intrinsic heterogeneity of the 32D population. The slower rate of proliferation on immobilized SCF can be attributed to a couple of factors.

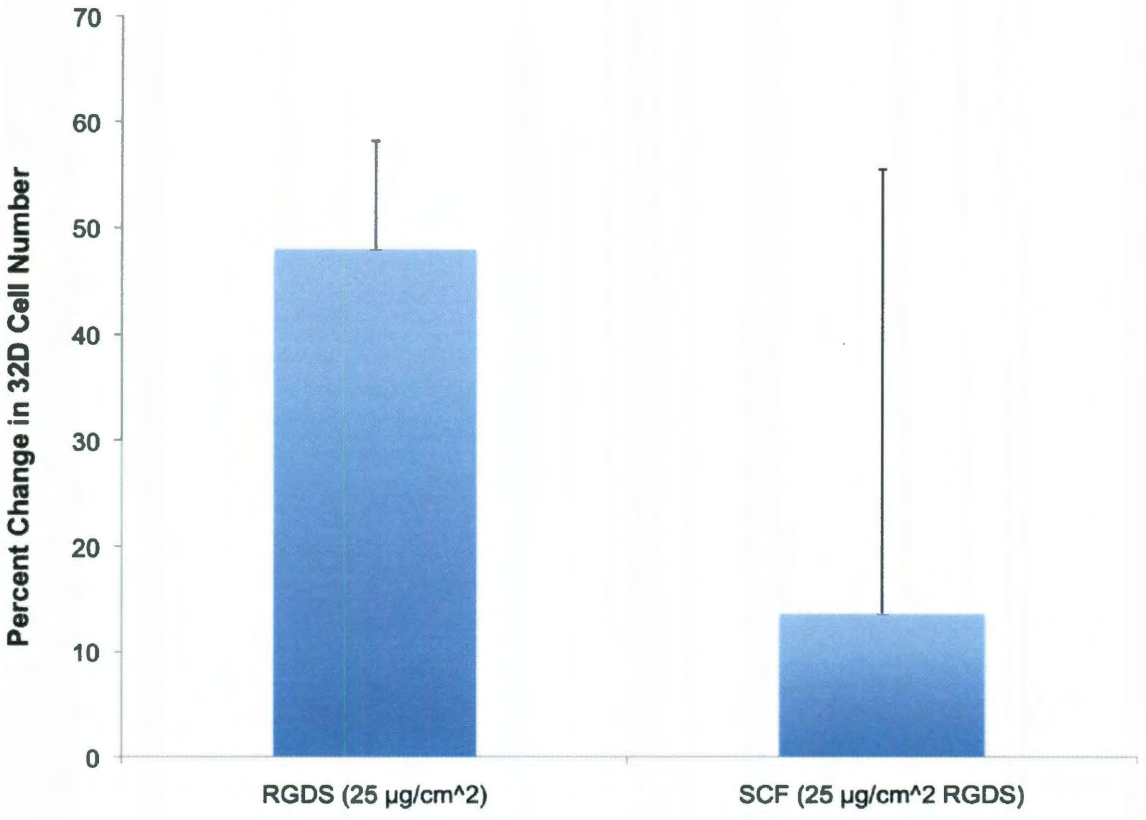

Figure 3.8: SCF does not affect the proliferation of 32D cells. 32D cells proliferated at a higher rate on gels without SCF in a 48 hr. time period, although the rates were not significantly different due to the heterogeneity of 32D cells. Bars represent mean + standard deviation (n=4)

Firstly, as aforementioned, adhesive interactions between hydrogels and cells can be quite strong and adversely affect cells' abilities to proliferate (161). Cells may find it difficult or be unable to leave the surface and divide. Alternatively, SCF signaling could be acting to maintain the 32Ds in a more undifferentiated state. Typically, HSCs are in a quiescent state, proliferating at a very slow rate, while hematopoietic progenitors proliferate rapidly. Immobilized SCF allows for persistent activation of the c-kit receptor as well as promotes the expression of the VLA-4 and VLA-5 integrins, which all work *in vivo* to retain HSCs in the niche and have been implicated in the self-renewal of HSCs *in vitro* (122, 191-194, 208, 220, 227-229, 232-234). In combination with TPO and Flt3,

SCF has also been shown to prevent differentiation for short periods of *in vitro* culture (241). In addition, membrane bound SCF has been shown to maintain HSCs in culture for longer periods than its soluble form, indicating its role in slowing or preventing differentiation (209). The ability to influence the proliferation rates, and potentially the differentiation, of hematopoietic cells by altering the components of the hydrogel matrix demonstrates the potential of this culture system to drive cell behavior. The PEG hydrogel system is beneficial because it allows complete control over the interactions between the matrix and the cells. The immobilization of SCF on the hydrogel surface leads to an increase in cell adhesion potentially through the activation of the c-kit receptor and $\alpha 5\beta 1$ integrins on the surfaces of 32Ds.

3.3.4 32D Cell Spreading

A better understanding of how SCF can affect cell behavior such as cell spreading can aid in the design of the hydrogel system. 32D cells spread extensively on gels with covalently bound SCF compared to groups with only RGDS presented on the surfaces. Figure 3.9 shows images of 32D cells whose nuclei and actin filaments have been stained with DAPI (blue) and phalloidin (green) respectively. High magnification images show a definitive morphological change in cells when SCF is present on the surface as compared to gels containing RGDS alone.

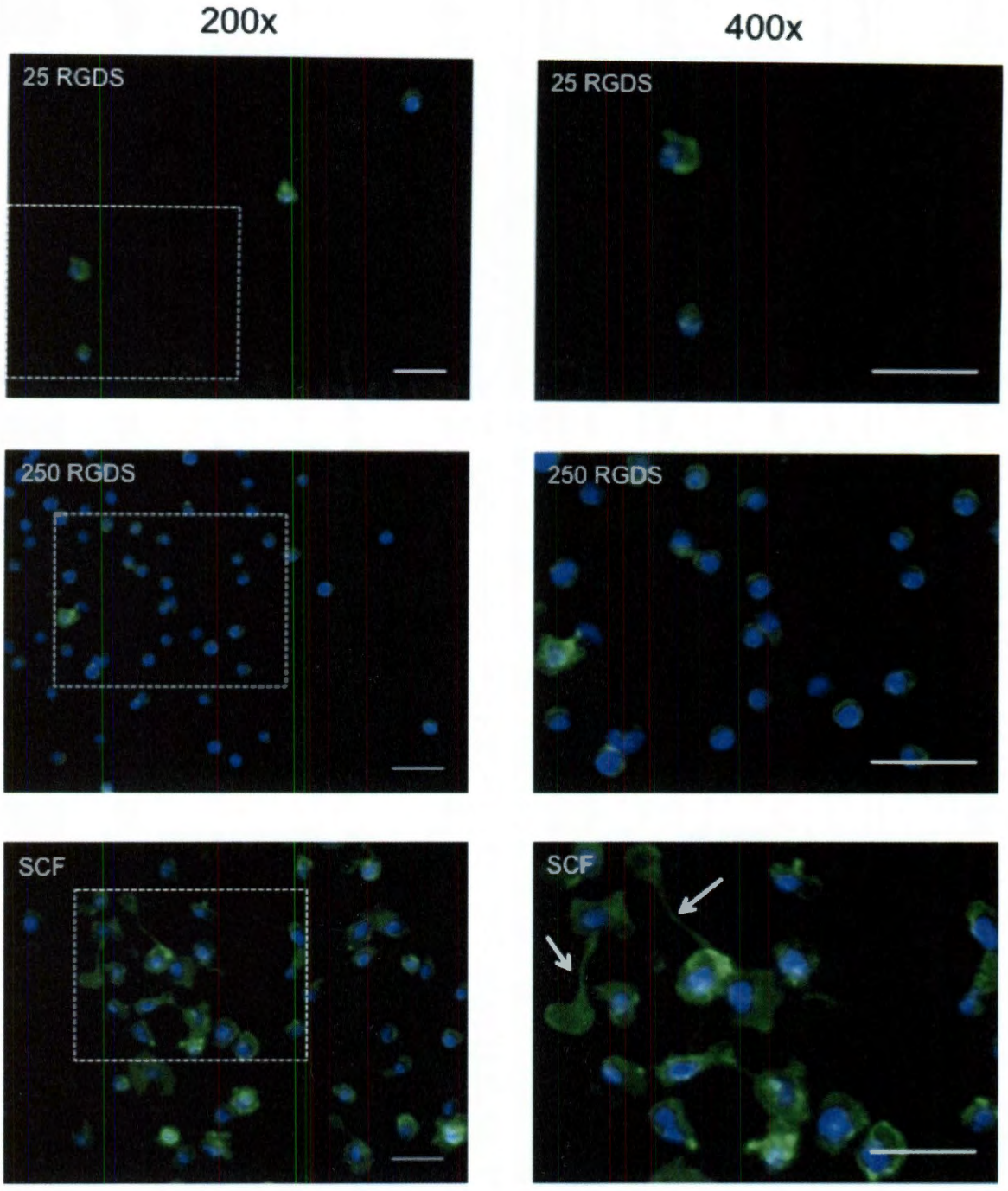

Figure 3.9: 32D cells spread extensively on hydrogels containing SCF. 32D cells were stained with DAPI (nuclei, blue) and phalloidin (actin filaments, green). The left panel is at 200x magnification. The right panel is a 400x image of the area designated by the white box in the left panel. Cells were round and had very little actin on gels with only RGDS. In contrast, cells were more spread in the presence of SCF with distinct filopodia (white arrows). Scale bars = 50 μm

32Ds were more spread and many had distinct filopodia extending across the gel surfaces containing SCF, indicated by white arrows in Figure 3.9. In contrast, 32Ds on gels with only RGDS remain round and appear smaller in size. We also noted clear differences in cell number consistent with our cell adhesion data. On PEG-DA gels and gels with a lower RGDS concentration (25 μg/cm^2), there are few cells present on surfaces after staining. In contrast, surfaces modified with SCF or high RGDS concentrations (250 μg/cm^2), there were many 32D cells on the gel surfaces.

To quantify the 32D cell areas on the hydrogels, individual cell areas were quantified using the phalloidin and DAPI images.

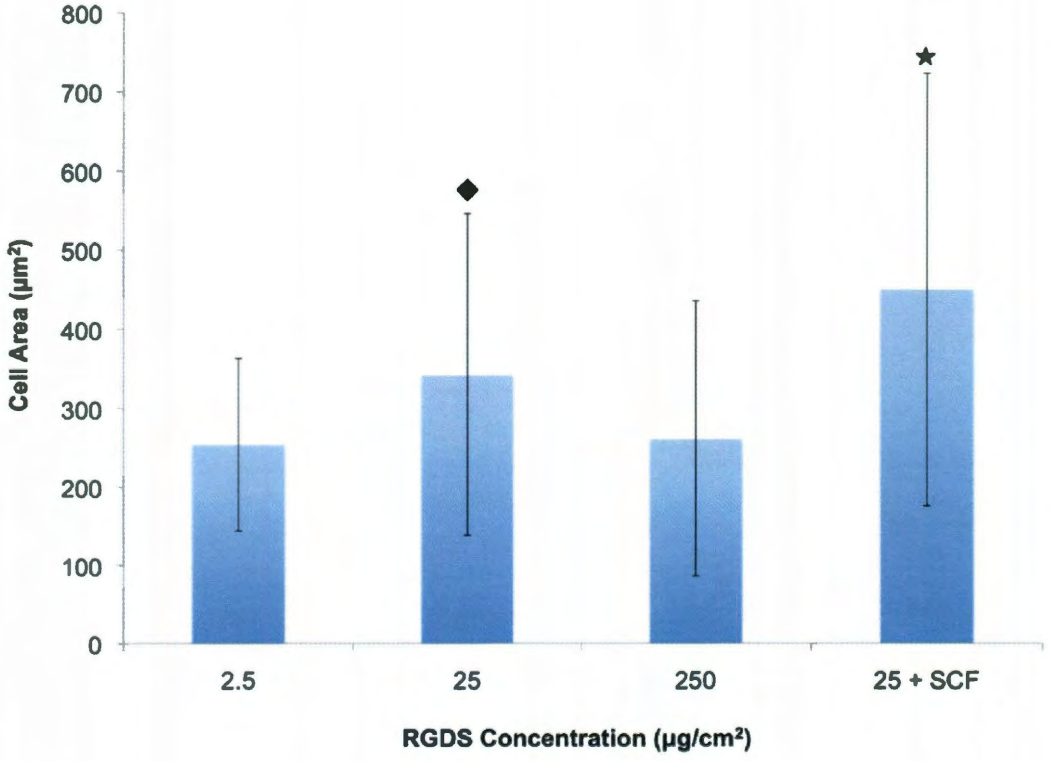

Figure 3.10: 32D cell area on bioactive hydrogels. 32D cells spread significantly on RGDS (25 μg/cm^2) with SCF (400 ng/cm^2) compared to all other groups. The wide distribution of cell size is due to the heterogeneity of 32D cells. Bars represent mean ± standard deviation (★ denotes significance compared to all other groups, ◆ denotes significance compared to 2.5 and 250 μg/cm^2 RGDS, n=58 (2.5 μg/cm^2 RGDS), 130 (25 μg/cm^2 RGDS), 863 (250 μg/cm^2 RGDS), 617 (SCF), $p < 0.05$)

When SCF was covalently immobilized on hydrogel surfaces there was a significant increase in the average cell size (Figure 3.10). The wide distribution of the data is a result of the heterogeneity of the 32D cell population. Cells are spread to different extents on the surfaces, which leads to a large range of cell sizes. To get a better sense of the distribution of cell sizes, the 32D cell areas were also plotted as histograms (Figure 3.11). The SCF hydrogels (with 25 μg/cm^2 PEG-RGDS) were compared to gels with the high RGDS concentration (250 μg/cm^2) because these gels had statistically similar numbers of adherent 32D cells.

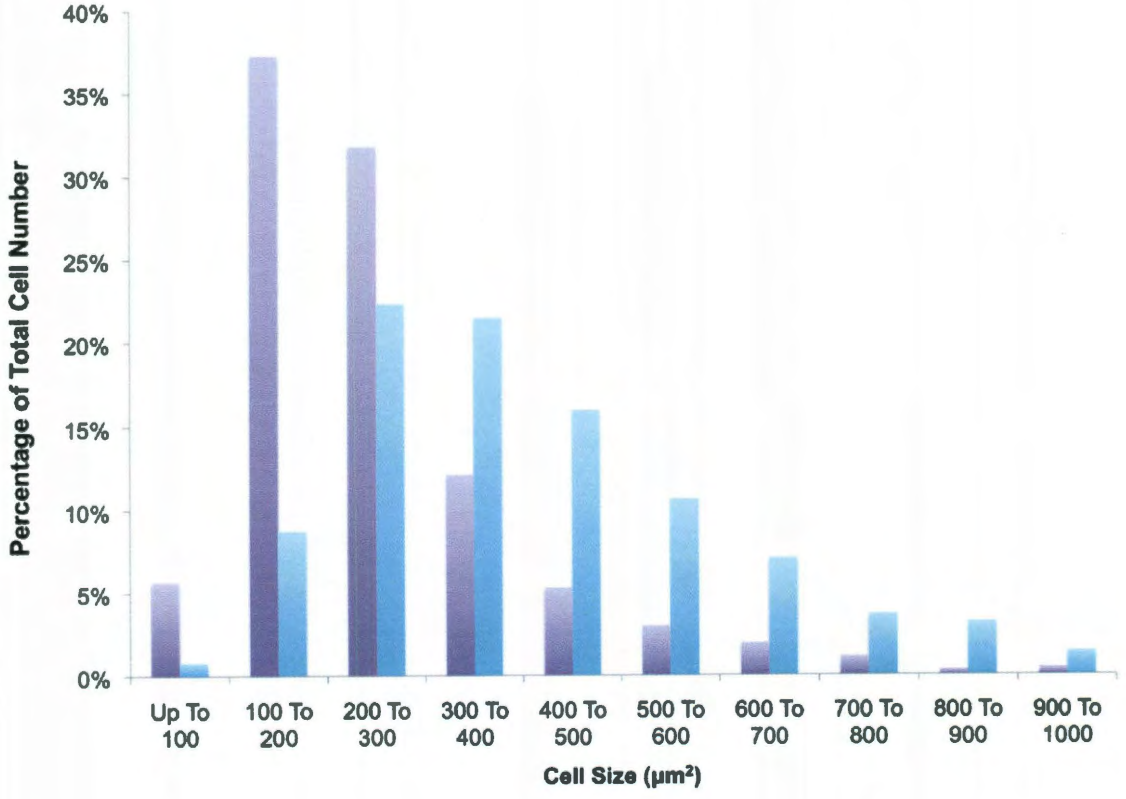

Figure 3.11: Distribution of 32D cell size on hydrogel surfaces. There is a shift in and broadening of the cell area distribution, indicating an increase in cell size on hydrogels containing SCF and 25 μg RGDS/cm^2. (**250 μg RGDS/cm^2**, **SCF and 25 μg RGDS/cm^2**)

On hydrogels modified with PEG-RGDS alone, 75% of the cells are in the 100-300 μm^2 range. With the addition of SCF, only 32% of the cells are in this range. There is a cell

area shift of approximately 100-200 μm^2 and a broadening of the distribution to include cells that are much larger, even some reaching 800-900 μm^2.

With the addition of SCF onto gel surfaces, the cells had a more spread morphology. The average cell size was larger, and the distribution of cell area was wider and shifted slightly right of PEG-RGDS alone. It is known that binding to both RGD and SCF activates multiple integrins on the cell surface (220). The integrins then cluster leading to the production of actin filaments and allowing the cells to move and spread on the gel surfaces. Integrin activation acts in a positive feedback loop causing a sustained upregulation of integrin expression and resulting in larger cell spread areas. In addition, many of these cells have a motile morphology indicated by filopodia extending outward from the cell centers. The binding of c-kit to SCF is known to promote cell motility, and we have mimicked this interaction and obtained this response by immobilizing SCF onto hydrogel surfaces (242-244). The addition of specific niche biomolecules to the gel surfaces has enabled control of 32D cell adhesion and morphology.

3.3.5 Primary Cell Expansion

To evaluate the ability of the system to expand primary HSC populations, we cultured cells in gel wells for 14 days and quantified the percent change in the total cell population. With the inclusion of SCF in the hydrogel matrix, we observed a definitive increase in hematopoietic cell number over 14 days in culture. Figure 3.12 shows phase contrast images captured at varying timepoints throughout the culture period. When primary c-kit$^+$, lin$^-$ cells were cultured on CS1 or RGDS alone, they tended to clump together in the center of the gel well. In hydrogel wells with SCF, the cells were more evenly distributed throughout the well, only forming clusters at later timepoints as

available space on the gel surface diminished.

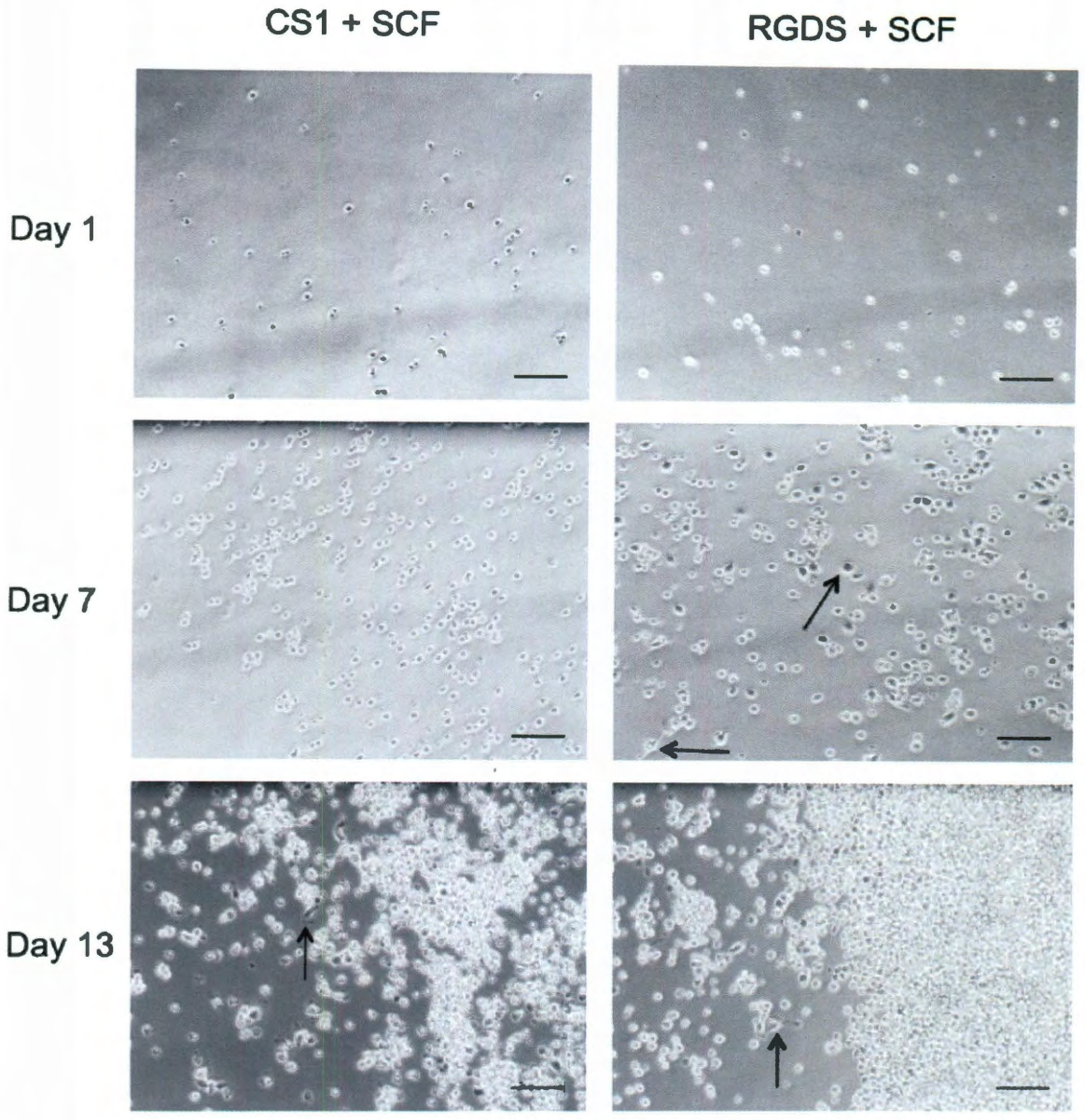

Figure 3.12: Primary cells cultured on immobilized SCF over 2 weeks. Primary cells proliferated on the hydrogels during two weeks in culture. Cells were well distributed over the hydrogel surfaces. Examples of cells with distinct morphological changes are designated with black arrows. Scale bars = 100 μm.

The primary cells were positively selected for c-kit, which binds to SCF and aids in cell adhesion (208, 220, 227-229, 232-234). Therefore, as expected, the cells were able to bind to the SCF immobilized on the surfaces reducing their tendency to bind to

each other. In addition, as aforementioned, the interaction between c-kit and SCF helps upregulate integrin expression, which leads to cell adhesion to both RGDS and CS1. This effect corresponds to 32D cell data previously shown, which indicated that the cells spread to a greater extent when hydrogel wells were modified with SCF in addition to adhesive peptides.

On gels with SCF, the primary cells proliferated extensively. Figure 3.13 shows the percent change in cell number after 14 days in culture. On gels with RGDS alone cell number increased 4558.2 ± 943.8%. The addition of SCF resulted in a significantly greater increase in primary cell number (9370.0 ± 2688.9%), and a similar trend was seen with the CS1 peptide. On CS1 alone cell number increased 4089.0 ± 1927.0% whereas the differential was 6373.4 ± 1447.3% with the addition of SCF to CS1. These results were not unexpected as SCF has been shown previously to act as a growth factor for HSCs and other hematopoietic cells, causing their proliferation (245, 246). The demonstration of an ability to trigger stem cell proliferation is significant since one of the major limiting factors in exploring new applications of HSCs in treating diseases is an insufficient HSC quantity. The inclusion of SCF in the hydrogel system drives cell proliferation, and it appears that the selection of specific fibronectin-derived peptide sequences may allow control over proliferation rates.

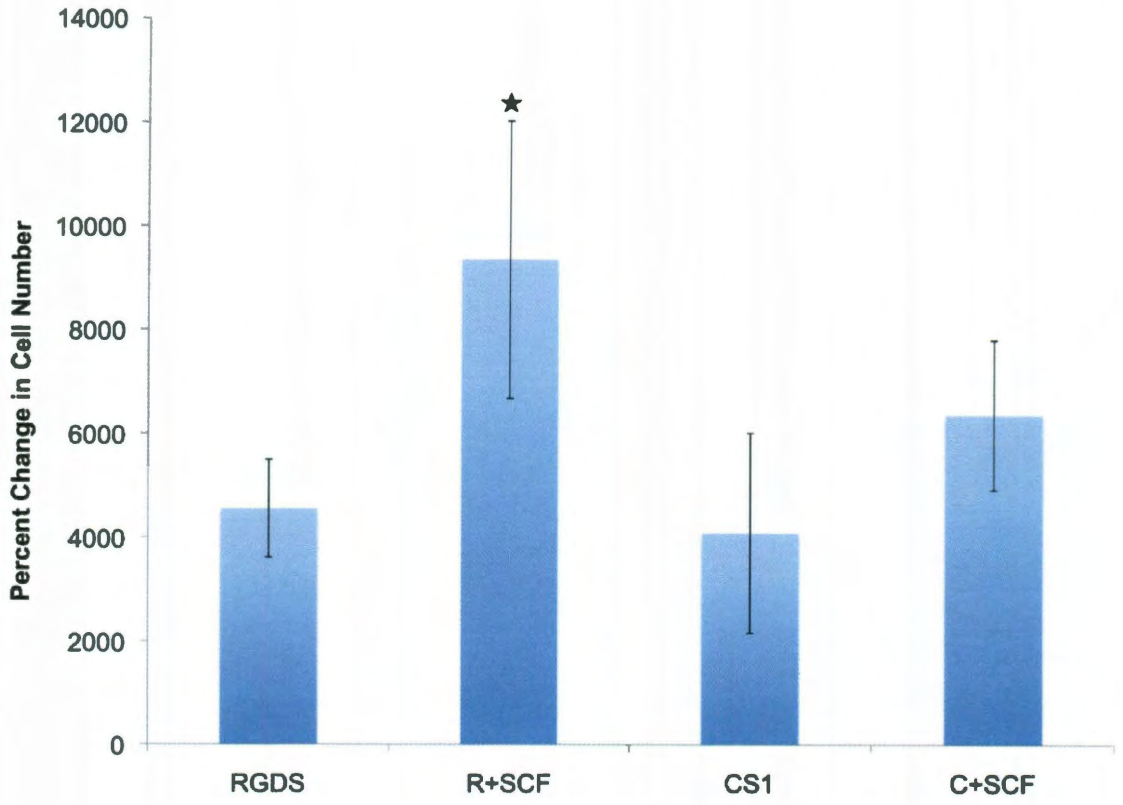

Figure 3.13: The addition of SCF to hydrogel surfaces results in primary cell expansion. On hydrogels with SCF, there was a significant increase in primary cell number after 14 days in culture compared with adhesive peptides alone. Bars represent mean ± standard deviation (★ denotes significance compared to CS1 and RGDS, n=3, $p < 0.05$)

Interestingly, the cells cultured on the surfaces with the combination of CS1 and SCF did not proliferative as extensively as those with RGDS and SCF. A previous study by Kapur *et al.* showed that hematopoietic progenitor cells proliferate in response to a combination of SCF and the α5β1 binding portion of FN (which contains RGDS) much more extensively than a combination of SCF and the α4β1 binding portion of FN (CS1) or a combination of both FN domains (247). The proliferative differences may also be due to the fact that adhesion to CS1 has been shown to expand HSCs with increased engraftment capabilities compared to the RGD fragment of FN (125). After an HSC transplant, only cells that are true LT-HSCs and have not begun to differentiate possess

the ability to engraft in host bone marrow and successfully repopulate the immune system. Again, hematopoietic cells that are less primitive proliferate at much faster rates than those that are undifferentiated. Thus, the differences in proliferation rates could indicate differences in the differentiation state of the cells. Another key factor in *ex vivo* expansion is the ability to prevent HSC differentiation. If the cells are no longer capable of self-renewal and engraftment, they will not be useful in therapeutic applications. As a result, the differentiation potential of expanded cells in the hydrogel wells was assessed with both a colony forming unit assay and flow cytometric analysis.

3.3.6 Primary Cell Differentiation

3.3.6.1 Colony Forming Unit Assay

To evaluate the functional potential of expanded cells we first conducted a colony forming unit assay. Figure 3.14 displays the distribution of colonies resulting from cells in each sample group. Compared to RGDS alone, RGDS with SCF generated more total colonies. In contrast, the addition of SCF to surfaces with CS1 decreased the number of colonies formed. However, neither of these changes was significant.

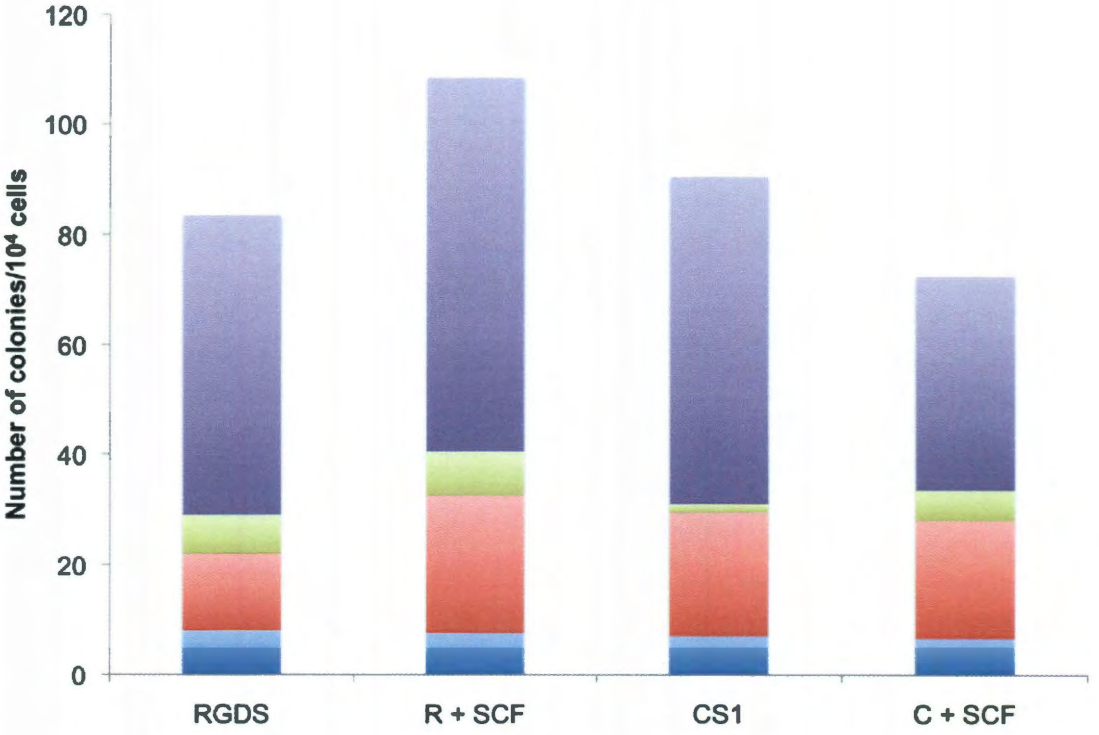

Figure 3.14: Colonies formed from expanded primary cells. Colonies formed in all groups. SCF promoted the formation of colonies from cells cultured on gels with RGDS but appeared to inhibit colony formation on gels with CS1. Neither of these changes was statistically significant. Bars are mean, n=2. (R=RGDS, C=CS1; **CFU-GEMM=Granulocyte, Erythrocyte, Megakaryocyte, Macrophage**, **CFU-GM=Granulocyte/Macrophage**, **CFU-G=Granulocyte**, **CFU-M=Macrophage**).

Figure 3.15 displays the colony data as a percentage of total colonies, and Figure 3.16 separates the data by colony type. The groups with SCF formed significantly similar numbers of GEMM colonies compared to their counterparts containing peptides only. However, in the RGDS and SCF group, the total number of colonies formed was greater than RGDS alone, meaning that quantitatively there were more undifferentiated cells in this group even though as a proportion of total cell number there were less. Conversely, the addition of SCF to the CS1 group not only reduced the percentage of primitive colonies, but also resulted in fewer primitive cells. Overall, the CS1 only group produced the highest proportion of primitive colonies, ~32%, which resulted in approximately the

same total number of primitive cells as the RGDS + SCF group when taking total cell number into account.

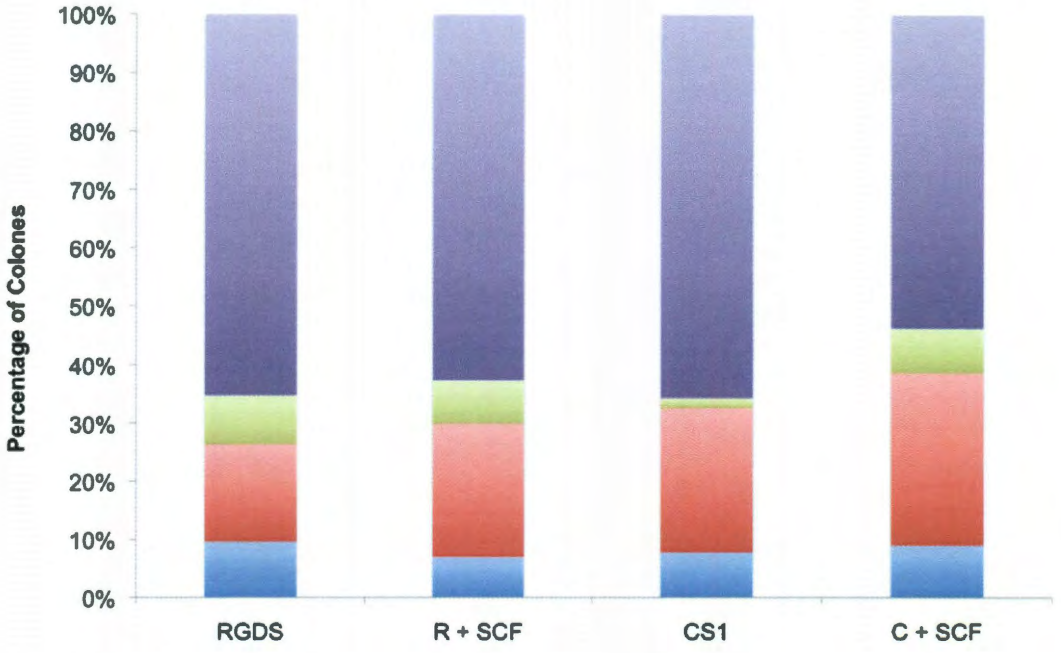

Figure 3.15: Distribution of colonies formed from cells expanded on gels with surface immobilized SCF. The percentage of primitive colonies (both GM and GEMM) is not significantly different between any of the groups. However, the addition of SCF does appear to promote the formation of GM colonies. Bars are mean, n=2. (R=RGDS, C=CS1; **CFU-GEMM=Granulocyte, Erythrocyte, Megakaryocyte, Macrophage**, **CFU-GM=Granulocyte/Macrophage**, **CFU-G=Granulocyte**, **CFU-M=Macrophage**).

The ability to form colonies, particularly those with several different cell types, indicates that the cells are in a more progenitor-like state. Each colony begins from one cell that exists in a progenitor-like state. In the assay, cells receive signals from soluble cytokines that cause them to proliferate and differentiate. Colonies that are composed of more than one type of progenitor cell indicate that the initial cell was less differentiated because it was able travel along several different pathways to form multiple cell types. The primitive state of the cell helps to predict if the cells will be capable of engraftment in the bone marrow and repopulation after implantation. In all of the sample groups, cells were maintained for 14 days with the potential to form GEMM and GM colonies. This

indicates that the system is capable of preventing the differentiation of some of the hematopoietic cells.

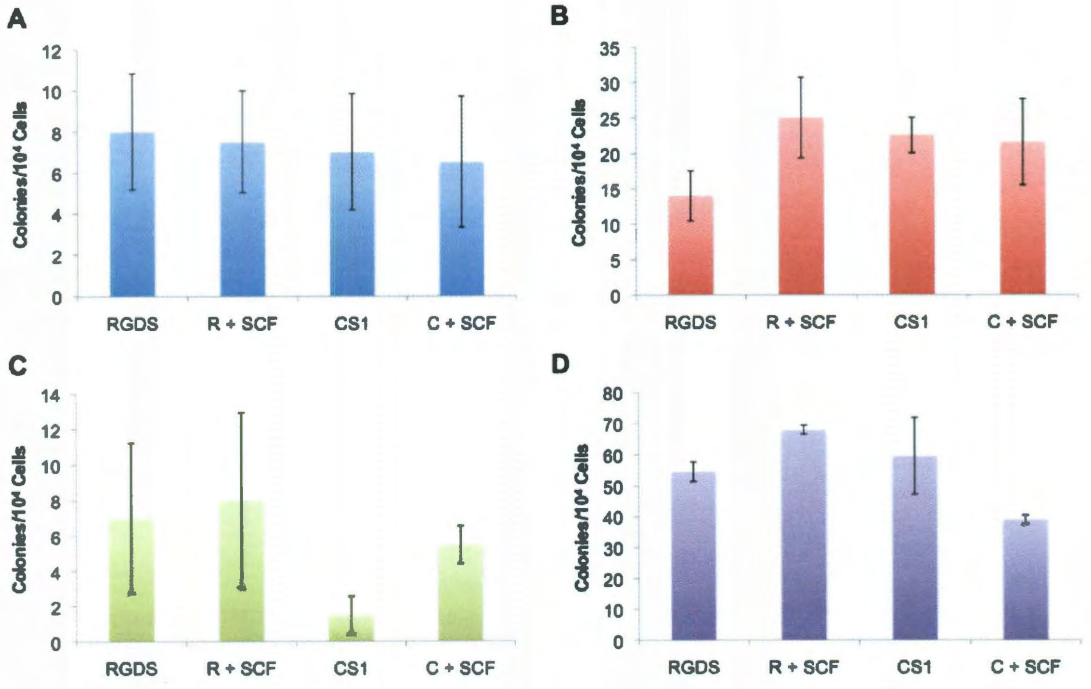

Figure 3.16: Individual colony formation organized by colony type from cells expanded on SCF functionalized hydrogels. The addition of SCF decreased GEMM formation in combination with CS1 and RGDS. There was an increase in GM formation on SCF with RGDS, but a slight decrease when SCF was in combination with CS1. However, none of these differences were significant. Bars are mean ± standard deviation, n=2. (R=RGDS, C=CS1; **A. CFU-GEMM=Granulocyte, Erythrocyte, Megakaryocyte, Macrophage, B. CFU-GM=Granulocyte/Macrophage, C. CFU-G=Granulocyte, D. CFU-M=Macrophage**)

The largest proportion of colonies in each group is macrophage. This is expected since the initial cell population of cells contained HSCs, multipotent progenitors, and even some committed progenitors. In addition, SCF-c-kit signaling can promote and is required for the differentiation of progenitor cells. This may be why we observed no significant differences in GM or GEMM colony formation between groups. It is hypothesized that if a purer population of HSCs is utilized, the number of less potent colonies may decrease. In contrast, SCF can also promote the self-renewal of HSCs, which is evident in the RGDS and SCF group. Though, the proportion of each type of

colony is similar compared to the RGDS only group, there is an increase in total colony number which means that all populations of cells are increasing, a condition that is only possible if the HSCs are self-renewing and not differentiating. Otherwise, there would be a significant shift in the proportion of macrophage and granulocyte colonies. It is interesting that the opposite trend occurs on the sample with both CS1 and SCF. Proportionally, there is an increase in macrophage and granulocyte colonies in addition to a decrease in the number of colonies formed, which means that on this surface cells appear to be losing their multipotent capabilities. The signaling mechanisms that lead to these observed differences between combinations of SCF with either CS1 or RGDS are unclear.

3.3.6.2 Flow Cytometry

Flow cytometry analysis was performed to complement the results obtained in the colony assay. Cells were sorted for a population with known repopulation capabilities: c-kit$^+$, Sca1$^+$, lin$^-$ (KSL). Plots generated from this data can be seen in Figure 3.17 (RGDS + SCF) and Figure 3.18 (CS1 + SCF). The data shows that most of the cells are c-kit$^-$, Sca1$^-$, lin$^+$ though a large proportion of total cells are still c-kit$^+$ and a majority of the lin$^-$ cells are c-kit$^+$. This was expected because many hematopoietic cells express c-kit until they become lineage-restricted progenitors (Figure 1.3). However, after 14 days in culture, a KSL population remains, indicating that the culture system is able to maintain this primitive population. This result also corresponds to the colony data, where a high number of colonies generated from more differentiated cells (such as macrophages), which could correlate with the large c-kit$^+$ population.

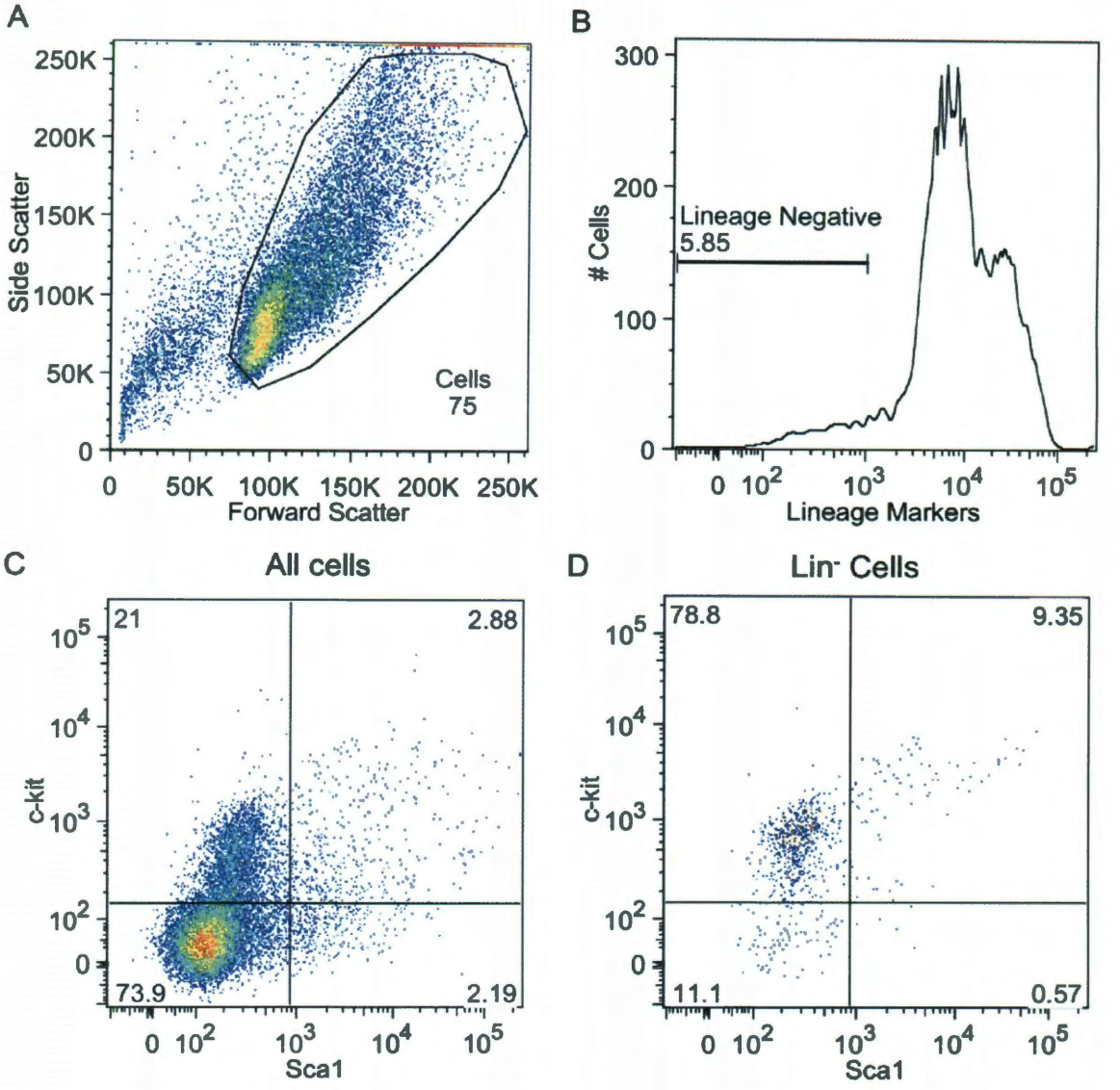

Figure 3.17: Flow cytometry analysis of c-kit$^+$, lin$^-$ cells after 14 days in culture on PEG-RGDS with PEG-SCF. A. Particles were gated to count only cells. B. Cells were gated to include those that were lin$^-$. C. A plot of all cells showing the fluorescence intensities of the Sca1 and c-kit markers. Cells were gated to delineate between positive and negative cells. D. A plot of lineage negative cells gated similarly to those in C. Numbers on the graphs indicate the percentage of cells falling within that gate.

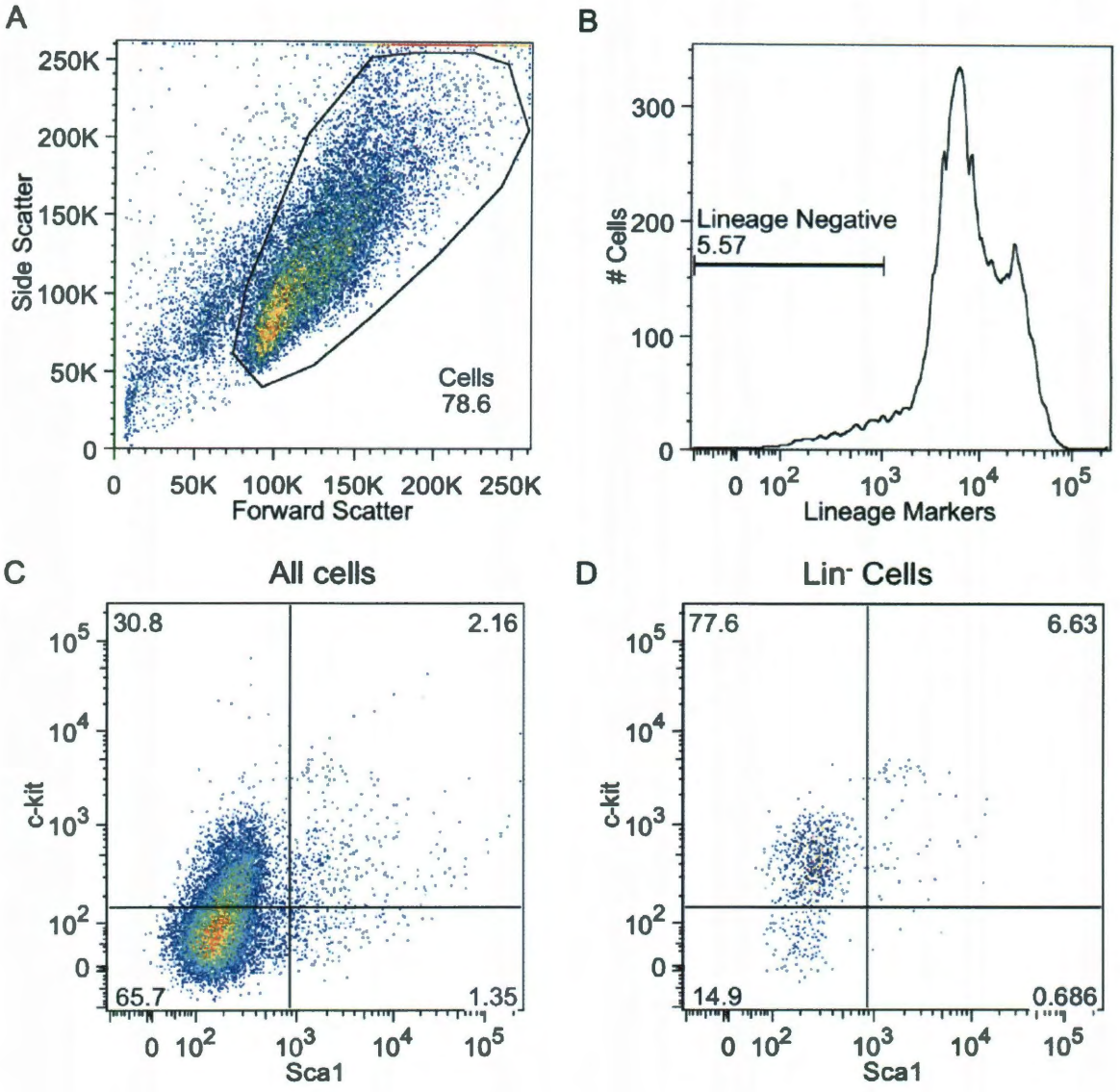

Figure 3.18: Flow cytometry analysis of c-kit$^+$, lin$^-$ cells after 14 days in culture on PEG-CS1 with PEG-SCF. A. Particles were gated to count only cells. B. Cells were gated for lin$^-$. C. All cells gated to delineate between positive and negative cells. D. A plot of lineage negative cells gated similarly to those in C. Numbers on the graphs indicate the percentage of cells falling within that gate.

In the quantification of this data, the percent changes in both the c-kit$^+$, lin$^-$ and the KSL populations significantly increased when SCF was added to the RGDS-containing hydrogel matrix, rising from 453.8 ± 65.0% to 1877.6 ± 1029.6% and 106.7 ± 99.2% to 660.0 ± 376.8% respectively (Figures 3.19 and 3.20). This corresponds directly with

what was observed in the colony assay with the increase in GM and GEMM colony numbers when taking total cell number into account. The percent change in c-kit$^+$, lin$^-$ and KSL number also increases on CS1 hydrogels with the addition of SCF from 308.4 ± 130.7% to 730.9 ± 338.3% and from 2.0 ± 84.1% to 169.9 ± 98.5% respectively, but these changes were not significant (Figures 3.19 and 3.20). This is contradictory to the results seen in the colony assay. This leads us to believe that the relationship between CS1 and SCF may be more complex and require further investigation.

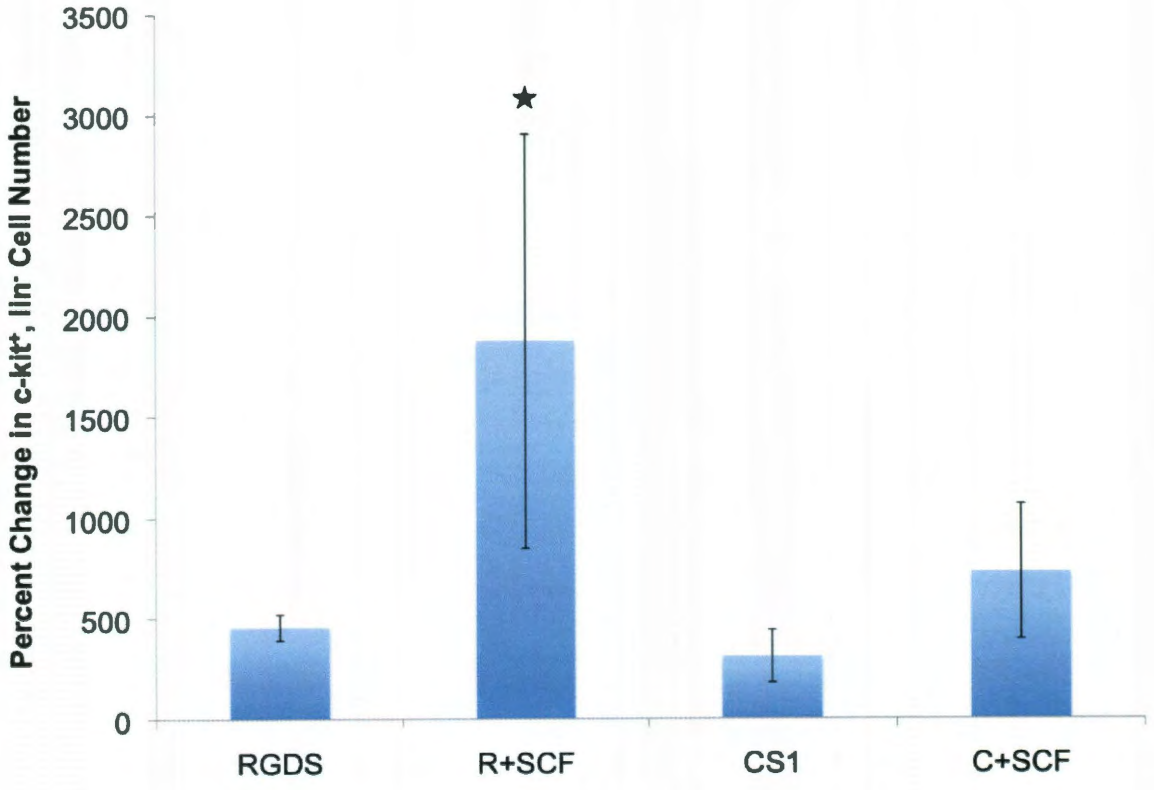

Figure 3.19: SCF immobilized on gel surfaces results in an increase in the c-kit$^+$, lin$^-$ population. Bars represent mean ± standard deviation. (R = RGDS, C = CS1), (★ denotes significance compared to RGDS and CS1, n=3, $p < 0.05$)

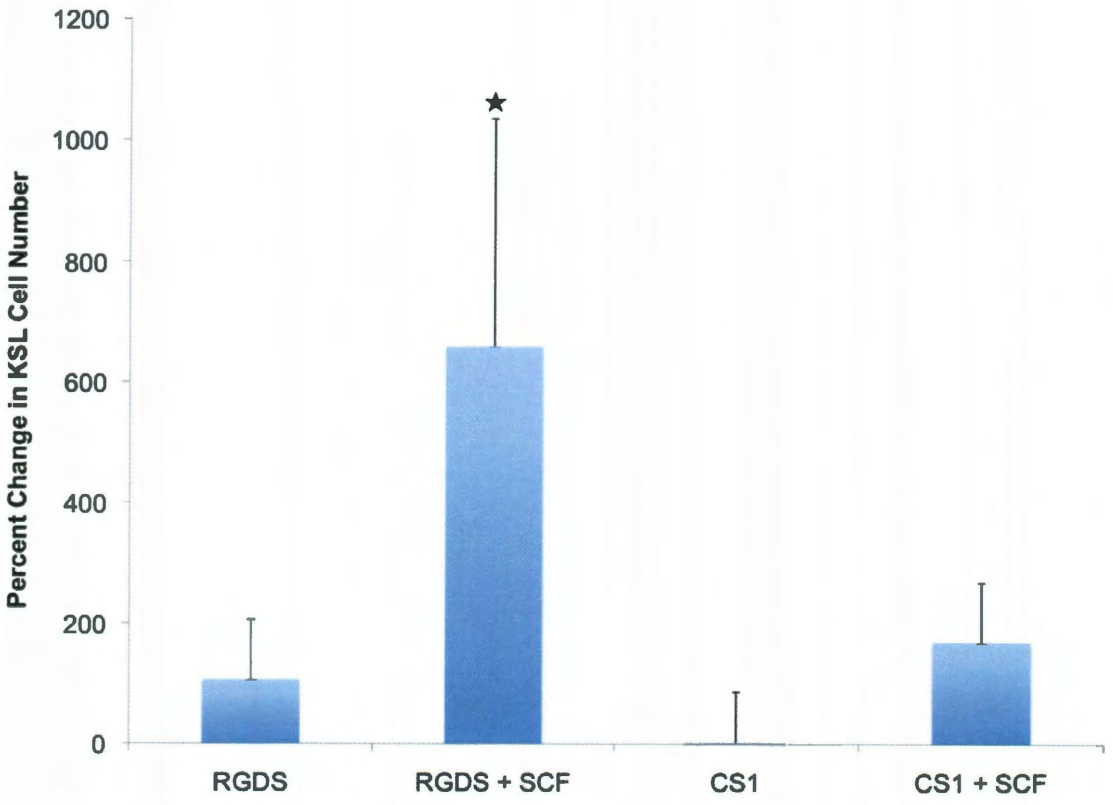

Figure 3.20: The addition of SCF to hydrogel wells causes a significant increase in the KSL population. Bars = mean + standard deviation. (★ denotes significance compared to RGDS and CS1, n=3, $p < 0.05$)

SCF is known to signal proliferation of multiple hematopoietic lineages but can also maintain HSCs in an undifferentiated state for short time periods especially in combination with other soluble cytokines (248). In its membrane-bound form, SCF is able to maintain HSCs in culture for two weeks longer than in its soluble version (209). We observed this in the hydrogel group containing both RGDS and SCF, where cells were triggered to proliferate but retained their ability to form primitive colonies, and a small population of cells expressed the KSL markers after 2 weeks in culture.

The combination of CS1 and SCF on hydrogel surfaces had varying results in terms of the analysis of differentiation potential. A previous study demonstrated that adhesion to CS1 is capable of preventing differentiation to a greater extent then RGDS

(125). This may be due to the fact that more primitive HSCs adhere specifically to CS1 (122). This was seen in the colony assay where a higher proportion of colonies were primitive (GM or GEMM). However, a similar trend was not observed in the expression of surface markers indicative of a HSC population. In addition, when SCF was added to the surfaces with CS1, we obtained contradictory results. In the colony assay, we observed a decrease in colony numbers as well as an increase in the proportion of more differentiated colonies. This could indicate that surface markers do not necessarily correlate with the colony-forming capabilities of HSCs. Baldridge *et al.* demonstrated that they could expand primitive KSL populations *in vivo* with a cocktail of cytokines, but these cells had reduced engraftment capabilities in subsequent transplantation assays despite the expression of these specific surface markers (93). These results stress the need for multiple *in vitro* and *in vivo* evaluation techniques.

3.4 Conclusions

The results in this chapter demonstrate the ability to immobilize SCF onto hydrogel surfaces at physiologically significant levels while maintaining its bioactivity. 32Ds adhere to surfaces with covalently bound SCF and RGDS at significantly greater levels than on hydrogels with RGDS alone. The cells were also able to spread to a greater extent on these surfaces and their cell area increased by 100-300 μm^2 on average. However, there was not a significant difference in cell proliferation on these samples. This study emphasizes the importance of SCF-c-kit signaling on cell adhesion. It also shows that we are capable of controlling HSC behavior through the design of our hydrogel scaffold.

With primary cells, significant increases in total cell number were observed when SCF was added to either RGDS or CS1 samples, though cells proliferated to a greater extent on samples containing the RGDS peptide. In the RGDS group, there were significant increases in primitive populations in the presence of SCF as evidenced by both the colony assay and flow cytometric analysis. These increases were seen across all progenitor populations demonstrating that SCF is capable of expanding hematopoietic populations without adversely affecting their differentiation potential. Cells cultured on CS1 containing hydrogels had varying results. In the colony assay, both the colony number and the proportion of primitive colonies decreased. However, the flow cytometric analysis showed an opposite trend. This inconclusive data prompts further investigation into the relationship between SCF and CS1 signaling.

In conclusion, these studies show that HSC behavior can be influenced by careful design of the scaffold. In addition, they demonstrate the sensitivity of these cells to their environment and stress the importance of critical analysis of the cells after expansion. In the future, *in vivo* experiments must be conducted to validate that the expanded cells are capable of reconstitution.

Chapter 4: The Effects of Immobilized SDF1α on Hematopoietic Cell Behavior in Hydrogel Wells

4.1 Background

Stromal derived factor 1α (SDF1α) is a chemokine that can recruit HSCs to the bone marrow as well as retain them there. This chapter focuses on work conducted to investigate the effects of the chemokine SDF1α on hematopoietic cell behavior. 32D cells and a primary murine hematopoietic cell population (c-kit$^+$, lin$^-$) were cultured in hydrogel gel wells with surface immobilized SDF1α in combination with one of the adhesive ligands CS1 or RGDS. Cell adhesion, proliferation, spreading, and differentiation potential were quantified to characterize expanded hematopoietic cell populations.

4.1.1 Stromal Derived Factor 1α

SDF1α was incorporated into the hydrogel matrix due to its substantial role in HSC homing to and lodging in the stem cell niche. SDF1α is a small, 8 kDa cytokine consisting of 89 amino acids (Figure 4.1). It was first isolated from bone marrow stromal cell lines and characterized as a growth factor for pre-B cells (249). It belongs to the chemokine superfamily, and similarly to SCF, it can be found in both membrane bound and soluble forms in both the endosteal and vascular niche (250). SDF1α binds to CXC chemokine receptor 4 (CXCR4) on HSC membranes and is secreted and expressed by osteoblasts, endothelial cells, fibroblasts, and other stromal cells.

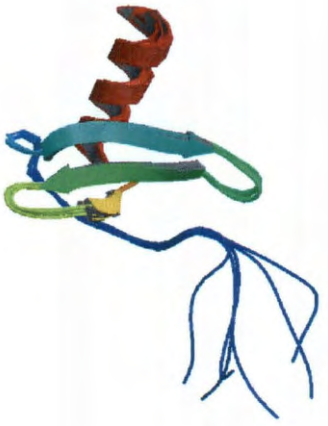

Figure 4.1: Structure of SDF1α. Image adapted from (251).

HSCs migrate selectively towards SDF1α and no other chemokines (252). This property means that SDF1α plays an integral role in HSC homing to the bone marrow niche as well as HSC mobilization to injury sites (253-255). In fact, HSCs treated with blocking antibodies to CXCR4 were unable to engraft after transplant (256). SDF1α is also expressed at high levels on the surfaces of reticular cells in the niche. Signaling between membrane-bound SDF1α and CXCR4 has been shown to maintain a pool of HSCs in an undifferentiated state *in vivo*, and it has been proposed that SDF1α supports the self-renewal of HSCs (67). SDF1α is also known to activate integrins on HSC surfaces and has been shown to stop rolling HSCs in flow experiments (239, 240). The ability of SDF1α to both attract HSCs and promote integrin expression helps to recruit HSCs and retain them in the niche (28, 34, 56).

4.1.2 Use of SDF1α in Biomimetic Scaffolds

SDF1α has not been used extensively in the culture of HSCs. Most *in vitro* experiments focus on HSC mobilization and migration in response to SDF1α or the effects of SDF1α and CXCR4 signaling on HSC engraftment. Bladergroen *et al.* worked

to create an *in vivo* niche by entrapping SDF1α within collagen scaffolds and then implanting the scaffolds subcutaneously in mice. To gauge the success of the implants, the scaffolds were excised after 5 weeks and the cells populating the scaffold were counted and characterized. Implants with SDF1α were populated with more hematopoietic cells than control scaffolds (257). Though this technique demonstrates a great deal of promise in supporting HSC development *in vivo*, it requires a source of HSCs within the transplant recipient to be successful and thus, may not be applicable in the treatment of certain diseases. In addition, some work has been done utilizing SDF1α in biomaterial scaffolds for wound healing and angiogenesis applications (258-263). In one study, an alginate hydrogel scaffold with encapsulated SDF1α was used to treat wounds created in the dorsal skin of mice and resulted in more rapid wound repair in seven days, as evaluated by remaining wound size, than control scaffolds (260). These studies demonstrate the ability to incorporate SDF1α into a scaffold while maintaining its bioactivity, though in all of these studies SDF1α was not covalently immobilized into the scaffold.

The work in this chapter takes advantage of the homing and lodging effects of SDF1α. SDF1α was immobilized onto hydrogel surfaces to retain HSCs on the gel surface by activating both the CXCR4 receptor and the VLA-4 and VLA-5 integrins, which could in turn promote adhesion of HSCs to CS1 and RGDS peptides also present on the surface. Hidalgo *et al.* demonstrated that SDF1α could modulate HSC adhesion by upregulating the expression of the VLA-4 integrin (264). Peled *et al.* observed that SDF1α activated both the VLA-4 and VLA-5 integrins on primary HSCs and that these integrins played a critical role in transendothelial migration during the homing process

(239). Figure 4.2 shows a schematic of the interplay between SDF1α and the VLA-4 and VLA-5 integrins. The ability to maintain HSCs close to the hydrogel surface is beneficial in HSC culture. By covalently tethering SDF1α to hydrogel surfaces, HSCs can be retained on the gel surface, enabling them to interact with other biomolecules, such as RGDS and CS1, which are also immobilized on the surface and can aid in HSC adhesion and expansion. In addition, SDF1α itself could prove beneficial in the maintenance of primitive HSC populations.

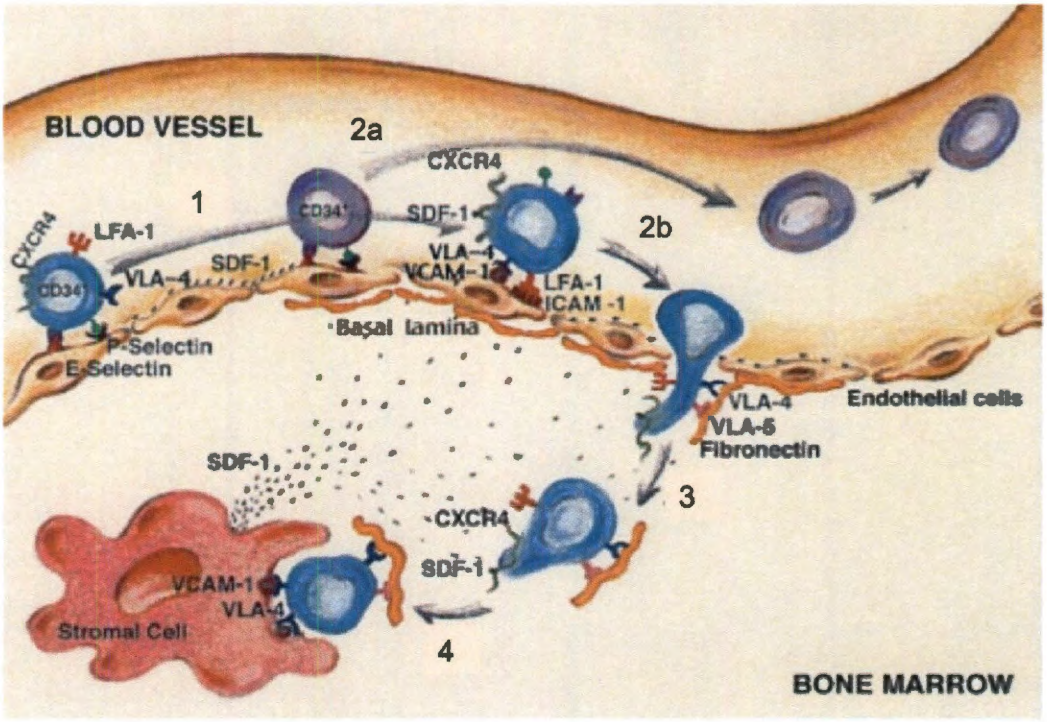

Figure 4.2: Process of transendothelial migration of HSCs triggered by the release of soluble SDF1α. 1. Circulating $CXCR4^{+}$ HSCs are slowed by interactions with selectins expressed by endothelial cells (ECs) in the bone marrow. 2a. Cells that do not express CXCR4 remain in the circulation following SDF1α stimulation. 2b. After stimulation by SDF1α and subsequent upregulation of LFA-1 and VLA-4 integrin expression, HSCs stop rolling and adhere to ECs. 3. The activation of CXCR4 increases both VLA-4 and VLA-5 expression and leads to transendothelial migration through adhesion to fibronectin and results in 4. The return of HSCs to the stem cell niche (homing). Figure adapted from (240).

4.2 Materials and Methods

All materials were obtained from Sigma unless otherwise noted.

4.2.1 Polymer Synthesis and Characterization

4.2.1.1 PEG-DA, PEG-RGDS, and PEG-CS1

PEGDA, PEG-RGDS, and PEG-CS1 were synthesized as described in Sections 2.2.1.1, 2.2.1.2, and 2.2.1.3.

4.2.1.2 PEG- SDF1α

To PEGylate SDF1α, the same technique was employed as for PEG-SCF (Section 3.2.1.3). 3400 MW Acrylate PEG-SVA was reacted with carrier-free murine SDF1α (R&D) at a molar ratio of 18:1 (PEG-SVA:SDF1α). The reactions were conducted in PBS (pH 8.0) overnight at 4° C. To determine the degree of conjugation, a Western blot was performed on the PEGylated and unmodified forms of the proteins using a 15% Tris-HCl precast polyacrylamide gel. The antibodies that were used included a rabbit polyclonal antibody to SDF1α (Abcam) and a secondary goat polyclonal antibody against rabbit IgG conjugated with horseradish peroxidase (Abcam). To detect the proteins on the blot, the ECL chemiluminescent Western blotting analysis system was applied, and chemiluminescent images of the blot were captured using an LAS 4000.

4.2.1.3 Bioactivity of PEG-SDF1α

To evaluate the bioactivity of PEGylated SDF1α, a migration assay utilizing transwells with 3 μm pores was performed. This pore diameter is required due to the relatively small size of hematopoietic cells (10 μm in diameter) and has been used in previous work to study hematopoietic cell migration (265). Three media formulations were put into the well plate below the transwells: control media (RPMI 1640 containing 10% heat-inactivated FBS, 10% IL-3 culture supplement, and 1% penicillin, streptomycin), control media with SDF1α (100 ng/ml), and control media with PEG-

SDF1α (100 ng SDF1α/ml). 32D cells were seeded into the top of the transwell in the control media at 6000 cells/cm^2. Images of the bottom of the well plate were taken after 72 hrs. in culture (37°C, 5% CO_2), and migrated cells were counted using ImageJ software.

4.2.1.4 Surface Immobilization and Quantification of SDF1α

6 kDa PEG-DA hydrogel wells were fabricated as described in Section 2.2.2.1. PEG-SDF1α was covalently conjugated to the surfaces of hydrogel wells in the same fashion as PEG-SCF (Section 3.2.1.5). A solution containing PEG-SDF1α, either PEG-CS1 or PEG-RGDS, and the photoinitiator 2,2-dimethoxy-2-phenyl acetophenone (10 μl/ml of polymer solution) in HBS was made. 10 μl of the solution was added to each well to obtain surface concentrations of 400 ng SDF1α per cm^2 and 25 μg or 250 μg of PEG-peptide (CS1 or RGDS) per cm^2. Groups of four wells were exposed together underneath long wavelength UV light (365 nm, 10 mW/cm^2) for 3 min. to crosslink the biomolecules into place. To determine the amount of SDF1α on surfaces the 10 μl solution in each gel well was collected after crosslinking and analyzed using the Quantikine ELISA kit for SDF1α (R&D) similarly to the process described in Section 3.2.1.6. Gels were soaked in PBS containing 0.1% NaN_3 overnight to allow any uncrosslinked protein to diffuse out of the gel. The soak solution was also assayed with the ELISA kit.

4.2.2 Cell Maintenance

4.2.2.1 32D Cell Culture

32D cells were kept in culture as previously described in Section 2.2.3.1.

4.2.2.2 Primary c-kit$^+$, lin$^-$ Cell Isolation and Culture

Primary c-kit$^+$, lin$^-$ cells were isolated from murine whole bone marrow and maintained as noted in Section 2.2.3.2.

4.2.2.3 Cell Seeding into Hydrogel Wells

32D cells were seeded into the hydrogel wells at 5000 cells/cm^2. The experimental groups consisted of wells with 400 ng/cm^2 SDF1α and 25 μg/cm^2 RGDS. PEG-DA and PEG-RGDS gels (25 and 250 μg/cm^2) served as controls. Each group consisted of 4 gel wells. 32Ds were cultured for 6 days at 37°C and 5% CO_2 with media renewal every 2 to 3 days.

c-kit$^+$ lin$^-$ cells were seeded in gel wells ([SDF1α]=400 ng/cm^2, [RGDS]=25 μg/cm^2 or ([SDF1α]=400 ng/cm^2, [CS1]=25 μg/cm^2) at 13,000 cells/cm^2. Gel wells with only RGDS or CS1 (25 μg peptide/cm^2) served as controls. Each group consisted of 4 gel wells. Media was added around gels to keep them hydrated. Cells were kept in culture for 14 days at 37°C and 5% CO_2 with media renewal every 2 to 3 days. After culture, the cells from each group were combined so that enough cells were available for flow cytometry. The experiment was conducted a total of three times.

4.2.3 Evaluation of Hematopoietic Cells in Culture

The adhesion, proliferation, and spreading of 32D cells were quantified as stated in Sections 2.2.4.1-2.2.4.3 to determine the effects of SDF1α on these properties.

c-kit$^+$ lin$^-$ cell expansion and differentiation potential were evaluated similarly to the methods in Sections 2.2.4.3-2.2.4.5

4.2.4 Statistical Analysis

One-way ANOVAs and Tukey's post-hoc analyses were performed to evaluate statistical differences between groups in all studies using a 95% probability level ($p<0.05$).

4.3 Results and Discussion

4.3.1 Polymer Synthesis and Characterization

4.3.1.1 PEG- SDF1α

Western blot analysis (Figure 4.3) confirmed PEGylation of SDF1α. A band can be seen in the protein-only lane at 8 kDa, whereas, in the PEG-SDF1α lane, there is a shift in molecular weight to 14 kDa. Additionally, there is a smear in this lane indicating that the protein has been decorated with multiple PEG chains.

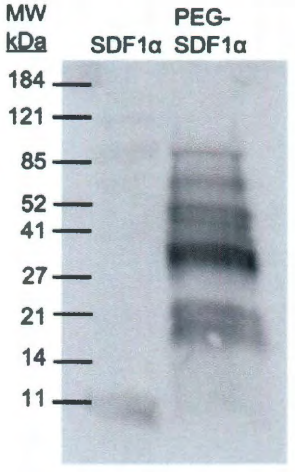

Figure 4.3: Western blot of SDF1α and PEG-SDF1α. There is a band present in the SDF1α lane near 8 kDa. In the PEG-SDF1α lane you can see a smear beginning around 14 kDa indicating the protein has been successfully conjugated to PEG chains. (MW=molecular weight)

4.3.1.2 Bioactivity of SDF1α

After confirming successful PEGylation, a migration assay was performed to determine if the PEGylated form of SDF1α maintained its bioactivity. The addition of SDF1α and PEG-SDF1α to the media promoted significant 32D cell migration through

the transwell membrane (Figure 4.4). However, the presence of the PEG chains did appear to diminish some of the SDF1α bioactivity. In the future, the molar ratio of PEG-SVA to SDF1α can be optimized to reach native levels of bioactivity. In addition, the concentration of SDF1α can be increased to compensate for the decrease in bioactivity.

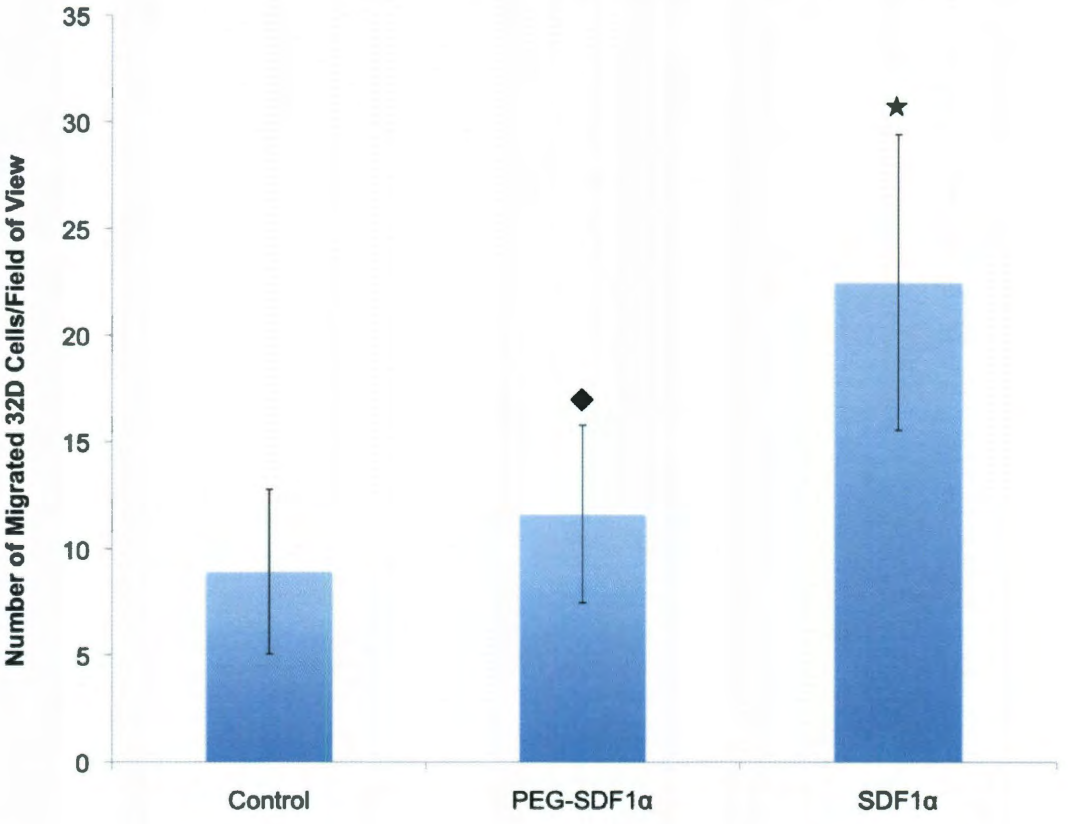

Figure 4.4: Bioactivity of PEGylated SDF1α. 32D cells were seeded into the top well of a transwell plate. The bottom well contained control media, control media with SDF1α, or control media with PEG-SDF1α. After 48 hrs., cells that migrated to the bottom well were counted. Cells migrated significantly in response to SDF1α and PEG- SDF1α compared to the control. Data is displayed as mean ± standard deviation. (★ denotes significance compared to control and PEG-SDF1α, ◆ denotes significance compared to control, n=54, $p < 0.05$)

4.3.1.3 Quantification of SDF1α on Gel Surfaces

To validate that SDF1α was covalently immobilized on hydrogel surfaces we conducted an ELISA on the conjugation and gel soak solutions after surface conjugation.

The surface concentration of SDF1α was calculated to be 98% of the initial protein added to the surface: 88.3 ± 0.5 ng/cm^2.

4.3.2 32D Cell Adhesion

We observed a significant increase in adherent 32D cells when SDF1α (400 ng/cm^2) was added to the surfaces of gels with 25 μg/cm^2 RGDS compared to RGDS alone (Figure 4.5). After 48 hrs., the number of cells on gels with SDF1α was 6577.2 ± 2623.1 cells/cm^2 compared to 2278.9 ± 1775.6 cells/cm^2 on RGDS alone. The activation of the CXCR4 receptor on HSC surfaces has been shown previously to activate both the VLA-4 and VLA-5 receptors and help retain HSCs in the niche (240). We can continuously upregulate the expression of both of these integrins by surface immobilizing SDF1α onto the hydrogel. This stabilization not only prevents protein from being endocytosed or otherwise cleared away, but it also causes the SDF1α to act similarly to a membrane bound protein as opposed to a soluble cytokine, which could increase cell motility away from the hydrogel. In turn, the interaction of the CXCR4 receptor with SDF1α on the gel surface allows for close proximity of the upregulated VLA-5 integrins to the gel surface where they can bind to RGDS.

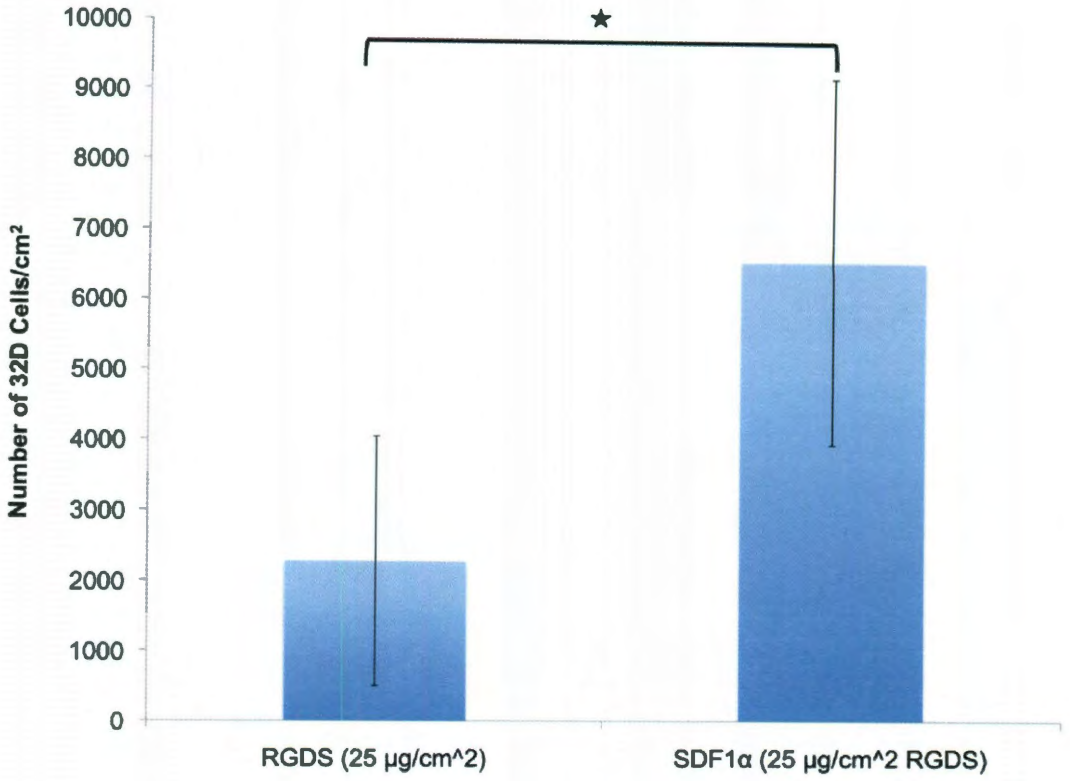

Figure 4.5: 32D cell adhesion on surfaces with immobilized SDF1α. On gels with RGDS concentrations of 25 µg/cm^2, there was a significant increase in 32D cell adhesion when SDF1α was also present on the surface. Data is displayed as mean ± standard deviation. (★ denotes significance, n=4, $p < 0.05$)

Interestingly, the addition of SDF1α to gel surfaces with higher RGDS concentrations (250 µg/cm^2) did not result in an increase in 32D cell adhesion (Figure 4.6). Recall that a similar response was seen with the SCF protein in Chapter 3. This finding could be attributed to the presence of more RGDS molecules, which allow the 32Ds to adhere to the gel through multiple integrins. In addition, the activation of RGDS can act as a positive feedback loop resulting in the expression of more VLA-5 integrins thus promoting more cell adhesion (127). As a result, the addition of SDF1α to the surface does not increase cell adhesion because the cells are already expressing sufficient integrins to bind to the surface at a high degree.

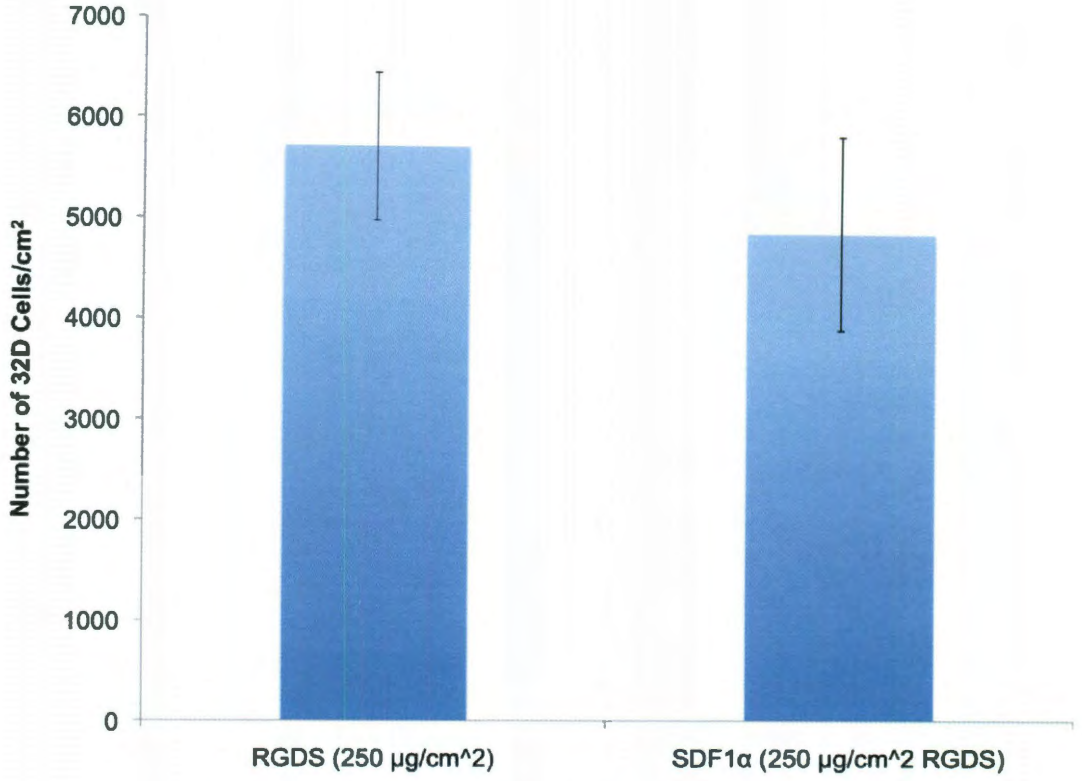

Figure 4.6: Cell adhesion on gels with high RGDS concentrations (250 µg/cm^2). The addition of SDF1α to the gel surfaces does not significantly affect cell adhesion. Data is displayed as mean ± standard deviation. (n=4)

4.3.3 32D Cell Proliferation

32D cell proliferation was evaluated by calculating the increase in adherent cells between days 2 and 4 and days 4 and 6 (48 hr. time periods) utilizing image analysis. The addition of SDF1α did not promote the proliferation of 32D cells (Figure 4.7). On gels with only RGDS the increase in cell number over 48 hrs. was 48.1 ± 10.2% while the percent increase on gels with SDF1α was 24.2 ± 13.3%. This could be due to a number of factors. Firstly, the concentrations of cells on the surfaces were very different. As shown by the adhesion data, there were twice as many cells on gels with SDF1α compared to those with RGDS alone. The higher density of the cells on the gel surfaces may be negatively influencing their proliferation through cell-cell signaling. Limited space on the gel surface may also result in proliferating cells leaving the surface. 32D

cells are a semi-adherent cell line that can survive in suspension, and the number of cells in the media was not quantified. Another possible explanation is that cells may not be able to proliferate as rapidly if they are adhering strongly to the gel surface (161, 266). As aforementioned, this has been previously reported on PEG hydrogels where smooth muscle cell proliferation decreased as the concentration of adhesive ligand increased (161). Furthermore, the cells may have returned to a more quiescent state. SDF1α has been shown to maintain a pool of HSCs *in vivo*, and signaling via the CXCR4 receptor could be turning on signaling pathways involved in HSC homeostasis during which HSCs proliferate quite slowly (35). However, the difference between the two proliferation rates was not significant and these alternative explanations require further study to warrant any definitive conclusions.

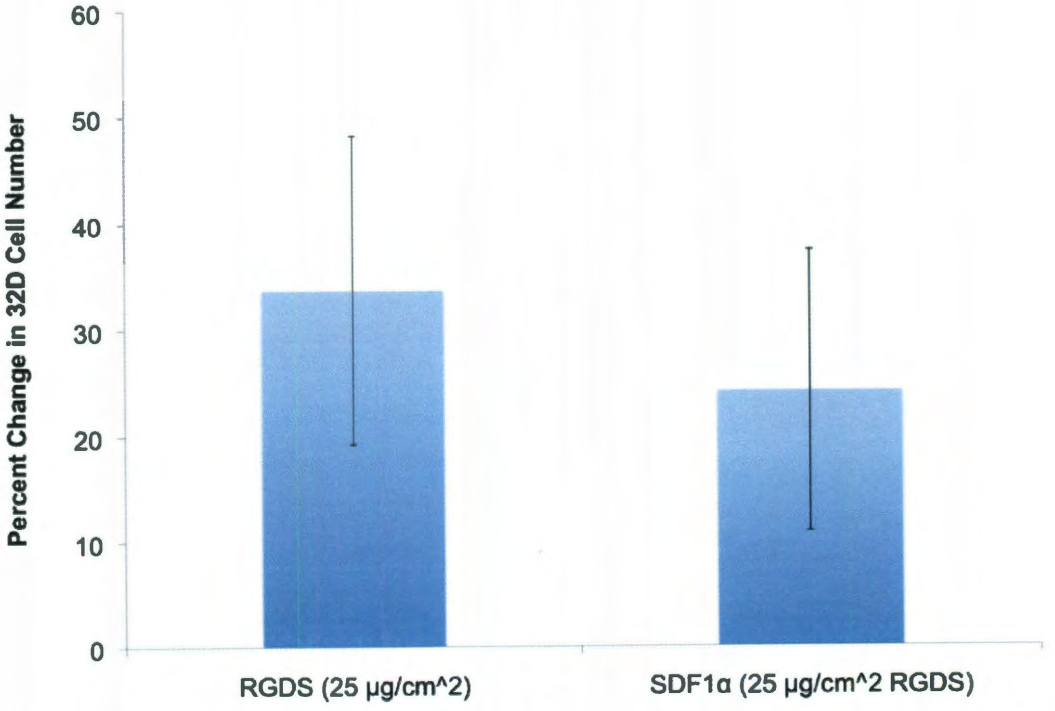

Figure 4.7: 32D cell growth over 48 hrs. on hydrogels with immobilized RGDS and SDF1α. Cell proliferation was not significantly affected by the addition of SDF1α; however, the proliferation rate did decrease slightly. Data is displayed as mean ± standard deviation. (n=4)

4.3.4 32D Cell Spreading

To visualize and quantify 32D cell spreading on surfaces with RGDS and SDF1α, cells were stained with DAPI (nuclei) and phalloidin (actin). Figure 4.8 shows representative images of cells spreading across the gels. Compared to cells on PEG-RGDS, the cells on gels with SDF1α are more spread and have filopodia extending from their centers (denoted by white arrows).

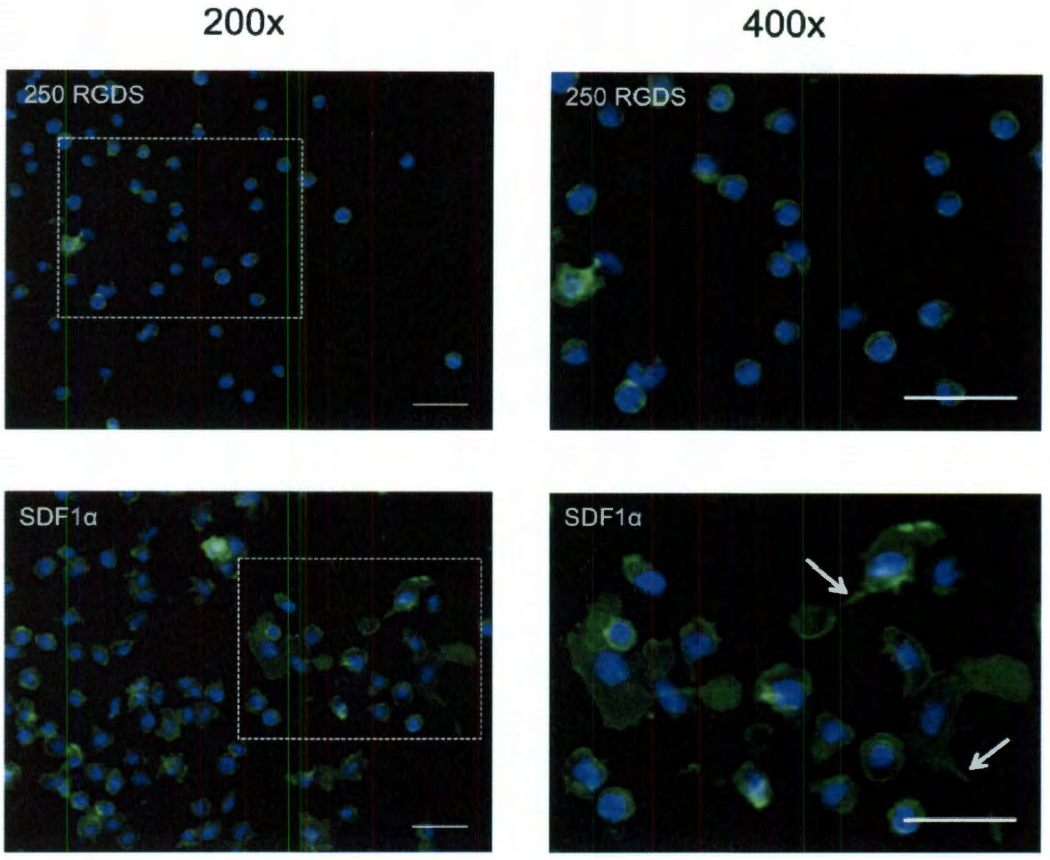

Figure 4.8: 32D morphology on bioactive PEG hydrogels with covalently immobilized SDF1α. The left column is at 200x magnification, and the right column is a 2x magnification (total magnification 400x) of the dotted box outlined in the left column. Actin filaments are stained with phalloidin (green) and nuclei are stained with DAPI (blue). With the covalent incorporation of SDF1α onto the surfaces, the cells appeared more spread, and distinct filopodia can be seen extending from many of the cells (denoted with arrows). Scale bars = 50 μm

Cells are well dispersed across the entire surface of the gels. To determine the average cell area, the area of phalloidin staining was quantified and divided by the number of

nuclei (Figure 4.9). We chose to compare the SDF1α group to RGDS gels with the high concentration of RGDS (250 μg/cm^2) due to similarity in cell density (resulting in similar available areas/cell for spreading). The average cell area increased significantly from 260.6 ± 175.1 μm^2 to 366.5 ± 246.9 μm^2 with the incorporation of SDF1α onto surfaces. Similarly to surfaces with both SCF and RGDS, the average cell areas had large standard deviation due to the heterogeneity of the 32D cell population.

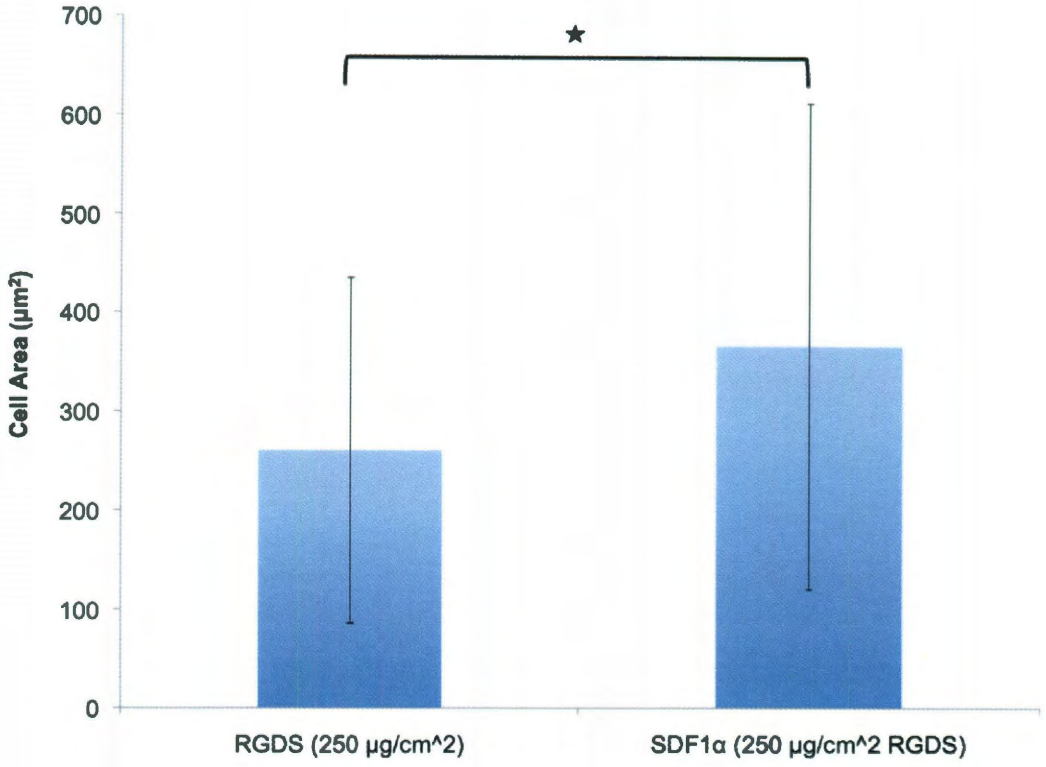

Figure 4.9: Average 32D cell area on hydrogels with immobilized RGDS and SDF1α. The average cell size significantly increased with the addition of SDF1α (400 ng/cm^2) onto gel surfaces. Data is displayed as mean ± standard deviation. (★ denotes significance, n=863 (250 μg/cm^2 RGDS), 631 (SDF1α), $p < 0.05$)

The diversity of cells on the surfaces resulted in a wide distribution of cell sizes. Thus, the cell area was also plotted as a histogram of cell sizes (Figure 4.10). On surfaces containing only RGDS, the highest percentage of cells was centered around 100 – 300

μm^2; with the addition of SDF1α onto the surfaces, there is a shift in cell size to center on 200 – 400 μm^2 and an increase in the percentage of cells that range from 400-1000 μm^2.

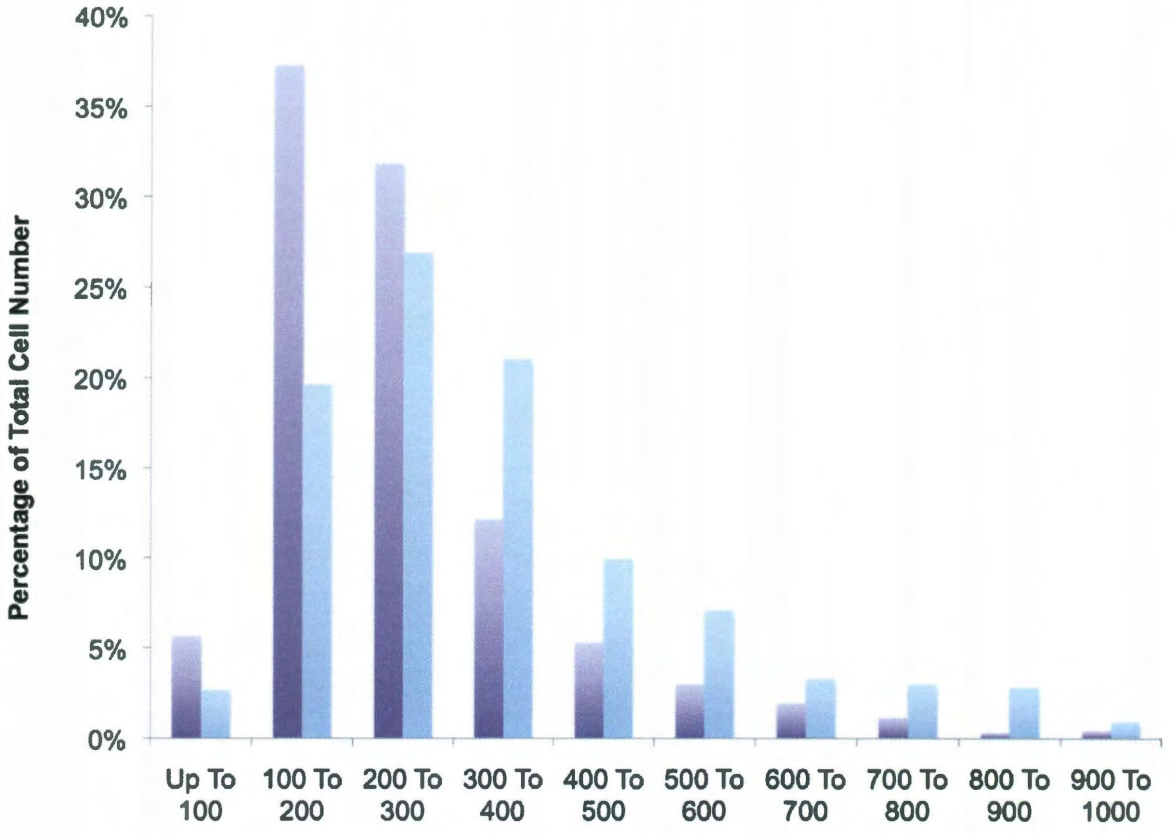

Figure 4.10: Distribution of 32D cell sizes on surface immobilized RGDS and SDF1α. With the addition of SDF1α (400 ng/cm^2) onto surfaces with RGDS (25 μg/cm^2), there is a shift in cell size from 100-200 μm^2 to 200-300 μm^2. There is also a higher percentage of cells at larger areas on surfaces with SDF1α. **(250 μg RGDS/cm^2, SDF1α and 25 μg RGDS/cm^2)**

SDF1α is a critical signaling molecule in HSC mobility. The capability of HSCs to move into and out of the HSC niche depends on their ability to adhere to extracellular matrix proteins as well as other cells through integrins on their surface. Thus, the interplay between activation of the CXCR4 receptor and integrin expression has been the subject of numerous studies. The expression of VLA-4 and VLA-5 – as well as other integrins – is upregulated as a result of SDF1α signaling (239, 240, 264). This appears to be the case on gel surfaces with immobilized SDF1α. The CXCR4 receptor is

continuously activated triggering the expression of VLA-5 integrins, which in turn bind to multiple RGD molecules causing the cells to spread. The presence of filopodia on the surface may also signify that cells are moving across the surface. Intracellularly, SDF1α signaling can result in actin polymerization in megakaryocytes (267). Furthermore, Fruehauf *et al.* observed podia formation in 32Ds in response to stimulation with SDF1α. The podia formation was associated with cell motility on fibronectin coated glass surfaces. (250). As aforementioned, SDF1α is a chemokine that is specific for hematopoietic cells. *In vivo*, cells migrate exclusively towards soluble SDF1α released by injured tissues during mobilization and by the bone marrow during homing. The podia formation suggests that SDF1α has triggered the 32Ds to migrate across the gel surfaces. Time-lapse studies could be employed in future studies to study the effects of immobilized SDF1α on cell migration.

4.3.5 Primary Cell Expansion

The effects of SDF1α on primary cell expansion were also investigated. c-kit$^+$ lin$^-$ primary hematopoietic progenitor cells were cultured on hydrogel surfaces with SDF1α in combination with either CS1 or RGDS for 14 days. Figure 4.11 shows representative images of the cells on both sets of gels during the culture period. Cells were fairly well dispersed after 24 hrs. but over time the cells began to cluster. Morphological changes in the cells were not observed until later timepoints (black arrows on Day 13 images in Figure 4.11).

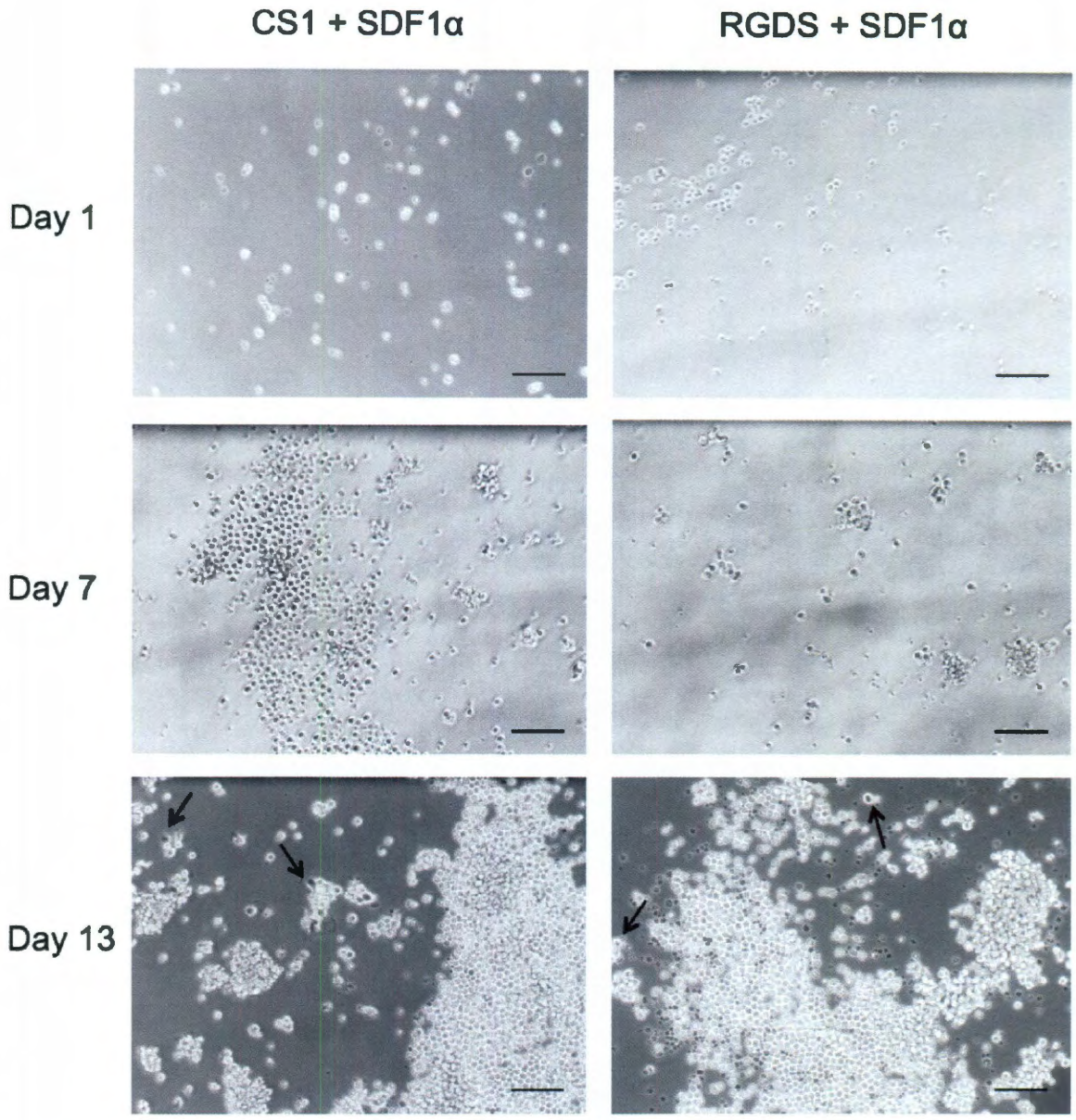

Figure 4.11: c-kit$^+$, lin$^-$ primary hematopoietic cells on hydrogels with surface immobilized SDF1α with PEG-CS1 or PEG-RGDS. Cells were maintained on the gels throughout the two weeks. After 14 days, some cells had started to spread (denoted with black arrows). The cells tended to clump together and were not evenly dispersed across the entire gel surface. (Scale bars = 100 μm)

With the inclusion of SDF1α in the hydrogel matrix, we did not see a significant change in cell expansion when compared to the peptides alone (Figure 4.12). On gels with CS1 and SDF1α, the percent change in cell number rose from 4089.0 ± 1927.0 percent to 5747.9 ± 2730.1 percent. On gels with RGDS and SDF1α there was a very

small decrease in the percent change in cell number from 4558.2 ± 943.8 to 4304.0 ± 1892.1 percent.

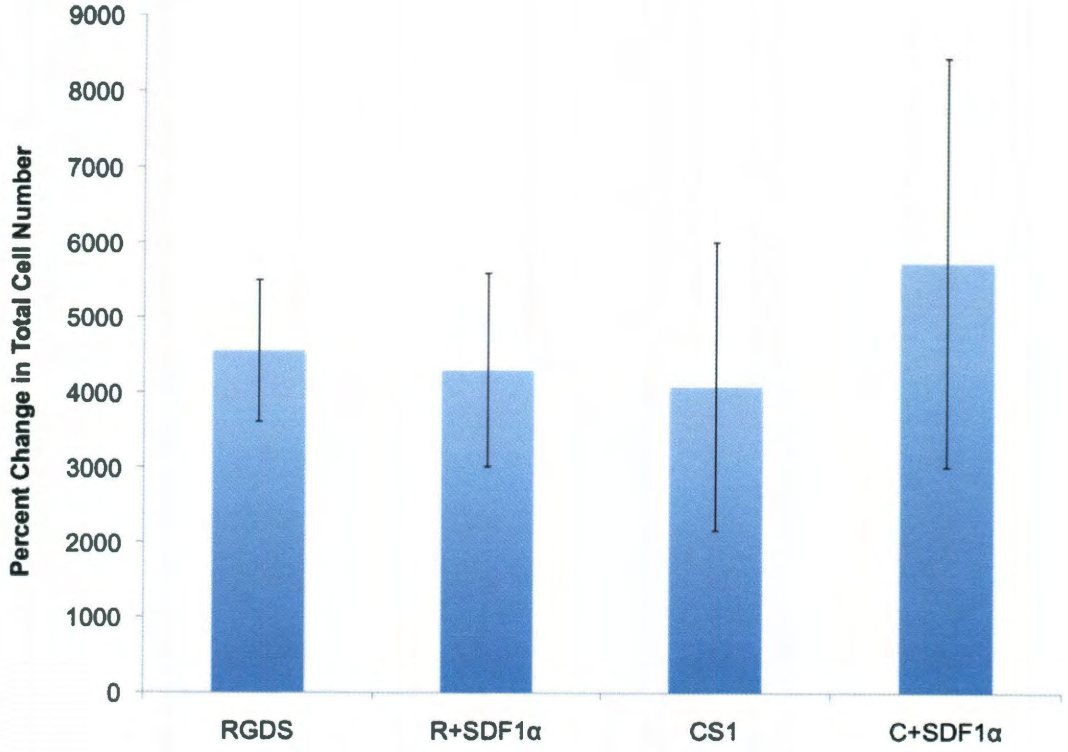

Figure 4.12: The total expansion of primary cells on surface immobilized SDF1α after 14 days in culture. Expansion was not significantly affected by the presentation of surface SDF1α, though there was a slight increase in cell number on gels with both CS1 and SDFα, though it was not statistically significant. (R=RGDS, C=CS1) Data is displayed as mean ± standard deviation (n=3).

Most *in vitro* studies performed with SDF1α have shown its role in cell migration and adhesive interactions with the ECM and stromal cells. Very little work has investigated the effect SDF1α has on hematopoietic cell proliferation. Rosu-Myles *et al.* demonstrated that the addition of SDF1α to primary hematopoietic cell cultures promoted the expansion and maintenance of committed progenitor cells (268). However, a significant change in cell expansion was not observed with the immobilization of SDF1α onto hydrogel surfaces. One reason for this may be that the initial population of cells expressed c-kit and none of the lineage markers, meaning they had not necessarily

become committed progenitors. There was a trend of differential effects on expansion depending on the adhesive peptide sequence that was used in conjunction with SDF1α. When CS1 was used with SDF1α, there was an increase in primary cell expansion. This implies that the effects of SDF1α on cell expansion depend on adhesion through the VLA-4 integrin. Hidalgo *et al.* showed that VLA-4 dependent adhesion to CS1 could be upregulated by SDF1α, which establishes a relationship between the two molecules. In addition, a lack of VLA-4 expression has been shown to negatively impact HSC self-renewal (269). Taken together, these findings suggest that the activation of multiple VLA-4 integrins in response to SDF1α signaling via the CXCR4 receptor results in the proliferation of hematopoietic progenitors.

Furthermore, though total cell expansion is not significant compared to peptide only controls, SDF1α could be promoting or slowing the proliferation of certain cell types. Cells that are less differentiated tend to proliferate at slower rates than those that have become more committed progenitors (127). Li *et al.* found that by using a small peptide analogue of SDF1α in HSC culture they could improve the engraftment potential of HSCs though they did not observe an increase in total cell number (270). In addition, the reduced bioactivity of PEG-SDF1α may be hindering its ability to interact with primary HSCs. To further study how SDF1α affected hematopoietic cell behavior the differentiation potential of the final cell populations on the gel surfaces was analyzed.

4.3.6 Primary Cell Differentiation

4.3.6.1 Colony Forming Unit Assay

To assess the differentiation potential of cells grown in the hydrogel wells, a colony assay and a flow cytometric analysis were performed. Figure 4.13 shows the

number and distribution of colonies formed from cells collected from hydrogel surfaces after 14 days in culture. As we observed on SCF, the colonies that formed were predominately macrophage. The total number of colonies increased in samples from gels containing SDF1α and RGDS but decreased slightly on SDF1α and CS1. Figure 4.14 displays the same colony data as a percentage of total colonies. On samples with SDF1α, there were a higher percentage of primitive GM and GEMM colonies compared to the peptides alone.

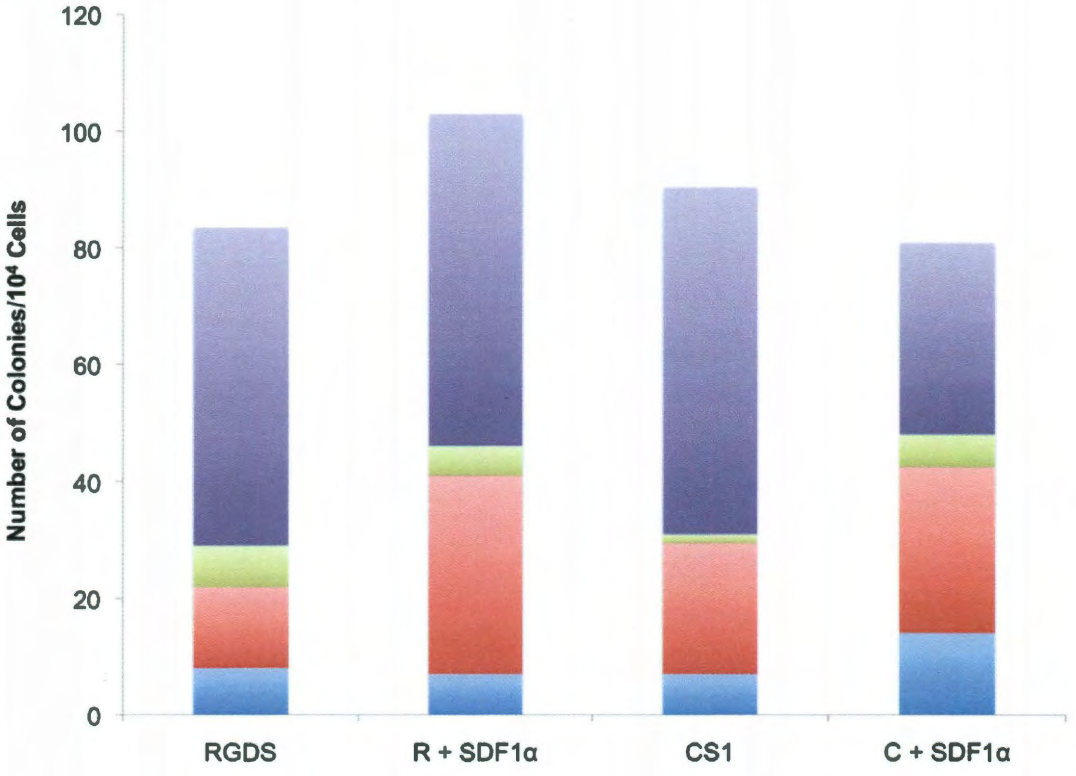

Figure 4.13: Colony distribution of colonies formed from cells expanded on gels with surface immobilized SDF1α. Total colony number increased on samples expanded on SDF1α in combination with RGDS. Bars are mean, n=2. (R=RGDS, C=CS1; **CFU-GEMM=Granulocyte, Erythrocyte, Megakaryocyte, Macrophage, CFU-GM=Granulocyte/Macrophage, CFU-G=Granulocyte, CFU-M=Macrophage**)

Figure 4.15 presents the data as individual colony formation, which demonstrates the same trends. However, none of the noted differences were statistically significant. This

is likely due to a low sample size, and thus, the experiments should be repeated to determine if the findings are a true response by the primary cells to the addition of SDF1α.

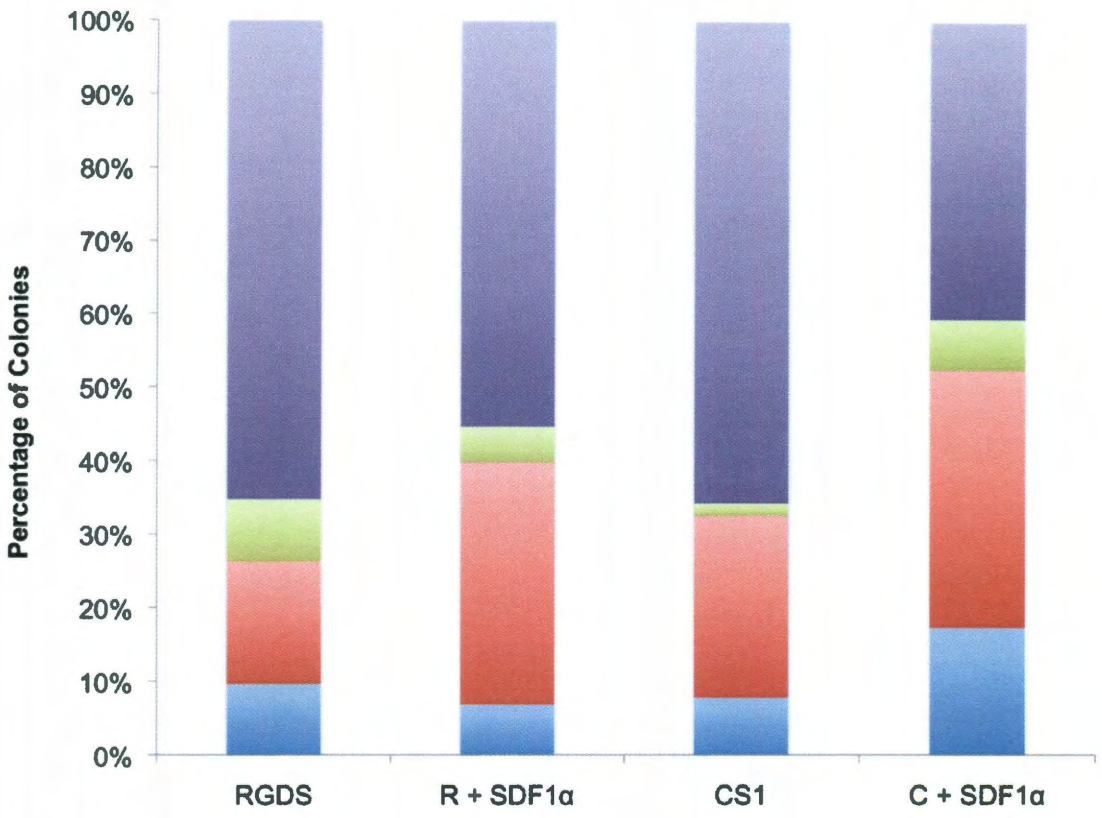

Figure 4.14: Distribution of colonies formed from cells expanded on gels with surface immobilized SDF1α. The percentage of primitive colonies (both GM and GEMM) is not significantly different between any of the groups. However, the addition of SDF1α does appear to promote the formation of GEMM and GM colonies particularly in combination with CS1. Bars are mean, n=2. (R=RGDS, C=CS1; **CFU-GEMM=Granulocyte, Erythrocyte, Megakaryocyte, Macrophage**, **CFU-GM=Granulocyte/Macrophage**, **CFU-G=Granulocyte**, **CFU-M=Macrophage**)

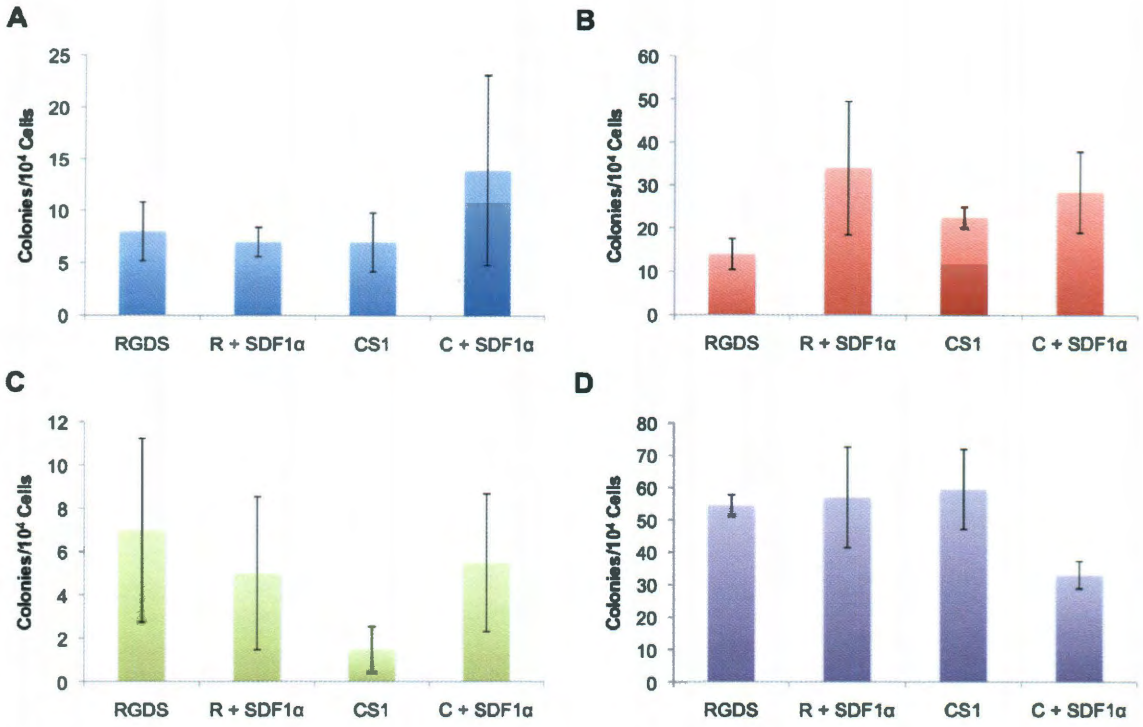

Figure 4.15: Individual colony formation organized by colony type from cells expanded on SDF1α functionalized hydrogels. The addition of SDF1α in combination with CS1 increased GEMM formation. There was an increase in GM formation on all samples with SDF1α. However, none of these differences were significant. Bars are mean ± standard deviation, n=2. (R=RGDS, C=CS1; **A. CFU-GEMM=Granulocyte, Erythrocyte, Megakaryocyte, Macrophage, B. CFU-GM=Granulocyte/Macrophage, C. CFU-G=Granulocyte, D. CFU-M=Macrophage**)

4.3.6.2 Flow Cytometry

Figures 4.16 and 4.17 display the flow cytometry plots generated by samples with SDF1α. When comparing the two, we note that both the lin^- and $c\text{-}kit^+$ populations are greater in cells cultured on CS1 and SDF1α than those cultured on RGDS and SDF1α. However, the percent increases in the $c\text{-}kit^+$, lin^- population are fairly similar: 350-450% (Figure 4.18). The percent increase in the primitive KSL population does not change significantly with the addition of SDF1α though there is a trend of increasing KSL population on gels with both CS1 and SDF1α (Figure 4.19).

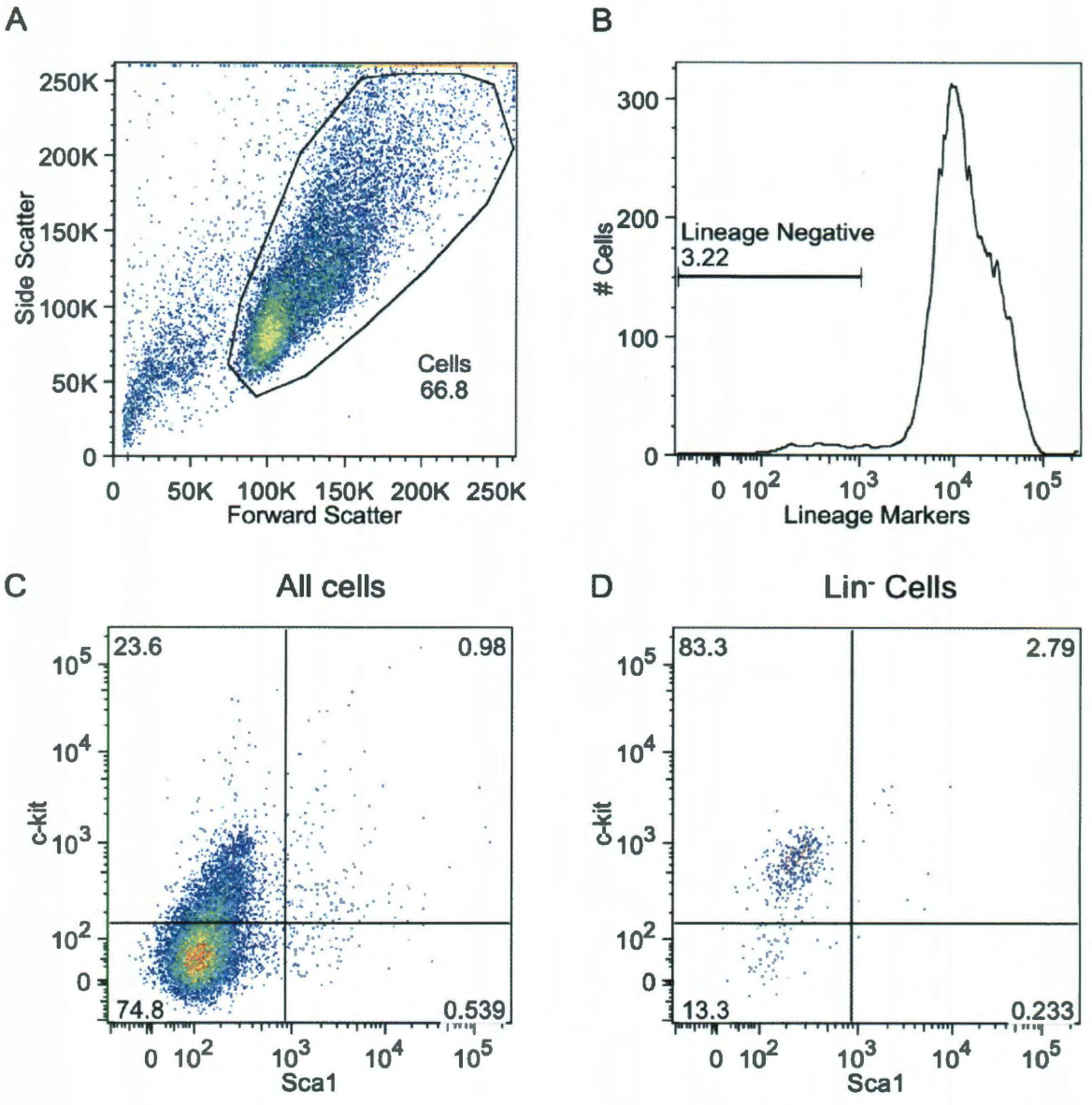

Figure 4.16: Flow cytometry analysis of c-kit$^+$, lin$^-$ cells after 14 days in culture on PEG-RGDS with PEG-SDFα. A. Particles were first gated to count cells. B. Cells were then gated for those that were lin$^-$. C. A plot of all cells gated for positive and negative Sca1 and c-kit expression. D. A plot of lineage negative cells gated exactly as in C. Numbers on the plots indicate the percentage of cells falling within that gate.

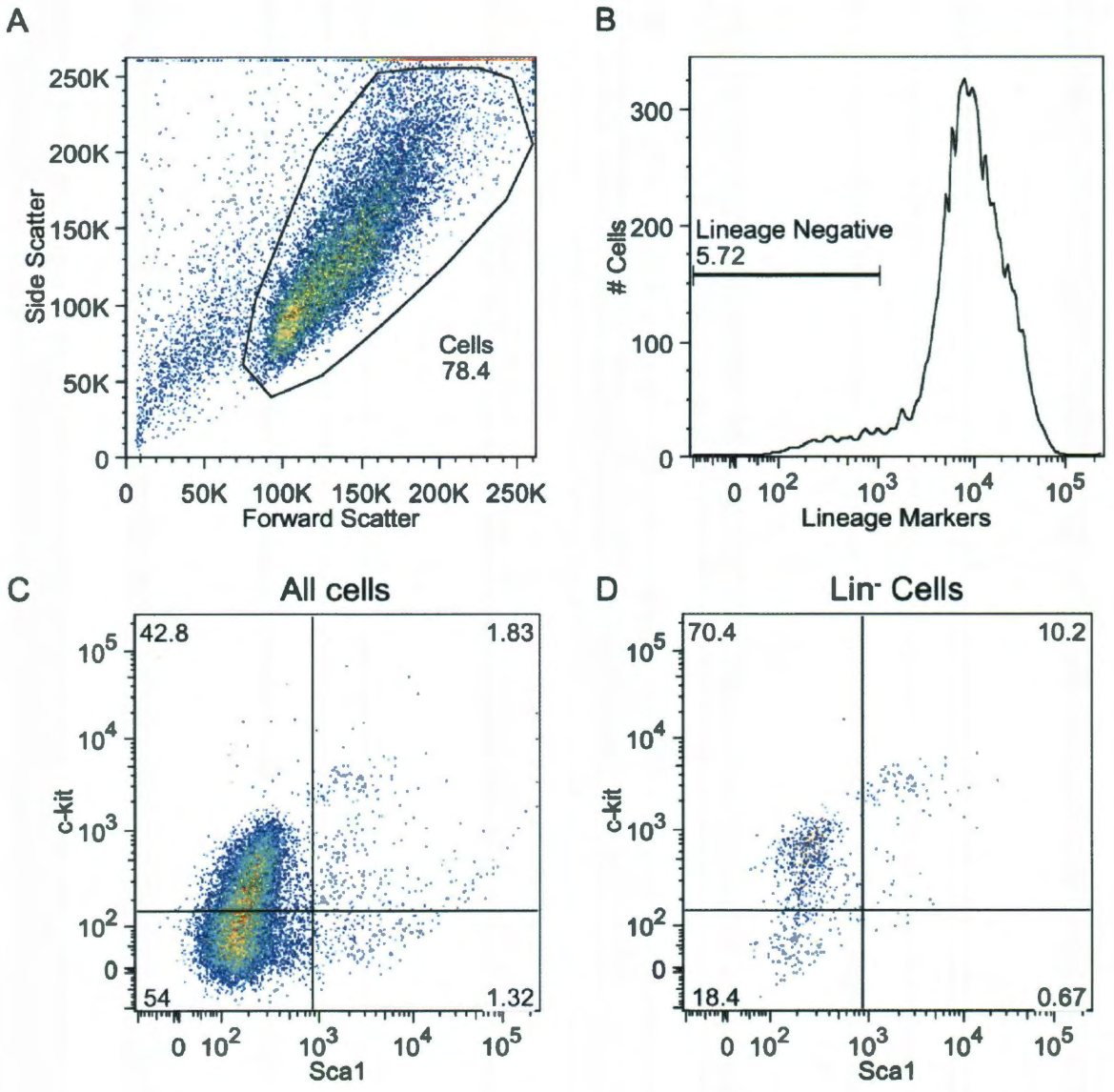

Figure 4.17: Flow cytometry analysis of c-kit$^+$, lin$^-$ cells after 14 days in culture on PEG-CS1 with PEG-SDF1α A. Particles were gated to count cells. B. All of the cells were gated for those that did not express lineage markers. C. A plot of all cells gated for positive and negative Sca1 and c-kit expression. D. A plot of lineage negative cells with gates described in C. Numbers on the graphs indicate the percentage of cells falling within that gate.

The data from these studies is somewhat inconclusive. Similarly to previous work in this thesis, there is a significant amount of differentiation occurring during the culture period. This is expected since a heterogeneous population of progenitor cells is used, many of which have already begun the differentiation process before being seeded

into the hydrogel wells. In previous work, SDF1α has been shown to aid in the maintenance of a primitive pool of HSCs *in vivo* and may be implicated in HSC self-renewal (271). The presence of SDF1α on gel surfaces did not promote significant cell proliferation, but it appeared to inhibit some degree of differentiation particularly in combination with CS1. Preliminary results in both the colony assay and flow cytometry supported this theory. When SDF1α was immobilized on gel surfaces with RGDS the effects on the proliferation and differentiation potential of primary cells seem to be minimal. These results may be due to an additive effect of CS1 and SDF1α. As previously described, the binding of CXCR4 to SDF1α results in activation of VLA-4 (240, 264). In addition, binding to CS1 via the VLA-4 integrin has been shown to maintain HSCs in a less differentiated state (122, 125). The ability to keep the HSCs undifferentiated in an *in vitro* system is critical because only the most primitive HSCs are capable of successful engraftment after transplantation. This work shows that the immobilization of SDF1α onto the surfaces of hydrogel wells can prevent some degree of HSC differentiation.

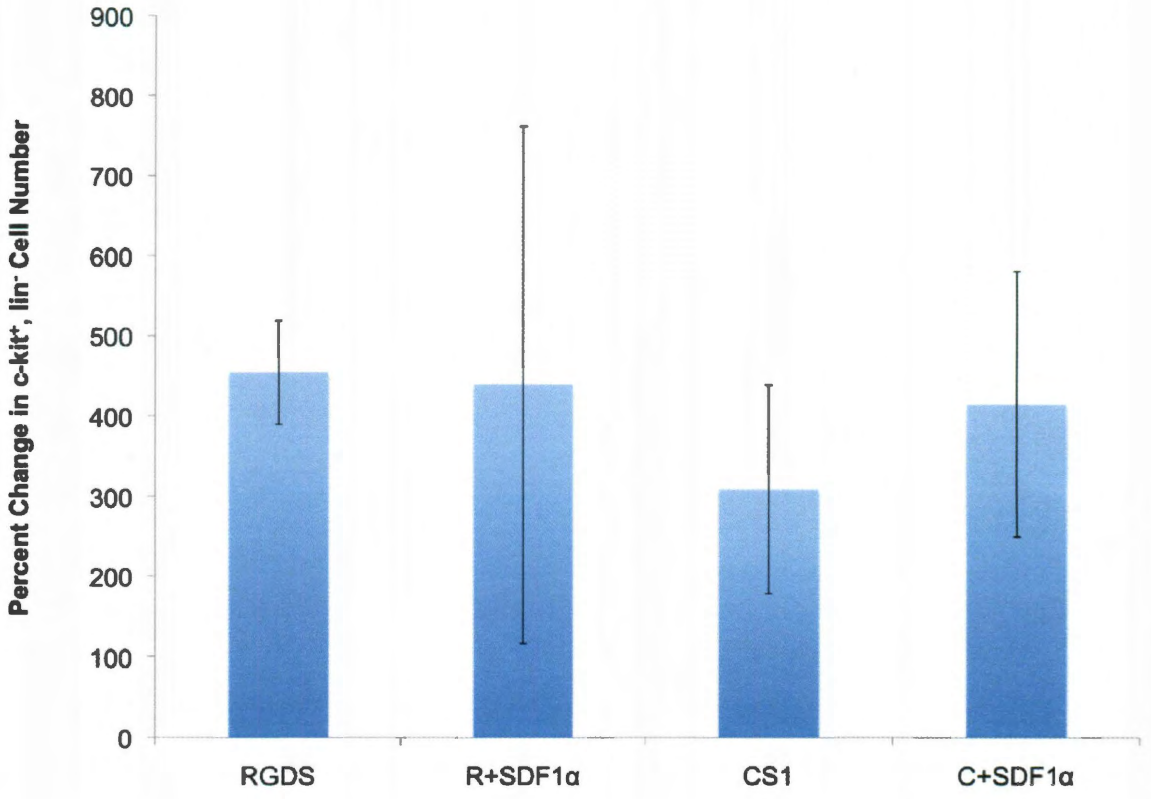

Figure 4.18: Increase in c-kit$^+$, lin$^-$ cells over 14 days in culture. The addition of SDF1α to surfaces had no significant effect on c-kit$^+$, lin$^-$ cell proliferation, though there was a slight increase in cell number on gels with the combination of CS1 and SDF1α compared to CS1 alone. Data is displayed as mean ± standard deviation. (n=3) (R=RGDS, C=CS1)

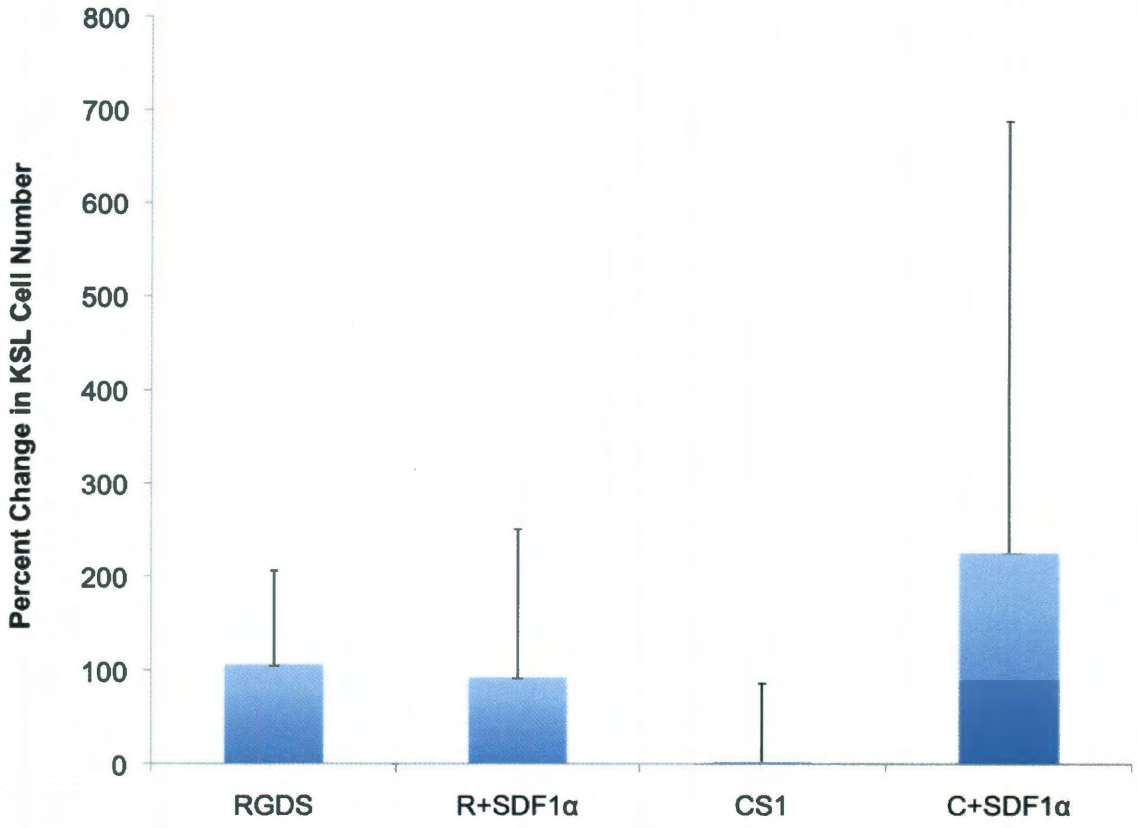

Figure 4.19: Expansion of the primitive KSL population on gels with covalently immobilized SDF1α. On gels with RGDS and SDF1α, the primitive cell population was unchanged compared to controls with RGDS alone. On gels with CS1 and SDF1α, there was an increase in the KSL population compared to controls. However, this increase was not deemed significant. Data is displayed as mean + standard deviation. (n=3) (R=RGDS, C=CS1)

4.4 Conclusions

SDF1α was included in the hydrogel matrix in an attempt to retain HSCs on the gel surface and inhibit their differentiation. In addition, the inclusion of SDF1α on gel surfaces could theoretically help to select for HSCs that are positive for the CXCR4 receptor, which is the protein that SDF1α binds to *in vivo*. CXCR4 expression is correlated with the ability to successfully home to the bone marrow cavity after transplantation, and overexpression of CXCR4 has been shown to improve this repopulation ability (272-274).

SDF1α was successfully PEGylated though its bioactivity was reduced as a result of this process. With 32D cells, there was an increase in the number of adherent cells after 48 hrs. when cells were cultured on immobilized SDF1α. Surface bound SDF1α also caused a decrease in cell proliferation and a corresponding increase in total cell area. Primary cells cultured in hydrogel wells functionalized with SDF1α did not proliferate significantly compared to peptide only controls. However, cells cultured on SDF1α were able to form more primitive colonies than peptide controls, particularly cells cultured on SDF1α in combination with CS1. This suggests that there may be an additive effect of surface immobilized SDF1α and CS1 in terms of maintaining primitive HSC populations, though the data was not significant. In future studies, SDF1α could be used in combination with SCF to ascertain whether these two proteins can work together to both promote proliferation and inhibit differentiation.

Chapter 5: Effects of Surface Immobilized Jagged1 on the Expansion of Hematopoietic Stem Cells in Hydrogel Wells

5.1 Background

SCF and SDF1α were found to promote hematopoietic stem cell expansion and inhibit differentiation, respectively. These successes led to the investigation of another niche molecule, Jagged1 (JAG1). Unlike SCF and SDF1α, which are found in both soluble and membrane-bound forms, JAG1 is only expressed in the endosteal and vascular niches as a transmembrane protein. Several types of stromal cells in the HSC niche display JAG1, which plays an integral role in HSC fate. The interaction between JAG1 and Notch1 has been implicated in HSC self-renewal and the prevention of differentiation. This chapter focuses on the effects of surface immobilized JAG1 on HSC behavior. HSCs were cultured within JAG1-modifed hydrogel wells for 14 days, and the differentiation potential of the expanded cells was characterized by the ability to form primitive colonies and the expression of surface markers indicative of HSC populations.

5.1.1 Jagged1

JAG1 is a transmembrane protein that is a member of the Notch family of receptors. The Notch signaling pathway is conserved between many mammalian species and has roles in many basic cell functions including growth and differentiation (71). The signaling is intracellular occurring between Notch receptors (Notch 1-4) and Notch ligands (Jagged 1 and 2 and Delta-like 1, 3, and 4). When Notch ligands bind to Notch receptors, the Notch receptor is cleaved by proteases and the intracellular portion of the receptor travels to the nucleus where it promotes or suppresses gene expression (Figure 5.1) (69). In the HSC niche, JAG1 is expressed by osteoblasts whereas HSCs,

hematopoietic progenitors, and mature blood cells all express the Notch1 receptor, which binds to JAG1 (275-277).

This signaling pathway has been shown to influence HSCs self-renewal and differentiation during *in vitro* and *in vivo* experiments (72, 278-282). Stier *et al.* transduced hematopoietic progenitor cells to express Notch1 and found these cells preferentially engaged in self-renewal over differentiation (279). Varnum-Finney *et al.* also transduced cells to overexpress Notch1 and found that they could maintain HSCs with repopulation capabilities for up to 8 months compared to cells that were not transduced and died within 25 days in culture. The expression of Notch1 can also inhibit the differentiation of HSCs even in the presence of cytokines that normally drive differentiation (72). The inhibition of Notch signaling has led to accelerated differentiation of HSCs *in vitro* and a depletion of the HSC pool *in vivo* (281). However, JAG1 and Notch1 are not necessary for these processes as shown by *in vivo* animal experiments in which these proteins are knocked out indicating some redundancies in this family of signaling molecules (73-76).

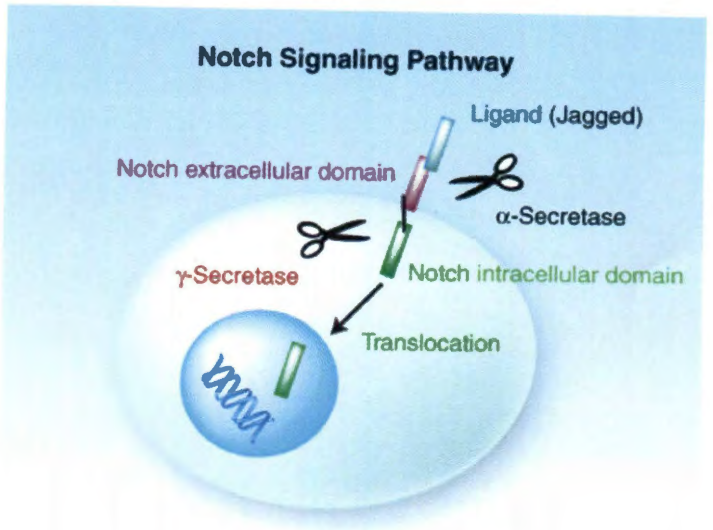

Figure 5.1: Jagged-Notch signaling pathway. When Jagged binds to Notch, the intracellular domain of Notch is proteolytically cleaved and translocates to the nucleus where it can alter gene expression. Figure adapted from (283).

5.1.2 JAG1 for HSC Expansion

JAG1-Notch signaling has been exploited for use in the *in vitro* expansion of HSCs (103, 275, 277, 284). After hematopoietic progenitor cells were cultured on stromal cells expressing JAG1, they were able to form four times as many colonies as control cells (275). Karanu *et al.* added soluble JAG1 to HSC cultures to promote proliferation and obtained populations of HSCs capable of *in vivo* reconstitution (103). Furthermore, the immobilization of JAG1 onto microbeads has been shown to promote the expansion of primitive HSC colonies *in vitro* (277, 284),

These studies show the potential for using JAG1 in an *ex vivo* culture system. However, they are all limited to some extent. The use of a stromal cell feeder layer triggers many signaling pathways that make the system difficult to control. Soluble factors are cleared quickly and must be constantly replenished into the media. Immobilizing the proteins on a sepharose bead addresses these issues, but it does not allow the complex tunability that is available in the PEG hydrogel system. The following

work investigates how the incorporation of JAG1 onto PEG hydrogel surfaces affects HSC behavior.

5.2 Materials and Methods

All materials were obtained from Sigma unless otherwise noted.

5.2.1 Polymer Synthesis and Characterization

5.2.1.1 PEG-DA, PEG-RGDS, PEG-CS1

PEG-DA, PEG-CS1, and PEG-RGDS were synthesized as previously described (Sections 2.2.1.1 and 2.2.1.3). PEG-RGDS made using the PEG-SVA derivative was employed for these studies.

5.2.1.2 PEG-JAG1

PEG-JAG1 was synthesized following the same methods as the production of PEG-SCF and PEG-SDF1α (Sections 3.2.1 and 4.2.1). A chimeric protein composed of the extracellular domain of rat JAG1 and the Fc portion of the human IgG_1 antibody (R&D) was reacted with PEG-SVA at a molar ratio of 84.7:1 (PEG-SVA: JAG1) overnight in PBS (pH = 8.0) at 4° C. The extracellular domain of rat Jagged1 shows 99% homology with the murine extracellular domain.

To confirm PEGylation, a Western blot was conducted on the PEGylated and naturally occurring forms of the proteins using a 15% Tris-HCl precast polyacrylamide gel. A primary rabbit polyclonal antibody to rat JAG1 (Abcam) and a secondary goat polyclonal antibody against rabbit IgG conjugated with horseradish peroxidase (Abcam) were used to stain the blot. To detect the proteins, the ECL chemiluminescent Western blotting analysis system was applied, and chemiluminescent images of the blot were taken using an LAS 4000.

5.2.1.3 Bioactivity of PEG-JAG1

To determine if the activity of the protein was maintained after PEGylation, a functional ELISA was performed. Rat Notch1 (R&D) was immobilized on immunoabsorbent 96 well plates at concentrations of 0.5 μg/ml overnight at 4° C. A sandwich ELISA was then performed on JAG1 and PEG-JAG1 using the Rat Jagged1 Duo Set (R&D) to determine the degree of binding to Notch1.

5.2.1.4 Surface Immobilization and Quantification

JAG1 in combination with either RGDS or CS1 (25 μg/cm^2) was immobilized onto the surfaces of hydrogel wells at concentrations of 200 and 400 ng/cm^2 using methods detailed in Section 2.2.2.2. To quantify the concentration of protein on the hydrogel surface, an ELISA was performed as previously described (Section 3.2.1.6) using the Rat Jagged1 Duo Set.

5.2.2 Cell Maintenance

5.2.2.1 Primary c-kit$^+$, lin$^-$ Cell Isolation and Culture

Primary c-kit$^+$, lin$^-$ cells were isolated from murine whole bone marrow and maintained as described in Section 2.2.3.2.

5.2.2.2 Cell Seeding into Hydrogel Wells

c-kit$^+$ lin$^-$ cells were seeded in gel wells ([JAG1]=400 ng/cm^2, [RGDS]=25 μg/cm^2 or ([JAG1]=400 ng/cm^2, [CS1]=25 μg/cm^2) at densities of 13,000 cells/cm^2. Gel wells with only RGDS or CS1 (25 μg peptide/cm^2) served as controls. Each group consisted of 4 gel wells. Media was added around gels to keep them hydrated. Cells were kept in culture for 14 days at 37°C and 5% CO_2 with media renewal every 2 to 3

days. After culture, the cells from each group were combined so that enough cells were available for flow cytometry. The experiment was conducted a total of three times.

5.2.3 Evaluation of Expanded Hematopoietic Cells

Primary cell expansion and differentiation potential (colony forming unit assay and flow cytometry) were performed as previously described in Sections 2.2.4.3-2.2.4.5.

5.2.4 Statistical Analysis

One-way ANOVAs and Tukey's post-hoc analyses were performed to evaluate statistical differences between groups in all studies using a 95% probability level ($p<0.05$).

5.3 Results and Discussion

5.3.1 Polymer Synthesis and Characterization

5.3.1.1 PEG-JAG1

To confirm JAG1 had been successfully PEGylated, a Western blot was performed. Figure 5.2 shows the results of this assay. There is a band present at 180 kDa, the molecular weight of the chimeric JAG1 protein, in the JAG1 lane. In the PEG-JAG1 lane, a smear can be seen with an increased molecular weight. This indicates successful PEGylation of JAG1.

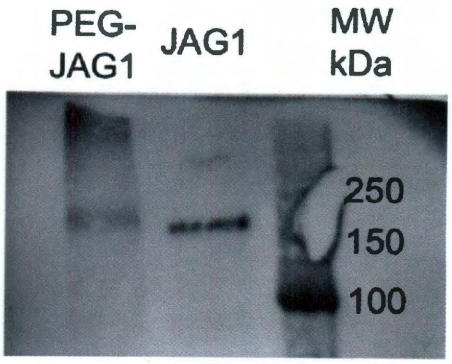

Figure 5.2: Western blot of PEG-JAG1. There is an increase in molecular weight (MW) after the conjugation reaction indicating that JAG1 has been successfully PEGylated. The smear occurs as a result of multiple PEG chains reacting with the protein.

5.3.1.2 Bioactivity of PEG-JAG1

A functional ELISA was conducted to determine the activity of PEG-JAG1. The PEG-JAG1 demonstrated the ability to bind successfully to Notch1 as indicated by a detectable colorimetric change upon completion of the ELISA. However, the change was quite low and suggests that PEGylation may have affected the activity of the protein. In future work, this assay will require optimization to accurately quantify the degree of JAG1:Notch1 binding.

5.3.1.3 Quantification of JAG1 on Gel Surfaces

An ELISA was used to quantify the concentration of JAG1 on the hydrogel surfaces. Approximately 99% of the solution that was added to the gel was covalently immobilized onto the surface resulting in approximately 87.92 ± 1.27 ng of JAG1 on each well surface.

5.3.2 Primary Cell Expansion

c-kit$^+$, lin$^-$ cells were cultured in hydrogel wells for 14 days. Figure 5.3 shows phase contrast images of cells at varying timepoints during culture. The cells mostly remain rounded. At early timepoints, cells are evenly distributed, but over time, the cells

cluster together in the center of the gel well.

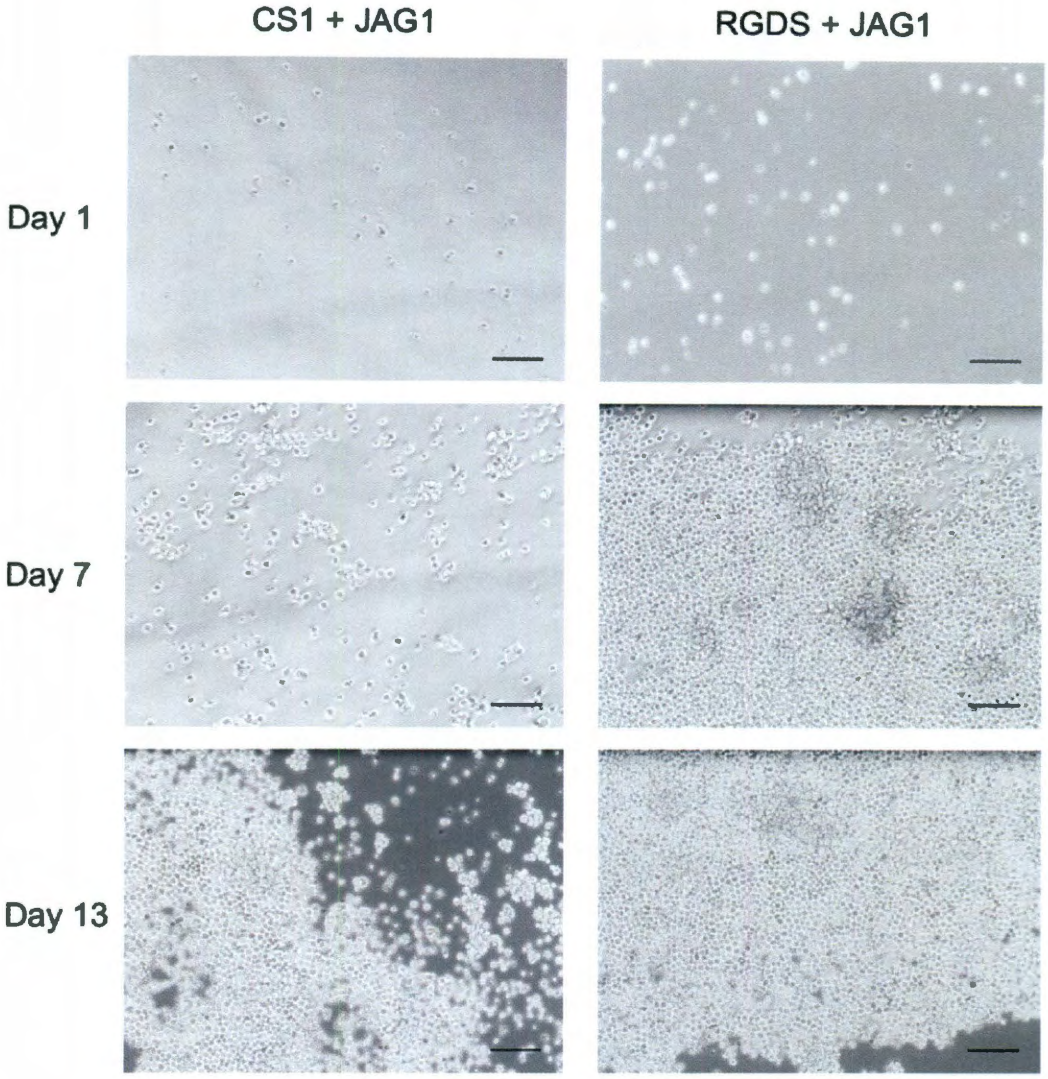

Figure 5.3: c-kit$^+$, lin$^-$ cells on hydrogel surfaces modified with JAG1 and CS1 or RGDS. Primary cells were cultured for 14 days in hydrogel wells. The images show an increase in cell number over time indicating cell proliferation. (Scale bars = 100 μm)

The expansion of c-kit$^+$, lin$^-$ cells was quantified by calculating the percent change between initial cell number and final cell number at day 14 (Figure 5.4). This data shows no significant changes in cell number with the addition of JAG1 to gel

surfaces. The percent change in all groups is approximately 4000%.

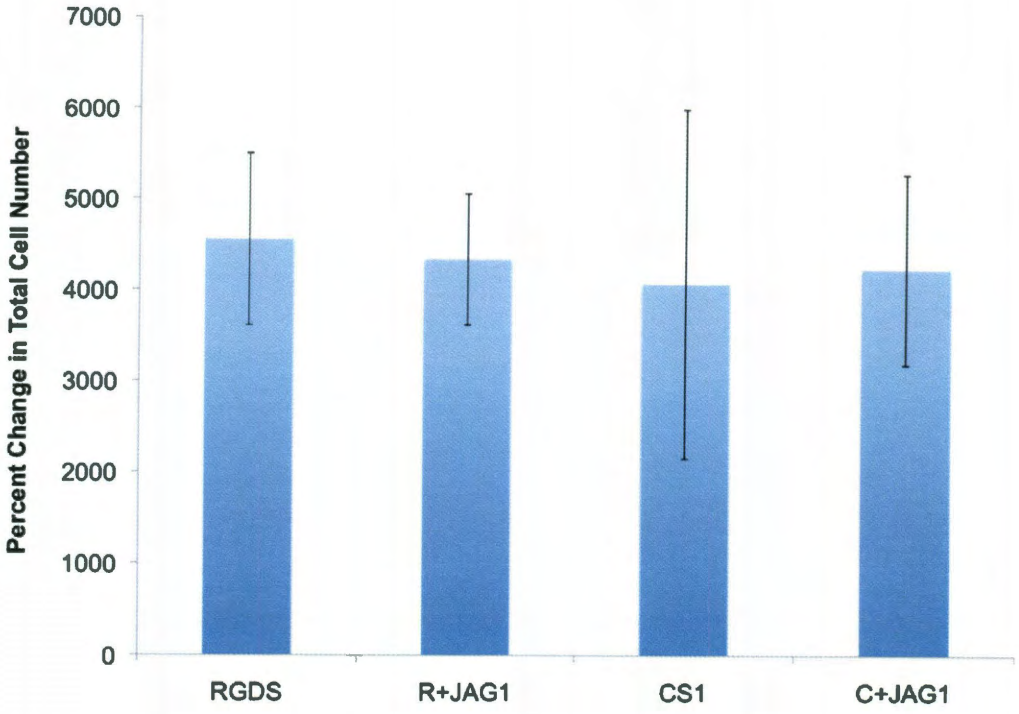

Figure 5.4: Total cell expansion on bioactive hydrogel surfaces functionalized with JAG1 after 2 weeks in culture. There was not a significant effect on cell expansion when JAG1 was added to the surfaces. Bars are mean ± standard deviation. (n=3) (R=RGDS, C=CS1)

Previous work has demonstrated the ability to add JAG1 to HSC cultures through expression by stromal cell feeder layers and immobilization on beads to promote HSC expansion (275, 277, 284). However, cell expansion in response to JAG1 in this system was not significantly affected, positively or negatively. One reason for this could be a diminished activity of the JAG1 protein by PEGylation and subsequent immobilization on the hydrogel surface. The bioactivity assay suggested that the JAG1 was somewhat limited in its ability to bind Notch1, and if this were the case, the ability of JAG1 to signal cell expansion through binding to Notch1 would be diminished. Another explanation is that the JAG1 does not have an additive effect in combination with the RGDS and CS1 peptides. A survey of the literature found that no previous studies had

been conducted with both JAG1 and either of these peptides (or FN) for the purposes of HSC expansion or maintenance. The addition of RGDS or CS1 to the surface was shown to promote expansion compared to FN plates and PEG-DA in Chapter 2, and the cell expansion observed in response to these peptides might mask any effects that JAG1 has on the culture. This was seen previously in Chapters 3 and 4 where high RGDS concentrations masked the effects of SCF and SDF1α on 32D cell adhesion and spreading.

In addition, the heterogeneity of the initial cell population could have lead to increases in some cell populations with corresponding decreases in others even though the total cell expansion was not increased compared to controls. Some studies have demonstrated that JAG1 does not promote significant HSC expansion (103, 278). Its main effect was the ability to retain HSCs in a more quiescent, undifferentiated state. A great deal of work has shown that triggering the JAG1-Notch signaling pathway can prevent HSC differentiation (72, 103, 278, 279, 281, 282). Therefore, the differentiation potential of the cell populations on hydrogels was also evaluated after two weeks in culture.

5.3.3 Primary Cell Differentiation

5.3.3.1 Colony Forming Unit Assay

To first evaluate the differentiation potential of the expanded c-kit$^+$, lin$^-$ cells, a colony assay was conducted. After expansion, primary cells were cultured in methylcellulose media for 10-14 days, and the colonies that formed were counted and scored. Four types of colonies were evaluated: CFU -G, -M, -GM, and -GEMM (G=Granulocyte, M=Macrophage, GM=Granulocyte, Macrophage, and

GEMM=Granulocyte, Erythrocyte, Macrophage, Megakaryocyte). As shown in Figure 5.5, similar number of colonies formed from cells cultured in all groups, ranging from around 70 from cells cultured on CS1+JAG1 functionalized gels to 90 on the CS1 only control.

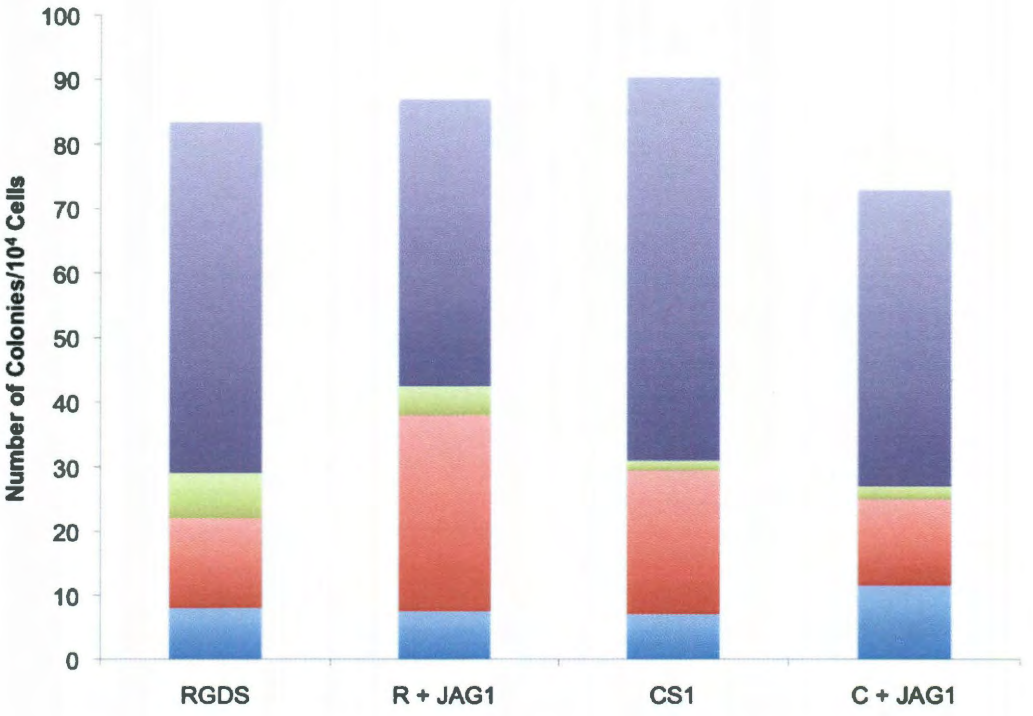

Figure 5.5: Colony formation from cells expanded on gels with surface immobilized JAG1. There is no significant difference in colony formation between groups. With the addition of JAG1 to the RGDS surface, there were more primitive GM and GEMM colonies than the other groups. In the CS1+JAG1 group, the highest number of GEMM colonies formed. Bars are mean, n=2. (R=RGDS, C=CS1; **CFU-GEMM=Granulocyte, Erythrocyte, Megakaryocyte, Macrophage, CFU-GM=Granulocyte/Macrophage, CFU-G=Granulocyte, CFU-M=Macrophage**)

The cells cultured on hydrogels functionalized with both RGDS and JAG1 formed the most primitive GM and GEMM colonies, whereas in the CS1 and JAG1 group, the most GEMM colonies formed. This can be seen more clearly in Figure 5.6, which displays a distribution of the colonies that grew as a percentage of the total number of colonies, and Figure 5.7, which shows individual colony formation for each group.

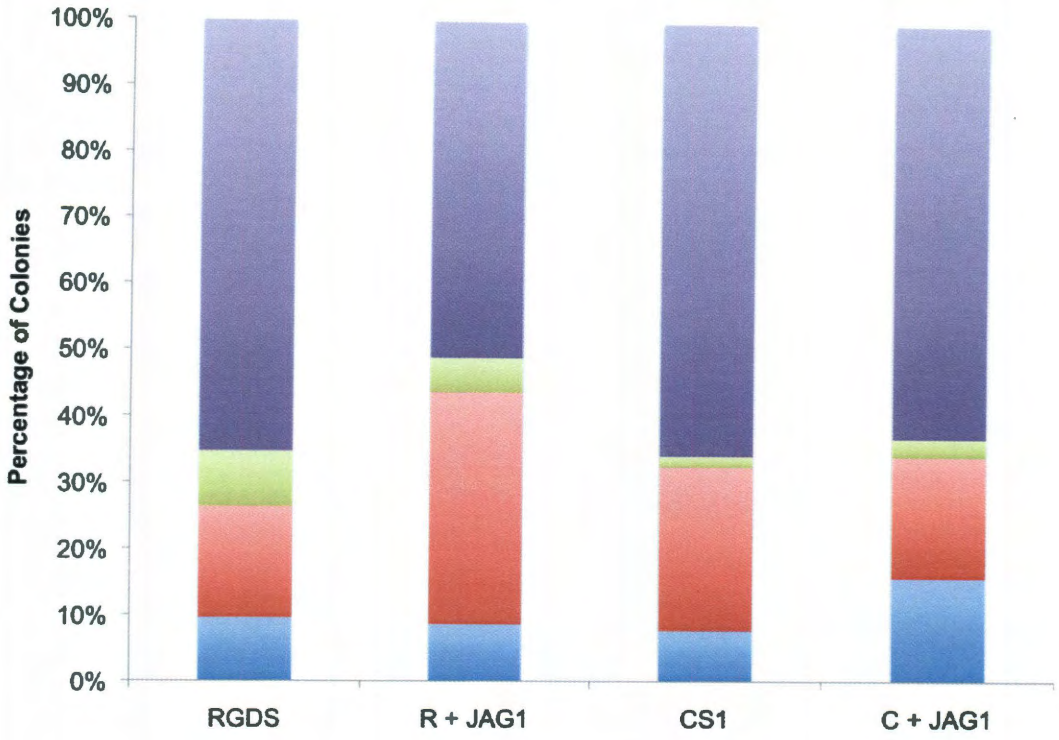

Figure 5.6: Distribution of colonies formed from cells expanded on gels with surface immobilized JAG1. The percentage of primitive colonies (both GM and GEMM) is highest in the RGDS and JAG1 group. The addition of JAG1 also seems to promote the formation of the most primitive, GEMM colonies in combination with CS1. Bars are mean, n=2. (R=RGDS, C=CS1; **CFU-GEMM=Granulocyte, Erythrocyte, Megakaryocyte, Macrophage, CFU-GM=Granulocyte/Macrophage, CFU-G=Granulocyte, CFU-M=Macrophage**)

These results suggest that the addition of JAG1 to the surfaces of the hydrogels is helping to maintain the HSCs in a more primitive state. However, none of the differences between the groups were significant. This can be attributed to a small sample size as well as diversity amongst the primary cell populations that were used. Flow cytometric analysis was done on the cells to further confirm and better quantify these results.

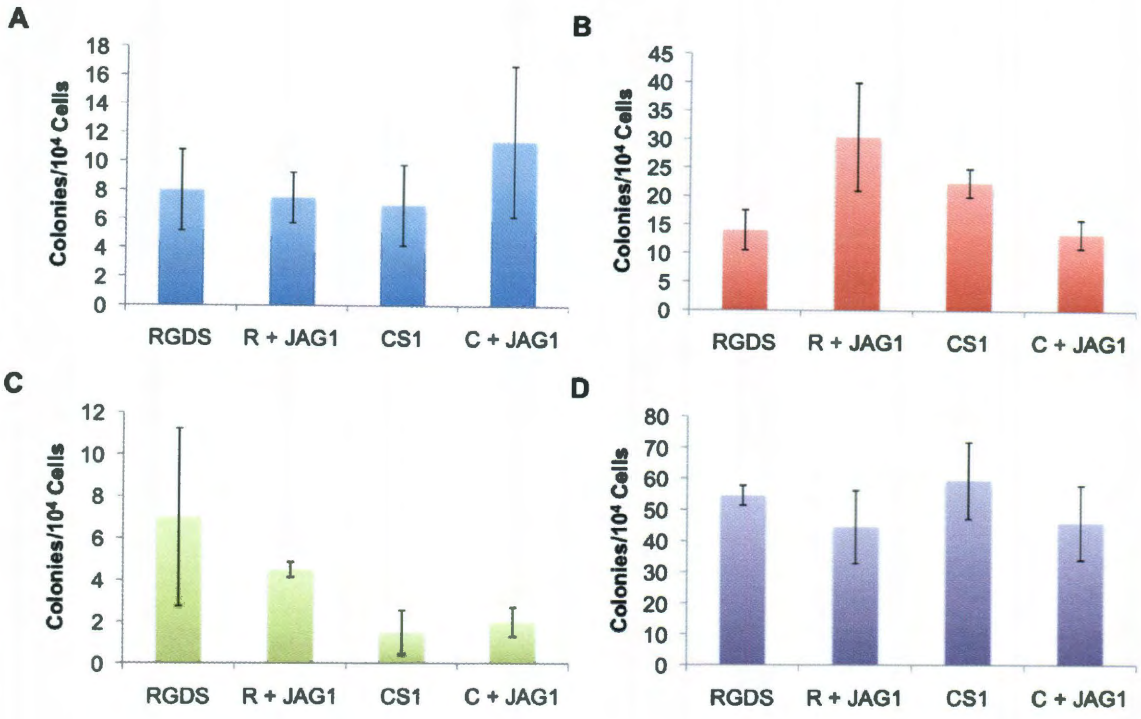

Figure 5.7: Individual colony formation organized by colony type from cells expanded on JAG1 functionalized hydrogels. The addition of JAG1 increases GEMM formation in combination with CS1 and GM formation with RGDS. Concurrently, there is an increase in M formation on gels with only RGDS or CS1. However, none of the differences were statistically significant. Bars are mean ± standard deviation, n=2. (R=RGDS, C=CS1; **A. CFU-GEMM=Granulocyte, Erythrocyte, Megakaryocyte, Macrophage, B. CFU-GM=Granulocyte/Macrophage, C. CFU-G=Granulocyte, D. CFU-M=Macrophage**)

5.3.3.2 Flow Cytometry

Flow cytometry was employed to evaluate the expression of specific surface markers by primary cells after the culture period. The pattern of expression was then compared to the initial expression of these molecules to determine differences between the initial and final cell populations. The total cell number was taken into account to consider the absolute changes in the population. Cells were stained with c-kit, Sca1, and a cocktail of lineage markers.

Representative plots from the analysis (one sample) can be seen in Figures 5.8 and 5.9. These data show that there is an increase in the expression of lineage markers

and a decrease in the expression of c-kit and Sca1 markers after 14 days in culture as compared to immediately following sorting (Figure 2.11).

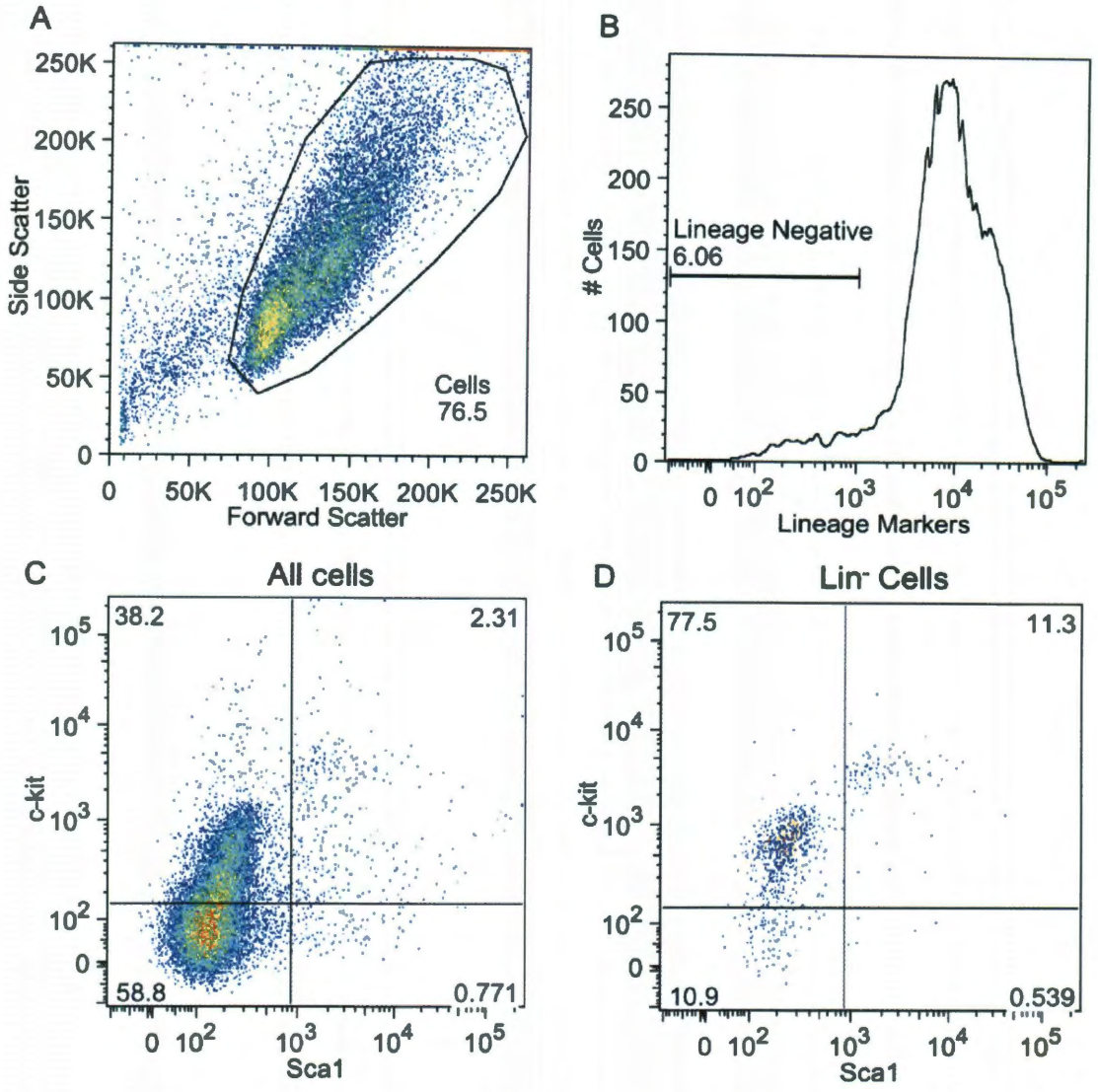

Figure 5.8: Flow cytometry analysis of c-kit$^+$, lin$^-$ cells after 14 days in culture on hydrogels functionalized with PEG-RGDS and PEG-JAG1. A. Particles were gated to count cells. B. Cells were then gated to count those that were lineage negative (lin$^-$). C. A plot of all cells gated for expression of Sca1 and c-kit. D. A plot of lineage negative cells gated similarly to C. Axes without units are relative fluorescent intensity. Numbers on the plots denote the percentage of cells within that specific gate.

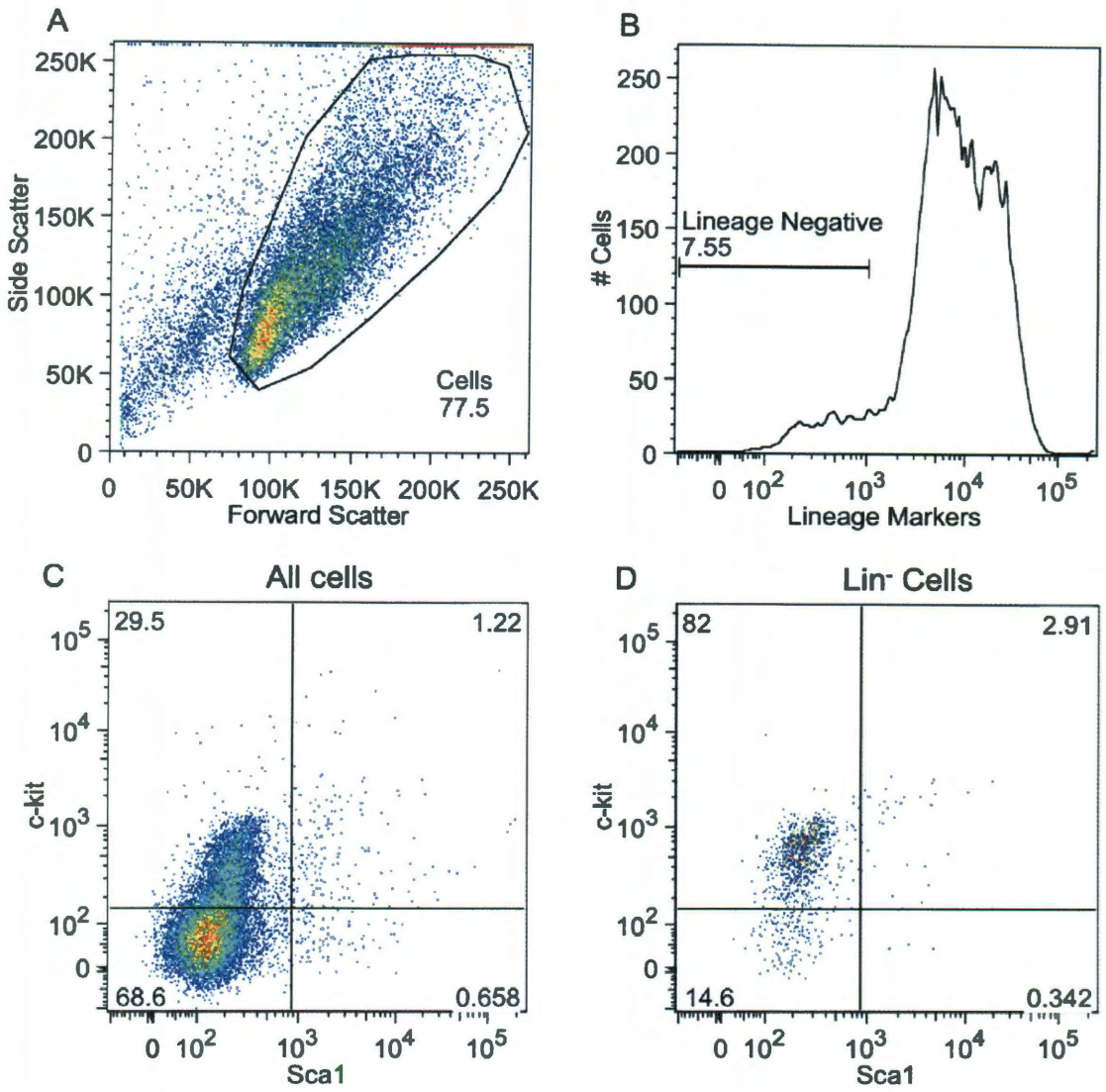

Figure 5.9: Flow cytometry analysis of c-kit$^+$, lin$^-$ cells after 14 days in culture on hydrogels functionalized with PEG-CS1 and PEG-JAG1. A. Particles were gated to count cells. B. Cells were then gated for expression of lineage markers. C. A plot of all cells gated for positive or negative expression of Sca1 and c-kit. D. A plot of lineage negative cells gated similarly to C. Axes without units are relative fluorescent intensity. Numbers on the plots denote the percentage of cells within that specific gate.

This data correlates with what has been observed previously in the culture system with SCF and SDF1α in Chapters 3 and 4. However, as can be seen in Figure 5.10, there is an increase in the c-kit$^+$, lin$^-$ population from gels functionalized with both RGDS and JAG1 that is higher than RGDS alone, and there is a slight increase in this population on gels with CS1 and JAG1. The same trend is seen with the KSL population (Figure 5.11), and

these observations correlate with the results of the colony assay. Though none of the increases is statistically significantly, the fact that similar results were obtained from the two assays suggests that JAG1 is helping to keep cells in a more primitive state.

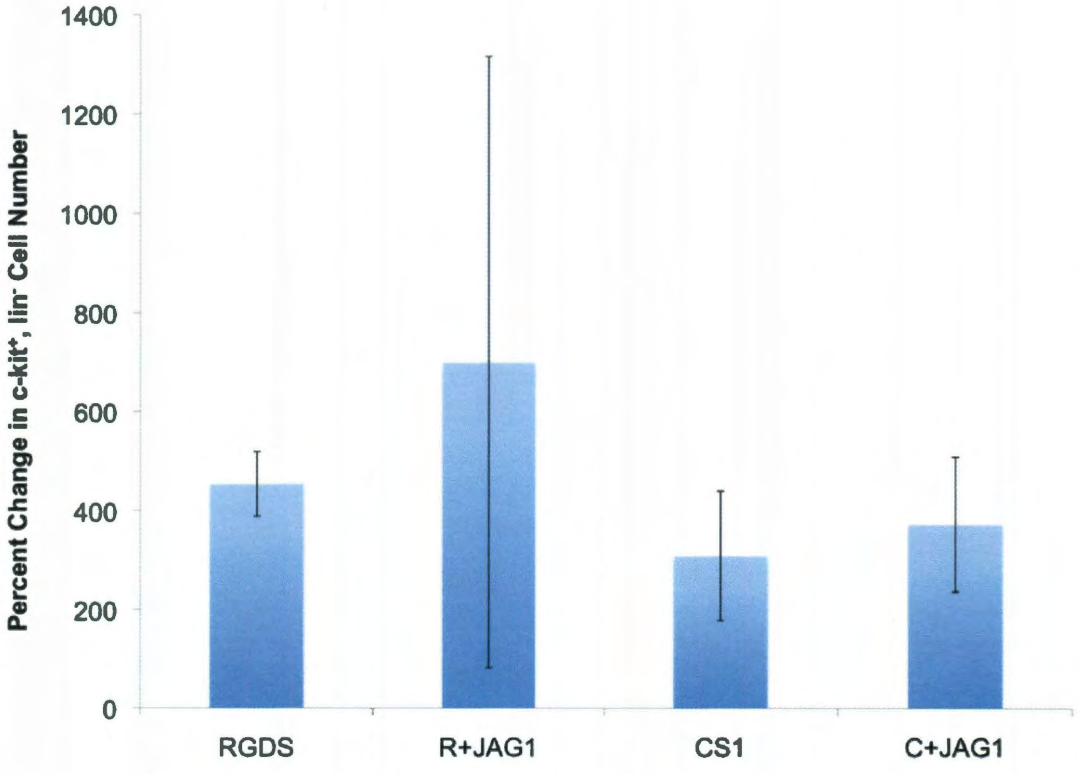

Figure 5.10: Increase in c-kit$^+$, lin$^-$ population during 14 days in culture on gels functionalized with JAG1. The addition of JAG1 to gel surfaces resulted in slight increases to the c-kit$^+$ lin$^-$ population compared to the peptides alone. However, neither of the differences was significant. Data is displayed as mean ± standard deviation. (n=3) (R=RGDS, C=CS1)

JAG1 has been shown in previous work to be capable of maintaining HSCs when added to culture media or immobilized on beads (275, 277, 284). Though some work has shown the ability to utilize JAG1 for HSC expansion, other contradictory work shows relatively little effect on HSC proliferation (103, 278).

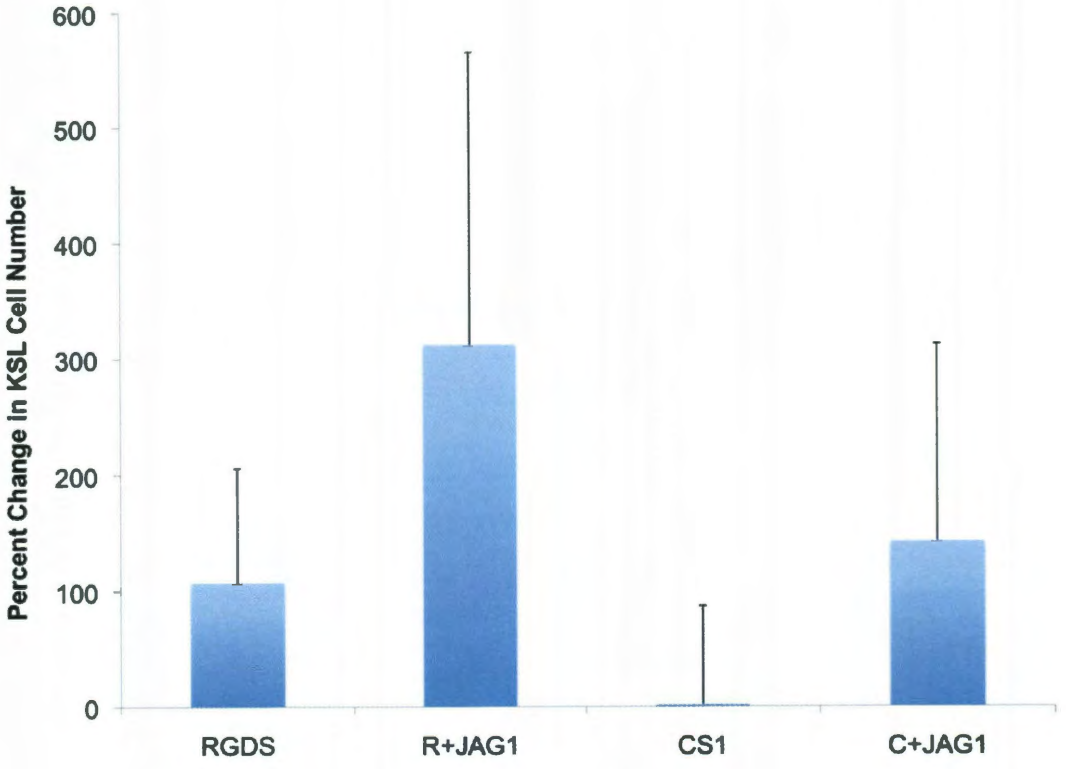

Figure 5.11: Expansion of the primitive KSL population on gels with covalently immobilized JAG1. On gels with RGDS and JAG1, the primitive KSL population increased compared to controls with RGDS alone. On gels with CS1 and JAG1, there was also an increase in the KSL population compared to controls with CS1 alone. However, the increases were not calculated to be significant. Data is displayed as mean + standard deviation. (n=3) (R=RGDS, C=CS1)

In one study, cells were cultured in media containing JAG1. JAG1 did not affect cell expansion compared to controls but the cells cultured in media with JAG1 were capable of repopulation in irradiated hosts (103). In a similar study, Walker *et al.* cultured HSCs on a feeder layer of stromal cells expressing JAG1. HSCs cultured in these conditions did not expand significantly but were retained in an undifferentiated state (278). The culture of HSCs on hydrogel wells functionalized with JAG1 supports these findings. The addition of JAG1 to the gel surfaces did not significantly alter the proliferation of the HSCs compared to controls. It did, however, result in cell populations that were able to both form primitive colonies and express specific markers that denote HSC populations.

5.4 Conclusions

JAG1-Notch signaling within the HSC niche has been shown to play a role in the maintenance of HSCs. To recapitulate this interaction, JAG1 was successfully PEGylated while retaining its bioactivity. The PEGylated protein was surface immobilized onto hydrogel wells in combination with RGDS or CS1 and the effects of JAG1 on HSC expansion and differentiation were evaluated. Though the total cell expansion was not affected by the incorporation of JAG1 into the hydrogel matrix, there were increases in the absolute numbers of cells within primitive HSC populations. These results suggest that hydrogel wells with covalently immobilized JAG1 are capable of maintaining the HSCs in an undifferentiated state through signaling via the Notch receptor expressed on HSC membranes. The ability to maintain HSCs *ex vivo* utilizing the hydrogel system could greatly benefit HSC research field by enabling the generation of large HSC populations as well as providing a way to study basic HSC biology.

Chapter 6: Hematopoietic Stem Cell Behavior in Hydrogel Wells Functionalized with IFNγ

6.1 Background

Interferon-γ (IFNγ) is known to play a significant role in the immune system. Recent studies have shown that it can influence HSC behavior, specifically proliferation and differentiation. As opposed to previous work detailed in this thesis that was dedicated to preserving the multipotency of HSCs, the following studies investigate the ability to use IFNγ to promote HSC differentiation. The ability to trigger differentiation along specific pathways using PEG hydrogel wells would broaden the clinical applicability of the system. In the following work, IFNγ was functionalized onto hydrogel well surfaces and its effects on primary HSC proliferation and differentiation were evaluated after 14 days in culture.

6.1.1 Interferon γ

IFNγ is part of a larger interferon family that was first discovered in 1957 due to its ability to impede viral replication (285, 286). IFNγ is an inflammatory cytokine produced by T helper cells to help regulate immune responses to infection (287). The overexpression of IFNγ has been linked to several anemic diseases though the mechanism through which this occurs is still under investigation (92). IFNγ binds to a heterodimeric receptor on the surfaces of hematopoietic cells, interferon gamma receptors 1 and 2, and stimulates the Jak/Stat signaling pathway (92) (Figure 6.1).

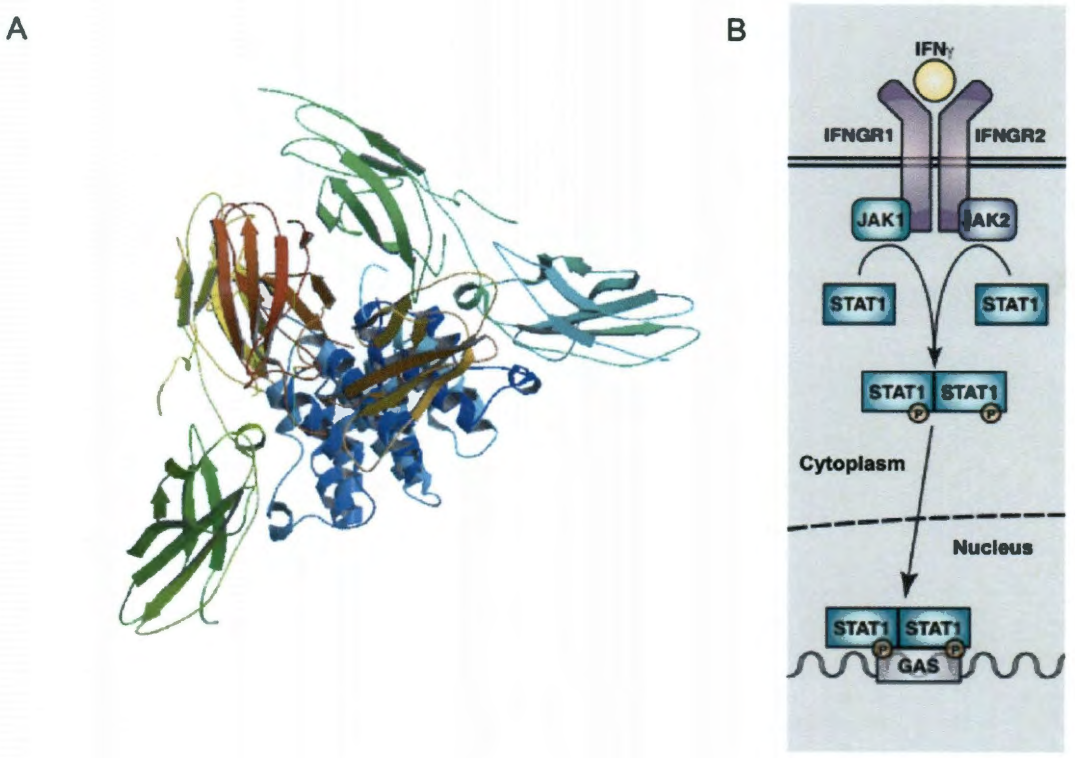

Figure 6.1: Structure of IFNγ and its receptor. A. The crystal structure of IFNγ complexed with its heterodimeric receptor (IFNγ Receptors 1 and 2, IFNGR1-2). Image adapted from (288) B. The signaling cascade triggered by the binding of IFNγ with IFNGR1-2. Upon this binding, Jak1/2 phosphorylate Stat1, which forms a homodimer and translocates to the nucleus where it can promote/suppress gene expression. Image adapted from (92).

IFNγ is considered a negative hematopoietic regulator and has been shown to aid in myeloid and lymphoid homeostasis by inhibiting overproduction (289, 290). Typically this results in a suppression of hematopoiesis or in cell apoptosis (291-295). In some hematopoietic populations, IFNγ has been shown to promote differentiation, specifically down myeloid pathways (92, 296, 297). In contrast, IFNγ can also promote the proliferation of primitive hematopoietic stem cells *in vivo* and *in vitro*, particularly in combination with other cytokines and growth factors. As a result, it has been investigated for use in *ex vivo* expansion systems.

6.1.2 IFNγ for HSC Expansion

IFNγ can stimulate the proliferation of HSCs and *in vitro* hematopoiesis when added to culture media (93, 287, 296, 298-302). This effect is typically seen in conjunction with other cytokine cocktails where the presence of IFNγ can augment cell proliferation but does not promote it singularly. For example, Hwang *et al.* demonstrated that the addition of IFNγ could rescue cells from apoptosis and enhance HSC growth but only in the presence of SDF1α (296). Shiohara *et al.* (1993, 1994) observed similar effects with SCF. When SCF and IFNγ were added together to an *in vitro* culture, there was an increase in the development of both primitive and mature hematopoietic populations (298, 299). These results suggest that IFNγ can play a dual role in the hematopoietic system, triggering both proliferation and apoptosis depending on other signaling factors that are present.

Zhao *et al.* and Baldridge *et al.* both demonstrated that long-term repopulating HSC (LT-HSC) populations can be triggered to proliferate by the addition of exogenous IFNγ to *in vitro* cultures (93, 287). In addition, Baldridge *et al.* injected IFNγ into mice and subsequently collected whole bone marrow for transplantation (93). They observed an increase in *in vivo* LT-HSC number in donor mice, but a reduced ability of these cells to engraft in transplant recipients. Other studies have also demonstrated that this increase in proliferation is accompanied by the differentiation of the cells (287, 297). Due to its ability to act on primitive HSC populations, IFNγ was immobilized onto the surfaces of hydrogel wells in an attempt to drive HSC proliferation and differentiation. The ability to better control and understand these processes can aid in the design of an expansion system with clinical relevance.

6.2 Materials and Methods

All materials were obtained from Sigma unless otherwise noted.

6.2.1 Polymer Synthesis and Characterization

6.2.1.1 PEG-DA, PEG-RGDS, PEG-CS1

PEG-DA, PEG-CS1, and PEG-RGDS were synthesized as aforementioned (Sections 2.2.1.1 and 2.1.1.3). PEG-RGDS made using PEG-SVA was utilized in these studies.

6.2.1.2 PEG-IFNγ

PEG-IFNγ was synthesized with the methods used in the production of PEG-SCF, PEG-SDF1α, and PEG-JAG1 (Sections 3.2.1.3, 4.2.1.2, 5.2.1.2). Murine IFNγ (R&D) was reacted with PEG-SVA at a molar ratio of 100:1 (PEG-SVA: IFNγ) in PBS (pH = 8.0) at 4° C overnight. To confirm PEGylation, a Western blot was performed on the PEGylated and naturally occurring forms of the proteins using a 15% Tris-HCl precast polyacrylamide gel. A primary rabbit polyclonal antibody to murine IFNγ (Abcam) and a secondary goat polyclonal antibody against rabbit IgG conjugated with horseradish peroxidase (Abcam) were used to stain the blot. To detect the stained proteins, the ECL chemiluminescent Western blotting analysis system was applied, and chemiluminescent images of the blot were taken using an LAS 4000.

6.2.1.3 Bioactivity of PEG-IFNγ

To evaluate the activity of IFNγ after PEGylation similar methods were used as when determining the activity of PEG-SCF in Section 3.2.2. 32D cells were seeded into TCPS plates at a density of 5,000 cells/cm^2 in three formulations of media: control media (RPMI-1640 with 10% IL-3 supplement), control media with IFNγ (200 ng/ml) and control media with PEG-IFNγ (200 ng IFNγ/ml). The cells were imaged at 24 h and 5

days. The number of cells at each timepoint was counted using ImageJ software as described in Section 2.2.4.1, and the percent increase in 32D cell number was quantified.

6.2.1.4 Surface Immobilization and Quantification

PEG-DA hydrogel wells were functionalized with IFNγ at concentrations of 200 and 400 ng/cm^2 in combination with either RGDS or CS1 (25 μg/cm^2) as previously described (Section 2.2.2.2). To quantify the concentration of IFNγ on the gel surface, an ELISA was conducted as explained in Section 3.2.1.6 using the mouse IFNγ Quantikine ELISA Kit.

6.2.2 Cell Maintenance

6.2.2.1 Primary c-kit$^+$, lin$^-$ Cell Isolation and Culture

Primary c-kit$^+$, lin$^-$ cells were isolated from murine whole bone marrow and maintained as described in Section 2.2.3.2.

6.2.2.2 Cell Seeding into Hydrogel Wells

c-kit$^+$ lin$^-$ cells were seeded in gel wells ([IFNγ]=400 ng/cm^2, [RGDS]=25 μg/cm^2 or ([IFNγ]=400 ng/cm^2, [CS1]=25 μg/cm^2) at densities of 13,000 cells/cm^2 in volumes of 10 μl. Gel wells with only RGDS or CS1 (25 μg peptide/cm^2) served as controls. Each group consisted of 4 gel wells. Media was added around gels to keep them hydrated. Cells were kept in culture for 14 days at 37°C and 5% CO_2 with media renewal every 2 to 3 days. After culture, the cells from each group were combined so that enough cells were available for flow cytometry. The experiment was conducted a total of three times.

6.2.3 Evaluation of Expanded Hematopoietic Cells

Primary cell expansion and differentiation potential (colony forming unit assay and flow cytometry) were assessed as stated in Sections 2.2.4.3-2.2.4.5.

6.2.4 Statistical Analysis

One-way ANOVAs and Tukey's post-hoc analyses were performed to evaluate statistical differences between groups in all studies using a 95% probability level ($p<0.05$).

6.3 Results and Discussion

6.3.1 Polymer Synthesis and Characterization

6.3.1.1 PEG-IFNγ

To determine if IFNγ was successfully PEGylated, a Western blot was conducted. Figure 6.2 shows an image of the blot after staining. There is a band in the IFNγ lane at 12-15 kDa that reflects the molecular weight of the monomer and band near 30 kDa that represents the IFNγ dimer. In the PEG-IFNγ lane, there is a smear beginning at 25 kDa. The increase in molecular weight indicates that the protein has been PEGylated with multiple PEG chains.

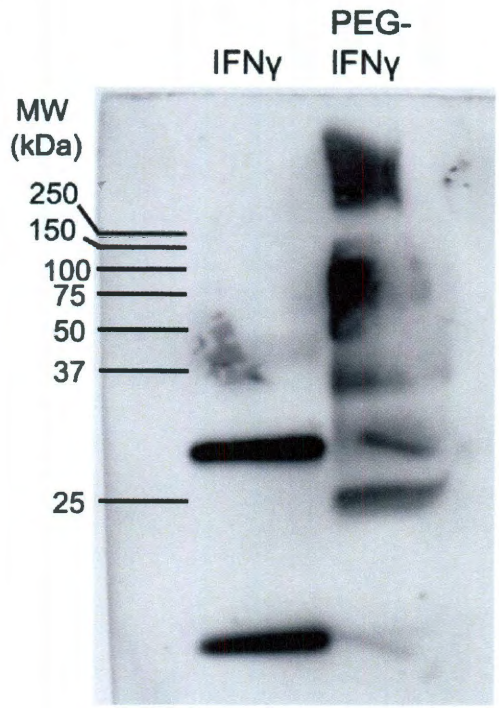

Figure 6.2: Western blot image of IFNγ. There is an increase in molecular weight (MW) after the conjugation reaction indicating that IFNγ has been successfully PEGylated. The smear occurs as a result of multiple PEG chains reacting with the protein. The MW of IFNγ is ~12-15 kDa.

6.3.1.2 Bioactivity of PEG-IFNγ

To assess the activity of the protein after PEGylation, 32D cells were cultured in control media as well as media containing 200 ng/ml IFNγ or PEG-IFNγ. After 5 days in culture, the percent change in cell number was calculated. Cells proliferated significantly in media containing IFNγ or PEG-IFNγ when compared to the control media (Figure 6.3). In addition, there was no significant difference between the percent changes in cell number in the IFNγ and PEG-IFNγ groups. These results demonstrate that the PEGylation of the protein did not significantly affect its activity.

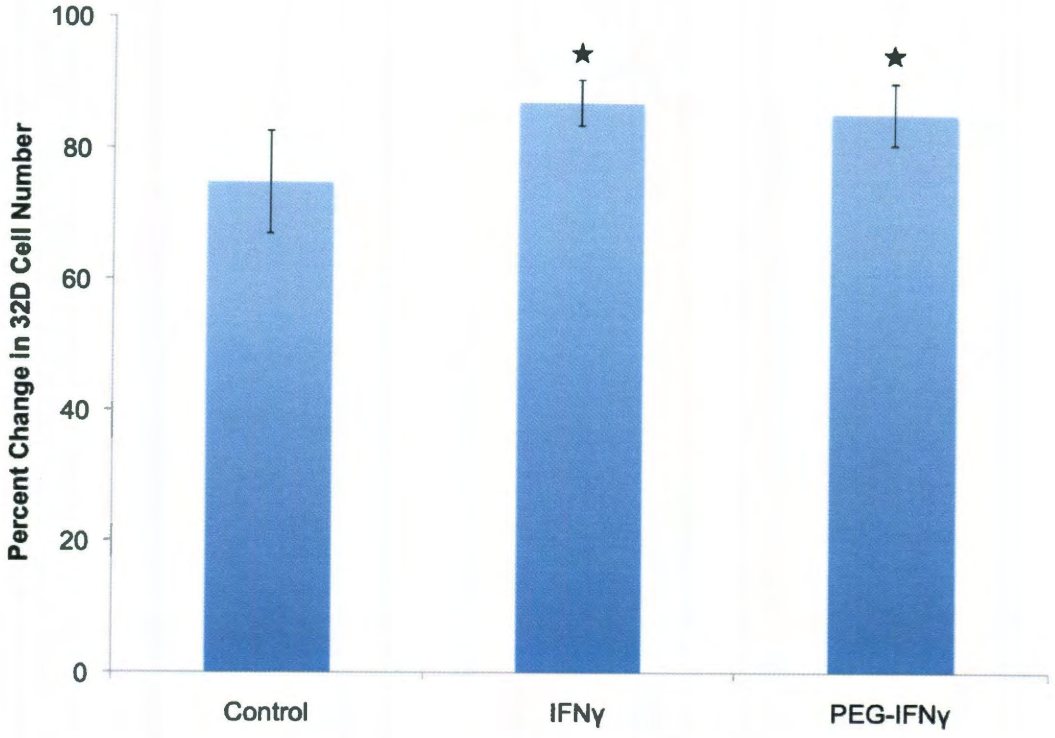

Figure 6.3: Bioactivity of PEGylated IFNγ. 32D cells were cultured in control media and in media containing 200 ng/ml IFNγ or PEG-IFNγ. There was a significant increase in the percent change in cell number in wells with either IFNγ or PEG-IFNγ compared to control media. There was not a significant difference between IFNγ and PEG-IFNγ. Bars are mean ± standard deviation. (★ denotes significance compared to control, n=8, $p < 0.05$)

6.3.1.3 Quantification of Surface IFNγ

An ELISA was used to quantify the percentage of IFNγ that was not conjugated to the hydrogel surface, and the surface concentration was back calculated from this data. Approximately 99% of the PEGylated protein that was added to the gel was covalently immobilized onto the surface resulting in 87.26 ± 0.213 ng of IFNγ on each hydrogel well surface.

6.3.2 Primary Cell Expansion

One of the main objectives of an *in vitro* HSC culture system is the promotion of HSC self-renewal. To monitor c-kit$^+$, lin$^-$ cell expansion on hydrogels functionalized

with IFNγ, phase contrast images were taken at varying timepoints throughout the 2 week culture period (Figure 6.4). Cell proliferation is sustained on both gel surfaces containing IFNγ, but it appears that the cells proliferated to a greater extent on surfaces containing both RGDS and IFNγ. The cells maintain their rounded shape and remain approximately 10 μm in diameter. The percent change in cell number was quantified by counting the final cell number from each group and comparing it to the initial number (Figure 6.5). This data correlates with the phase contrast images, showing a significant increase in cell number on gels with surface immobilized RGDS and IFNγ compared to all other groups.

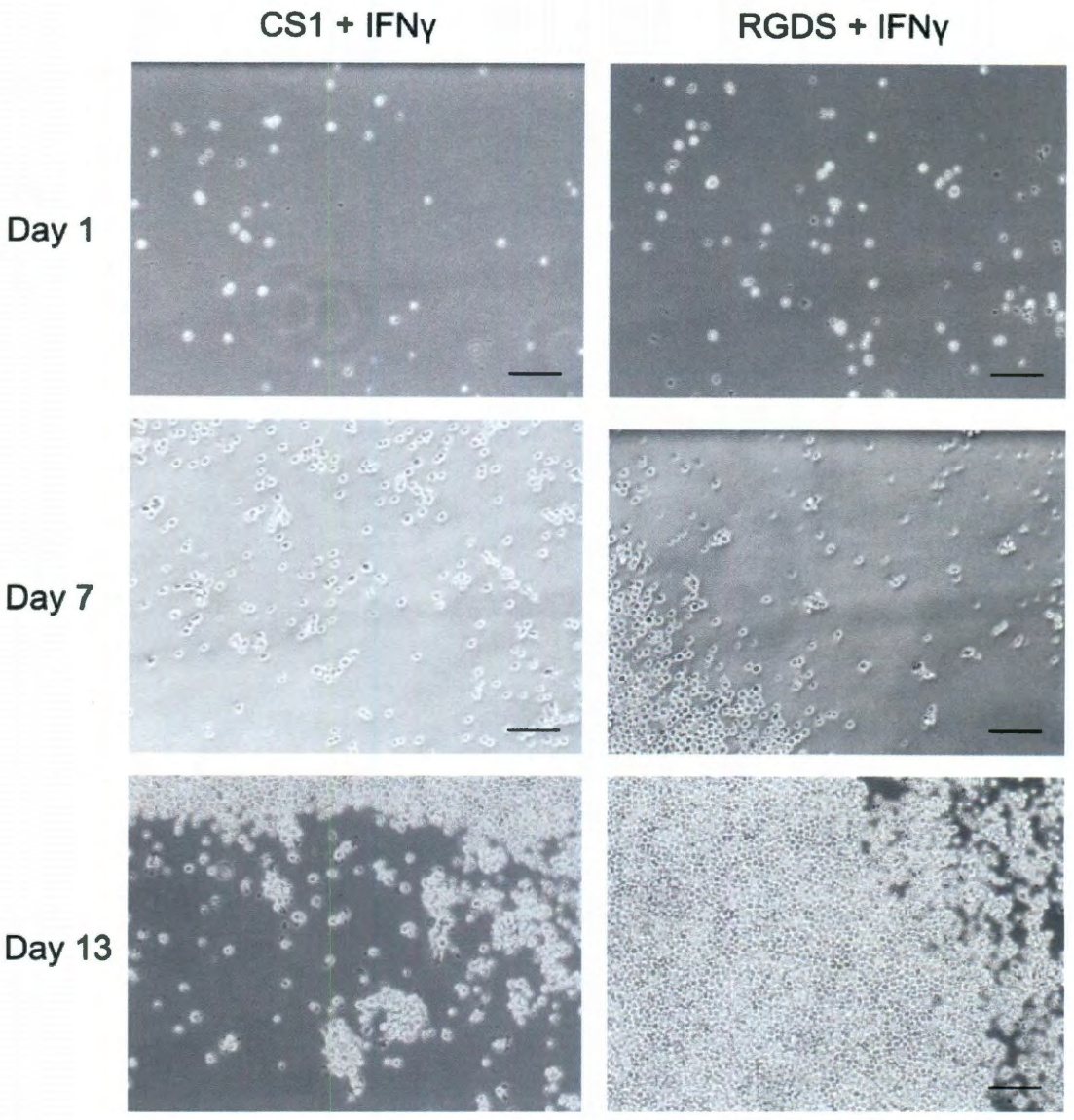

Figure 6.4: c-kit$^+$, lin$^-$ cells on hydrogels functionalized with IFNγ and RGDS or CS1. Cells proliferated extensively within gel wells with both RGDS and IFNγ, as indicated by increasing number of cells present in the field of view over time. Scale bars = 100 μm.

Traditionally, IFNγ has been regarded as a negative regulator of hematopoiesis and a cytokine that often triggers apoptosis (92, 291, 303). In contrast, several groups have shown success in using IFNγ to stimulate hematopoietic cell proliferation (93, 287, 296-302). Interestingly, most studies that report HSC proliferation are performed with other cytokines, such as SDF1α, SCF, IL-3 or TPO, present in the media. Shiohara *et al.*

(1993, 1994) have shown that the combination of soluble SCF and IFNγ can work together to promote HSC expansion (298, 299).

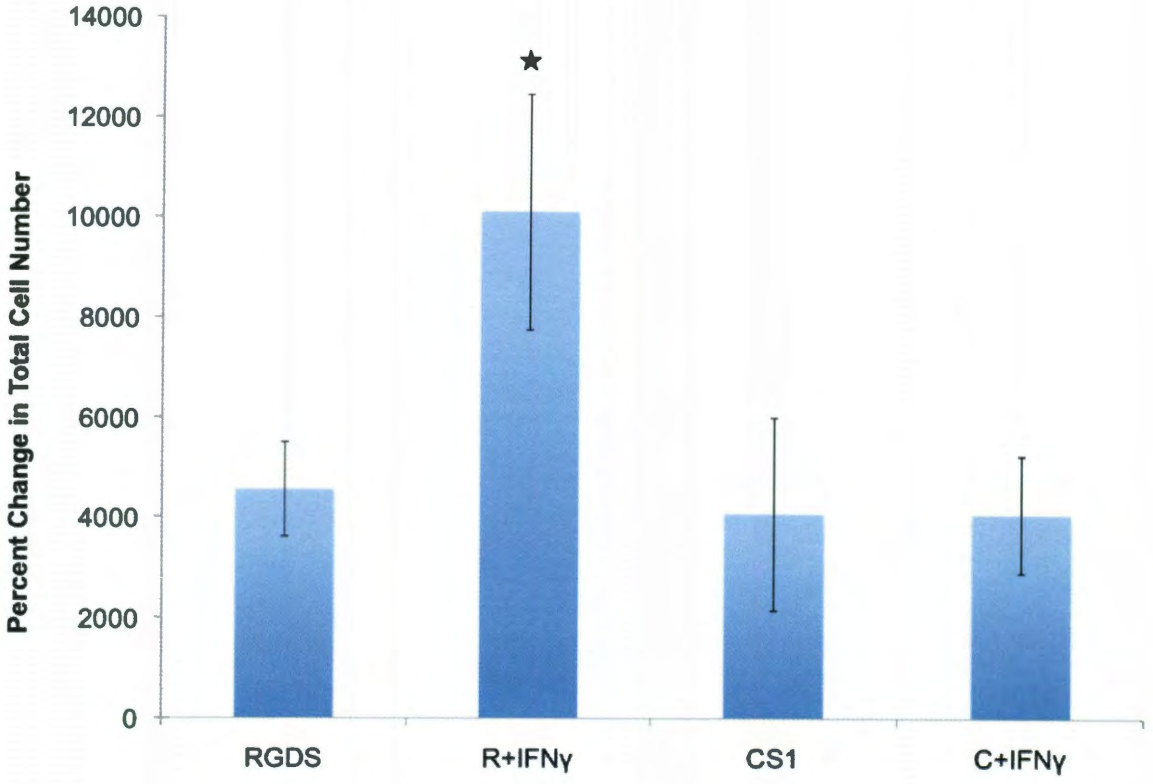

Figure 6.5: Total cell expansion on hydrogel surfaces with immobilized IFNγ after 2 weeks in culture. There was a significant increase in cell expansion on gels with both RGDS and IFNγ compared to all other samples. Bars are mean ± standard deviation. (R=RGDS, C=CS1; RGDS, ★ denotes significance compared to all other groups, n=3, $p < 0.05$)

The results described in this chapter support these findings; primary cells were cultured on hydrogels functionalized with IFNγ in media containing soluble SCF. The cells proliferated significantly in gel wells in response to the IFNγ and RGDS on the surfaces. However, when IFNγ was added to gel wells with CS1, there was no significant effect on cell proliferation. This is similar to what was observed with SCF and CS1 in Chapter 3. When in combination with RGDS, cells on gels functionalized with SCF and IFNγ proliferate extensively, but this does not occur when the proteins are immobilized with CS1. Previous work has shown differing effects of binding via the α4β1 integrin, the

integrin that binds to the CS1 portion of fibronectin. Kapur *et al.* found that binding via the α4β1 integrin led to the apoptosis of erythrocyte progenitor cells, while binding with the α5β1 integrin led to cell survival and proliferation (247). However, other studies have shown hematopoietic cell proliferation in response to binding via both integrins (122, 191). Additionally, HSC culture on CS1 has resulted in cells that were less differentiated when compared to RGDS (122, 125). This was also seen in Chapter 4 where cells cultured on gels modified with a combination of CS1 with SDF1α. It is unclear why HSCs in the culture system do not proliferate in response to cytokines such as SCF and IFNγ when they are cultured on surfaces with immobilized CS1 as significantly as when these cytokines are immobilized in combination with RGDS. It is possible that adhesion to CS1 is helping to retain HSCs in a quiescent state, which in turn, slows their proliferation rate. To better characterize the cells expanded in hydrogel wells with surface immobilized IFNγ, a colony forming assay and flow cytometric analysis of stem cell surface markers were performed.

6.3.3 Primary Cell Differentiation

6.3.3.1 Colony Forming Unit Assay

The colony assay was conducted as a functional assay to determine which pathways the expanded cells could differentiate down. Four types of colonies were evaluated: CFU -G, -M, -GM, and -GEMM. Figure 6.6 shows the colonies that formed from the expanded cells as a function of the hydrogel surface.

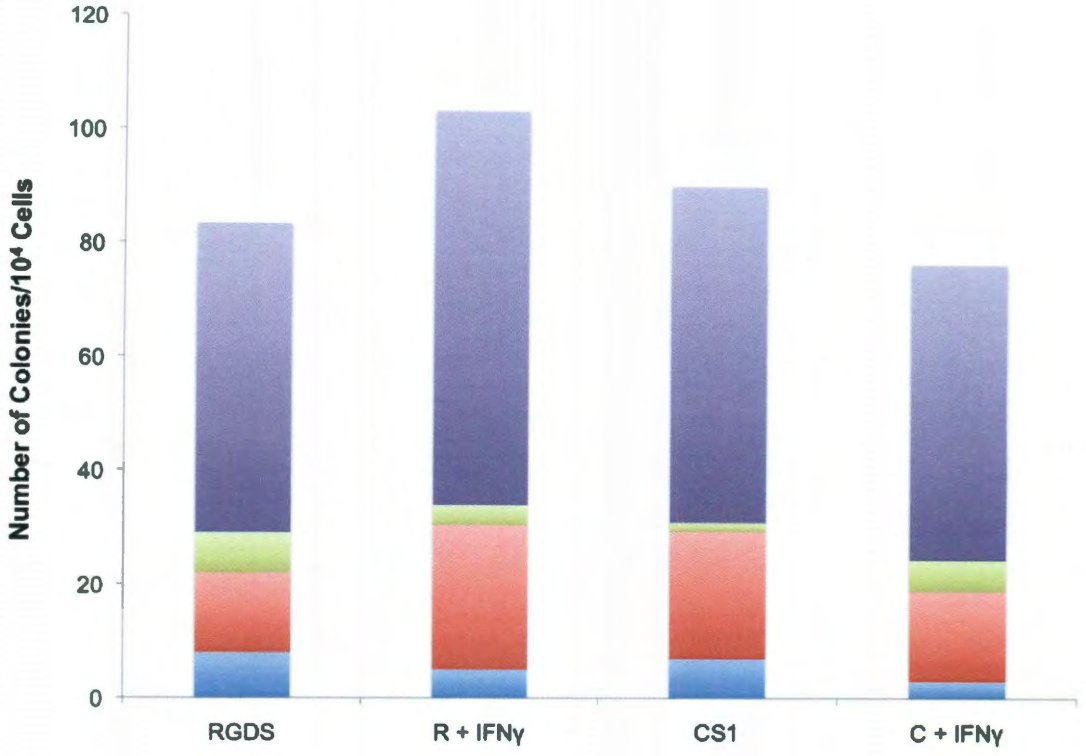

Figure 6.6: Colony formation from cells expanded on gels with surface immobilized IFNγ. The group with both RGDS and IFNγ formed the most colonies. There is also appears to be an increase in total primitive colonies on RGDS and IFNγ compared to RGDS and a decrease in the formation of these colonies on CS1 and IFNγ. Bars are mean, n=2. (R=RGDS, C=CS1; **CFU-GEMM=Granulocyte, Erythrocyte, Megakaryocyte, Macrophage**, **CFU-GM=Granulocyte/Macrophage**, **CFU-G=Granulocyte**, **CFU-M=Macrophage**)

Cells expanded in gel wells functionalized with RGDS and IFNγ formed the highest number of colonies: 100 colonies/10^4 cells, and CS1 and IFNγ formed the lowest around 75 colonies/10^4 cells. Figures 6.7 shows the colony distribution per group displayed as a percentage of the total colony formation.

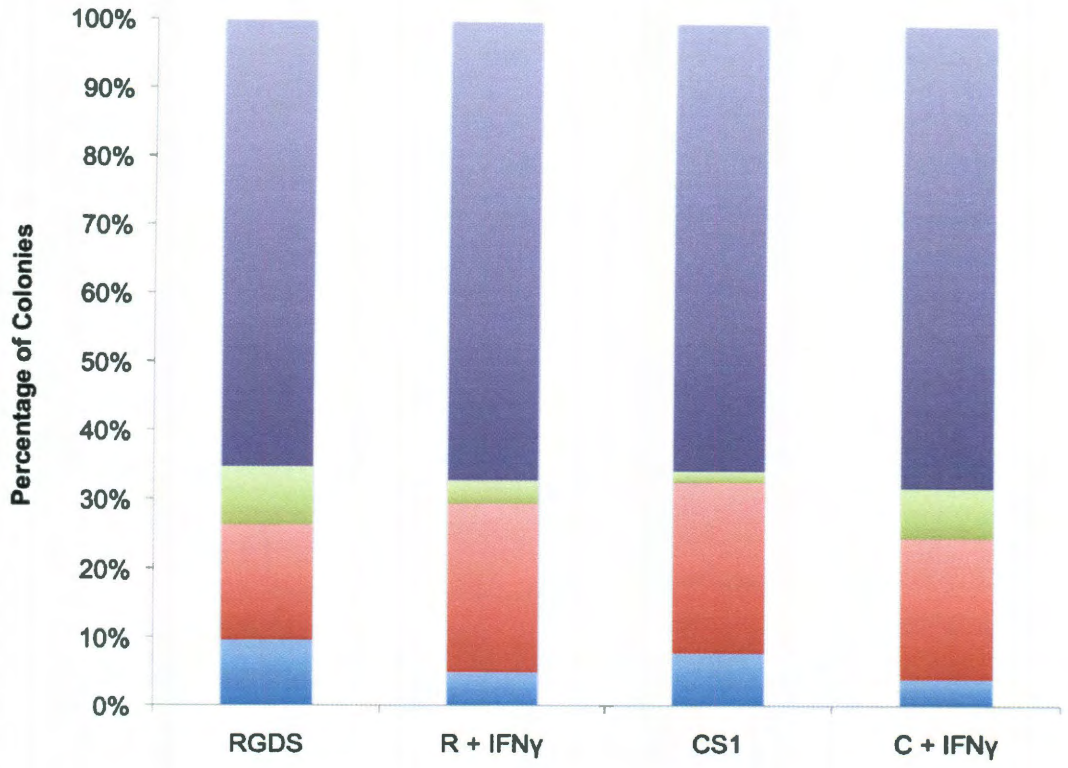

Figure 6.7: Distribution of colonies formed from cells expanded on gels with surface immobilized IFNγ. The percentage of primitive colonies (both GM and GEMM) is not significantly different between any of the groups. However, the addition of IFNγ appears to limit the formation of the most primitive GEMM colonies. Bars are mean, n=2. (R=RGDS, C=CS1; **CFU-GEMM=Granulocyte, Erythrocyte, Megakaryocyte, Macrophage**, **CFU-GM=Granulocyte/Macrophage**, **CFU-G=Granulocyte**, **CFU-M=Macrophage**)

Though the percentage of GM and GEMM colonies appears to be relatively similarly between all groups, there is a slight decrease in GEMM formation from cells cultured on hydrogels with surface immobilized IFNγ in both the RGDS and CS1 groups. This can be seen more clearly in Figure 6.8 where individual colony data is displayed. Though none of the differences are significant, these results suggest that IFNγ is triggering differentiation to some extent. Primitive GM colonies are still forming, but there is a loss in the ability to form the most primitive GEMM colonies compared to controls without IFNγ.

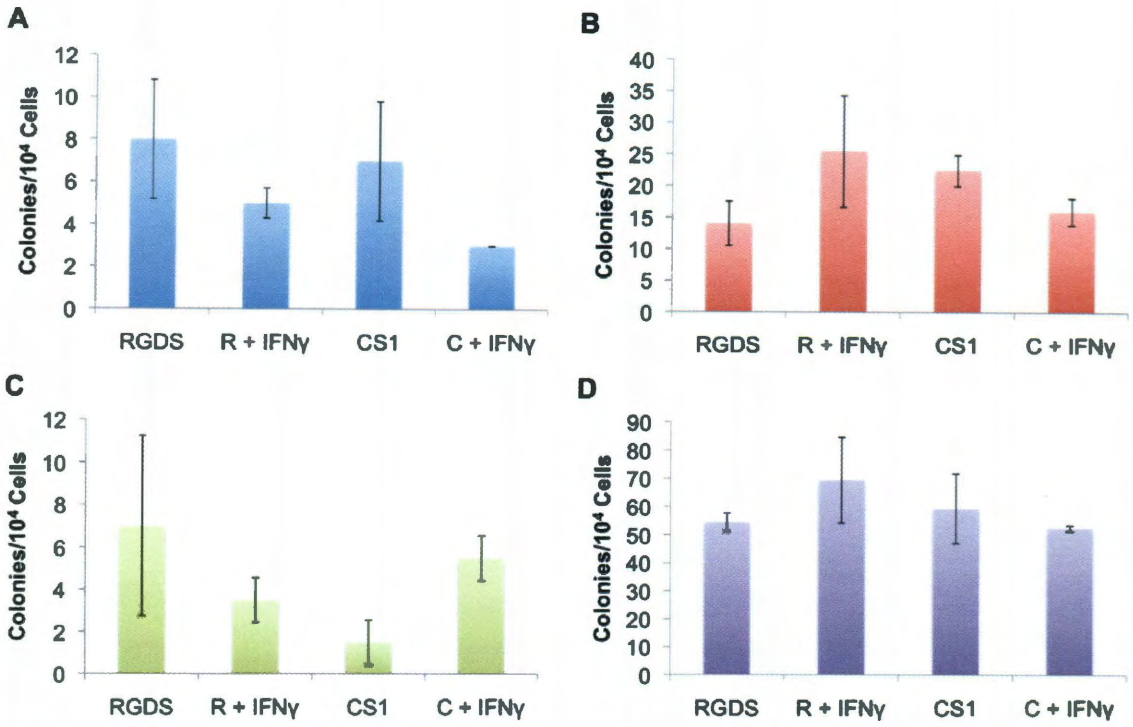

Figure 6.8: Individual colony formation organized by colony type from cells expanded on IFNγ functionalized hydrogels. The addition of IFNγ decreased GEMM formation in combination with CS1 and RGDS. There was a slight increase in GM formation on RGDS with IFNγ, but on CS1 and IFNγ this number decreased. Bars are mean ± standard deviation. (n=2) (R=RGDS, C=CS1; **A. CFU-GEMM=Granulocyte, Erythrocyte, Megakaryocyte, Macrophage, B. CFU-GM=Granulocyte/Macrophage, C. CFU-G=Granulocyte, D. CFU-M=Macrophage**)

6.3.3.2 Flow Cytometry

To further confirm these results, flow cytometry analysis was performed to quantify the expression of specific surface markers known to denote primitive HSC populations. Cells were stained for c-kit, Sca1, and lineage markers. Figures 6.9 and 6.10 show representative plots of the flow cytometry data. Similarly to previous work in the hydrogel system, there is a decrease in the percentage of total cells that are lin^- and $c\text{-}kit^+$. However, this decrease does not seem to be as extensive as with other proteins.

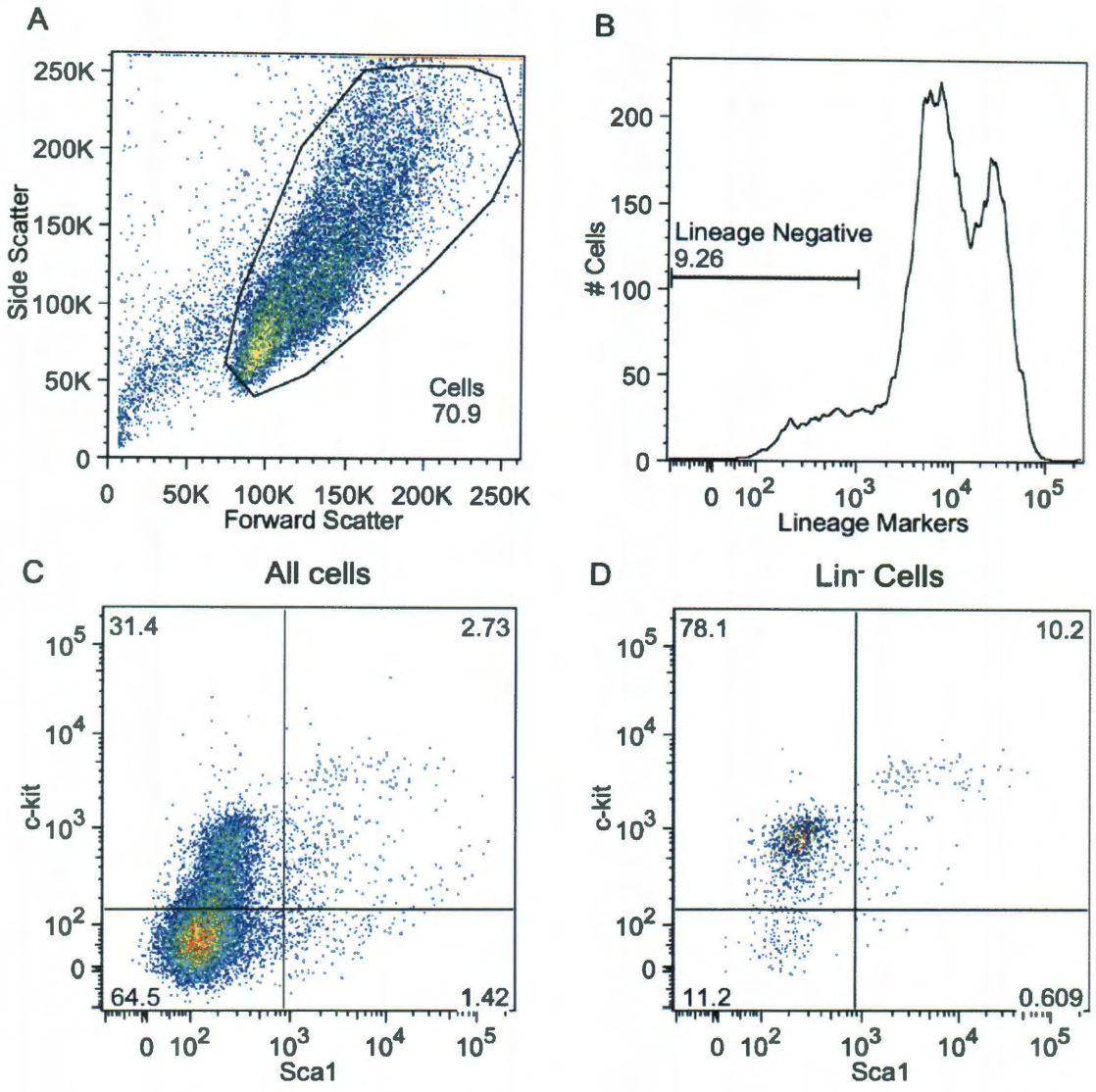

Figure 6.9: Flow cytometry analysis of c-kit$^+$, lin$^-$ cells after 14 days in culture on hydrogels functionalized with PEG-RGDS and PEG-IFNγ. A. Particles were gated to count cells. B. Cells were then gated to count those that were lineage negative (lin$^-$). C. A plot of all cells gated for expression of Sca1 and c-kit. D. A plot of lineage negative cells gated similarly to C. Axes without units are relative fluorescent intensity. Numbers on the plots denote the percentage of cells within that specific gate.

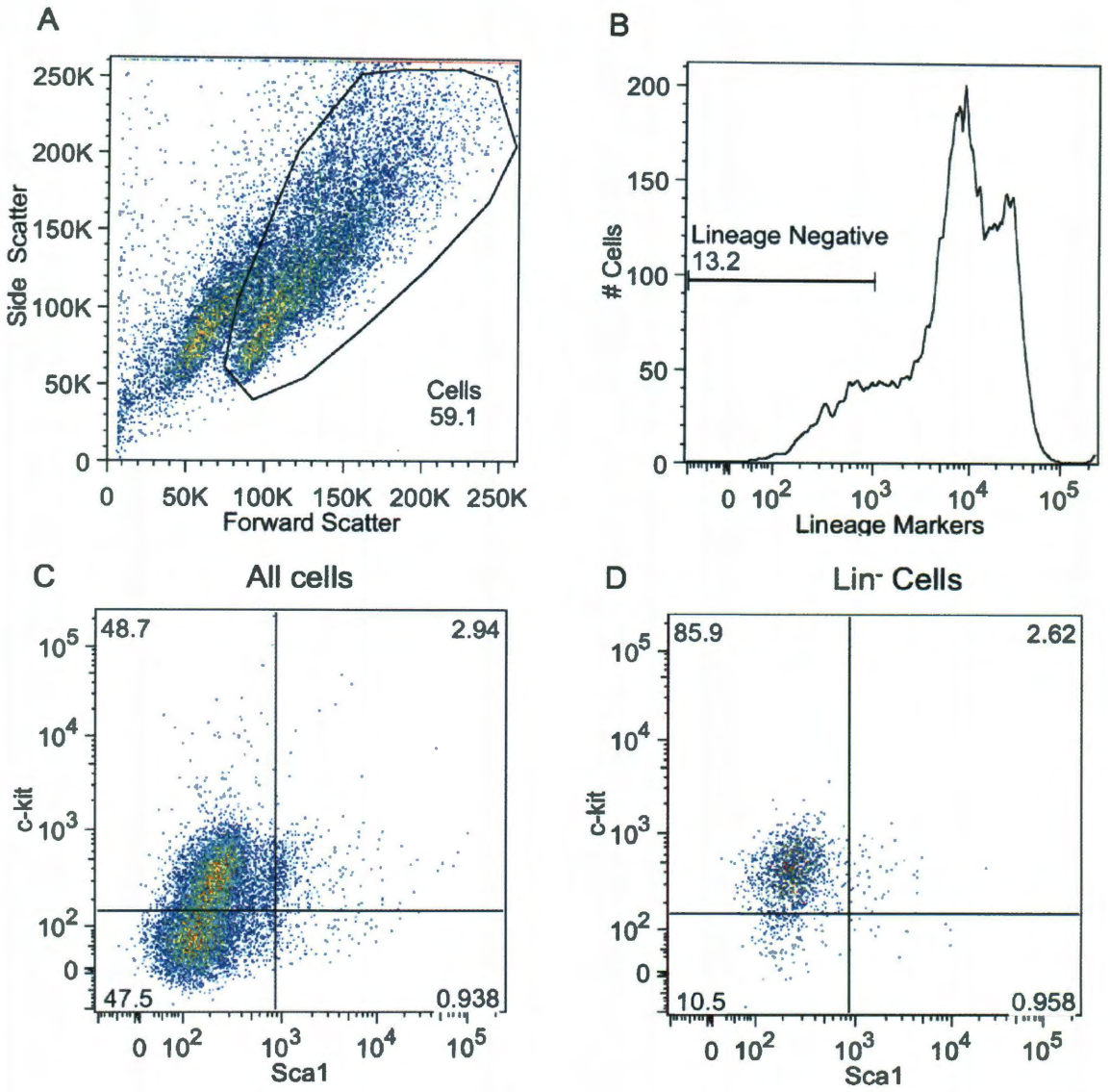

Figure 6.10: Flow cytometry analysis of c-kit$^+$, lin$^-$ cells after 14 days in culture on hydrogels functionalized with PEG-CS1 and PEG-IFNγ. A. Particles were first gated to count cells. B. Cells were then gated for those that did not express lineage markers. C. A plot of all cells gated for positive and negative Sca1 and c-kit markers. D. A plot of lineage negative cells gated similarly to C. Axes without units are relative fluorescent intensity. Numbers on the plots denote the percentage of cells within each gate.

Figure 6.11 shows the percent change in the number of c-kit$^+$, lin$^-$ cells during the 14 day culture. c-kit$^+$, lin$^-$ cells cultured on gels with RGDS and IFNγ expanded significantly compared to all other groups. Cells cultured on gels with CS1 and IFNγ

showed a slight increase in the c-kit$^+$, lin$^-$ population compared to CS1 alone though this change was not significant.

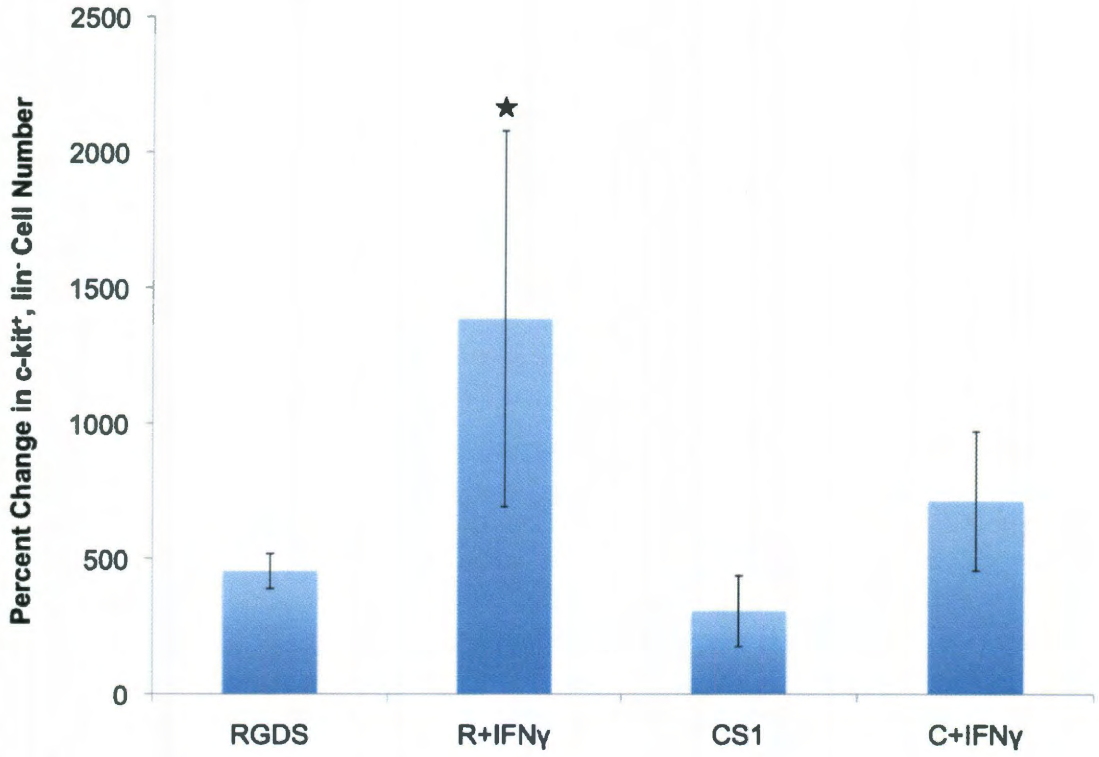

Figure 6.11: Increase in c-kit$^+$, lin$^-$ population during 14 days in culture on gels functionalized with IFNγ. The addition of IFNγ to surfaces with RGDS significantly increased the total population of c-kit$^+$ lin$^-$ cells. There was also a slight increase in cell number on gels with the combination of CS1 and IFNγ, though this change was not significant. Data is displayed as mean ± standard deviation. (R=RGDS, C=CS1; ★ denotes significance compared to all other groups, n=3, $p < 0.05$)

The percent changes in the primitive KSL population of HSCs can be seen in Figure 6.12. The KSL population increased significantly on samples with both RGDS and IFNγ compared to all other groups. However, the combination of CS1 and IFNγ did not demonstrate a significant change in the KSL population though it was slightly higher than CS1 alone.

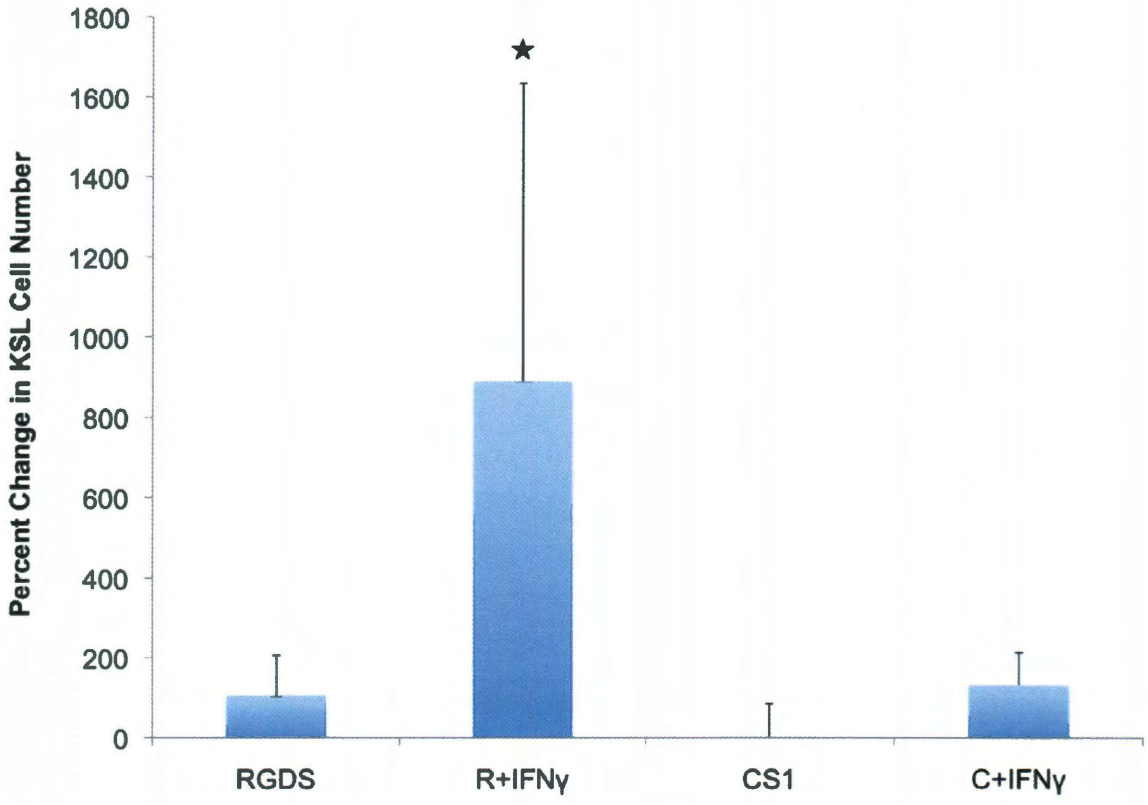

Figure 6.12: Expansion of the primitive KSL population on gels with covalently immobilized IFNγ. On gels with RGDS and IFNγ, the primitive KSL population increased significantly compared to all other groups. On gels with CS1 and IFNγ, there was also an increase in the KSL population compared to controls with CS1 alone, though this change was not significant. Data is displayed as mean + standard deviation. (R=RGDS, C=CS1; ★ denotes significance compared to all other groups, n=3, $p < 0.05$)

These results are somewhat counterintuitive when taking the colony results into account. Previous work has demonstrated that IFNγ triggers differentiation during *in vitro* culture (93, 292, 297). Baldridge *et al.* showed that cells expanded *in vivo* with IFNγ showed a reduced ability to engraft (93). Yang *et al.* also showed that IFNγ could trigger HSC proliferation but led to differentiation (297). The CFU assay results support these findings. Cells expanded on gel surfaces with surface immobilized IFNγ showed a reduced ability to form GEMM colonies. However, the flow cytometry data shows a significant increase in the KSL population when cells were grown on IFNγ functionalized

hydrogels. This suggests that IFNγ can prevent the differentiation of the HSCs. However, we do not see the same result on surfaces with IFNγ and CS1; the percent change in the KSL population is minimal, though greater than on control gels with CS1 only. This supports the results from the CFU assay and suggests that the hypothesis that the combination of CS1 and IFNγ prevents differentiation is inaccurate.

The conflicting colony and flow cytometry data for samples with RGDS and IFNγ is likely because the two assays evaluate distinct cell properties. The colony assay evaluates HSC functionality whereas the flow cytometric analysis assesses the expression of primitive surface markers. Baldridge *et al.* demonstrated that while they were able to expand the KSL population, the cells showed reduced engraftment potential (93). The cells maintained their expression of the primitive KSL markers but they were no longer able to home to the bone marrow and repopulate the immune system upon transplantation. This indicates that they have started down the differentiation pathway. This is similar to what I observed. Cells expanded on IFNγ and RGDS still expressed the primitive surface markers but were unable to form GEMM and GM colonies that are composed of more than one colony. This demonstrates a reduced ability to differentiate down multiple pathways. These results show that the functionalization of the hydrogel with IFNγ can drive and support differentiation, which makes the system more versatile and could lead to the generation of more mature blood cell populations. However, the somewhat contradictory results of the colony assay and flow cytometry analysis emphasize the need to conduct multiple *in vitro* and *in vivo* assay to characterize the cell populations grown within the hydrogel wells.

6.4 Conclusions

IFNγ has been used successfully to promote HSC expansion at the expense of driving HSC differentiation. This work demonstrated the ability to PEGylate IFNγ while retaining its activity. Primary c-kit$^+$, lin$^-$ cells were cultured in hydrogel wells functionalized with IFNγ and either RGDS or CS1 for two weeks. Cells expanded on gels with surface immobilized RGDS and IFNγ showed significant cell proliferation compared to controls. In contrast, the combination of CS1 and IFNγ did not promote cell proliferation. Though the cells cultured on RGDS and IFNγ showed high percent changes in both the c-kit$^+$, lin$^-$ and KSL populations, the colony data demonstrated the inability of these cells to form primitive GEMM colonies. These results show the versatility of the hydrogel system. In the previous chapters, bioactive factors were added in an attempt to retain the differentiation potential of HSCs. In contrast, the work in this chapter functionalized the hydrogel surface with a cytokine known to initiate differentiation and triggered the cells to begin this process.

Chapter 7: Encapsulation of Hematopoietic Stem Cells in Bioactive Degradable Hydrogels

7.1 Background

The ability to recapitulate the bone marrow microenvironment in three dimensions has the potential to maintain HSCs in culture for long periods because a three-dimensional system would better represent the native bone marrow architecture. This chapter focuses on the translation of the two-dimensional hydrogel well system into a three-dimensional biomimetic hydrogel. In preliminary, proof-of-concept studies, primary c-kit$^+$ hematopoietic cells were encapsulated within protease sensitive hydrogels and viability was assessed after encapsulation. After culture for 2 or 4 weeks, hydrogels were degraded to retrieve the hematopoietic cells and the differentiation potential of the cells was evaluated.

7.1.1 Cell Encapsulation within Degradable PEG Hydrogels

Poly(ethylene glycol) hydrogels can be rendered enzymatically biodegradable by flanking a degradable peptide sequence, targeted to a specific enzyme, with monoacrylated PEG chains (167, 183). The PEG chains can subsequently be photopolymerized to form a hydrogel that has protease sensitive molecules within its matrix. Cells can also be included in the prepolymer solution and become entrapped within the hydrogel matrix during polymer crosslinking (See Figure 2.3). Several protease sensitive peptide sequences have been studied and characterized. Patterson *et al.* (2010, 2011) studied the ability of three proteases to degrade an array of peptide sequences and discovered varying degrees of sensitivity to the proteases as well as significant effects on degradation rate (181, 182). The selection of a peptide sequence for

cell encapsulation relies heavily on the application and the enzyme activity of cells that are being encapsulated.

Encapsulation strategies have been used for the engineering of numerous three-dimensional tissues ranging from the pancreas to bone (304-310). In these studies, cells are first entrapped within a polymer scaffold. Over time, the cells release proteases to gradually remodel and degrade the scaffold and create a functional tissue absent of synthetic components. There have been some attempts to encapsulate cells for hematopoietic stem cell expansion; however, most of these studies have focused on the encapsulation of stromal cells for HSC maintenance (110, 311). Encapsulation allows stromal cell-HSC signaling through soluble cytokines and prevents cell-cell contact, which is beneficial for clinical applications since xenogeneic stromal cells are often used.

A couple of groups have investigated the use of encapsulation strategies for *ex vivo* HSC expansion. Levee *et al.* encapsulated whole bone marrow within an alginate-poly-L-lysine copolymer and observed total cell growth after 16-19 days in culture, though most of the cells were more differentiated hematopoietic progenitors (312). Yuan *et al.* demonstrated the ability to encapsulate cord blood hematopoietic stem cells within alginate scaffolds; their results showed an improvement in hematopoietic cell expansion after 12 days in their three-dimensional scaffolds compared to conventional two-dimensional cell culture (313). These studies demonstrate the ability to encapsulate hematopoietic cells and culture them in three dimensions. However, alginate scaffolds do not offer the same degree of tunability as the PEG hydrogel based system. As opposed to alginate scaffolds, PEG hydrogels are biologically inert. PEG gels can be rendered bioactive by covalently immobilizing individual biomolecules into the hydrogel matrix,

allowing researchers to investigate the effects of individual molecules on cell behavior (151). In addition, alginate scaffolds degrade slowly over time due to hydrolysis, whereas the degradation rate of synthetic PEG scaffolds can be tailored by the inclusion of specific degradable peptide sequences (151, 314). Sections 2.1.1-2.1.3 contain a more extensive discussion of the advantages of synthetic PEG hydrogels.

7.1.2 Advantages of Encapsulation for HSC Expansion

The encapsulation of HSCs within a three-dimensional hydrogel matrix mimics the native structure of the bone marrow cavity more accurately than two-dimensional culture on hydrogel surfaces. A precise recapitulation of the *in vivo* microenvironment will likely lead to the ability to maintain HSCs in *ex vivo* culture (32, 62). Physical entrapment also helps to contain these highly motile cells during culture. In two-dimensional systems, cells frequently leave the surface and grow in suspension. Furthermore, encapsulation ensures HSC interaction with biomolecules covalently tethered to the hydrogel matrix, such as RGDS or SCF, which can help control HSC behavior.

Fedorovich *et al.* demonstrated that photopolymerization of mesenchymal stem cells (MSC) within a methacrylated hyaluronic acid hydrogel did not negatively impact the cells' viability or differentiation potential (315). The ability to successfully encapsulate MSCs, which are also bone marrow derived, suggests that the photopolymerization process may not be harmful to HSCs. The speed of the photopolymerization process ensures that the cells are distributed homogenously throughout the scaffold.

The peptide sequence GGGPQGIWGQGK (PQ) was selected for incorporation into the PEG backbone due to its ability to be degraded by several MMPs (183). This peptide sequence has been successfully incorporated into PEG hydrogels to promote the vascularization of tissue-engineered constructs (310). Moon *et al.* encapsulated a coculture of endothelial cells and pericyte precursors within a degradable PEG-PQ-PEG hydrogel and observed degradation of the hydrogel as vascular networks formed (310).

In contrast, significant degradation of the hydrogels by the HSCs is not expected because the encapsulated cells are retained within a synthetic niche environment and not stimulated by outside signals to mobilize. During homeostasis, HSCs are lodged within the niche and their enzymatic activity is fairly low. Matrix metalloproteinase (MMP) activity is upregulated during the mobilization and homing processes; specifically, MMP 2 and 9 expression increases on mobilized hematopoietic cells (57). This allows cells to both exit and enter the bone marrow. After *ex vivo* culture, a protease solution will be added to the media to degrade the hydrogel and allow retrieval of the expanded cells for analysis.

7.2 Materials and Methods

All materials were obtained from Sigma unless otherwise noted.

7.2.1 Polymer Synthesis and Characterization

7.2.1.1 Peptide Synthesis

NH_2-GGGPQG↓IWGQGK-COOH (PQ) was synthesized using solid-state peptide synthesis following the principles of Fmoc chemistry with an Apex 396 peptide synthesizer (AAPPTec, Louisville, KY). The arrow denotes the site of cleavage within the sequence. The peptide was cleaved from the resin with trifluoroacetic acid (TFA). The TFA was removed by rotary evaporation followed by peptide precipitation and

washing in diethyl ether. To confirm successful synthesis, the peptide was analyzed using matrix-assisted laser desorption ionization time of flight mass spectrometry (MALDI-ToF; Bruker Daltonics, Billerica, MA).

7.2.1.2 PEG-PQ-PEG Synthesis

PQ peptide was reacted with PEG-SVA at a molar ratio of 1:2.2 (PQ:PEG-SVA) in PBS (pH 8.0) at 4°C overnight to form PEG-PQ-PEG (Figure 7.1). The sample was then dialyzed against milliQ water to remove unconjugated peptide from the sample. The solution containing the peptide was lyophilized and then run on GPC to confirm successful conjugation to PEG.

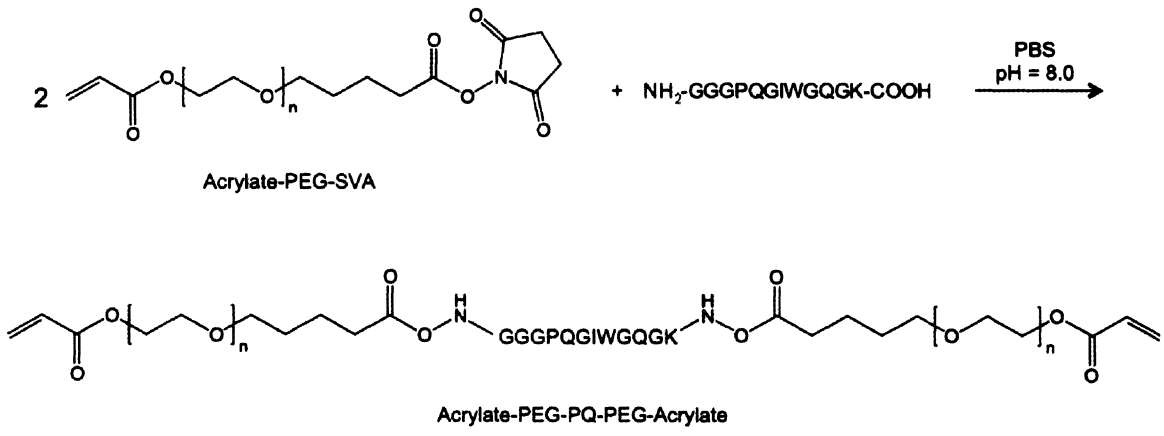

Figure 7.1: PEG-PQ-PEG synthesis. PEG-SVA is reacted with GGGPQGIWGQGK (PQ) at a 2.2:1 molar ratio in PBS at pH 8.0 at 4°C overnight. The resulting product is a diacrylate PEG chain with the degradable PQ sequence sandwiched between the two PEG segments. The site of degradation occurs between G and I. The acrylate groups on each end of the chain can crosslink together, similarly to PEG-DA, to form a hydrogel.

7.2.1.3 PEG-Biomolecule Synthesis

PEG -RGDS, -SCF, -JAG1, and –IFNγ were all synthesized as previously described in Sections 2.2.1.3, 3.2.1.3, 5.2.1.2, and 6.2.1.2 respectively.

7.2.2 Cell Encapsulation and Maintenance

7.2.2.1 Primary Cell Isolation and Culture

Primary murine whole bone marrow was isolated and purified as described in Section 2.2.3.2. Whole bone marrow was magnetically sorted using the EasySep® Mouse CD117 (cKIT) Positive Selection Kit (Stem Cell Technologies) following the manufacturer's protocol. Sorted cells were immediately counted and encapsulated within the PEG-PQ-PG hydrogel.

7.2.2.2 Encapsulation Procedure

A solution containing 10% (w/v) PEG-PQ and 2 mM PEG-RGDS was made in HBS (pH 7.4) containing 1.5% triethanolamine. PEG-SCF, PEG-JAG1, and PEG-IFNγ were also added to individual polymer solutions at concentrations of 400 ng/ml. Eosin Y was added to the solution at a concentration of 10 μM in conjunction with 3.5 μl/ml NVP to serve as a photoinitiator for polymer crosslinking. This solution was sterilized via filtration in a laminar flow hood using a 0.22 μm PES syringe filter. Cells were centrifuged at 200 x g for 5 min. and resuspended in the polymer solution at a concentration of 20 x 10^6 cells/ml. Four 10 μl cell-laden polymer droplets were pipetted onto a Sigmacote-modified glass slide. Two 380 μm PTFE spacers were placed on the edges of the slide, and an untreated glass slide was rested on these spacers to sandwich the gel solution between the slides. The slides were clamped together and placed under a white light lamp (250 mW/cm^2) (Fiber Lite, Dolan Jenner, Boxborough, MA) for 45 sec. A schematic of the process can be seen in Figure 7.2. After crosslinking, gels were immediately transferred to ultra-low attachment 48 well plates with 400 μl media using a

sterile spatula. Cells were maintained in StemSpan media supplemented with 50 ng/ml soluble SCF.

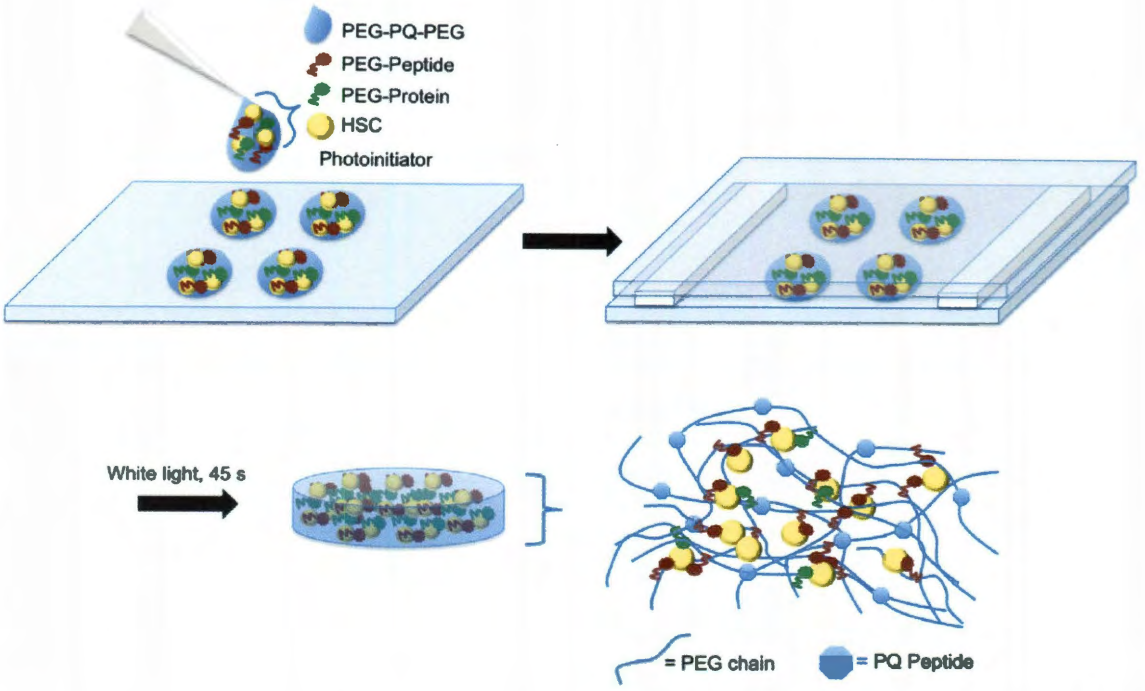

Figure 7.2: Encapsulation of HSCs in degradable PEG-PQ-PEG hydrogels. Four 10 µl droplets containing PEG-PQ-PEG (10% w/v), 2 mM PEG-RGDS, 400 ng/ml PEG-Protein, the Eosin Y photoinitiator, and HSCs (20 x 10^6 cells/ml) are pipetted onto a Sigmacoted glass slide. Two PTFE spacers are placed on either side of the droplets, and an untreated glass slide is placed on top. The slides are clamped together and exposed to white light for 45 s. The resulting hydrogels have cells entrapped within the polymer matrix. To collect cells after culture, a collagenase solution is added to degrade the gels by cleaving the PQ peptide and thus the polymer chains.

7.2.2.3 Culture Parameters

Gels were maintained in culture for 2 and 4 week time periods in incubators with 5% CO_2 at 37°C. Media was replenished every 2-3 days by removing half the media volume per well and replacing it with fresh media.

7.2.2.4 Viability Assessment

To determine the viability of the primary cells after encapsulation and during the culture period, we stained cells contained in gels with the Live/Dead® Cell

Viability/Cytotoxicity Kit for mammalian cells (Invitrogen) after 3, 7, 10, and 14 days and 5 weeks. A Live/Dead solution of PBS containing 2 µl/ml ethidium homodimer (2 mM) and 0.5 µl/ml calcein AM (4 mM) was made. Media was removed from gels and the Live/Dead solution was added followed by incubation for 20 min. at 37°C with 5% CO_2. After the incubation period, the gels were imaged on an inverted Zeiss Axiovert 135 inverted microscope equipped with an EXFO X-Cite 120 Fluorescent Illumination System, using a Jenoptik ProgRes C5 CCD camera. Images in both the "live" (excitation/emission: 494/517 nm) and "dead" (excitation/emission: 517/617 nm) channels were captured. To quantify the percentage of live cells, live and dead cells from the same field of view were counted in ImageJ software using a similar protocol as in Section 2.2.4.1. The number of live cells was divided by the total number of cells for each field of view to determine the percentage of live cells. Ten fields of view for three gels were analyzed at each timepoint.

7.2.3 Cell Retrieval

After the culture period, cells were retrieved from gels by placing gels in a new well plate in an HBS solution containing 0.1 mg/ml collagenase type IV (MMP-2) and 0.36 mM $CaCl_2$. The gels were degraded in an incubator at 37°C with 5% CO_2 for 1 hr. During the incubation time, the gels were agitated every 10 -15 min. to aid in the degradation process. After hydrogel degradation was complete, the cells were immediately centrifuged at 200 x g for 5 min., resuspended in media, and counted.

7.2.4 Cell Proliferation

To monitor cell proliferation within the gels over the time course of the studies, phase contrast images were captured using the Zeiss Axiovert 135 inverted microscope

and Jenoptik CCD camera. Cell proliferation was quantified by counting cells retrieved from each gel after degradation. The starting cell density and initial cell viability were used to determine the initial cell number/gel.

7.2.5 Evaluation of Differentiation Potential

7.2.5.1 Colony Forming Unit Assay

To assess the differentiation potential of cells after encapsulation within hydrogels, a colony forming unit assay was performed as described in Section 2.2.4.4. Briefly, 10,000 cells per sample were resuspended in 1 ml of MCM, plated into 6 wells of a low attachment 48 well plate, and incubated at 37°C with 5% CO_2. The colonies that formed were counted and characterized after 10-14 days in culture. MCM was added to wells that appeared to be drying out or contained rapidly proliferating colonies (indicated by colorimetric changes in the phenol red containing MCM).

7.2.5.2 Flow Cytometry

To support results seen in the colony assay, we analyzed cells using flow cytometry if there were sufficient cells remaining after cell retrieval (>100,000 cells). Cells were stained for c-kit, Sca1, and lineage markers using the protocol described in Section 2.2.4.5.

7.2.6 Statistical Analysis

One-way ANOVAs and Tukey's post-hoc analyses were performed to evaluate statistical differences between groups in all studies using a 95% probability level ($p<0.05$).

7.3 Results and Discussion

7.3.1 Polymer Synthesis and Characterization

7.3.1.1 Peptide Synthesis

To confirm that we synthesized the correct peptide sequence, we used mass spectrometry to determine the molecular weight of the final product. The mass spectrometry data in Figure 7.3 shows a peak at ~1140 kDa, which matches the molecular weight of the PQ sequence. Though this does not validate the correct order of the sequence, the ability to degrade in a collagenase solution (described in Section 7.2.3), supports that the sequence was synthesized in the correct order.

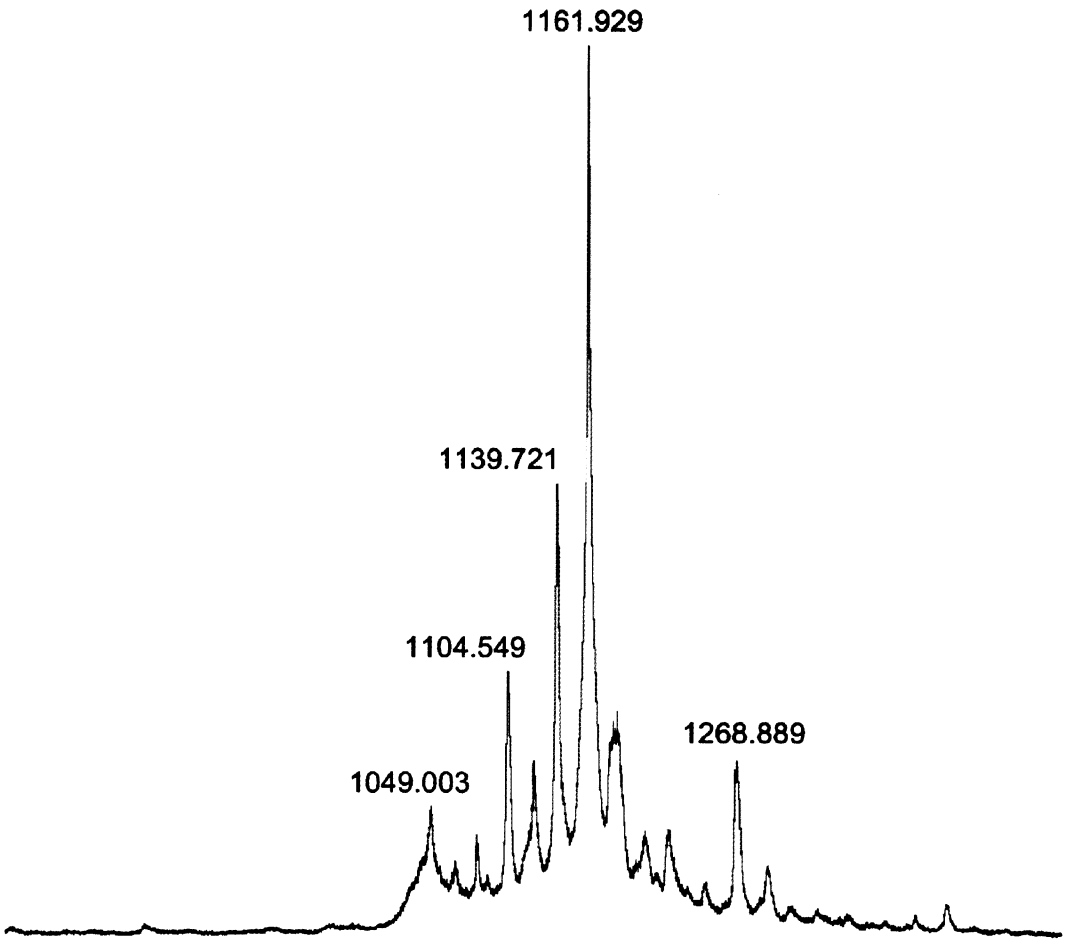

Figure 7.3. Mass spectrometry plot of PQ peptide. There is a peak at ~1140 kDa indicating the presence of a molecule at the predicted molecular weight of the PQ peptide.

7.3.1.2 PEG-PQ-PEG

GPC was performed on the sample to confirm PEGylation of the PQ peptide. Figure 7.4 shows the resulting plot. After conjugation, there is a peak that appears much earlier during data collection than when the PEG-SVA control is run by itself. This shift indicates an increase in molecular weight. It is possible that the peptide was only functionalized with one PEG chain, but the ability to form a gel from the polymer indicates that two acrylated PEG chains flank the PQ. The conjugation efficiency was calculated to be near 80%.

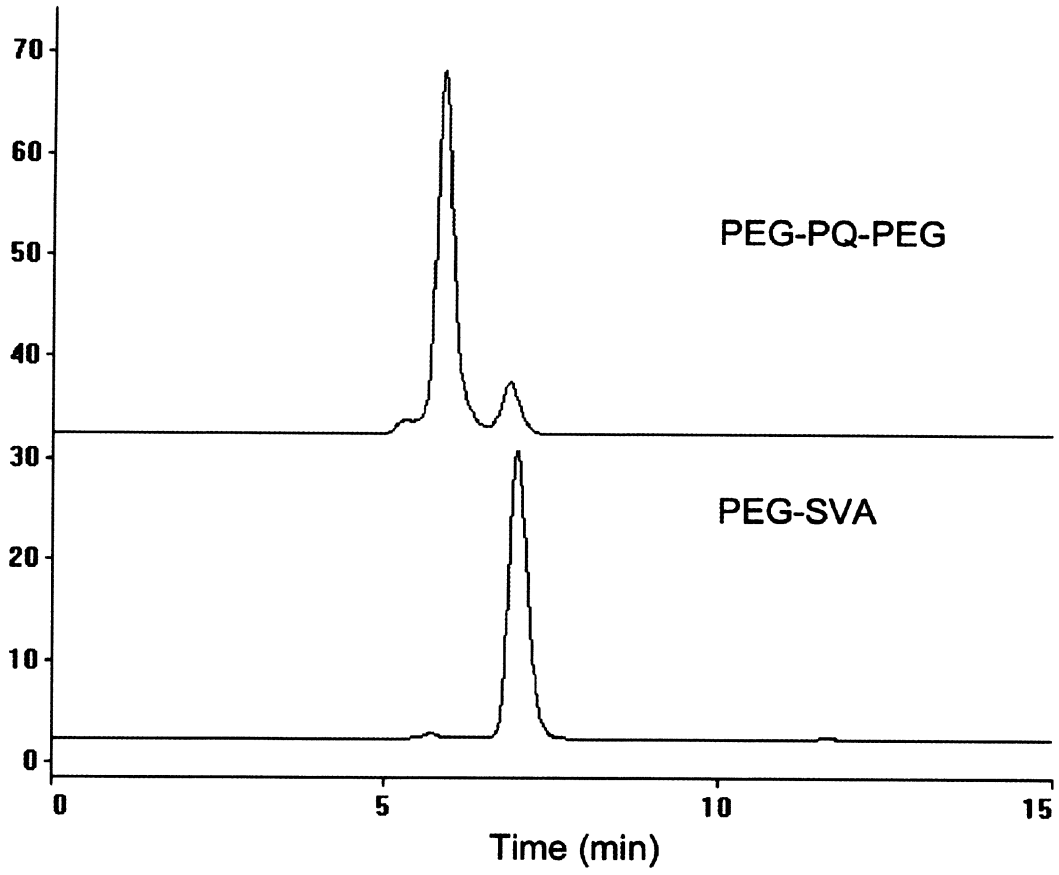

Figure 7.4: Gel permeation chromatography (GPC) analysis of PEG-PQ-PEG. PEG-PQ-PEG flows more quickly through the column and is detected earlier than PEG-SVA. This indicates an increase in molecular weight after the reaction and successful conjugation to the peptide. The percent conjugation was calculated to be approximately 80%.

7.3.2 Cell Viability within PEG Hydrogels

To ensure that the cells remained viable after the encapsulation process, a live/dead assay was conducted. Fluorescent images of primary c-kit$^+$ cells entrapped within gels can be seen in Figure 7.5. Live cells are able to process calcein AM to create a fluorescent product that appears green in the images. Ethidium homodimer binds to DNA and then fluoresces red; it can only enter cells whose membranes have been compromised, such as dead cells. The images show that primary cells are viable after encapsulation and that viability is maintained throughout the culture period despite the presence of some dead cells.

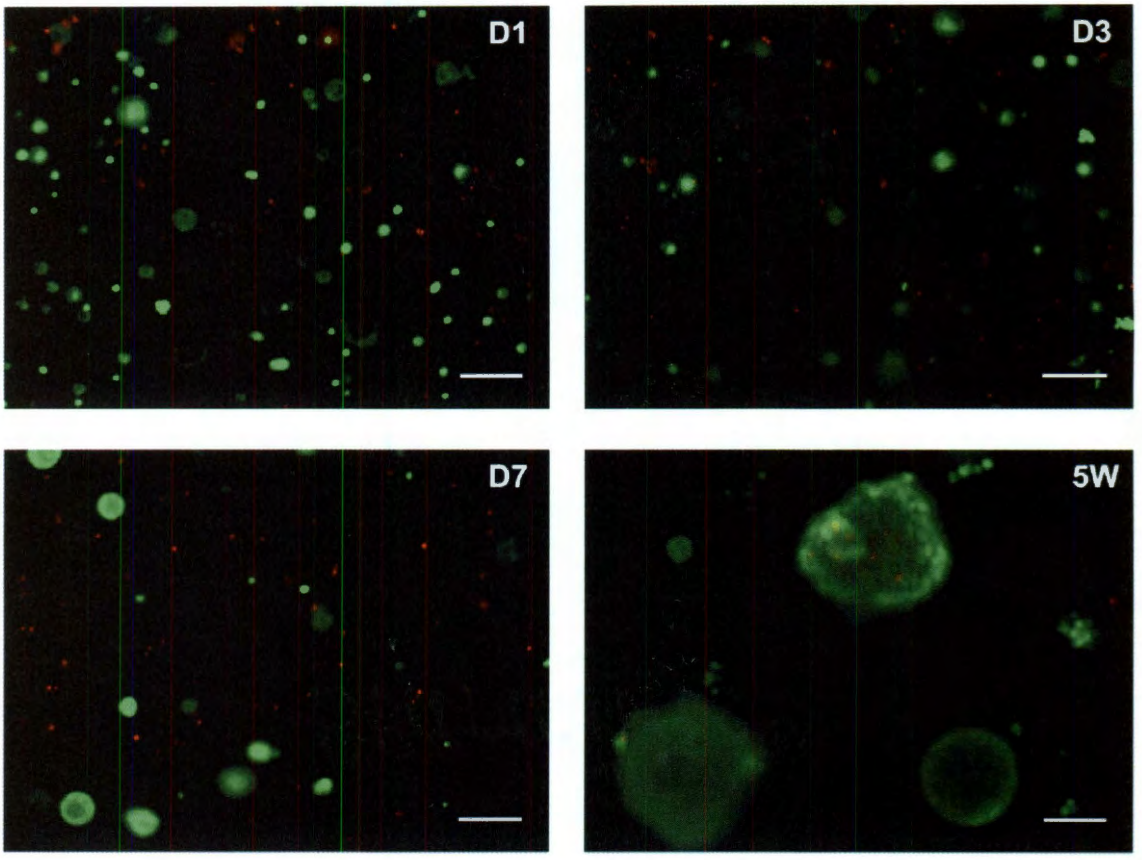

Figure 7.5: Viability of encapsulated c-kit$^+$ cells within PEG-PQ-PEG hydrogels with immobilized RGDS. Cells that are viable appear green and those that are dead appear red. The images were taken 24 h (D1), 3 days (D3), 7 days (D7), and 5 weeks (5W) after encapsulation. Viable cells remained after one week in culture and appeared to proliferate in clusters, indicated by the increase in viable cell size over time. Scale bars = 100 μm.

Figure 7.6 displays the quantification of the viability data. At day 3, approximately 30% of the cells remain alive. Though this is fairly low, the cell viability appears to recover at 7, 10, and 14 days, indicating that cells are not only alive but are also replicating. The percent increase in cell viability is significant at all timepoints compared to day 3. This demonstrates that a portion of the HSC population can

withstand the encapsulation procedure and is able to proliferate within the gel.

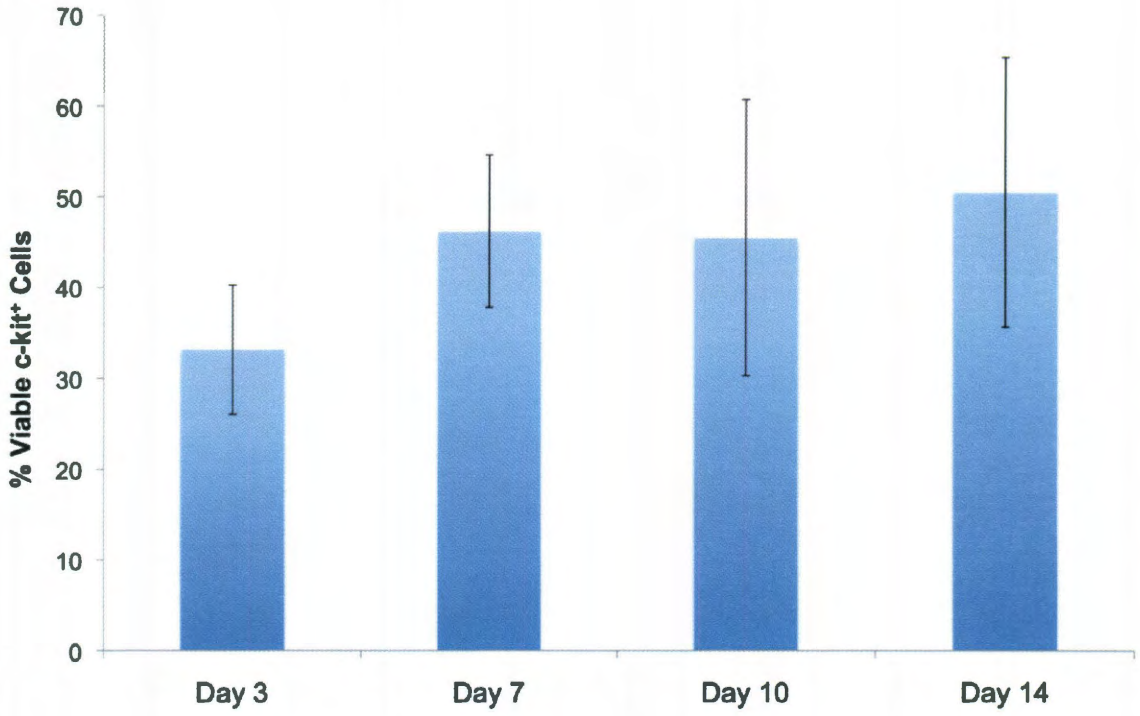

Figure 7.6: Primary cell viability in PEG-PQ-PEG hydrogels. Cell viability was assessed at Days 3, 7, 10, and 14 using the Live/Dead Viability/Cytotoxicity Assay. The percentage of live cells was determined by counting the number of live and dead cells and dividing the live cells by the total number of cells. Cells were counted using ImageJ software. After three days, only 30% of the cells were viable, but at later timepoints the cells appeared to recover. The viability increased to approximately 50% and was maintained at this level. Bars are mean ± standard deviation.

Though the cell viability is lower than what has been previously observed with other cell types (314, 316, 317), these results confirm the ability to maintain initial HSC viability over time. Furthermore, the percent of viable cells increases over time, signifying that the cells are proliferating. Previous work has shown that cell types have varying sensitivity to photoinitiators (316). Intrinsically, HSCs may be more affected by the photoinitiator system and could have increased susceptibility to cell death due to their primitive nature and recent harvest. Besides sensitivity to the photoinitiator, the low

percentage of viable cells at early timepoints could be the result of several other factors. Primarily, there are no steps devoted to the removal of dead or dying cells between the cell harvest and the encapsulation process. Thus, cells that die as result of the isolation process contribute to the total percentage of dead cells after encapsulation.

There are several steps in the procedure that can contribute to cell death. The isolation procedure from the bone marrow is fairly harsh. Cells are flushed from the bone and then washed multiple times with several steps that involve centrifugation. Secondly, during the magnetic sorting, cells are sorted in a laminar flow hood but are outside of an incubator setting for a prolonged period. Thus, once cells are ready to undergo the encapsulation procedure, they have been significantly stressed and may not be robust enough to survive the encapsulation procedure. It is possible that allowing the cells to recover from the harvest and sorting procedures in media within an incubator before encapsulation could increase the cell viability percentage. However, the differentiation potential of HSCs is highly time-sensitive, and waiting just a few hours before placing the cells into the culture system could negatively impact the differentiation potential of the cells. Conversely, the LT-HSC portion of the c-kit$^+$ hematopoietic progenitor population may be more sensitive to the encapsulation process and may make up a larger percentage of the dead cells within the gel. Thus, waiting to encapsulate may be crucial to ensuring that a greater number of primitive HSCs survive. Future work includes studies to determine the ideal timeframe for cell isolation, purification, and encapsulation that maximizes both cell viability and differentiation potential.

7.3.3 Cell Proliferation within Gels

Figure 7.7 shows phase contrast images at various timepoints. The black arrows designate clusters of cells that are proliferating within the gel. These clusters also support the hypothesis that the HSCs are unable to degrade the gel. They are able to displace the gel to create space for new cells, but the clusters are tightly packed throughout the culture period and cells do not seem to spread within the gel matrix. Cells also appear to proliferate on the surfaces of the gels.

To quantify the increase in cell number in the gel, cells were counted after the degradation of the gel. In all groups, a decrease in cell number was observed. This does not correlate with what was observed in the well plates and the phase contrast images in Figure 7.7. After the cells are retrieved from the hydrogel, they are highly susceptible to sticking to the low attachment well plates. To remedy this, degradation was performed in a microcentrifuge tube in later studies. This resulted in more efficient retrieval, and in preliminary studies with this method, there was an approximately 50% increase in cell number after 4 weeks in culture. However, the process will need to be repeated to determine significance.

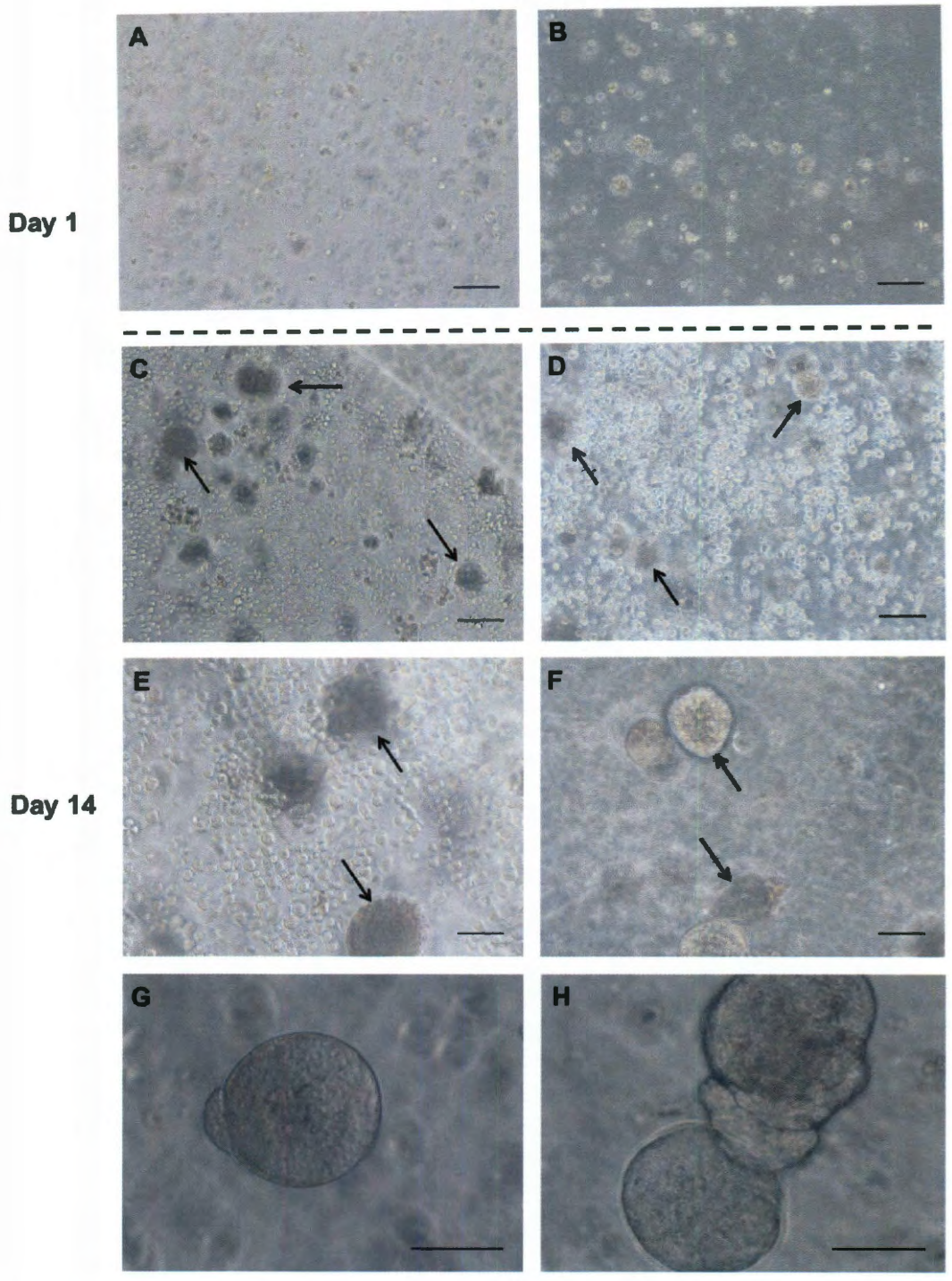

Figure 7.7: Representative phase contrast images of c-kit$^+$ cells encapsulated within degradable biomimetic PEG-PQ-PEG hydrogels at days 1 and 14. Cells are disperse and less dense after 24 h. At day 14, cells have proliferated within and on top of the gel. The cells do not degrade the gel, but displace it to make space for forming cell clusters. Black arrows denote these cell clusters. Scale bar = 100 μm in A-D, Scale bar = 50 μm in E-H. Immobilized bioactive factors within the PEG-PQ-PEG hydrogel: A. 2 mM RGDS; B, C, E, G. 2 mM RGDS and 400 ng/ml SCF; D, F, H. 2 mM RGDS and 400 ng/ml IFNγ

7.3.4 Differentiation Potential

The ideal *ex vivo* culture system should not only maintain the viability of the cells but should also prevent rapid differentiation of the HSCs. To evaluate the differentiation potential of encapsulated cells after 2 or 4 weeks in culture, two assays were performed: the colony forming unit assay and flow cytometric analysis.

7.3.4.1 Colony Forming Unit Assay

The results from the colony forming unit assay are displayed in Figure 7.8. All sample groups were able to form colonies, which is a characteristic of less differentiated cell types.

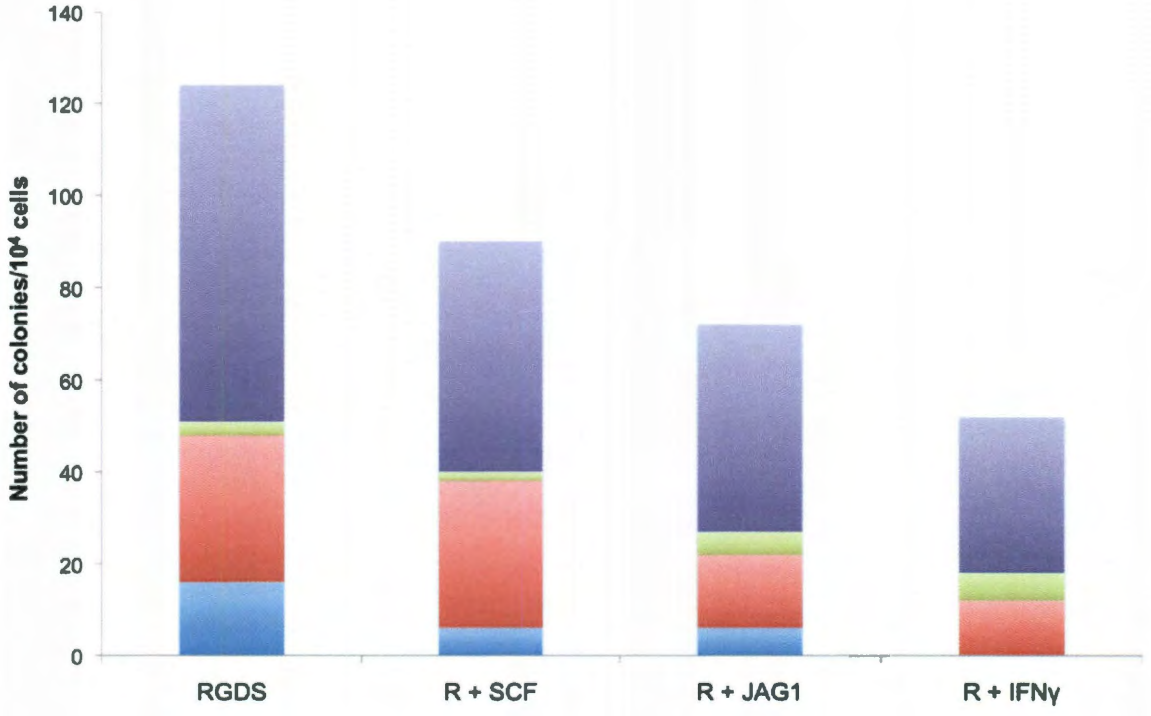

Figure 7.8: Colonies formed from c-kit$^+$ cells after 14 days of encapsulation. Cells encapsulated in RGDS formed the most colonies, 124, and the cells were still able to form primitive GM and GEMM colonies. Though cells encapsulated in gels with SCF and JAG1 did not form as many colonies as in RGDS alone (90 and 72 respectively), the cells still retained the ability to form primitive colonies. In gels with IFNγ, the cells were not able to form GEMM colonies and the total colony number was much lower than other sample groups. (R=RGDS; **CFU-M=Macrophage, CFU-G=Granulocyte, CFU-GM=Granulocyte/Macrophage, CFU-GEMM=Granulocyte, Erythrocyte, Megakaryocyte, Macrophage**)

The RGDS group formed the most colonies while the sample with IFNγ formed the least. However, the changes were not significant due to a small sample size. The distribution of colonies is shown in Figure 7.9. The samples with RGDS only, SCF, and JAG1 exhibited similar distributions of colonies. RGDS had the highest percentage of GEMM colonies (12%) while SCF had the highest percentage of primitive GM and GEMM colonies (45%). The IFNγ group had the highest percentage of more committed colonies (G and M) at around 65%.

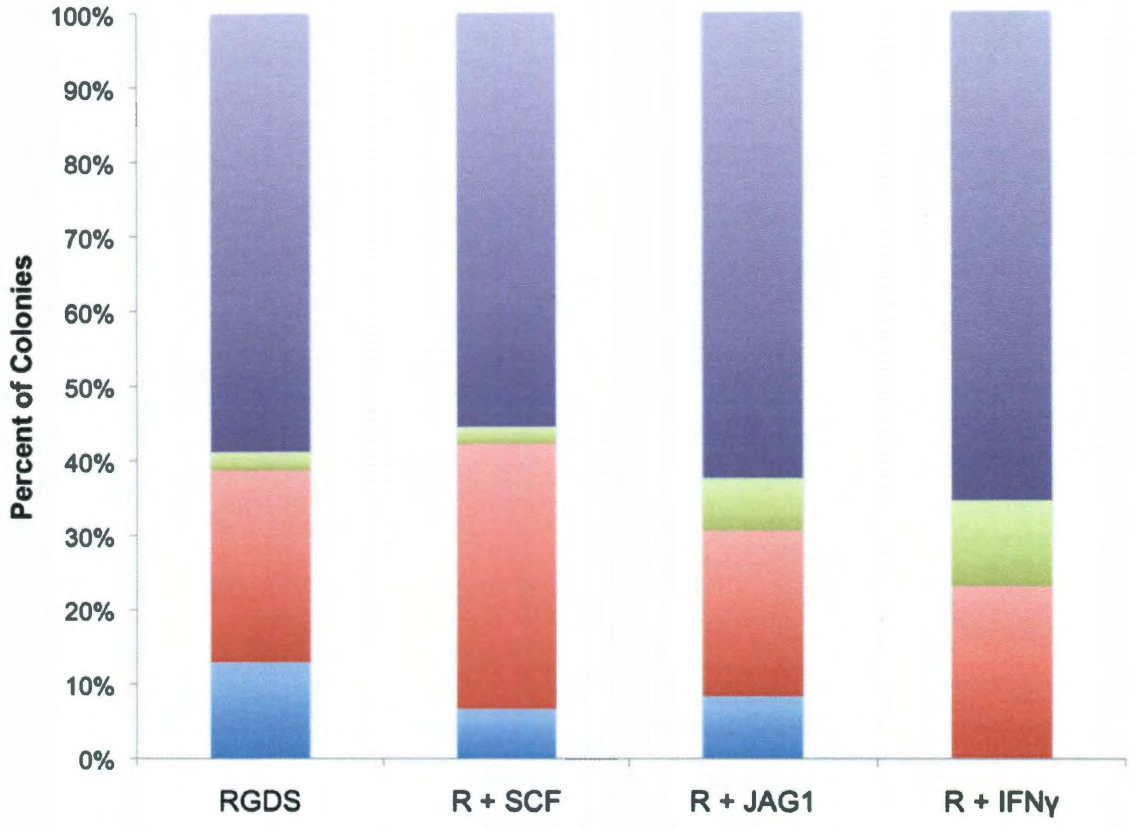

Figure 7.9: Colony distribution as a proportion of total colony number. The distribution of colonies was fairly similar between RGDS, SCF and JAG1. The group containing RGDS only formed the highest percentage of GEMM colonies (~12%), while the group with SCF had the most primitive colonies (GM and GEMM) at around 42%. IFNγ had the highest percentage of more committed progenitors (G and M) at around 80%. (R=RGDS; **CFU-M=Macrophage, CFU-G=Granulocyte, CFU-GM=Granulocyte/Macrophage, CFU-GEMM=Granulocyte, Erythrocyte, Megakaryocyte, Macrophage**)

7.3.4.2 Flow Cytometry

Due to the large loss of cells during the degradation procedure (described above), there were a limited number of samples that could be analyzed with flow cytometry. Figure 7.10 displays data collected on cells encapsulated within a PEG-PQ hydrogel functionalized with PEG-RGDS. There are a high percentage of cells, approaching 90%, that remain c-kit$^+$ after 4 weeks in culture. In addition, 67% of the cells are lin-, and 9% of the cells make up a KSL population. This is an improvement on what was observed on gel surfaces with surface immobilized RGDS, where 45% of the cells are c-kit$^+$, 7% are lin$^-$, and 5% make up the KSL population after expansion. Even though the initial population was broader, the percentage of KSL cells is increased when compared to cells cultured on surfaces. However, this is data collected from only one sample (three gels) and will need to be repeated to verify these results.

Taken together, this data shows that the encapsulation procedure can aid in maintaining HSCs in an undifferentiated state. The reduced number of differentiated cells could be due to the morphology of the cell inside the gel. Because the cells were not able to degrade the gel and spread significantly, they retained their rounded shape. This may help signal the cell to remain in its multipotent state. Several groups have investigated at the effects of cell shape on the differentiation of another bone marrow derived stem cell, mesenchymal stem cells (MSC), and have observed that cell shape is a critical factor in the pathways along which the cell differentiates (318-321). McBeath *et al.* showed that cell shape affects endogenous RhoA activity. By promoting this activity, MSCs differentiate down osteogenic pathways, and by blocking this activity, MSCs become adipogenic (318). Kilian et al. observed similar results on surfaces with adhesive ligands of similar surface areas but of distinct shapes. MSCs differentiated down

adipogenic or osteogenic pathways, independent of soluble signaling, due to differences in cytoskeletal tension, a downstream effect of RhoA signaling (320). Thus, the shape of HSCs may play a critical role in the differentiation status of HSCs.

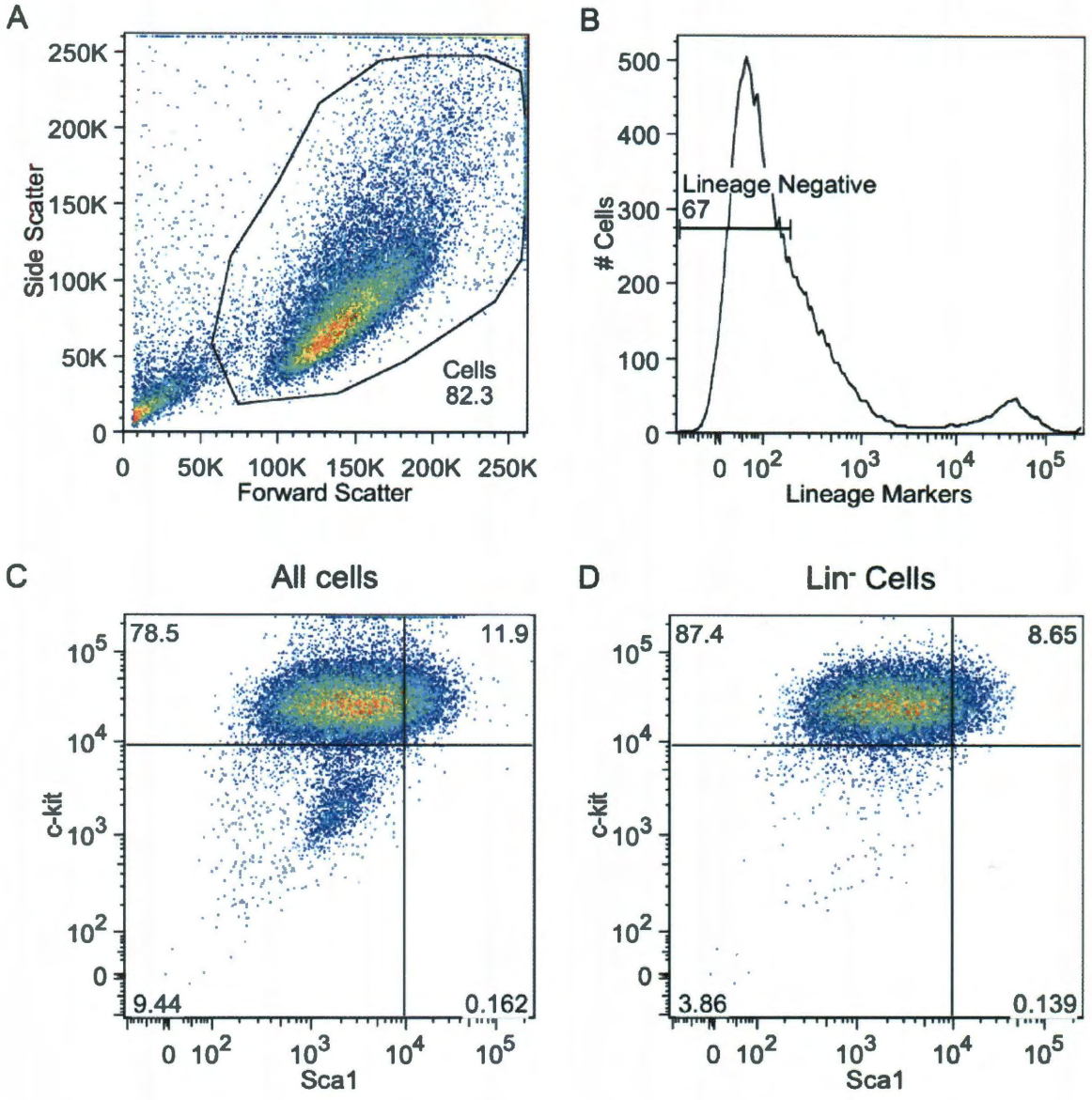

Figure 7.10: Flow cytometric analysis of c-kit$^+$ cells after culture in degradable PEG hydrogels with 2 mM RGDS. A. Particles were gated to exclude debris and cell aggregates. B. The cells were gated to include those that did not express lineage markers. C. Cells were gated to delineate between c-kit and Sca1 positive and negative cells. D. Lineage negative cells were gated as in C. Axes that do not have units are relative fluorescent intensity. Numbers on the graphs denote the percentage of cells within each gate.

Interestingly, these results contradict some of what was seen in two-dimensional culture. In three dimensions, the addition of proteins to the polymer matrix resulted in reduced total colony formation and only slight differences in the distribution of colonies compared to the RGDS alone. In contrast, in two-dimensional culture, it was observed that the addition of SCF to the hydrogel surface led to greater colony formation and no differences in the distribution of the colonies when compared to RGDS. In addition, cells cultured on hydrogels with surface immobilized JAG1 formed similar numbers of colonies but a greater number of primitive colonies compared to RGDS in two-dimensions. On IFNγ, the cells formed more total colonies compared to the peptide alone in two dimensions but showed a reduced ability to form primitive colonies in both two and three dimensions. Thus, in each group, there was a marked difference between two and three-dimensional culture. It is unclear what the source of these differences is. It may be related to the way the proteins are displayed in three-dimensional culture. In addition, because the cells form such large clusters, it is possible that the HSCs are responding more to stimuli from one another as opposed to cues from the matrix, particularly cells in the centers of the clusters. However, the colony data is preliminary and only represents one experimental group; thus, the findings should be confirmed before making any definitive claims.

The encapsulation process keeps HSCs in constant contact with the gel. They are unable to leave, and as a result are in close proximity to immobilized adhesive peptides and signaling proteins within the gel. The continuous interaction with these factors and subsequent activation of specific surface receptors like c-kit, Notch, and the VLA-4 and VLA-5 integrins can help maintain HSCs in a state of self-renewal and prevent their

differentiation. By functionalizing the gel with proteins known to trigger differentiation, like IFNγ, the potential of the cells could be altered as shown by the limited ability of cells in these samples to form less primitive GM and GEMM colonies. The ability to affect HSC fate through the encapsulation process and signaling molecules immobilized within the gel is a powerful tool in the development of an *ex vivo* culture system.

7.4 Conclusions

A three-dimensional system that accurately recapitulates the *in vivo* HSC microenvironment could enable the generation of HSC populations with clinical applicability. These studies show that HSCs can be successfully encapsulated within hydrogels in a manner that maintains their viability and allows them to proliferate without compromising their differentiation potential. Incorporating different proteins within the hydrogel matrix altered the differentiation potential of the cells. For example, the addition of IFNγ to the gels prevented the cells from forming primitive GEMM colonies. This system exhibits great promise in the maintenance of HSCs in long-term culture though several more studies should be conducted to confirm these preliminary results. Future studies will focus on the clinical applicability of the cells after encapsulation and culture.

Chapter 8: The Biomimetic PEG Hydrogel System for HSC Expansion

8.1 Introduction

Hematopoietic stem cells (HSC) have been successfully used in bone marrow transplants to treat blood cancers and other diseases. They have the potential to be used in therapies for numerous other diseases, and research using HSCs for the treatment of diabetes, chronic ischemia, liver disease, as well as others, is currently underway. However, the expansion of HSCs into other therapeutic applications is hindered by a shortage of HSC donors and the inability to culture HSCs *ex vivo* since the cells rapidly begin to differentiate or apoptose when removed from their *in vivo* microenvironment. The development of a culture system that recapitulates the HSC niche could aid in the generation of clinically relevant populations of HSCs. The work in this thesis demonstrated the ability to utilize a bioactive PEG hydrogel to mimic the HSC microenvironment and expand these cells *ex vivo* in both two and three dimensions.

8.2 32D Cell Culture in PEG Hydrogel Wells

The design of the hydrogel system began with the formation of PEG hydrogel wells. Wells were utilized to prevent cell migration off of the hydrogel and ensure interaction between cells and specific biomolecules immobilized on the gel surfaces. To begin this process, a mold consisting of photoresist pillars was created using microfabrication techniques. Unmodified PEG-DA was polymerized around the pillars to create a hydrogel well base, and the bottoms of the hydrogel wells were subsequently functionalized with biomolecules.

In initial experiments, 32D cells, a myeloid progenitor cell line, were used to observe how RGDS—a fibronectin-derived adhesive peptide sequence, SCF—a cytokine

involved in HSC self-renewal, and SDF1α—a chemokine integral in HSC homing and mobilization—affect cell adhesion, spreading, and proliferation. These studies demonstrated that the incorporation of RGDS, SCF, and SDF1α onto gel surfaces could encourage cell adhesion. By increasing the surface RGDS concentration, the number of adherent 32D cells was increased after 48 hrs. in culture. The inclusion of either SCF or SDF1α with RGDS (25 $\mu g/cm^2$) allowed a significantly greater number of 32D cells to adhere compared to the peptide alone at similar concentrations. The degree of cell spreading was also influenced by the presence of SCF and SDF1α. When compared to RGDS surfaces (250 μg RGDS/cm^2) with similar 32D cell densities, cells spread to a significantly greater extent and exhibited distinct filopodia. A histogram of the cell areas showed that there was an approximately 100-200 μm^2 increase in the average 32D cell size and a higher percentage of large cells (>700 μm^2) on gels with surface immobilized SCF and SDF1α.

These studies demonstrated the functional potential of the hydrogel culture system and allowed for the optimization of hydrogel parameters such as the surface concentration of biomolecules. Hydrogel wells successfully retained hematopoietic cells on the gel surface, and biomolecules tethered to the gel surfaces maintained their bioactivity and were capable of altering hematopoietic cell behavior. Though the scaffold was capable of modulating certain 32D cell behavior, the effects on primary HSCs also required investigation to determine the ability of the hydrogel system to maintain HSCs in an undifferentiated state.

8.3 Primary Cell Culture in Bioactive Hydrogel Wells

To gain a better understanding of the effects of the culture system on primary HSC expansion and differentiation, c-kit$^+$, lin$^-$ cells were isolated from murine whole bone marrow. RGDS, CS1, SCF, SDF1α, JAG1, and IFNγ were covalently immobilized on the surfaces of hydrogel wells, and c-kit$^+$, lin$^-$ primary cells were cultured in the gel wells for two weeks. JAG1 is a transmembrane protein expressed by stromal cells in the niche that can promote HSC expansion while retaining HSCs in an undifferentiated state. In contrast, IFNγ is a cytokine that can encourage HSC proliferation at the expense of initiating the differentiation process.

When RGDS and CS1 were added to gel surfaces, there was an increase in total cell expansion compared to PEG-DA and FN plate controls. The combination of SCF or IFNγ with RGDS or CS1 on gel surfaces significantly increased total cell expansion as compared to the peptides alone. JAG1 and SDF1α displayed minimal effects on total cell expansion. Figure 8.1 displays the quantified data for total cell expansion for all groups. The ability of the gel to encourage self-renewal is a fundamental necessity in a culture system for generating large HSC populations. These findings demonstrate that the inclusion of specific bioactive elements into the hydrogel culture system can promote HSC self-renewal.

In a clinical setting, only undifferentiated HSCs are able to repopulate the immune system of the host after transplantation. Therefore the differentiation potential of expanded cells was evaluated with two assays to predict the likelihood of success in *in vivo* engraftment experiments. The colony forming unit (CFU) assay was used to assess the functional capability of the cells to differentiate down multiple pathways. In addition,

flow cytometric analysis was used to investigate the expression of specific surface markers indicative of HSCs, c-kit and Sca1, and the absence of lineage markers.

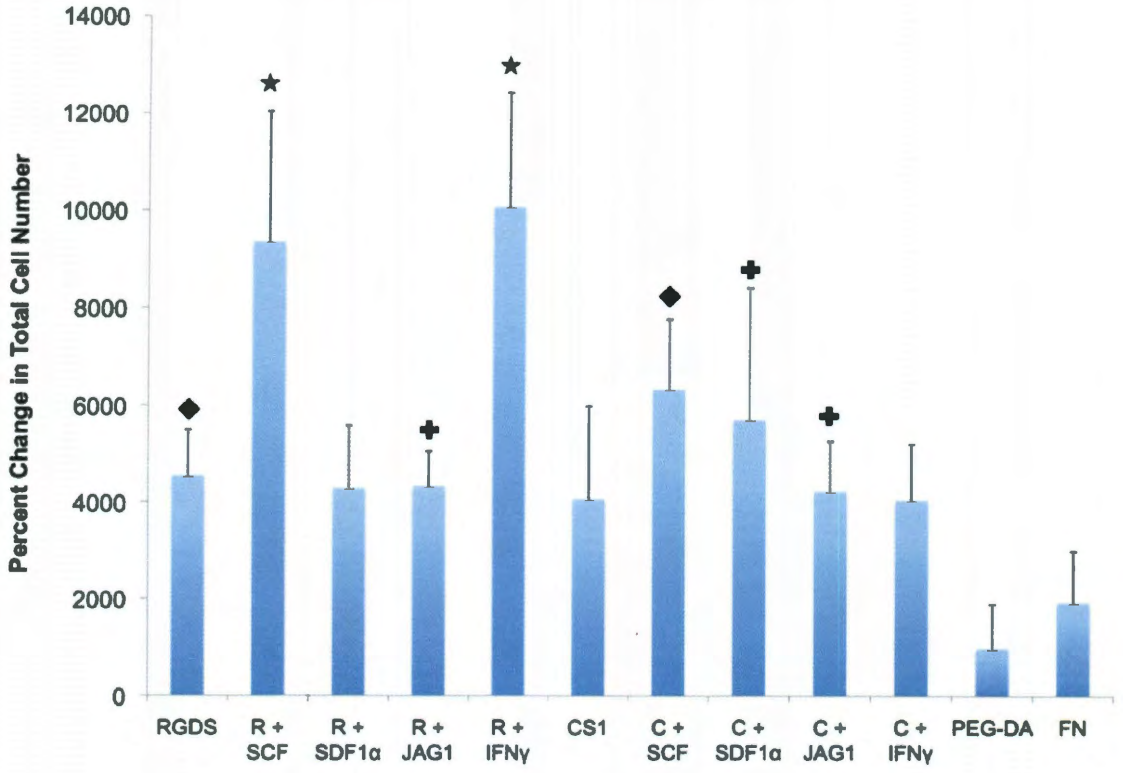

Figure 8.1: Percent change in total cell population after 14 days in culture within hydrogel wells functionalized with biomolecules. Bars are mean ± standard deviation (★ denotes significance compared to peptide, PEG-DA, and FN controls, ◆ denotes significance compared to PEG-DA and FN controls, ✚ denotes significance compared to PEG-DA control, n=3, $p < 0.05$) (R=RGDS, C=CS1)

A compilation of the results from the CFU assay from all samples is displayed in Figure 8.2 while the results from flow cytometry are shown in Figures 8.3 and 8.4. In all samples, with the exception of PEG-DA, CFU-GEMM colonies, the most primitive, were able to form from expanded cells, indicating that cells have remained in a more undifferentiated state. In addition, there was a small KSL population present in all groups after the two-week culture period, though the percentage of KSL cells out of the total population decreased in all groups.

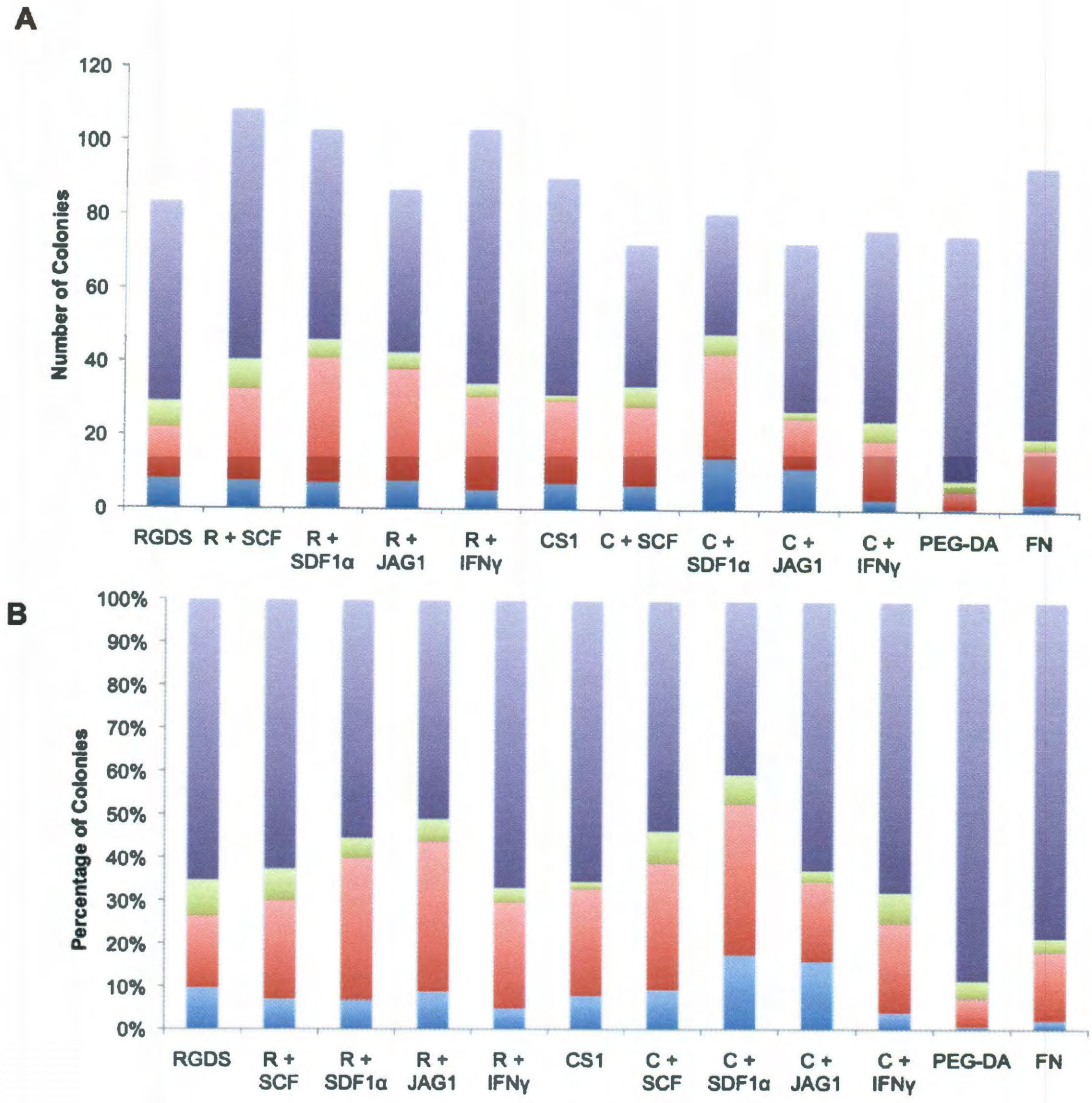

Figure 8.2: Colony formation of c-kit$^+$, lin$^-$ cells cultured for 14 days on hydrogel surfaces functionalized with biomolecules A. Total colony formation B. Distribution of colonies as a percent of total colony number. Bars are means, n=2. (**CFU-M=Macrophage, CFU-G=Granulocyte, CFU-GM=Granulocyte/Macrophage, CFU-GEMM=Granulocyte, Erythrocyte, Megakaryocyte, Macrophage**)

The cells that were expanded on hydrogel wells functionalized with CS1 and RGDS formed more primitive colonies than cells from the control groups on PEG-DA and FN plates. In contrast, the controls had a high quantity of KSL cells, though the expression of these markers does not necessarily signify that the cells are able to differentiate down multiple lineages. Due to its significant effect on HSC proliferation,

samples with SCF generated the highest quantity of undifferentiated cells, which was supported by data from both the colony assay and flow cytometry. JAG1 was able to preserve the cells in an undifferentiated state, but it did not significantly expand the cells meaning it did not generate a large HSC population in culture. The presence of SDF1α resulted in no apparent improvement on cell expansion, but it did retain the differentiation potential of cells when it was functionalized on hydrogel surfaces with CS1 compared to RGDS and CS1 controls. IFNγ expanded primary cells significantly but also lead to substantial HSC differentiation. Similarly to cells expanded on PEG-DA and FN controls, the cells on IFNγ could not form primitive colonies, but they did express surface markers indicative of undifferentiated HSCs. Table 8.1 gives an overview of the effects of each biomolecule on hematopoietic cell behavior. The "+" designates that the biomolecule(s) promoted the desired cell behavior while the "-" denotes that the behavior was inhibited. Note that a "+" for differentiation potential means the immobilized biomolecule prevented HSC differentiation. The number of pluses and minuses shows the relative degree of the effect compared to other bioactive factors.

It is interesting that there were differential effects on cell behavior depending on the peptide that was immobilized on gel surfaces in combination with proteins. It suggests that there may be synergistic or antagonistic effects of these combinations of molecules on HSC signaling pathways. Further investigation could help to elucidate these effects in more detail. These findings demonstrate the ability to design the hydrogel system to alter HSC expansion and differentiation. Controlling these processes more precisely may lead to the generation of HSC populations that can be used clinically.

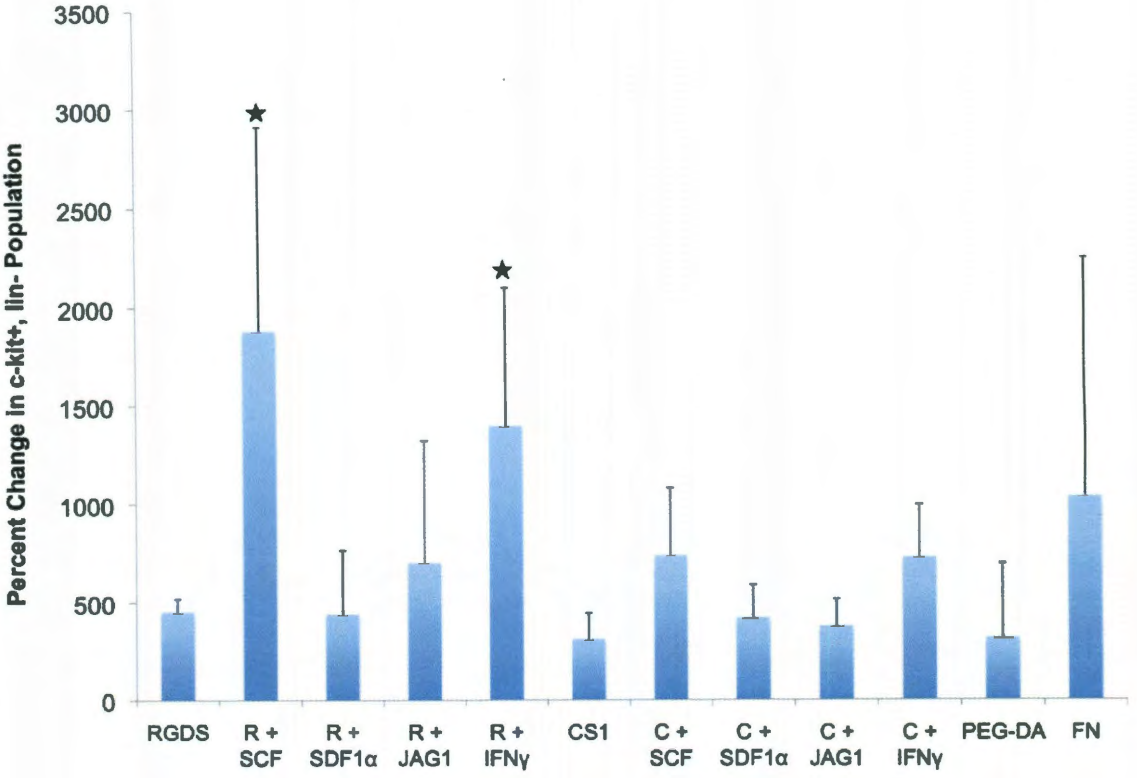

Figure 8.3: Percent change in c-kit$^+$, lin$^-$ population after 14 days in culture within hydrogel wells functionalized with biomolecules. Bars are mean + standard deviation (n=3) (★ denotes significance compared to peptide control, R=RGDS, C=CS1)

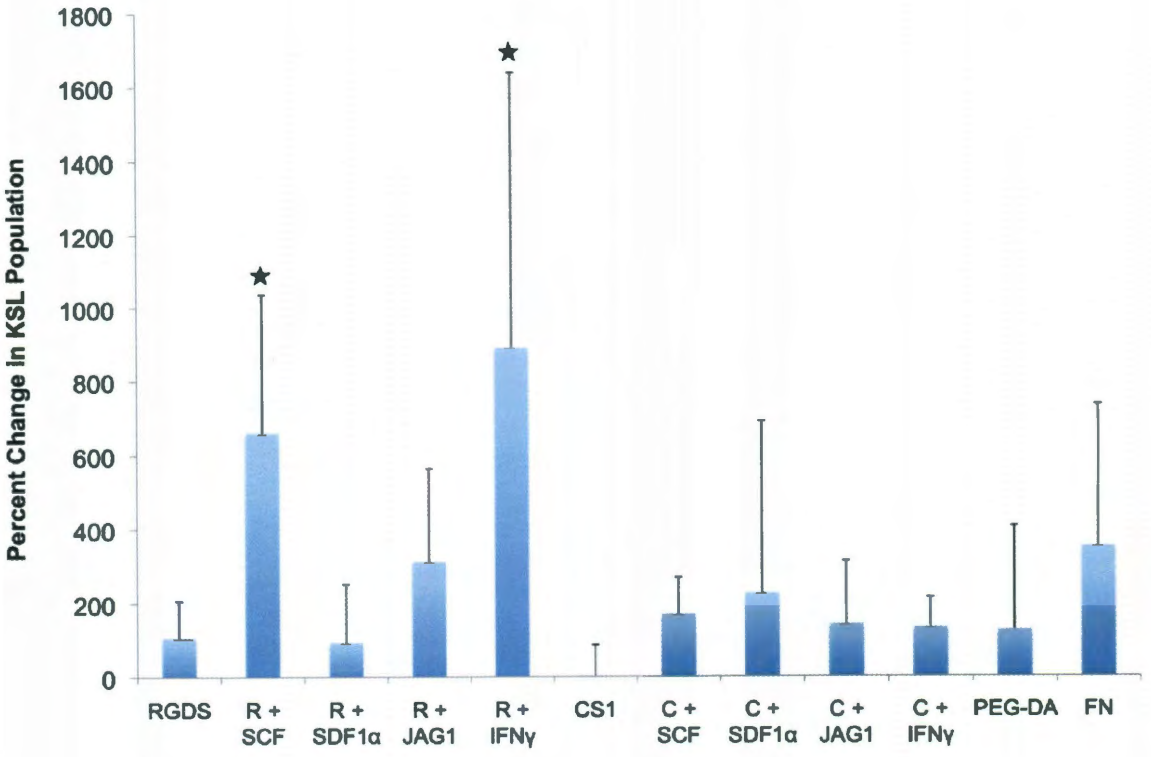

Figure 8.4: Percent change in KSL population after 14 days in culture within hydrogel wells functionalized with biomolecules. Bars are mean + standard deviation (★ denotes significance compared to peptide control, n=3, $p < 0.05$) (R=RGDS, C=CS1)

8.4 Primary HSC Culture in Three-dimensional Bioactive PEG Hydrogels

HSCs were cultured in a three-dimensional PEG hydrogel to more accurately mimic the *in vivo* microenvironment. Furthermore, entrapping cells within the hydrogel prevents significant cell migration and keeps cells in close contact with bioactive elements incorporated into the polymer matrix. HSCs were encapsulated within a biodegradable PEG scaffold and cultured for 2-5 weeks. The results showed the ability of the three-dimensional hydrogel to maintain HSC viability for a period of 5 weeks, though there is some cell death at early timepoints likely due to both the isolation and encapsulation procedures. Within the hydrogels, HSCs proliferate to form cell clusters, which are unable to degrade the gel substantially. After culture, cells were retrieved through degradation of the gel in collagenase-containing media and evaluated for

differentiation potential using both the CFU assay and flow cytometry. Preliminary results indicate that encapsulation helped to maintain the HSCs in an undifferentiated state though, based on results from the colony assay, it appeared that the addition of SCF, JAG1, and IFNγ all lead to differentiation. This is somewhat contradictory to what was seen in two-dimensions, with the exception of IFNγ, but may be due to a low sample size. This technique showed great potential in the generation of HSC population *ex vivo* but still requires additional investigation to confirm these promising results.

Table 8.1: Overview of the effects of surface immobilized bioactive factors on hematopoietic cell behavior. "+" signifies that the surface promoted the desired behavior while "–" signifies that the surface inhibited the desired behavior. (Note: for differentiation potential, the plus signifies that it retained the differentiation potential of the cells.) The number of pluses or minuses indicates a relative degree compared to other samples.

				Differentiation Potential	
	32D Cell Adhesion	32D Cell Spreading	Primary Cell Expansion	Colony Assay	Flow Cytometry
RGDS	++	-	+	+	+
R + SCF	+++	++	+++	+	++
R + SDF1α	+++	++	+	++	+
R + JAG1	N/A	N/A	+	++	+
R + IFNγ	N/A	N/A	+++	--	++
CS1	N/A	N/A	+	+	-
C + SCF	N/A	N/A	++	++	+
C + SDF1α	N/A	N/A	+	++	+
C + JAG1	N/A	N/A	+	+	+
C + IFNγ	N/A	N/A	+	-	-
PEG-DA	-	-	-	-	+
FN	N/A	N/A	-	-	+

8.5 Conclusions and Future Work

The aim of the work in this thesis was the development of an *ex vivo* culture system capable of expanding HSC populations while preventing significant differentiation. Currently this is not possible, and the ability to generate large HSC populations has tremendous clinical relevance. The PEG-DA hydrogel system was designed to mimic the *in vivo* HSC microenvironment or niche. The advantage of using a PEG-based system resides in the ability to easily tailor its properties. The PEG-DA matrix is not intrinsically bioactive, but biomolecules can be selectively incorporated within the PEG matrix allowing one to study the effects of individual molecules on cell behavior. The studies in this thesis functionalized hydrogels with molecules from the niche known to affect HSC expansion and differentiation. The results demonstrated the ability to control HSC fate by tethering specific biomolecules or combinations of biomolecules to the polymer scaffold in both two and three dimensions. This system shows the potential to maintain HSCs *ex vivo* and with further optimization and refinement, it could one day be used for therapeutic applications.

However, to reach that point, there are still many experiments that need to be conducted before this system can be used clinically. Thus far, the culture system has been utilized for the culture of a heterogeneous population with many highly proliferative progenitors. The use of a more primitive population for future studies may result in the generation of HSC populations with fewer macrophage progenitors. In addition, several of the experiments with primary cells can be repeated to obtain significant differences between experimental groups and uncover the source of conflicting results. Because the experiments were performed with cells from different populations of mice, there are similar trends but different quantitative results from each experiment, which results in

large standard deviations. Repeating the studies will help to confirm that the results that were obtained are significant. In addition, most of the studies in this thesis were limited to two weeks. Previous work has demonstrated the ability to successfully maintain HSCs in culture for similar time periods. The ability of the PEG hydrogel system to extend this time frame still requires further investigation.

Several more experiments could also be conducted combining the different bioactive factors. For example, IFNγ has been shown to expand HSCs when it is used in combination with SCF and SDF1α (296, 298, 299). Perhaps, IFNγ works to encourage HSC proliferation while SCF and/or SDF1α can retain HSCs in an undifferentiated state. Combinations of SCF or IFNγ with JAG1 could also cause significant proliferation while maintaining differentiation potential. Furthermore, other cytokines like erythropoietin (EPO), a hormone that triggers erythrocyte production *in vivo*, could be investigated in combination with SCF or IFNγ to generate populations of mature blood cells. A combination of SCF and EPO was previously shown to promote the proliferation and survival of erythroid progenitor cells (322). This is incredibly relevant to clinical applications as blood shortages are common, particularly for rare blood types. These kinds of studies could assist in the biological design of a hydrogel that has better control over HSC behavior.

Most importantly, *in vivo* studies are required to investigate engraftment capabilities of expanded cells. The ability to form colonies or express a combination of surface markers is irrelevant if the cells are unable to repopulate the immune system. HSCs that are implanted after expansion should be able to home to the bone marrow, engraft, and reconstitute the immune system. Furthermore, bone marrow cells from the

transplant recipient should also be capable of these processes when implanted into a secondary recipient. If this system shows success in *in vivo* experiments, it will likely have significant clinical benefits.

Bibliography

1. Sorrentino BP (2004) Clinical strategies for expansion of haematopoietic stem cells. *Nature reviews. Immunology* 4:878-88.

2. Copelan E a (2006) Hematopoietic stem-cell transplantation. *The New England journal of medicine* 354:1813-26.

3. Jenq RR, Brink MRM van den (2010) Allogeneic haematopoietic stem cell transplantation: individualized stem cell and immune therapy of cancer. *Nature reviews. Cancer* 10:213-21.

4. Shenoy S (2007) Has stem cell transplantation come of age in the treatment of sickle cell disease? *Bone marrow transplantation* 40:813-21.

5. García-Bosch O, Ricart E, Panés J (2010) Review article: stem cell therapies for inflammatory bowel disease - efficacy and safety. *Alimentary pharmacology & therapeutics* 32:939-52.

6. Annaloro C, Onida F, Lambertenghi Deliliers G (2009) Autologous hematopoietic stem cell transplantation in autoimmune diseases. *Expert review of hematology* 2:699-715.

7. Isgrò A, Marziali M, Sodani P, Gaziev J, Lucarelli G (2009) The impact of hematopoietic stem cell transplantation on the management of thalassemia. *Expert review of hematology* 2:335-44.

8. Dazzi F, Laar JM van, Cope A, Tyndall A (2007) Cell therapy for autoimmune diseases. *Arthritis research & therapy* 9:206.

9. Weissman IL, Shizuru J a (2008) The origins of the identification and isolation of hematopoietic stem cells, and their capability to induce donor-specific transplantation tolerance and treat autoimmune diseases. *Blood* 112:3543-53.

10. Burt RK et al. (2008) Clinical applications of blood-derived and marrow-derived stem cells for nonmalignant diseases. *JAMA : the journal of the American Medical Association* 299:925-36.

11. Forrester JS, Price MJ, Makkar RR (2003) Stem cell repair of infarcted myocardium: an overview for clinicians. *Circulation* 108:1139-45.

12. Sanberg PR, Willing AE, Cahill DW (2002) Novel cellular approaches to repair of neurodegenerative disease: from Sertoli cells to umbilical cord blood stem cells. *Neurotoxicity research* 4:95-101.

13. Moraleda JM et al. (2006) Adult stem cell therapy: dream or reality? *Transplant immunology* 17:74-7.

14. Kondo M et al. (2003) Biology of hematopoietic stem cells and progenitors: implications for clinical application. *Annual review of immunology* 21:759-806.

15. Lagasse E et al. (2000) Purified hematopoietic stem cells can differentiate into hepatocytes in vivo. *Nature medicine* 6:1229-34.

16. Gussoni E et al. (1999) Dystrophin expression in the mdx mouse restored by stem cell transplantation. *Nature* 401:390-4.

17. Ianus A, Holz GG, Theise ND, Hussain MA (2003) In vivo derivation of glucose-competent pancreatic endocrine cells from bone marrow without evidence of cell fusion. *The Journal of clinical investigation* 111:843-50.

18. 2008 Biennial Report of The C.W. Bill Young Cell Transplantation Program (2008) *2008 Biennial Report of The C.W. Bill Young Cell Transplantation Program* (Bethesda, MD).

19. Kerrigan D, Hollen K, Kelly J, Hollen B (2006) Blood Stem Cell Transplants. *Understanding Cancer*. Available at: http://www.cancer.gov/cancertopics/understandingcancer/stemcells [Accessed June 14, 2011].

20. Kindt T, Goldsby RA, Osborne BA (2007) *Immunology* (W. H. Freeman and Company, New York). 6th Ed.

21. Moore T, Ikeda A (2010) Bone Marrow Transplantation. *Medscape Reference*. Available at: http://emedicine.medscape.com/article/1014514-overview#showall [Accessed June 20, 2011].

22. Sandmaier BM, Mackinnon S, Childs RW (2007) Reduced intensity conditioning for allogeneic hematopoietic cell transplantation: current perspectives. *Biology of blood and marrow transplantation : journal of the American Society for Blood and Marrow Transplantation* 13:87-97.

23. Giralt S et al. (1997) Engraftment of allogeneic hematopoietic progenitor cells with purine analog-containing chemotherapy: harnessing graft-versus-leukemia without myeloablative therapy. *Blood* 89:4531-6.

24. McSweeney PA et al. (2001) Hematopoietic cell transplantation in older patients with hematologic malignancies: replacing high-dose cytotoxic therapy with graft-versus-tumor effects. *Blood* 97:3390-400.

25. Baron F et al. (2005) Graft-versus-tumor effects after allogeneic hematopoietic cell transplantation with nonmyeloablative conditioning. *Journal of clinical oncology : official journal of the American Society of Clinical Oncology* 23:1993-2003.

26. Majhail NS, Brunstein CG, Wagner JE (2006) Double umbilical cord blood transplantation. *Current opinion in immunology* 18:571-5.

27. U.S. Transplant Data by Disease Report (2011) U.S. Transplant Data by Disease Report. *Bone Marrow and Cord Blood Donation and Transplantation.* Available at: http://bloodcell.transplant.hrsa.gov/RESEARCH/index.html [Accessed June 21, 2011].

28. Lapidot T, Petit I (2002) Current understanding of stem cell mobilization: the roles of chemokines, proteolytic enzymes, adhesion molecules, cytokines, and stromal cells. *Experimental hematology* 30:973-81.

29. Devine SM, Lazarus HM, Emerson SG (2003) Clinical application of hematopoietic progenitor cell expansion: current status and future prospects. *Bone marrow transplantation* 31:241-52.

30. Wu A, Siminovitch L, Till J, McCulloch E (1968) Evidence for a Relationship between Mouse Hemopoietic Stem Cells and Cells Forming Colonies in Culture. *Proceedings of the National Academy of Sciences of the United States of America* 59:1209-1215.

31. Till JE, McCulloch EA (1961) A direct measurement of the radiation sensitivity of normal mouse bone marrow cells. *Radiation Research* 14:213–222.

32. Lutolf MP, Blau HM (2009) Artificial stem cell niches. *Advanced materials (Deerfield Beach, Fla.)* 21:3255-68.

33. Lutolf MP, Gilbert PM, Blau HM (2009) Designing materials to direct stem-cell fate. *Nature* 462:433-41.

34. Wilson A, Trumpp A (2006) Bone-marrow haematopoietic-stem-cell niches. *Nature reviews. Immunology* 6:93-106.

35. Cheshier SH, Morrison SJ, Liao X, Weissman IL (1999) In vivo proliferation and cell cycle kinetics of long-term self-renewing hematopoietic stem cells. *Proceedings of the National Academy of Sciences of the United States of America* 96:3120-5.

36. Fuchs E, Tumbar T, Guasch G (2004) Socializing with the neighbors: stem cells and their niche. *Cell* 116:769-78.

37. Watt FM, Hogan BL (2000) Out of Eden: stem cells and their niches. *Science (New York, N.Y.)* 287:1427-30.

38. Bryder D, Rossi DJ, Weissman IL (2006) Hematopoietic Stem Cells: The Paradigmatic Tissue-Specific Stem Cell. *American Journal Of Pathology* 169:338-346.

39. Wilson A et al. (2007) Dormant and self-renewing hematopoietic stem cells and their niches. *Annals of the New York Academy of Sciences* 1106:64-75.

40. Morrison SJ, Weissman IL (1994) The long-term repopulating subset of hematopoietic stem cells is deterministic and isolatable by phenotype. *Immunity* 1:661-73.

41. Spangrude GJ, Heimfeld S, Weissman IL (1988) Purification and Characterization of Mouse Hematopoietic Stem Cells. *Science* 241:58.

42. Ikuta K, Weissman IL (1992) Evidence that hematopoietic stem cells express mouse c-kit but do not depend on steel factor for their generation. *Proceedings of the National Academy of Sciences of the United States of America* 89:1502-6.

43. Osawa M, Hanada K, Hamada H, Nakauchi H (1996) Long-Term Lymphohematopoietic Reconstitution by a Single CD34-Low/Negative Hematopoietic Stem Cell. *Science (New York, N.Y.)* 273:242-5.

44. Ema H et al. (2006) Adult mouse hematopoietic stem cells: purification and single-cell assays. *Nature protocols* 1:2979-87.

45. Goodell MA, Brose K, Paradis G, Conner AS, Mulligan RC (1996) Isolation and functional properties of murine hematopoietic stem cells that are replicating in vivo. *The Journal of experimental medicine* 183:1797.

46. Robinson SN, Seina SM, Gohr JC, Kuszynski C a, Sharp JG (2005) Evidence for a qualitative hierarchy within the Hoechst-33342 "side population" (SP) of murine bone marrow cells. *Bone marrow transplantation* 35:807-18.

47. Kiel MJ et al. (2005) SLAM family receptors distinguish hematopoietic stem and progenitor cells and reveal endothelial niches for stem cells. *Cell* 121:1109-21.

48. Blank U, Karlsson G, Karlsson S (2008) Signaling pathways governing stem-cell fate. *Blood* 111:492-503.

49. Morrison SJ, Weissman IL (1994) The long-term repopulating subset of hematopoietic stem cells is deterministic and isolatable by phenotype. *Immunity* 1:661-73.

50. Adolfsson J et al. (2001) Upregulation of Flt3 expression within the bone marrow Lin(-)Sca1(+)c-kit(+) stem cell compartment is accompanied by loss of self-renewal capacity. *Immunity* 15:659-69.

51. Yang L et al. (2005) Identification of Lin(-)Sca1(+)kit(+)CD34(+)Flt3- short-term hematopoietic stem cells capable of rapidly reconstituting and rescuing myeloablated transplant recipients. *Blood* 105:2717-23.

52. Camargo FD, Chambers SM, Drew E, McNagny KM, Goodell M a (2006) Hematopoietic stem cells do not engraft with absolute efficiencies. *Blood* 107:501-7.

53. Matsuzaki Y, Kinjo K, Mulligan RC, Okano H (2004) Unexpectedly efficient homing capacity of purified murine hematopoietic stem cells. *Immunity* 20:87-93.

54. Uchida N, Dykstra B, Lyons KJ, Leung FYK, Eaves CJ (2003) Different in vivo repopulating activities of purified hematopoietic stem cells before and after being stimulated to divide in vitro with the same kinetics. *Experimental hematology* 31:1338-47.

55. Wagers AJ, Sherwood RI, Christensen JL, Weissman IL (2002) Little evidence for developmental plasticity of adult hematopoietic stem cells. *Science (New York, N.Y.)* 297:2256-9.

56. Kopp H-G, Avecilla ST, Hooper AT, Rafii S (2005) The bone marrow vascular niche: home of HSC differentiation and mobilization. *Physiology (Bethesda, Md.)* 20:349-56.

57. Pruijt JF et al. (1999) Prevention of interleukin-8-induced mobilization of hematopoietic progenitor cells in rhesus monkeys by inhibitory antibodies against the metalloproteinase gelatinase B (MMP-9). *Proceedings of the National Academy of Sciences of the United States of America* 96:10863-8.

58. Möhle R, Haas R, Hunstein W (1993) Expression of adhesion molecules and c-kit on CD34+ hematopoietic progenitor cells: comparison of cytokine-mobilized blood stem cells with normal bone marrow and peripheral blood. *Journal of hematotherapy* 2:483-9.

59. Takamatsu Y et al. (1998) Osteoclast-mediated bone resorption is stimulated during short-term administration of granulocyte colony-stimulating factor but is not responsible for hematopoietic progenitor cell mobilization. *Blood* 92:3465-73.

60. Nakagawa T, Nabeshima Y-I, Yoshida S (2007) Functional identification of the actual and potential stem cell compartments in mouse spermatogenesis. *Developmental cell* 12:195-206.

61. Kai T, Spradling A (2004) Differentiating germ cells can revert into functional stem cells in Drosophila melanogaster ovaries. *Nature* 428:564-9.

62. Di Maggio N et al. (2011) Toward modeling the bone marrow niche using scaffold-based 3D culture systems. *Biomaterials* 32:321-9.

63. Brannan CI et al. (1991) Steel-Dickie mutation encodes a c-kit ligand lacking transmembrane and cytoplasmic domains. *Proceedings of the National Academy of Sciences of the United States of America* 88:4671-4.

64. Kollet O, Dar A, Lapidot T (2007) The multiple roles of osteoclasts in host defense: bone remodeling and hematopoietic stem cell mobilization. *Annual review of immunology* 25:51-69.

65. Shizuru J a, Negrin RS, Weissman IL (2005) Hematopoietic stem and progenitor cells: clinical and preclinical regeneration of the hematolymphoid system. *Annual review of medicine* 56:509-38.

66. Kiel MJ, Morrison SJ (2008) Uncertainty in the niches that maintain haematopoietic stem cells. *Nature reviews. Immunology* 8:290-301.

67. Sugiyama T, Kohara H, Noda M, Nagasawa T (2006) Maintenance of the hematopoietic stem cell pool by CXCL12-CXCR4 chemokine signaling in bone marrow stromal cell niches. *Immunity* 25:977-88.

68. Wagner W et al. (2007) Molecular and secretory profiles of human mesenchymal stromal cells and their abilities to maintain primitive hematopoietic progenitors. *Stem cells (Dayton, Ohio)* 25:2638-47.

69. Radtke F, Wilson A, Mancini SJC, MacDonald HR (2004) Notch regulation of lymphocyte development and function. *Nature immunology* 5:247-53.

70. Reya T, Clevers H (2005) Wnt signalling in stem cells and cancer. *Nature* 434:843-50.

71. Artavanis-Tsakonas S (1999) Notch Signaling: Cell Fate Control and Signal Integration in Development. *Science* 284:770-776.

72. Kumano K et al. (2001) Notch1 inhibits differentiation of hematopoietic cells by sustaining GATA-2 expression. *Blood* 98:3283-9.

73. Han H et al. (2002) Inducible gene knockout of transcription factor recombination signal binding protein-J reveals its essential role in T versus B lineage decision. *International immunology* 14:637-45.

74. Mancini SJC et al. (2005) Jagged1-dependent Notch signaling is dispensable for hematopoietic stem cell self-renewal and differentiation. *Blood* 105:2340-2.

75. Radtke F et al. (1999) Deficient T cell fate specification in mice with an induced inactivation of Notch1. *Immunity* 10:547-58.

76. Saito T et al. (2003) Notch2 is preferentially expressed in mature B cells and indispensable for marginal zone B lineage development. *Immunity* 18:675-85.

77. Yin T, Li L (2006) The stem cell niches in bone. *Journal of Clinical Investigation* 116:1195.

78. Arai F et al. (2004) Tie2/angiopoietin-1 signaling regulates hematopoietic stem cell quiescence in the bone marrow niche. *Cell* 118:149-61.

79. Staal FJT, Clevers HC (2005) WNT signalling and haematopoiesis: a WNT-WNT situation. *Nature reviews. Immunology* 5:21-30.

80. Rattis FM, Voermans C, Reya T (2004) Wnt signaling in the stem cell niche. *Current opinion in hematology* 11:88-94.

81. Reya T et al. (2003) A role for Wnt signalling in self-renewal of haematopoietic stem cells. *Nature* 423:409-14.

82. Barker JE (1997) Early transplantation to a normal microenvironment prevents the development of Steel hematopoietic stem cell defects. *Experimental hematology* 25:542-7.

83. Barker JE (1994) Sl/Sld hematopoietic progenitors are deficient in situ. *Experimental hematology* 22:174-7.

84. Wilson A et al. (2004) c-Myc controls the balance between hematopoietic stem cell self-renewal and differentiation. *Genes & development* 18:2747-63.

85. Zhang J et al. (2003) Identification of the haematopoietic stem cell niche and control of the niche size. *Methods in Molecular Biology* 425:0-5.

86. Muguruma Y et al. (2006) Reconstitution of the functional human hematopoietic microenvironment derived from human mesenchymal stem cells in the murine bone marrow compartment. *Blood* 107:1878-87.

87. Kiel MJ, Radice GL, Morrison SJ (2007) Lack of evidence that hematopoietic stem cells depend on N-cadherin-mediated adhesion to osteoblasts for their maintenance. *Cell stem cell* 1:204-17.

88. Nilsson SK et al. (2005) Osteopontin, a key component of the hematopoietic stem cell niche and regulator of primitive hematopoietic progenitor cells. *Blood* 106:1232-9.

89. Sell S ed. (2004) *Stem Cells Handbook* (Humana Press, Totowa, NJ).

90. Adams GB et al. (2006) Stem cell engraftment at the endosteal niche is specified by the calcium-sensing receptor. *Nature* 439:599-603.

91. Ivanović Z et al. (2000) Incubation of murine bone marrow cells in hypoxia ensures the maintenance of marrow-repopulating ability together with the expansion of committed progenitors. *British journal of haematology* 108:424-9.

92. Baldridge MT, King KY, Goodell M a (2011) Inflammatory signals regulate hematopoietic stem cells. *Trends in immunology* 32:57-65.

93. Baldridge MT, King KY, Boles NC, Weksberg DC, Goodell M a (2010) Quiescent haematopoietic stem cells are activated by IFN-gamma in response to chronic infection. *Nature* 465:793-7.

94. LaIuppa J a, McAdams T a, Papoutsakis ET, Miller WM (1997) Culture materials affect ex vivo expansion of hematopoietic progenitor cells. *Journal of biomedical materials research* 36:347-59.

95. Tsai S, Bartelmez S, Sitnicka E, Collins S (1994) Lymphohematopoietic progenitors immortalized by a retroviral vector harboring a dominant-negative retinoic acid receptor can recapitulate lymphoid, myeloid, and erythroid development. *Genes & development* 8:2831-41.

96. Turner ML, Masek LC, Hardy CL, Parker a C, Sweetenham JW (1998) Comparative adhesion of human haemopoietic cell lines to extracellular matrix components, bone marrow stromal and endothelial cultures. *British journal of haematology* 100:112-22.

97. Fox N, Priestley G, Papayannopoulou T, Kaushansky K (2002) Thrombopoietin expands hematopoietic stem cells after transplantation. *The Journal of clinical investigation* 110:389-94.

98. Sitnicka E et al. (1996) The effect of thrombopoietin on the proliferation and differentiation of murine hematopoietic stem cells. *Blood* 87:4998-5005.

99. Kirito K, Fox N, Kaushansky K (2003) Thrombopoietin stimulates Hoxb4 expression: an explanation for the favorable effects of TPO on hematopoietic stem cells. *Blood* 102:3172.

100. Buza-Vidas N et al. (2006) Cytokines regulate postnatal hematopoietic stem cell expansion: opposing roles of thrombopoietin and LNK. *Genes & development* 20:2018-23.

101. Ema H, Takano H, Sudo K, Nakauchi H (2000) In vitro self-renewal division of hematopoietic stem cells. *The Journal of experimental medicine* 192:1281-8.

102. Willert K et al. (2003) Wnt proteins are lipid-modified and can act as stem cell growth factors. *Nature* 423:448-52.

103. Karanu FN et al. (2000) The notch ligand jagged-1 represents a novel growth factor of human hematopoietic stem cells. *The Journal of experimental medicine* 192:1365-72.

104. Diehl a, Stoelting S, Nadrowitz R, Wagner T, Peters SO (2007) Improved hematopoietic stem cell engraftment following ex vivo expansion of murine marrow cells with SCF and Flt3L. *Cytotherapy* 9:532-8.

105. Haan G de et al. (2003) In vitro generation of long-term repopulating hematopoietic stem cells by fibroblast growth factor-1. *Developmental cell* 4:241-51.

106. McNiece IK, Almeida-Porada G, Shpall EJ, Zanjani E (2002) Ex vivo expanded cord blood cells provide rapid engraftment in fetal sheep but lack long-term engrafting potential. *Experimental hematology* 30:612-6.

107. Petzer A, Zandstra P, Piret J, Eaves C (1996) Differential Cytokine Effects on Primitive (CD34+CD38-) Human Hematopoietic Cells: Novel Responses to Flt3-Ligand and Thrombopoietin. *The Journal of experimental medicine* 183:2551.

108. Lu LS, Wang SJ, Auerbach R (1996) In vitro and in vivo differentiation into B cells, T cells, and myeloid cells of primitive yolk sac hematopoietic precursor cells expanded > 100-fold by coculture with a clonal yolk sac endothelial cell line.

Proceedings of the National Academy of Sciences of the United States of America 93:14782-7.

109. Hu L et al. (2006) Effects of human yolk sac endothelial cells on supporting expansion of hematopoietic stem/progenitor cells from cord blood. *Cell biology international* 30:879-84.

110. Fujimoto N et al. (2007) Microencapsulated feeder cells as a source of soluble factors for expansion of CD34(+) hematopoietic stem cells. *Biomaterials* 28:4795-805.

111. Jung Y et al. (2005) Cell-to-cell contact is critical for the survival of hematopoietic progenitor cells on osteoblasts. *Cytokine* 32:155-62.

112. Oostendorp R a J et al. (2005) Long-term maintenance of hematopoietic stem cells does not require contact with embryo-derived stromal cells in cocultures. *Stem cells (Dayton, Ohio)* 23:842-51.

113. Feugier P et al. (2002) Ex vivo expansion of stem and progenitor cells in co-culture of mobilized peripheral blood CD34+ cells on human endothelium transfected with adenovectors expressing thrombopoietin, c-kit ligand, and Flt-3 ligand. *Journal of hematotherapy & stem cell research* 11:127-38.

114. Dormady SP, Zhang XM, Basch RS (2000) Hematopoietic Progenitor Cells Grow on 3T3 Fibroblast Monolayers That Overexpress Growth Arrest-Specific Gene-6 (GAS6). *Proceedings of the National Academy of Sciences of the United States of America* 97:12260.

115. Roberts R a et al. (1987) Metabolically inactive 3T3 cells can substitute for marrow stromal cells to promote the proliferation and development of multipotent haemopoietic stem cells. *Journal of cellular physiology* 132:203-14.

116. Huang G-P et al. (2007) Ex vivo expansion and transplantation of hematopoietic stem/progenitor cells supported by mesenchymal stem cells from human umbilical cord blood. *Cell transplantation* 16:579-85.

117. Chitteti BR et al. (2010) Impact of interactions of cellular components of the bone marrow microenvironment on hematopoietic stem and progenitor cell function. *Blood* 115:3239-48.

118. Celebi B, Mantovani D, Pineault N (2011) Irradiated mesenchymal stem cells improve the ex vivo expansion of hematopoietic progenitors by partly mimicking the bone marrow endosteal environment. *Journal of immunological methods* 370:93-103.

119. Yamaguchi H et al. (1996) Umbilical vein endothelial cells are an important source of c-kit and stem cell factor which regulate the proliferation of haemopoietic progenitor cells. *British journal of haematology* 94:606-11.

120. Franke K, Pompe T, Bornhäuser M, Werner C (2007) Engineered matrix coatings to modulate the adhesion of CD133+ human hematopoietic progenitor cells. *Biomaterials* 28:836-43.

121. Dao M, Hashino K, Kato I, Nolta J (1998) Adhesion to fibronectin maintains regenerative capacity during ex vivo culture and transduction of human hematopoietic stem and progenitor cells. *Blood* 92:4612-21.

122. Yokota T et al. (1998) Growth-supporting activities of fibronectin on hematopoietic stem/progenitor cells in vitro and in vivo: structural requirement for fibronectin activities of CS1 and cell-binding domains. *Blood* 91:3263-72.

123. Lévesque JP, Haylock DN, Simmons PJ (1996) Cytokine regulation of proliferation and cell adhesion are correlated events in human CD34+ hemopoietic progenitors. *Blood* 88:1168-76.

124. Krämer a et al. (1999) Adhesion to fibronectin stimulates proliferation of wild-type and bcr/abl-transfected murine hematopoietic cells. *Proceedings of the National Academy of Sciences of the United States of America* 96:2087-92.

125. Jiang X-S et al. (2006) Surface-immobilization of adhesion peptides on substrate for ex vivo expansion of cryopreserved umbilical cord blood CD34+ cells. *Biomaterials* 27:2723-32.

126. Ma K et al. (2008) Electrospun nanofiber scaffolds for rapid and rich capture of bone marrow-derived hematopoietic stem cells. *Biomaterials* 29:2096–2103.

127. Lutolf MP, Doyonnas R, Havenstrite K, Koleckar K, Blau HM (2009) Perturbation of single hematopoietic stem cell fates in artificial niches. *Integrative biology : quantitative biosciences from nano to macro* 1:59-69.

128. Kobel S, Limacher M, Gobaa S, Laroche T, Lutolf MP (2009) Micropatterning of hydrogels by soft embossing. *Langmuir : the ACS journal of surfaces and colloids* 25:8774-9.

129. Feng Q, Chai C, Jiang XS, Leong KW, Mao HQ (2006) Expansion of engrafting human hematopoietic stem/progenitor cells in three-dimensional scaffolds with surface-immobilized fibronectin. *Journal of Biomedical Materials Research Part A* 78:781–791.

130. Chua K et al. (2007) Functional nanofiber scaffolds with different spacers modulate adhesion and expansion of cryopreserved umbilical cord blood hematopoietic stem/progenitor cells. *Experimental Hematology* 35:771-781.

131. Chua K-N et al. (2006) Surface-aminated electrospun nanofibers enhance adhesion and expansion of human umbilical cord blood hematopoietic stem/progenitor cells. *Biomaterials* 27:6043-51.

132. Bagley J, Rosenzweig M, Marks DF, Pykett MJ (1999) Extended culture of multipotent hematopoietic progenitors without cytokine augmentation in a novel three-dimensional device. *Experimental hematology* 27:496-504.

133. Diehl a, Stoelting S, Nadrowitz R, Wagner T, Peters SO (2007) Improved hematopoietic stem cell engraftment following ex vivo expansion of murine marrow cells with SCF and Flt3L. *Cytotherapy* 9:532-8.

134. Klug CA, Jordan CT eds. (2002) *Hematopoietic Stem Cell Protocols* (Humana Press, Totowa, NJ). 1st Ed.

135. Kirito K, Fox N, Kaushansky K (2003) Thrombopoietin stimulates Hoxb4 expression: an explanation for the favorable effects of TPO on hematopoietic stem cells. *Blood* 102:3172-8.

136. Christensen JL, Weissman IL (2001) Flk-2 is a marker in hematopoietic stem cell differentiation: a simple method to isolate long-term stem cells. *Proceedings of the National Academy of Sciences of the United States of America* 98:14541-6.

137. Kishimoto S et al. (2010) Immobilization, stabilization, and activation of human stem cell factor (SCF) on fragmin/protamine microparticle (F/P MP)-coated plates. *Journal of biomedical materials research. Part B, Applied biomaterials* 92:32-9.

138. Langer R, Peppas NA (2003) Advances in biomaterials, drug delivery, and bionanotechnology. *AIChE Journal* 49:2990-3006.

139. Hubbell JA (1998) Synthetic biodegradable polymers for tissue engineering and drug delivery. *Current Opinion in Solid State and Materials Science* 3:246-251.

140. Dinh SM, Liu P eds. (2003) *Advances in Controlled Drug Delivery* (American Chemical Society, Washington, DC).

141. Langer R, Tirrell DA (2004) Designing materials for biology and medicine. *Nature* 428:487-92.

142. Kim B, Peppas NA (2003) In vitro release behavior and stability of insulin in complexation hydrogels as oral drug delivery carriers. *International journal of pharmaceutics* 266:29-37.

143. Lu S, Anseth KS (2000) Release Behavior of High Molecular Weight Solutes from Poly(ethylene glycol)-Based Degradable Networks. *Macromolecules* 33:2509-2515.

144. Davis KA, Anseth KS (2002) Controlled release from crosslinked degradable networks. *Critical reviews in therapeutic drug carrier systems* 19:385-423.

145. Pratt AB, Weber FE, Schmoekel HG, Müller R, Hubbell JA (2004) Synthetic extracellular matrices for in situ tissue engineering. *Biotechnology and bioengineering* 86:27-36.

146. Schmedlen RH, Masters KS, West JL (2002) Photocrosslinkable polyvinyl alcohol hydrogels that can be modified with cell adhesion peptides for use in tissue engineering. *Biomaterials* 23:4325-32.

147. Nguyen KT, West JL (2002) Photopolymerizable hydrogels for tissue engineering applications. *Biomaterials* 23:4307-14.

148. Lee KY, Mooney DJ (2001) Hydrogels for tissue engineering. *Chemical reviews* 101:1869-79.

149. Drury JL, Mooney DJ (2003) Hydrogels for tissue engineering: scaffold design variables and applications. *Biomaterials* 24:4337-51.

150. Peppas N A, Hilt J Z, Khademhosseini A, Langer R (2006) Hydrogels in Biology and Medicine: From Molecular Principles to Bionanotechnology. *Advanced Materials* 18:1345-1360.

151. Peppas NA, Bures P, Leobandung W, Ichikawa H (2000) Hydrogels in pharmaceutical formulations. *European journal of pharmaceutics and biopharmaceutics : official journal of Arbeitsgemeinschaft für Pharmazeutische Verfahrenstechnik e.V* 50:27-46.

152. Van Vlierberghe S, Dubruel P, Schacht E (2011) Biopolymer-based hydrogels as scaffolds for tissue engineering applications: a review. *Biomacromolecules* 12:1387-408.

153. Nemir S, Hayenga HN, West JL (2010) PEGDA hydrogels with patterned elasticity: Novel tools for the study of cell response to substrate rigidity. *Biotechnology and bioengineering* 105:636-44.

154. Sershen S, West J (2002) Implantable, polymeric systems for modulated drug delivery. *Advanced drug delivery reviews* 54:1225-35.

155. Jeong B, Kim SW, Bae YH (2002) Thermosensitive sol-gel reversible hydrogels. *Advanced drug delivery reviews* 54:37-51.

156. Gombotz WR, Wang GH, Horbett T a, Hoffman a S (1991) Protein adsorption to poly(ethylene oxide) surfaces. *Journal of biomedical materials research* 25:1547-62.

157. Merrill EW et al. (1982) Platelet-compatible hydrophilic segmented polyurethanes from polyethylene glycols and cyclohexane diisocyanate. *Transactions - American Society for Artificial Internal Organs* 28:482-7.

158. Miller JS, West JL (2008) in *Micro and Nanoengineering of the Cell Microenvironment: Technologies and Applications*, eds Khademhosseini A, Borenstein J, Toner M (Artech House Publishers).First.

159. Metters A, Hubbell J (2005) Network formation and degradation behavior of hydrogels formed by Michael-type addition reactions. *Biomacromolecules* 6:290-301.

160. Pathak CP, Sawhney AS, Hubbell JA (1992) Rapid photopolymerization of immunoprotective gels in contact with cells and tissue. *Journal of the American Chemical Society* 114:8311–8312.

161. Mann BK, West JL (2002) Cell adhesion peptides alter smooth muscle cell adhesion, proliferation, migration, and matrix protein synthesis on modified surfaces and in polymer scaffolds. *Journal of biomedical materials research* 60:86–93.

162. Gobin AS, West JL (2002) Cell migration through defined, synthetic extracellular matrix analogues. *The FASEB Journal.*

163. Desmangles AI, Jordan O, Marquis-Weible F (2001) Interfacial photopolymerization of beta-cell clusters: approaches to reduce coating thickness using ionic and lipophilic dyes. *Biotechnology and bioengineering* 72:634-41.

164. Hubbell JA (1999) Bioactive biomaterials. *Current opinion in biotechnology* 10:123-9.

165. Lutolf MP, Hubbell JA (2003) Synthesis and physicochemical characterization of end-linked poly(ethylene glycol)-co-peptide hydrogels formed by Michael-type addition. *Biomacromolecules* 4:713-22.

166. Temenoff JS, Mikos AG (2000) Injectable biodegradable materials for orthopedic tissue engineering. *Biomaterials* 21:2405-12.

167. West JL, Hubbell J a (1999) Polymeric Biomaterials with Degradation Sites for Proteases Involved in Cell Migration. *Macromolecules* 32:241-244.

168. Hern DL, Hubbell J a (1998) Incorporation of adhesion peptides into nonadhesive hydrogels useful for tissue resurfacing. *Journal of biomedical materials research* 39:266-76.

169. Burdick JA, Anseth KS (2002) Photoencapsulation of osteoblasts in injectable RGD-modified PEG hydrogels for bone tissue engineering. *Biomaterials* 23:4315-23.

170. Burdick JA, Khademhosseini A, Langer R (2004) Fabrication of gradient hydrogels using a microfluidics/photopolymerization process. *Langmuir : the ACS journal of surfaces and colloids* 20:5153-6.

171. Gonzalez AL, Gobin AS, West JL, McIntire LV, Smith CW (2004) Integrin interactions with immobilized peptides in polyethylene glycol diacrylate hydrogels. *Tissue engineering* 10:1775-86.

172. Moon JJ, Lee S-H, West JL (2007) Synthetic biomimetic hydrogels incorporated with ephrin-A1 for therapeutic angiogenesis. *Biomacromolecules* 8:42-9.

173. Saik JE, Gould DJ, Watkins EM, Dickinson ME, West JL (2010) Covalently Immobilized Platelet Derived Growth Factor-BB Promotes Angiogenesis in Biomimetic Poly(ethylene glycol) Hydrogels. *Acta biomaterialia* 7:133-143.

174. Leslie-Barbick JE, Moon JJ, West JL (2009) Covalently-immobilized vascular endothelial growth factor promotes endothelial cell tubulogenesis in poly(ethylene glycol) diacrylate hydrogels. *Journal of biomaterials science. Polymer edition* 20:1763-79.

175. DeLong SA, Moon JJ, West JL (2005) Covalently immobilized gradients of bFGF on hydrogel scaffolds for directed cell migration. *Biomaterials* 26:3227-34.

176. Miller JS, Béthencourt MI, Hahn M, Lee TR, West JL (2006) Laser-scanning lithography (LSL) for the soft lithographic patterning of cell-adhesive self-assembled monolayers. *Biotechnology and bioengineering* 93:1060–1068.

177. Liu Tsang V et al. (2007) Fabrication of 3D hepatic tissues by additive photopatterning of cellular hydrogels. *The FASEB journal : official publication of the Federation of American Societies for Experimental Biology* 21:790-801.

178. Lee S-H, Moon JJ, West JL (2008) Three-dimensional micropatterning of bioactive hydrogels via two-photon laser scanning photolithography for guided 3D cell migration. *Biomaterials* 29:2962-8.

179. Hahn MS et al. (2006) Photolithographic patterning of polyethylene glycol hydrogels. *Biomaterials* 27:2519-24.

180. Hoffmann JC, West JL (2010) Three-dimensional photolithographic patterning of multiple bioactive ligands in poly(ethylene glycol) hydrogels. *Soft Matter* 6:5056.

181. Patterson J, Hubbell JA (2010) Enhanced proteolytic degradation of molecularly engineered PEG hydrogels in response to MMP-1 and MMP-2. *Biomaterials* 31:7836-45.

182. Patterson J, Hubbell JA (2011) SPARC-derived protease substrates to enhance the plasmin sensitivity of molecularly engineered PEG hydrogels. *Biomaterials* 32:1301-10.

183. Lutolf MP et al. (2003) Synthetic matrix metalloproteinase-sensitive hydrogels for the conduction of tissue regeneration: engineering cell-invasion characteristics. *Proceedings of the National Academy of Sciences of the United States of America* 100:5413-8.

184. Karp JM et al. (2007) Controlling size, shape and homogeneity of embryoid bodies using poly(ethylene glycol) microwells. *Lab on a chip* 7:786-94.

185. Moeller H-C, Mian MK, Shrivastava S, Chung BG, Khademhosseini A (2008) A microwell array system for stem cell culture. *Biomaterials* 29:752-63.

186. Jongpaiboonkit L, King WJ, Murphy WL (2009) Screening for 3D environments that support human mesenchymal stem cell viability using hydrogel arrays. *Tissue engineering. Part A* 15:343-53.

187. Bryant SJ, Anseth KS (2002) Hydrogel properties influence ECM production by chondrocytes photoencapsulated in poly(ethylene glycol) hydrogels. *Journal of biomedical materials research* 59:63-72.

188. Gunawan RC, King J a, Lee BP, Messersmith PB, Miller WM (2007) Surface presentation of bioactive ligands in a nonadhesive background using DOPA-tethered biotinylated poly(ethylene glycol). *Langmuir : the ACS journal of surfaces and colloids* 23:10635-43.

189. Giovino MA, Wang H, Sykes M, Yang Y-G (2005) Role of VLA-4 and VLA-5 in ex vivo maintenance of human and pig hematopoiesis in human stroma-supported long-term cultures. *Experimental hematology* 33:363-70.

190. Luo B et al. (2011) The Endoplasmic Reticulum Chaperone Protein GRP94 Is Required for Maintaining Hematopoietic Stem Cell Interactions with the Adult Bone Marrow Niche. *PloS one* 6:e20364.

191. Weinstein R et al. (1989) Dual role of fibronectin in hematopoietic differentiation. *Blood* 73:111-6.

192. Wayner E a, Kovach NL (1992) Activation-dependent recognition by hematopoietic cells of the LDV sequence in the V region of fibronectin. *The Journal of cell biology* 116:489-97.

193. Minguell JJ, Hardy CL, Tavassoli M (1993) Adhesive interaction of hemopoietic progenitor cell membrane with the RGD domain of fibronectin. *Biochimica et biophysica acta* 1151:120-6.

194. Garcia AS, Dellatore SM, Messersmith PB, Miller WM (2009) Effects of supported lipid monolayer fluidity on the adhesion of hematopoietic progenitor cell lines to fibronectin-derived peptide ligands for alpha5beta1 and alpha4beta1 integrins. *Langmuir : the ACS journal of surfaces and colloids* 25:2994-3002.

195. Jensen TW et al. (2004) Lipopeptides incorporated into supported phospholipid monolayers have high specific activity at low incorporation levels. *Journal of the American Chemical Society* 126:15223-30.

196. Okada S et al. (1992) In vivo and in vitro stem cell function of c-kit- and Sca-1-positive murine hematopoietic cells. *Blood* 80:3044-50.

197. Cuchiara MP, Allen ACB, Chen TM, Miller JS, West JL (2010) Multilayer microfluidic PEGDA hydrogels. *Biomaterials* 31:5491-7.

198. Chollet C et al. (2009) The effect of RGD density on osteoblast and endothelial cell behavior on RGD-grafted polyethylene terephthalate surfaces. *Biomaterials* 30:711-20.

199. Vuillet-Gaugler MH et al. (1990) Loss of attachment to fibronectin with terminal human erythroid differentiation. *Blood* 75:865-73.

200. Patel VP, Ciechanover a, Platt O, Lodish HF (1985) Mammalian reticulocytes lose adhesion to fibronectin during maturation to erythrocytes. *Proceedings of the National Academy of Sciences of the United States of America* 82:440-4.

201. Lemoine FM, Dedhar S, Lima GM, Eaves CJ (1990) Transformation-associated alterations in interactions between pre-B cells and fibronectin. *Blood* 76:2311-20.

202. Verfaillie CM, McCarthy JB, McGlave PB (1991) Differentiation of primitive human multipotent hematopoietic progenitors into single lineage clonogenic progenitors is accompanied by alterations in their interaction with fibronectin. *The Journal of experimental medicine* 174:693-703.

203. Sagar BMM, Rentala S, Gopal PNV, Sharma S, Mukhopadhyay A (2006) Fibronectin and laminin enhance engraftibility of cultured hematopoietic stem cells. *Biochemical and biophysical research communications* 350:1000-5.

204. Broxmeyer HE et al. (1991) The kit receptor and its ligand, steel factor, as regulators of hemopoiesis. *Cancer cells (Cold Spring Harbor, N.Y. : 1989)* 3:480-7.

205. Bernstein ID, Andrews RG, Zsebo KM (1991) Recombinant human stem cell factor enhances the formation of colonies by CD34+ and CD34+lin- cells, and the generation of colony-forming cell progeny from CD34+lin- cells cultured with interleukin-3, granulocyte colony-stimulating factor, or granulocyte-m. *Blood* 77:2316-21.

206. Doran MR et al. (2009) Surface-bound stem cell factor and the promotion of hematopoietic cell expansion. *Biomaterials* 30:4047-52.

207. McNiece IK, Langley KE, Zsebo KM (1991) Recombinant human stem cell factor synergises with GM-CSF, G-CSF, IL-3 and epo to stimulate human progenitor cells of the myeloid and erythroid lineages. *Experimental hematology* 19:226-31.

208. Miyazawa K et al. (1995) Membrane-bound Steel factor induces more persistent tyrosine kinase activation and longer life span of c-kit gene-encoded protein than its soluble form. *Blood* 85:641-9.

209. Toksoz D et al. (1992) Support of human hematopoiesis in long-term bone marrow cultures by murine stromal cells selectively expressing the membrane-bound and secreted forms of the human homolog of the steel gene product, stem cell factor. *Proceedings of the National Academy of Sciences of the United States of America* 89:7350-4.

210. Galli MC, Giardina PJ, Migliaccio AR, Migliaccio G (1993) The biology of stem cell factor, a new hematopoietic growth factor involved in stem cell regulation. *International journal of clinical & laboratory research* 23:70-7.

211. Anderson DM et al. (1990) Molecular cloning of mast cell growth factor, a hematopoietin that is active in both membrane bound and soluble forms. *Cell* 63:235-43.

212. McNiece IK, Briddell RA (1995) Stem cell factor. *Journal of leukocyte biology* 58:14-22.

213. Zsebo KM et al. (1990) Identification, purification, and biological characterization of hematopoietic stem cell factor from buffalo rat liver--conditioned medium. *Cell* 63:195-201.

214. Williams DE et al. (1990) Identification of a ligand for the c-kit proto-oncogene. *Cell* 63:167-74.

215. Nocka K, Buck J, Levi E, Besmer P (1990) Candidate ligand for the c-kit transmembrane kinase receptor: KL, a fibroblast derived growth factor stimulates mast cells and erythroid progenitors. *The EMBO journal* 9:3287-94.

216. Martin FH et al. (1990) Primary structure and functional expression of rat and human stem cell factor DNAs. *Cell* 63:203-11.

217. Besmer P (1991) The kit ligand encoded at the murine Steel locus: a pleiotropic growth and differentiation factor. *Current opinion in cell biology* 3:939-46.

218. Zhang Z, Zhang R, Joachimiak A, Schlessinger J, Kong XP (2000) Crystal structure of human stem cell factor: implication for stem cell factor receptor dimerization and activation. *Proceedings of the National Academy of Sciences of the United States of America* 97:7732-7.

219. Gilfillan AM, Tkaczyk C (2006) Integrated signalling pathways for mast-cell activation. *Nature reviews. Immunology* 6:218-30.

220. Kovach NL, Lin N, Yednock T, Harlan JM, Broudy VC (1995) Stem cell factor modulates avidity of alpha 4 beta 1 and alpha 5 beta 1 integrins expressed on hematopoietic cell lines. *Blood* 85:159-67.

221. Broxmeyer HE et al. (1995) Flt3 ligand stimulates/costimulates the growth of myeloid stem/progenitor cells. *Experimental hematology* 23:1121-9.

222. Jacobsen SE, Okkenhaug C, Myklebust J, Veiby OP, Lyman SD (1995) The FLT3 ligand potently and directly stimulates the growth and expansion of primitive murine bone marrow progenitor cells in vitro: synergistic interactions with interleukin (IL) 11, IL-12, and other hematopoietic growth factors. *The Journal of experimental medicine* 181:1357-63.

223. Veiby OP, Jacobsen FW, Cui L, Lyman SD, Jacobsen SE (1996) The flt3 ligand promotes the survival of primitive hemopoietic progenitor cells with myeloid as well as B lymphoid potential. Suppression of apoptosis and counteraction by TNF-alpha and TGF-beta. *Journal of immunology (Baltimore, Md. : 1950)* 157:2953-60.

224. McNiece IK, Briddell RA, Hartley CA, Andrews RG (1993) The role of stem cell factor in mobilization of peripheral blood progenitor cells: synergy with G-CSF. *Stem cells (Dayton, Ohio)* 11 Suppl 3:83-8.

225. Dührsen U et al. (1988) Effects of recombinant human granulocyte colony-stimulating factor on hematopoietic progenitor cells in cancer patients. *Blood* 72:2074-81.

226. Heimfeld S, Fogarty B, McGuire K, Williams S, Berenson RJ (1992) Peripheral blood stem cell mobilization after stem cell factor or G-CSF treatment: rapid enrichment for stem and progenitor cells using the CEPRATE immunoaffinity separation system. *Transplantation proceedings* 24:2818.

227. Dastych J, Metcalfe DD (1994) Stem cell factor induces mast cell adhesion to fibronectin. *Journal of immunology (Baltimore, Md. : 1950)* 152:213-9.

228. Bendall LJ et al. (1998) Stem cell factor enhances the adhesion of AML cells to fibronectin and augments fibronectin-mediated anti-apoptotic and proliferative signals. *Leukemia : official journal of the Leukemia Society of America, Leukemia Research Fund, U.K* 12:1375-82.

229. Wang L-S, Liu H-J, Jia X-X, Dong B, Wu C-T (2002) [Stem cell factor enhances the adhesion of hematopoietic cells to fibronectin]. *Zhongguo shi yan xue ye xue za zhi / Zhongguo bing li sheng li xue hui = Journal of experimental hematology / Chinese Association of Pathophysiology* 10:93-6.

230. Tushinski RJ, McAlister IB, Williams DE, Namen AE (1991) The effects of interleukin 7 (IL-7) on human bone marrow in vitro. *Experimental hematology* 19:749-54.

231. McNiece IK, Langley KE, Zsebo KM (1991) The role of recombinant stem cell factor in early B cell development. Synergistic interaction with IL-7. *Journal of immunology (Baltimore, Md. : 1950)* 146:3785-90.

232. Lyman SD, Jacobsen SE (1998) c-kit ligand and Flt3 ligand: stem/progenitor cell factors with overlapping yet distinct activities. *Blood* 91:1101-34.

233. Avraham H et al. (1992) Interaction of human bone marrow fibroblasts with megakaryocytes: role of the c-kit ligand. *Blood* 80:1679-84.

234. Long MW, Briddell R, Walter AW, Bruno E, Hoffman R (1992) Human hematopoietic stem cell adherence to cytokines and matrix molecules. *The Journal of clinical investigation* 90:251-5.

235. McCarthy KF, Ledney GD, Mitchell R (1977) A deficiency of hematopoietic stem cells in steel mice. *Cell and tissue kinetics* 10:121-6.

236. Miyazawa K et al. (1994) Ligand-dependent polyubiquitination of c-kit gene product: a possible mechanism of receptor down modulation in M07e cells. *Blood* 83:137-45.

237. Yee NS, Langen H, Besmer P (1993) Mechanism of kit ligand, phorbol ester, and calcium-induced down-regulation of c-kit receptors in mast cells. *The Journal of biological chemistry* 268:14189-201.

238. Yee NS, Hsiau CW, Serve H, Vosseller K, Besmer P (1994) Mechanism of down-regulation of c-kit receptor. Roles of receptor tyrosine kinase, phosphatidylinositol 3'-kinase, and protein kinase C. *The Journal of biological chemistry* 269:31991-8.

239. Peled a et al. (1999) The chemokine SDF-1 stimulates integrin-mediated arrest of CD34(+) cells on vascular endothelium under shear flow. *The Journal of clinical investigation* 104:1199-211.

240. Peled a et al. (2000) The chemokine SDF-1 activates the integrins LFA-1, VLA-4, and VLA-5 on immature human CD34(+) cells: role in transendothelial/stromal migration and engraftment of NOD/SCID mice. *Blood* 95:3289-96.

241. Luens KM et al. (1998) Thrombopoietin, kit ligand, and flk2/flt3 ligand together induce increased numbers of primitive hematopoietic progenitors from human CD34+Thy-1+Lin- cells with preserved ability to engraft SCID-hu bone. *Blood* 91:1206-15.

242. Tan BL et al. (2003) Genetic evidence for convergence of c-Kit- and alpha4 integrin-mediated signals on class IA PI-3kinase and the Rac pathway in regulating integrin-directed migration in mast cells. *Blood* 101:4725-32.

243. Schofield KP, Rushton G, Humphries MJ, Dexter TM, Gallagher JT (1997) Influence of interleukin-3 and other growth factors on alpha4beta1 integrin-mediated adhesion and migration of human hematopoietic progenitor cells. *Blood* 90:1858-66.

244. Nilsson G, Butterfield JH, Nilsson K, Siegbahn A (1994) Stem cell factor is a chemotactic factor for human mast cells. *Journal of immunology (Baltimore, Md. : 1950)* 153:3717-23.

245. Hassan HT, Zander A (1996) Stem cell factor as a survival and growth factor in human normal and malignant hematopoiesis. *Acta haematologica* 95:257-62.

246. Sharma S et al. (2006) Stem cell c-KIT and HOXB4 genes: critical roles and mechanisms in self-renewal, proliferation, and differentiation. *Stem cells and development* 15:755-78.

247. Kapur R, Cooper R, Zhang L, Williams DA (2001) Cross-talk between alpha(4)beta(1)/alpha(5)beta(1) and c-Kit results in opposing effect on growth and

survival of hematopoietic cells via the activation of focal adhesion kinase, mitogen-activated protein kinase, and Akt signaling pathways. *Blood* 97:1975-81.

248. Verfaillie CM (1993) Soluble factor(s) produced by human bone marrow stroma increase cytokine-induced proliferation and maturation of primitive hematopoietic progenitors while preventing their terminal differentiation. *Blood* 82:2045-53.

249. Nagasawa T, Kikutani H, Kishimoto T (1994) Molecular cloning and structure of a pre-B-cell growth-stimulating factor. *Proceedings of the National Academy of Sciences of the United States of America* 91:2305-9.

250. Fruehauf S, Srbic K, Seggewiss R, Topaly J, Ho A (2002) Functional characterization of podia formation in normal and malignant hematopoietic cells. *Journal of leukocyte biology* 71:425.

251. Veldkamp CT et al. (2009) Monomeric structure of the cardioprotective chemokine SDF-1/CXCL12. *Protein science : a publication of the Protein Society* 18:1359-69.

252. Wright DE (2002) Hematopoietic Stem Cells Are Uniquely Selective in Their Migratory Response to Chemokines. *Journal of Experimental Medicine* 195:1145-1154.

253. Aiuti A, Webb I, Bleul C, Springer T (1997) The Chemokine SDF-1 Is a Chemoattractant for Human CD34+ hematopoietic progenitor cells and Provides a New Mechanism to Explain the Mobilization of CD34+ Progenitors to Peripheral Blood. *The Journal of Experimental Medicine* 185:111-120.

254. Bleul CC, Fuhlbrigge RC, Casasnovas JM, Aiuti a, Springer T a (1996) A highly efficacious lymphocyte chemoattractant, stromal cell-derived factor 1 (SDF-1). *The Journal of experimental medicine* 184:1101-9.

255. Netelenbos T et al. (2002) Proteoglycans guide SDF-1-induced migration of hematopoietic progenitor cells progenitor cell (HPC) trafficking to the bone mar-Cell cultures. *Journal of Leukocyte Biology* 72:353-362.

256. Peled A et al. (1999) Dependence of human stem cell engraftment and repopulation of NOD/SCID mice on CXCR4. *Science (New York, N.Y.)* 283:845-8.

257. Bladergroen B a et al. (2009) In vivo recruitment of hematopoietic cells using stromal cell-derived factor 1 alpha-loaded heparinized three-dimensional collagen scaffolds. *Tissue engineering. Part A* 15:1591-9.

258. Rabbany SY et al. (2010) Continuous delivery of stromal cell-derived factor-1 from alginate scaffolds accelerates wound healing. *Cell transplantation* 19:399-408.

259. Sarkar A, Tatlidede S, Scherer SS, Orgill DP, Berthiaume F (2011) Combination of stromal cell-derived factor-1 and collagen-glycosaminoglycan scaffold delays contraction and accelerates reepithelialization of dermal wounds in wild-type mice.

Wound repair and regeneration : official publication of the Wound Healing Society [and] the European Tissue Repair Society 19:71-9.

260. Henderson PW et al. Stromal-derived factor-1 delivered via hydrogel drug-delivery vehicle accelerates wound healing in vivo. *Wound repair and regeneration : official publication of the Wound Healing Society [and] the European Tissue Repair Society* 19:420-5.

261. Zhang G et al. (2007) Controlled release of stromal cell-derived factor-1 alpha in situ increases c-kit+ cell homing to the infarcted heart. *Tissue engineering* 13:2063-71.

262. Sun G et al. (2011) Functional neovascularization of biodegradable dextran hydrogels with multiple angiogenic growth factors. *Biomaterials* 32:95-106.

263. Frederick JR et al. (2010) Stromal cell-derived factor-1alpha activation of tissue-engineered endothelial progenitor cell matrix enhances ventricular function after myocardial infarction by inducing neovasculogenesis. *Circulation* 122:S107-17.

264. Hidalgo A et al. (2001) Chemokine stromal cell-derived factor-1alpha modulates VLA-4 integrin-dependent adhesion to fibronectin and VCAM-1 on bone marrow hematopoietic progenitor cells. *Experimental hematology* 29:345-55.

265. Merzouk A et al. (2004) Rational Design of Chemokine SDF-1 Analogs with Agonist Activity for the CXCR4 Receptor and the Capacity to Rapidly Mobilize PMN and Hematopoietic Progenitor Cells in Mice. *Letters in Drug Design & Discovery* 1:126-134.

266. Neff JA, Tresco PA, Caldwell KD (1999) Surface modification for controlled studies of cell-ligand interactions. *Biomaterials* 20:2377-93.

267. Rivière C et al. (1999) Phenotypic and functional evidence for the expression of CXCR4 receptor during megakaryocytopoiesis. *Blood* 93:1511-23.

268. Rosu-Myles M, Bhatia M (2003) SDF-1 enhances the expansion and maintenance of highly purified human hematopoietic progenitors. *The hematology journal : the official journal of the European Haematology Association / EHA* 4:137-45.

269. Priestley GV, Scott LM, Ulyanova T, Papayannopoulou T (2006) Lack of alpha4 integrin expression in stem cells restricts competitive function and self-renewal activity. *Blood* 107:2959-67.

270. Li K et al. (2006) Small peptide analogue of SDF-1alpha supports survival of cord blood CD34+ cells in synergy with other cytokines and enhances their ex vivo expansion and engraftment into nonobese diabetic/severe combined immunodeficient mice. *Stem cells (Dayton, Ohio)* 24:55-64.

271. Sugiyama T, Kohara H, Noda M, Nagasawa T (2006) Maintenance of the hematopoietic stem cell pool by CXCL12-CXCR4 chemokine signaling in bone marrow stromal cell niches. *Immunity* 25:977-88.

272. Lapidot T, Kollet O (2002) The essential roles of the chemokine SDF-1 and its receptor CXCR4 in human stem cell homing and repopulation of transplanted immune-deficient NOD/SCID and NOD/SCID/B2m(null) mice. *Leukemia : official journal of the Leukemia Society of America, Leukemia Research Fund, U.K* 16:1992-2003.

273. Voermans C et al. (2001) In vitro migratory capacity of CD34+ cells is related to hematopoietic recovery after autologous stem cell transplantation. *Blood* 97:799-804.

274. Spencer A, Jackson J, Baulch-Brown C (2001) Enumeration of bone marrow "homing" haemopoietic stem cells from G-CSF-mobilised normal donors and influence on engraftment following allogeneic transplantation. *Bone marrow transplantation* 28:1019-22.

275. Jones P et al. (1998) Stromal expression of Jagged 1 promotes colony formation by fetal hematopoietic progenitor cells. *Blood* 92:1505-11.

276. Milner LA, Kopan R, Martin DI, Bernstein ID (1994) A human homologue of the Drosophila developmental gene, Notch, is expressed in CD34+ hematopoietic precursors. *Blood* 83:2057-62.

277. Kertész Z et al. (2006) In vitro expansion of long-term repopulating hematopoietic stem cells in the presence of immobilized Jagged-1 and early acting cytokines. *Cell biology international* 30:401-5.

278. Walker L et al. (1999) The Notch/Jagged pathway inhibits proliferation of human hematopoietic progenitors in vitro. *Stem cells (Dayton, Ohio)* 17:162-71.

279. Stier S, Cheng T, Dombkowski D, Carlesso N, Scadden DT (2002) Notch1 activation increases hematopoietic stem cell self-renewal in vivo and favors lymphoid over myeloid lineage outcome. *Blood* 99:2369-78.

280. Calvi LM et al. (2003) Osteoblastic cells regulate the haematopoietic stem cell niche. *Nature* 425:841-6.

281. Duncan AW et al. (2005) Integration of Notch and Wnt signaling in hematopoietic stem cell maintenance. *Nature immunology* 6:314-22.

282. Varnum-Finney B et al. (2000) Pluripotent, cytokine-dependent, hematopoietic stem cells are immortalized by constitutive Notch1 signaling. *Nature medicine* 6:1278-81.

283. Chumsri S, Matsui W, Burger AM (2007) Therapeutic implications of leukemic stem cell pathways. *Clinical cancer research : an official journal of the American Association for Cancer Research* 13:6549-54.

284. Varnum-Finney B et al. (1998) The Notch ligand, Jagged-1, influences the development of primitive hematopoietic precursor cells. *Blood* 91:4084-91.

285. Isaacs A, Lindenmann J, Valentine RC (1957) Virus interference. II. Some properties of interferon. *Proceedings of the Royal Society of London. Series B, Containing papers of a Biological character. Royal Society (Great Britain)* 147:268-73.

286. Isaacs A, Lindenmann J (1957) Virus interference. I. The interferon. *Proceedings of the Royal Society of London. Series B, Containing papers of a Biological character. Royal Society (Great Britain)* 147:258-67.

287. Zhao X et al. (2010) Brief report: interferon-gamma induces expansion of Lin(-)Sca-1(+)C-Kit(+) Cells. *Stem cells (Dayton, Ohio)* 28:122-6.

288. Thiel DJ et al. (2000) Observation of an unexpected third receptor molecule in the crystal structure of human interferon-gamma receptor complex. *Structure (London, England : 1993)* 8:927-36.

289. Dalton DK, Haynes L, Chu CQ, Swain SL, Wittmer S (2000) Interferon gamma eliminates responding CD4 T cells during mycobacterial infection by inducing apoptosis of activated CD4 T cells. *The Journal of experimental medicine* 192:117-22.

290. Murray PJ, Young RA, Daley GQ (1998) Hematopoietic remodeling in interferon-gamma-deficient mice infected with mycobacteria. *Blood* 91:2914-24.

291. Selleri C, Sato T, Anderson S, Young NS, Maciejewski JP (1995) Interferon-gamma and tumor necrosis factor-alpha suppress both early and late stages of hematopoiesis and induce programmed cell death. *Journal of cellular physiology* 165:538-46.

292. Raefsky EL, Platanias LC, Zoumbos NC, Young NS (1985) Studies of interferon as a regulator of hematopoietic cell proliferation. *Journal of immunology (Baltimore, Md. : 1950)* 135:2507-12.

293. Zoumbos NC, Djeu JY, Young NS (1984) Interferon is the suppressor of hematopoiesis generated by stimulated lymphocytes in vitro. *Journal of immunology (Baltimore, Md. : 1950)* 133:769-74.

294. Zoumbos NC, Gascon P, Djeu JY, Young NS (1985) Interferon is a mediator of hematopoietic suppression in aplastic anemia in vitro and possibly in vivo. *Proceedings of the National Academy of Sciences of the United States of America* 82:188-92.

295. Maciejewski J, Selleri C, Anderson S, Young NS (1995) Fas antigen expression on CD34+ human marrow cells is induced by interferon gamma and tumor necrosis factor alpha and potentiates cytokine-mediated hematopoietic suppression in vitro. *Blood* 85:3183-90.

296. Hwang J-H et al. (2006) Interferon gamma has dual potential in inhibiting or promoting survival and growth of hematopoietic progenitors: interactions with stromal cell-derived factor 1. *International journal of hematology* 84:143-50.

297. Yang L et al. (2005) IFN-gamma negatively modulates self-renewal of repopulating human hemopoietic stem cells. *Journal of immunology (Baltimore, Md. : 1950)* 174:752-7.

298. Shiohara M, Koike K, Nakahata T (1993) Synergism of interferon-gamma and stem cell factor on the development of murine hematopoietic progenitors in serum-free culture. *Blood* 81:1435-41.

299. Shiohara M, Koike K, Nakahata T, Komiyama A (1994) Hematopoietic progenitors and synergism of interferon-gamma and stem cell factor. *Leukemia & lymphoma* 14:203-11.

300. Kurz K, Gluhcheva Y, Zvetkova E, Konwalinka G, Fuchs D (2010) Interferon-gamma-mediated pathways are induced in human CD34(+) haematopoietic stem cells. *Immunobiology* 215:452-7.

301. Caux C, Moreau I, Saeland S, Banchereau J (1992) Interferon-gamma enhances factor-dependent myeloid proliferation of human CD34+ hematopoietic progenitor cells. *Blood* 79:2628-35.

302. Brugger W et al. (1993) Ex vivo expansion of enriched peripheral blood CD34+ progenitor cells by stem cell factor, interleukin-1 beta (IL-1 beta), IL-6, IL-3, interferon-gamma, and erythropoietin. *Blood* 81:2579-84.

303. Snoeck HW et al. (1994) Interferon gamma selectively inhibits very primitive CD342+CD38- and not more mature CD34+CD38+ human hematopoietic progenitor cells. *The Journal of experimental medicine* 180:1177-82.

304. Lin C-C, Anseth KS (2009) Glucagon-like peptide-1 functionalized PEG hydrogels promote survival and function of encapsulated pancreatic beta-cells. *Biomacromolecules* 10:2460-7.

305. Wang D-A et al. Bioresponsive phosphoester hydrogels for bone tissue engineering. *Tissue engineering* 11:201-13.

306. Seidlits SK et al. (2010) The effects of hyaluronic acid hydrogels with tunable mechanical properties on neural progenitor cell differentiation. *Biomaterials* 31:3930-40.

307. Zhang C et al. (2011) Oligo(trimethylene carbonate)-poly(ethylene glycol)-oligo(trimethylene carbonate) triblock-based hydrogels for cartilage tissue engineering. *Acta biomaterialia.*

308. Hu X, Li D, Gao C (2011) Chemically cross-linked chitosan hydrogel loaded with gelatin for chondrocyte encapsulation. *Biotechnology journal.*

309. Matyash M et al. (2011) Novel soft alginate hydrogel strongly supports neurite growth and protects neurons against oxidative stress. *Tissue engineering. Part A.*

310. Moon JJ et al. (2010) Biomimetic hydrogels with pro-angiogenic properties. *Biomaterials* 31:3840-7.

311. Liu Y et al. (2009) Effects of encapsulated rabbit mesenchymal stem cells on ex vivo expansion of human umbilical cord blood hematopoietic stem/progenitor cells. *Journal of microencapsulation* 26:130-42.

312. Levee MG, Lee GM, Paek SH, Palsson BO (1994) Microencapsulated human bone marrow cultures: a potential culture system for the clonal outgrowth of hematopoietic progenitor cells. *Biotechnology and bioengineering* 43:734-9.

313. Yuan Y et al. (2011) Ex vivo amplification of human hematopoietic stem and progenitor cells in an alginate three-dimensional culture system. *International journal of laboratory hematology.*

314. Nicodemus GD, Bryant SJ (2008) Cell encapsulation in biodegradable hydrogels for tissue engineering applications. *Tissue engineering. Part B, Reviews* 14:149-65.

315. Fedorovich NE et al. (2009) The effect of photopolymerization on stem cells embedded in hydrogels. *Biomaterials* 30:344-53.

316. Williams CG, Malik AN, Kim TK, Manson PN, Elisseeff JH (2005) Variable cytocompatibility of six cell lines with photoinitiators used for polymerizing hydrogels and cell encapsulation. *Biomaterials* 26:1211-8.

317. Franco CL, Price J, West JL (2011) Development and optimization of a dual-photoinitiator, emulsion-based technique for rapid generation of cell-laden hydrogel microspheres. *Acta biomaterialia* 7:3267-76.

318. McBeath R, Pirone DM, Nelson CM, Bhadriraju K, Chen CS (2004) Cell shape, cytoskeletal tension, and RhoA regulate stem cell lineage commitment. *Developmental cell* 6:483-95.

319. Ruiz SA, Chen CS (2008) Emergence of patterned stem cell differentiation within multicellular structures. *Stem cells (Dayton, Ohio)* 26:2921-7.

320. Kilian KA, Bugarija B, Lahn BT, Mrksich M (2010) Geometric cues for directing the differentiation of mesenchymal stem cells. *Proceedings of the National Academy of Sciences of the United States of America* 107:4872-7.

321. Luo W, Jones SR, Yousaf MN (2008) Geometric control of stem cell differentiation rate on surfaces. *Langmuir : the ACS journal of surfaces and colloids* 24:12129-33.

322. Wang W, Horner DN, Chen WLK, Zandstra PW, Audet J (2008) Synergy between erythropoietin and stem cell factor during erythropoiesis can be quantitatively

described without co-signaling effects. *Biotechnology and bioengineering* 99:1261-72.

Appendix

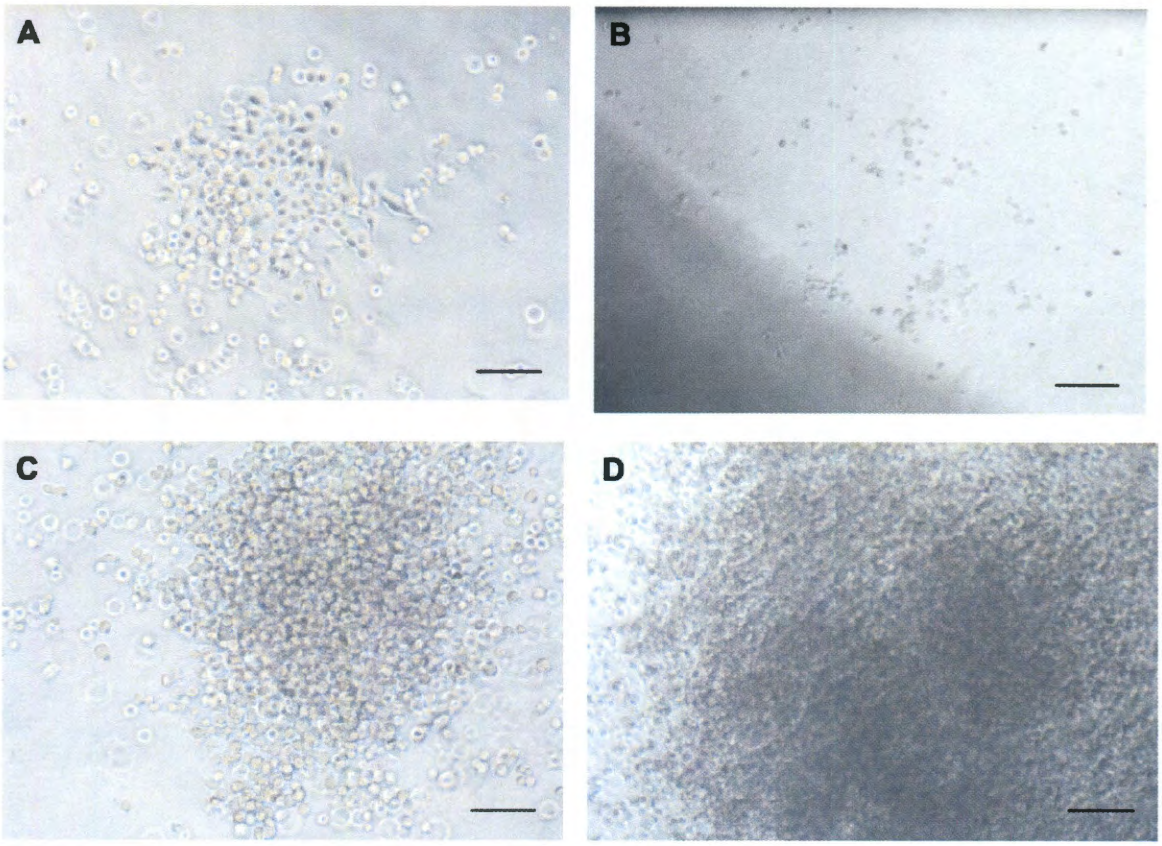

Figure A1: Colonies formed during the colony forming unit assay. A. CFU-M, Cells are distinct, uniform, and large in size compared to cells in CFU-G colonies; B. CFU-G, Cells are smaller and distinct; C. CFU-GM, Colonies are large, and cells are distinguishable and multiple cell sizes are present; D. CFU-GEMM, Colonies are large and individual cells are indistinguishable at the colony centers. There is also a brown or reddish hue to the colonies. Multiple cell sizes are present.